Impacts of ocean acidification and warming on Arctic calcifying key species: Benthic coralline red alga (*Lithothamnion glaciale*) and pelagic thecosome pteropods (*Limacina helicina* & *L. retroversa*)

Dissertation

zur Erlangung des akademischen Grades
eines Doktors der Naturwissenschaften

-Dr. rer. nat.-

an der Mathematisch-Naturwissenschaftlichen Fakultät
der Christian-Albrechts Universität zu Kiel

vorgelegt von
Jan Büdenbender
Kiel, Dezember 2015

Erste/r Gutachter/in: Prof. Dr. Ulf Riebesell
Zweite/r Gutachter/in: Prof. Dr. Frank Melzner

Tag der mündlichen Prüfung: 15.02.2016

Zum Druck genehmigt:

gez. Prof. Dr. Wolfgang J. Duschl
(Der Dekan)

Content

1 Summary

Over the last two centuries human activities significantly changed the Earth system. Atmospheric CO_2 concentrations were increased by ~25% in only 50 years (1965 to 2015) through combustion of fossil fuels and changes in land use. This is a rate of change likely unprecedented in Earth history. Consequences of these activities are a warming climate mainly caused by the greenhouse effect of CO_2, and the 'acidification' of the world oceans. A doubling of surface ocean carbon dioxide- (CO_2) and proton- (H^+) and a 40% decrease of the carbonate ion (CO_3^{2-}) concentrations until the end of this century will probably affect many marine organisms, and are of concern for calcifying species. Due to low temperatures, the Arctic Surface Ocean will be one of the first to experience mean annual corrosive conditions for calcified organisms. This makes the Arctic Ocean a bellwether for global impacts of ocean acidification (OA) on marine life. Biogenic calcium carbonate often establishes ecological functions like being the fundament for species rich habitats in the case of hermatypic corals and crustose coralline algae (CCA) or impacting global carbon cycling embodied by coccolithophores, foraminifera and thecosome pteropods. The marine carbon cycle influences the destination of human CO2 emissions and the development of the global climate. Therefore, the ecological importance of CCA and pteropods, their involvement in the marine carbon cycle and their anticipated vulnerability to OA call for research on their fate in the future ocean.

This doctoral thesis investigates the effects of warming and ocean acidification on growth, calcification, dissolution, corrosion and survival of Arctic calcifying keystone species Lithothamnion glaciale (CCA) and Limacina helicina and retroversa (thecosome pteropods). As laboratory based experimental work with thecosome pteropods suffers from major restrictions, these being starvation and high mortality, part of this thesis deals with methodological improvements in this field.

The northern most known benthic habitat based on the unattached growth form of *L. glaciale* is described in an observational study. In an experimental study, calcification and dissolution rates of this alga under increased CO_2 concentrations were measured. Interpretation of experimental results let us propose Arctic CCA engineered habitats to suffer from annual net dissolution within this century.

Two experiments, investigating OA and warming impacts on thecosome pteropods, showed that OA will reduce pteropod growth rates and enhance shell corrosion. However, the effect of OA on future survival remains controversial and depends on cultivation conditions and temporal resolution in experimental studies. In a mesocosm study simulating OA at close to in-situ conditions, we observed OA independent survival of pteropods challenging the hypothesis of pteropod absence in future subsaturated waters.

Methodological aspects of this thesis are: the contribution to the development and successful implementation of large scale replicated mesocosm studies with the KOSMOS system which improved experimental pteropod work and the development of an instrument for handheld automated optical non destructive in-situ observations of particle and mesozooplankton dynamics in shelf and mesocosm systems.

2 Zusammenfassung

Menschliche Aktivitäten während der letzten zwei Jahrhunderte haben unseren Planeten nachhaltig beeinflusst. Die Verbrennung fossiler Kohlenstoffe und eine veränderte Landnutzung (Waldrodungen und intensive Agrarwirtschaft) führten, in nur 50 Jahren, zu einem Anstieg atmosphärischer CO_2 Konzentrationen um 25% (1965 bis 2015). Dies ist eine Zuwachsrate, die in den letzten 300 millionen Jahren nicht, vielleicht auch noch nie, in der Erdgeschichte vorgekommen ist. Konsequenzen dieser Aktivitäten sind ein sich erwärmendes Klima, bedingt durch den Treibhauseffekt von CO_2, und die 'Versauerung' der globalen Meere. Die Verdopplung der CO_2- und Protonen Konzentration, sowie eine 40%ige Verringerung der Carbonationen Konzentration des Oberflächenozean bis zum Ende des 21. Jahrhunderts werden die Biologie vieler mariner Lebewesen aber insbesondere die der kalzifizierenden Arten beeinflussen. Aufgrund seiner niedrigen Wassertemperatur wird der Arktische Ozean einer der ersten sein, in dem das Wasser korrosiv für kalzifizierende Arten sein wird. Das macht ihn zu einem Studienobjekt für potentielle Veränderungen, die die Ozeanversauerung (OA) auf die marine Biologie haben wird.

Manche dieser kalzifizierenden Arten erfüllen wichtige ökologische Funktionen im marinen System, wie z.B. Habitat bildende hermatypische Korallen- und Krustenrotalgen. Pelagische kalzifizierende Organismen wie Coccolithophoriden, Foraminiferen und thekosomate Flügelschnecken hingegen können den globalen Kohlenstoffkreislauf beeinflussen. Der marine Kohlenstoffkreislauf und eventuelle Veränderungen darin entscheiden mit über die weitere Entwicklung des globalen Klimas. Die ökologische Wichtigkeit kalzifizierender Organismen, deren Verwicklung in den marinen Kohlenstoffkreislauf und deren vermutliche Sensitivität für Veränderungen der marinen Carbonatchemie rufen nach wissenschaftlichen Untersuchungen dieser Arten und ihrem Schicksal im zukünftigen Ozean.

Die vorliegende Dissertation untersucht den Einfluss von Erwärmung und Ozeanversauerung auf Prozesse wie Wachstum, Kalzifizierung, Auflösung, Korrosion und Überleben in den arktischen kalzifizierenden Schlüsselarten *Lithothamnion glaciale* (Krustenrotale) und *Limacina helicina* und *retroversa* (Thekosome Flügelschnecken). Experimentelle Arbeit mit Flügelschnecken in Laboren ist durch Verhungern und erhöhte Mortalität beeinträchtigt, deshalb befasst sich ein Teil der Dissertation mit der Verbesserung von Methoden für Flügelschneckenexperimente.

In einer Studie wurde das nördlichste, bis jetzt bekannte, benthische Habitat beschrieben, das durch die unbefestigte Wuchsform von *L. glaciale* gebildet wird. In einer experimentellen Studie wurden Kalzifizierungs- und Auflösungsraten dieser Krustenrotalge in zukünftigen CO_2 Emissionsszenarien getestet. Die Befunde dieses Experiments lässt uns annehmen, dass auf Krustenrotalgen aufbauende arktische Habitate noch innerhalb des 21. Jahrhunderts von einer Nettoauflösung ihres Kalkskeletts betroffen sein werden.

In zwei Studien zu den Einflüssen von OA auf kalzifizierende Flügelschnecken wurde gezeigt, dass OA Wachstumsraten verringert und Schalenkorrosion erhöht. In einer Mesokosmen Studie haben wir OA unabhängige Überlebensraten gemessen, sogar in korrosivem Wasser. Diese Beobachtung stellt die allgemeine Annahme, dass Flügelschnecken in korrosiven Ozeanen zukünftig fehlen werden, in Frage.

Methodische Aspekte dieser Dissertation sind: die Beteiligung an der Entwicklung des KOSMOS Systems und dessen erfolgreiche Anwendung in umfassenden replizierten Mesokosmenstudien, die zu einer Verbesserung von Flügelschnecken-Experimenten geführt haben, und die

Entwicklung der KielVision, einer Kamera für automatisierte, nicht invasive, optische in-situ Messung von Partikel- und Mesozooplanktondynamiken in Küsten und Mesokosmensystemen.

3 Introduction

3.1 The human footprint in Earth history

Global element cycles are driven by living organisms throughout Earth history. For example, the first photosynthetic bacteria enriched the atmosphere over the time span of likely 1 giga-annum with oxygen from 0 to 20000 ppm (0.00002 ppm y^{-1}) (Kump 2008). The colonization of land by green plants, especially the evolution of trees, in the Permo-Carboniferous period (300 mega-annum ago) likely reduced the atmospheric CO_2 concentration by an order of magnitude, from ~ 5000 ppm to 500 ppm over the period of ~ 100 million years (0.000045 ppm y^{-1}) (Berner & Kothavala 2001). However, humans so far are the beings most efficient in altering global conditions. In only 200 years, atmospheric CO_2 concentration could be increased from 280 ppm to 400 ppm (~0.5 ppm y^{-1}) (IPCC 2007), four orders of magnitude faster than Permo-Carboniferus plants. Industrialization, ultimately driven by a globally triumphal procession of capitalism "the run for profit instead of safety" (Pirenne 1914), starting in the late 18th /early 19th century, was enabled by the application of steam machinery to manufacturing. This development was accompanied by an increasing need for energy. Energy was made usable through burning of easily accessible 'fossil fuels' like coal, oil and natural gas. Massive burning of fossil fuels, cement production and changes in land use introduced ~400 Pg of carbon from the fossil reservoir and the terrestrial biosphere to the atmosphere (Sabine et al. 2004). It can be expected, that dramatic effects like mass extinctions, as happened after past perturbation episodes, could be exceeded or at least triggered by the recent anthropogenic perturbation (Jackson 2008).

3.2 CO_2 and the global climate

The climate is a complex and interactive system, ultimately powered by solar radiation and based on dispersal of this energy over the Earth's components mainly through temperature, precipitation and wind dynamics (IPCC 2007). On the long-term incoming solar radiation is balanced by outgoing longwave radiation. On the short term this radiation balance can be altered in three ways: by changing the incoming radiation (e.g. changes in the sun's radiation output), by changing the fraction of solar radiation that is reflected (called 'albedo' e.g. by changes in cloud cover, atmospheric particles or vegetation), or by changing the outgoing longwave radiation leaving the Earth system (e.g. changes in greenhouse gas concentration). Such changes in the radiation balance would directly alter the Earth climate. Greenhouse gases act as a blanket for longwave radiation coming from the Earth surface. As e.g. clouds reflect shortwave radiation like the visible light coming in from the sun, greenhouse gases like CO_2 reflect longwave radiation going out from the Earth surface, thereby keeping the mean Earth surface temperature at about 14°C. Due to human activities the atmospheric CO_2 concentration has increased since the industrial revolution (Francey & Farquhar 1982, Keeling & Shertz 1992) changing the radiation balance between Earth and Space. This increased 'blanketing' of the Earth decreased the outgoing longwave radiation by about 1.6 Wm^{-2}, thereby warming the Earth surface by about 0.76°C (IPCC 2007). From 1955 to 1998 the oceans (0-3000m), by far the Earth's biggest reservoir for heat content, warmed by 0.037°C (Levitus et al. 2005).

3.3 Carbonate chemistry

In order to understand the impact of rising atmospheric CO_2 concentrations on the ocean and the ocean role in the climate, we will have a brief look at the marine carbonate system and the marine carbon cycle.

Atmospheric CO_2 is, via diffusion, in constant exchange with surface ocean CO_2, determined by Henry's Law:

$$[CO_2] = K_0 \, PCO_2 \quad (1)$$

K_0 being the temperature and salinity dependent Henry's constant and PCO_2 the atmospheric CO_2 partial pressure.

If CO_2 enters the water, it will partly form true carbonic acid (H_2CO_3), which further dissociates to bicarbonate ions (HCO_3^-), carbonate ions (CO_3^{2-}) and protons (H^+). Since carbonic acid [H_2CO_3] (squared brackets denote concentrations) is less than 0.3% and cannot be chemically separated from aqueous CO_2, both concentrations are by definition included in [CO_2], simplifying the equilibrium equation for the marine carbonate system to:

$$CO_2 + H_2O \overset{K_1}{\Leftrightarrow} HCO_3^- + H^+ \overset{K_2}{\Leftrightarrow} CO_3^{2-} + 2H^+ \quad (2)$$

Quantities of the individual ions are governed by the equilibrium constants K_1 and K_2 (or first and second dissociation constants of carbonic acid) depending on temperature, pressure and salinity. Stochiometric K_1^* and K_2^* look as follows:

$$K_1^* = \frac{[HCO_3^-][H^+]}{[CO_2]} \quad (3)$$

and

$$K_2^* = \frac{[CO_3^{2-}][H^+]}{[HCO_3^-]} \quad (4)$$

K^*_1 and K^*_2 have been determined analytically (reviewed in Lee et al. (2000)).

With the knowledge of K^*_1 and K^*_2 it is possible to calculate the relative proportions of CO_2, HCO_3^- and CO_3^{2-} in a given system. At increasing [CO_2] as a consequence of combustion of fossil fuels, [CO_3^{2-}] decreases, [H^+] increases and [HCO_3^-] in- or decreases slightly depending on the initial pH.

Two more concepts are necessary for describing the marine carbonate system, which is the sum of all dissolved inorganic carbon species (DIC):

$$DIC = [CO_2] + [HCO_3^-] + [CO_3^{2-}] \quad (5)$$

and the concept of total alkalinity (TA).

TA can be expressed in different ways. Dickson (1981) gives the following chemical definition: "The total alkalinity of a natural seawater is thus defined as the number of moles of hydrogen ion equivalent to the excess of proton acceptors (bases formed from weak acids with a dissociation constant $K \leq 10^{-4.5}$ at 25 °C and zero ionic strength) over proton donors (acids with $K > 10^{-4.5}$) in one kilogram of sample."

$$TA = [HCO_3^-] + 2[CO_3^{2-}] + [B(OH)_4^-] + [OH^-] + [HPO_4^{2-}] + 2[PO_4^{3-}] + [H_3SiO_4^-] + [NH_3^-] + [HS^-] + \ldots - [H^+] - [HSO_4^-] - [HF] - [H_3PO_4] - \ldots \quad (6)$$

TA can be determined analytically through titration of a seawater sample with a strong acid until the concentration of proton donors equals the concentration of proton acceptors. In this concept, TA can be regarded as buffer capacity of seawater.

From an electrochemical perspective, TA can be expressed as the charge surplus of conservative cations (Na^+, Mg^{2+}, K^+, Ca^{2+}) over conservative anions (Cl^-, SO_4^{2-}, F^-, Br^-), which is balanced by weak anions like (HCO_3^-, CO_3^{2-}, $B(OH)_4^-$, OH^-) (Wolf-Gladrow et al. 2007). Therefore, the sum of charges of the carbonate ions (TA) is conservative as well. Nevertheless, the concentrations of the individual compounds of the TA do change as a function of temperature, pressure and salinity. With this concept changes in alkalinity can be expressed as a consequence of changes in the pool of conservative ions, e.g. when Ca^{2+} is used for calcification or NO_3^{2-} for primary production.

Another concept of the carbonate system of particular interest for calcifying organisms is the solubility of calcium carbonate ($CaCO_3$) expressed as the $CaCO_3$ saturation state of seawater (Omega). Omega is a function of carbonate and calcium ion concentrations and depends on temperature, pressure, salinity and the crystal structure of the $CaCO_3$ species (Zeebe & Wolf-Gladrow 2001).

$$Omega = \frac{[Ca^{2+}][CO_3^{2-}]}{K_{sp}^*} \quad (7)$$

K_{sp}^* is a function of the carbonate crystal structure (aragonite, calcite or high Mg-calcite, temperature, pressure and salinity). In general, $CaCO_3$ is thermodynamically stable when Omega values are greater than 1, while dissolution is favored when Omega values are below 1. K_{sp}^* for the different crystal structures are determined experimentally with the K_{sp}^* of calcite being larger than the K_{sp}^* of aragonite. The literature has not agreed on a K_{sp}^* for high Mg-calcite and reports large offsets, e.g. from 5 times the solubility of aragonite to the solubility of calcite (Plummer & Mackenzie 1974, Morse et al. 2006). In natural seawater changes in $[Ca^{2+}]$ are small and closely related to changes in salinity (Zeebe & Wolf-Gladrow 2001), so Omega is mainly dependent on $[CO_3^{2-}]$.

3.4 Biological influences on carbonate chemistry

Photosynthesis, respiration and calcification are biological processes which interfere with marine carbonate chemistry. Photosynthesis decreases DIC by synthesizing organic carbon molecules from inorganic CO_2, called primary production.

$$6CO_2 + 6H_2O \rightarrow C_6H_{12}O_6 + 6O_2 \quad (8)$$

A consequence of CO_2 removal from the water is an increase in $[CO_3^{2-}]$ and a decrease in $[H^+]$ and $[CO_2]$, while TA stays constant. Minor changes in TA arise from photosynthesis associated nutrient uptake. Respiration represents the reverse reaction of photosynthesis and therefore has the reverse effect on the carbonate chemistry.

Calcification,

$$Ca^{2+} + CO_3^{2-} \rightarrow CaCO_3 \quad (9)$$

takes up Ca^{2+} and CO_3^{2-} from the water, and thereby decreases TA by two equivalents and DIC by one equivalent. The consequence of calcification for the carbonate system is an increase in $[CO_2]$ and $[H^+]$. The dissolution of $CaCO_3$ has the opposite effects on the carbonate chemistry.

3.5 Ocean acidification

A consequence of increasing atmospheric CO_2 concentration is increasing marine DIC (also called 'ocean carbonation' (Riebesell et al. 2009)). Due to the buffer capacity (see TA concepts) of the ocean, the CO_2 concentration in water changes only slightly.

$$CO_2 + H_2O + CO_3^{2-} \leftrightharpoons 2HCO_3^- \quad (10)$$

As $[CO_3^{2-}]$ decreases, Omega decreases eq. (7). However, a small part of the resulting HCO_3^- will dissociate into $CO_3^{2-}$and H^+ and therefore lower the pH (Zeebe & Wolfl-Gladrow 2001). This decrease in pH caused by the buffering of rising CO_2 concentrations was originally named 'ocean acidification' by Broecker & Clarke (2001) but was advertised more widely through the paper of Caldeira & Wickett (2003). Ocean acidification nowadays is used as a synonym for the invasion of anthropogenic CO_2 into the oceans and the associated changes in the marine carbonate chemistry (increasing $[CO_2]$ and $[H^+]$ and decreasing $[CO_3^{2-}]$). Ocean acidification (OA) is already measurable in the oceans. Mean surface pH has dropped by 0.1 unit from 8.2 to 8.1 corresponding to an increase in acidity of 30% since the pre-industrial time (Raven 2005). Models project a further pH decrease of 0.3 - 0.4 units by the end of the 21st century (Orr et al. 2005).

3.6 Climate change impacts on marine biota

Temperature is a basal and paramount parameter for life in general (i.e. Maxwell-Boltzmann energy distribution (Maxwell 1860)), which determines the rate of fundamental processes such as enzymatic reactions, diffusion and membrane transport (Brown et al. 2004). Changes in temperature therefore will affect metabolic rates, which ultimately determine life history traits, population growth and ecosystem processes (Hochachka & Somero 2002, O'Connor et al. 2007). Organisms through the process of evolution adapt to local environmental temperatures with optimal physiological responses matching temperatures that are close to the local average (Hoegh-Guldberg & Bruno 2010). Organisms are able to acclimatize to a range around these optimal environmental temperatures, but beyond this range acclimatization fails, mortality risk increases, fitness is reduced and populations decline or are driven to local extinction (Hochachka & Somero 2002). For example, a reduction in Antarctic krill densities (Atkinson et al. 2004) as well as tropical coral reef cover and performance are associated with increasing oceanic heat content (Hoegh-Guldberg et al. 2007). Biogeochemical aspects like global marine primary production are considered to be negatively affected, too. Warming likely increases the top-down effect in the marine food web, since respiration has a higher temperature sensitivity than photosynthesis (Lopez-Urrutia et al. 2006). This could lead to both reduced total food web biomass and a reduced animal to plant biomass ratio (O'Connor et al. 2009).

Impacts of OA on marine ecosystems have been extensively studied (Raven 2005, Fabry et al. 2008, Riebesell et al. 2009). Decreasing carbonate saturations will affect biogenetic calcification by corroding existing $CaCO_3$ structures and increasing the energy demand of active CO_3^{2-} uptake (Gattuso & Buddemeier 2000). From experimental studies we so far know that generally calcification rates will be reduced (Riebesell et al. 2000, Fabry et al. 2008). Despite calcification, also other physiological processes, occurring in all marine animals, are expected to be affected by OA. Increasing CO_2 will affect acid-base regulation, respiration, energy turnover and mode of metabolism, depending on the organisms regulatory capacities (Pörtner et al. 2004). OA induced changes in animal physiology may not be detrimental but are expected to affect long-term growth and reproduction, possibly harming population size and species diversity (Pörtner et al. 2004). On the other hand, ocean carbonation (Riebesell et al. 2009) in the surface ocean will be beneficial for autotrophic organisms. Especially algae with inefficient carbon concentrating mechanisms are thought to profit from increased CO_2 availability (Riebesell et al. 1993, Hein & Sand-Jensen 1997).

Why are we interested in climate change impacts on the marine biota? The marine biota is considered to significantly impact global climate, as happened before (see 3.1). In order to understand how marine biota can impact global climate we have to look at the global and the marine carbon cycle and the role of the marine biota in the so called 'biological pump'.

3.7 The marine carbon cycle

Carbon is cycled between global reservoirs, which can be separated into 'active' (mainly hydrosphere, biosphere & atmosphere) and 'conservative' reservoirs (the lithosphere) (Fortier et al. 1994, Ridgwell & Zeebe 2005). Separation is mainly defined by the timescales in which carbon is cycled within and between them. E.g. formation of fossil fuels, which is an organic carbon transfer from the biosphere through burial into the lithosphere, takes millions of years, while e.g. the transfer of inorganic carbon from the atmosphere into organic carbon in the hydrosphere during a spring bloom can take only a couple of days. With few on the next couple

of centuries, the deep ocean can also be counted to the conservative reservoirs, since carbon entering the deep ocean has a residence time of approximately 1000 years until it is cycled back to the atmosphere (Sarmiento & Gruber 2006).

The hydrosphere, dominated by the oceans, is by far the largest carbon reservoir, containing approximately 38000 PgC (Le Quéré et al. 2009), which is roughly 85% of the combined active reservoirs. Thus, changes in the marine carbon reservoir can significantly influence the atmospheric reservoir. The dominant process driving the global carbon cycle out of its historical balance is the immensely accelerated transfer of carbon from the lithosphere to the atmosphere, that means from a conservative to an active reservoir, by the burning of fossil fuels. From the global carbon cycle perspective the most interesting question is how this anthropogenic perturbation will affect the marine carbon cycle. The ocean has by far the largest buffer capacity for anthropogenic CO_2 (Gruber et al. 2009) and the largest carbon cycling rate of 5 to >12 PgC y^{-1} (Boyd & Trull 2007, Henson et al. 2011, Siegel et al. 2014) between a climate active reservoir, the surface ocean, and a climate conservative reservoir, the deep ocean. From 1800 AD to 1994 AD the oceans approximately removed 118 ± 19 Pg CO_2 from the atmosphere (Sabine et al. 2004), which is roughly 30% of the anthropogenic emitted carbon (compare 3.1). There are two main pathways, called ‘pumps’, through which carbon is cycled between the surface and the deep ocean: The physical pump and the biological pump (Sarmiento & Gruber 2006). These pumps together modulate the vertical distribution of carbon in the oceans.

The physical pump works at sites of deepwater formation. Surface water travelling towards the poles cools down, which increases CO_2 uptake capacity eq. (1) and ultimately sinks to the ocean floor exporting anthropogenic CO_2 from the atmosphere. The physical pump is responsible for approximately 35 to 40 % of the surface to deep ocean DIC difference (Toggweiler, Gnanadesikan, et al. 2003).

The biological pump, which can be subdivided into the soft tissue pump and the carbonate pump (Volk & Hoffert 1985), mediate the remaining fraction of the surface to deep ocean DIC gradient (Toggweiler, Murnane, et al. 2003). The tissue pump is driven by photosynthesizing plankton organisms fixing DIC into organic carbon, which eventually aggregates and sinks past the mixed surface layer depth. Most of this organic carbon is respired in deep waters by heterotrophic bacteria, increasing deep ocean DIC. However, a small portion of this sinking carbon reaches the ocean floor and is eventually buried in the sediments (Sarmiento & Gruber 2006). This is one way of how carbon is transferred back to the lithosphere. While the tissue pump provides a net export of surface ocean DIC and decreases surface ocean pCO_2, the carbonate pump also exports DIC bound in $CaCO_3$ but increases surface ocean pCO_2. During the process of calcification 0.6 moles of CO_2 are produced for every mole of $CaCO_3$ (Frankignoulle, Canon and Gattuso 1994). For this reason the carbonate pump is sometimes referred to as carbonate counter pump. While travelling along the global ocean conveyer belt, deep ocean DIC is temporarily excluded from climate active carbon reservoirs until it is up-welled to the ocean surface and released back into the atmosphere. Due to the physical and biological pump, the ocean keeps the atmospheric CO_2 concentration at a constantly lower level than without these pumps (Post et al. 1990).

Functioning of the biological part of the marine carbon cycle is determined by the entire marine community. Considering this thesis topic, I will confine further explanations of the biological pump to the role of calcifying organisms. Pelagic calcifying organisms like coccolithophores, foraminifera and pteropods have two involvements. They contribute to the carbonate counter pump and potentially play a strong role in the soft tissue pump. Global marine calcification is

projected to be (further) reduced in the coming decades caused by OA (Riebesell et al. 2000). Lower global calcification would increase surface ocean CO_2 uptake capacity by weakening the carbonate counter pump, being a negative feedback to climate change (Ridgwell et al. 2007). Nevertheless, this feedback is considered to be of small magnitude, since CO_2 production from global calcification accounts for only 2% of present-day CO_2 emissions from burning of fossil fuels (Frankignoulle et al. 1994). Secondly, biogenic $CaCO_3$ (= particulate inorganic carbon 'PIC') acts as ballast for sinking material and is considered to determine deep water particulate organic carbon 'POC' flux (Armstrong et al. 2002, Klaas & Archer 2002). Further, sinking POC, which makes it to the deep sea floor and eventually is buried in the sediments, is a very long-term sink for atmospheric CO_2. This makes the likely reduction of biogenic calcification through ocean acidification a potentially strong and durable positive feedback for climate change (Riebesell et al. 2009). Additional processes considered to make the large bite of carbon export through the soft tissue pump are the production of mucus increasing POC and PIC aggregation, repacking of POC into heavier and more streamline forms like fecal pellets and the mass sedimentation of phytoplankton blooms (Turner 2002).

3.8 Crustose coralline red algae

Crustose coralline red algae (CCA) encompass over 1600 described species and intraspecific taxa of Rhodophyta (Woelkerling 1988). The common characteristic of CCA is their reddish color and their crustose growth form, often recognized as pink paint on hard substrates in the coastal surface ocean (Fig. 1a, b & e) (Nelson 2009). During the Miocene CCA outcompete any other carbonate producers (Halfar & Mutti 2005), which is manifested in several 100 m thick rhodolith facies in tropical latitudes.

Figure 1 Examples of crustose coralline algae (CCA) habitats and growth forms: a) *Hydrolithon craspedium* pillars, Southern Line Islands, photographed by Maggy Johnson; b) CCA encrusted boulder, northern Svalbard, photographed by Karen Hissmann; c) Maerl habitat, northern Scotland photographed by Jeff Meadows; d) Assemblage of rhodoliths and encrusted stones, northern Svalbard by Karen Hissmann; e) Rhodoliths sampled at northern Svalbard, by Karen Hissmann.

Species of the genus *Lithothamnion* (Melobosidae, Coralinaceae) produce unattached growth forms called rhodoliths (Fig. 1d & e) and maerl (Fig. 1c) (Foster 2001). Rhodoliths generally derive from plants which completely enveloped small stones, mollusc shells or other material and

then continued to grow around this central core, which might be lost over time, thus creating the characteristic hollow inside (Fig. 1d). Maerl stems from fragments broken off crustose portions of attached or unattached plants which continue to grow independently (Foster 2001). Rhodoliths and maerl significantly increase biodiversity through their 3-dimensional structure and facilitate settlement and recruitment for many invertebrate and vertebrate species some being of economic importance (Steller et al. 2003, Kamenos et al. 2004a, b, c). CCA engineered habitats are considered to be equally important as kelp beds and forests or sea-grass meadows (Foster 2001). In high latitudes, rhodoliths can build up large calcareous beds covering several square kilometers of the sea floor (Freiwald & Henrich 1994, Foster 2001). Comparable to subtropic and tropic CCA habitats carbonate production of subarctic CCA habitats is high, although subarctic CCA experience much slower growth rates (Freiwald 1993, Roberts et al. 2002). High carbonate production is possible due to remarkably high standing stocks (Freiwald & Henrich 1994). Global contribution of CCA to calcium carbonate production has been approximated to be 1.8×10^9 t C yr^{-1} comparable to e.g. coral reef production (Gattuso et al. 1998, van der Heijden & Kamenos 2015).

The Corallinales differ from other calcareus aquatic plants as they deposit high Mg-calcite, not aragonite (Feely et al. 2004, Guinotte & Fabry 2008, Kuffner et al. 2008). These deposits are within their cell walls (Craigie 1990). The investigated species *Lithothamnion glaciale* (Kjellman 1883) produces $CaCO_3$ with a fraction of 13 - 25 mol% $MgCO_3$ (Kamenos et al. 2008). High Mg-calcite, with a fraction of 12 - 16 mol% $MgCO_3$, appears to be about 20% more soluble than aragonite (Morse et al. 2006). Therefore, CCA are among the most sensitive calcifying organisms with respect to OA in terms of solubility. The $CaCO_3$ content varies in algal species and can total up to 80-90% of the biomass (Bilan & Usov 2001).

Due to their use of phycobilins (besides the Chl *a*) as light harvesting pigment-protein CCA (like all Rhodophyta) in general are well adapted to low photon flux densities (Woelkerling 1990). To endure the dark period in polar regions with no irradiance during winter, CCA reduce or totally stop growth in the summer months to fully concentrate on accumulation and storing of carbohydrates (Lüning 1985). Due to low temperatures and light intensities, at which polar CCA have to live, they experience slow growth and a long life span. To date, probably *Clathromorphum nereostratum* (Lebednik 1976), a CCA species found at the Aleutian Islands (Alaska), with an age of approximately 700 years might be the oldest algae reported until now (Frantz et al. 2005). Due to long life spans and global representation in fossil sediments CCA are of interest for palaeoclimate scientists. Annual and subannual calcite bands allow aligning their climate information with geological time scales. Some slow growing species allow temperature reconstruction of bi-weekly resolutions back to the Holocene (Kamenos et al. 2008).

Considering their slow growth rates and their ecosystem functioning rhodolith and maerl habitats should be considered as ecologically important and essentially non-renewable resource (Foster 2001).

3.9 Pteropods

Pteropods are a cosmopolitan group of holoplanktonic mollusks comprising the orders Thecosomata and Gymnosomata (Lalli & Gilmer 1989). The name pteropod generates from two wing like parapodia, which morphogenetically is a bilobed foot enabling the holoplanktonic lifestyle. Thecosomata, in contrast to Gymnosomata, are characterized by a permanent shell (gymnosoms have a shell during an early life stage only), swarm formation (gymnosoms are generally of low abundance) and suspension feeding via a mucus web (gymnosoms are carnivorous and active predators) (Be & Gilmer 1977, Lalli & Gilmer 1989). Thecosome pteropods are the principal pelagic producers of aragonite (Fabry 1990). While their species richness is large in tropical oceans, only two species inhabit the North Atlantic and Arctic Ocean (Be & Gilmer 1977, Perissinotto 1992, Pakhomov & Perissinotto 1997, Pakhomov et al. 1997, Froneman & Pakhomov 1998, van der Spoel & Dadon 1999, Bernard & Froneman 2002, Pakhomov & Froneman 2004). *Limacina retroversa* (Fleming 1823) is a more temperate to sub-polar species, while *Limacina helicina* (Phipps 1773) regularly occurs in the high Arctic waters (Lalli & Gilmer 1989, Hunt et al. 2008). Limaciniids have a spirally coiled shell of sinistral orientation, which is vertically stretched in *L. retroversa* (Fig. 2b) and vertically flattened in *L. helicina* (Fig. 2d), distinguishing both species (Lalli & Gilmer 1989).

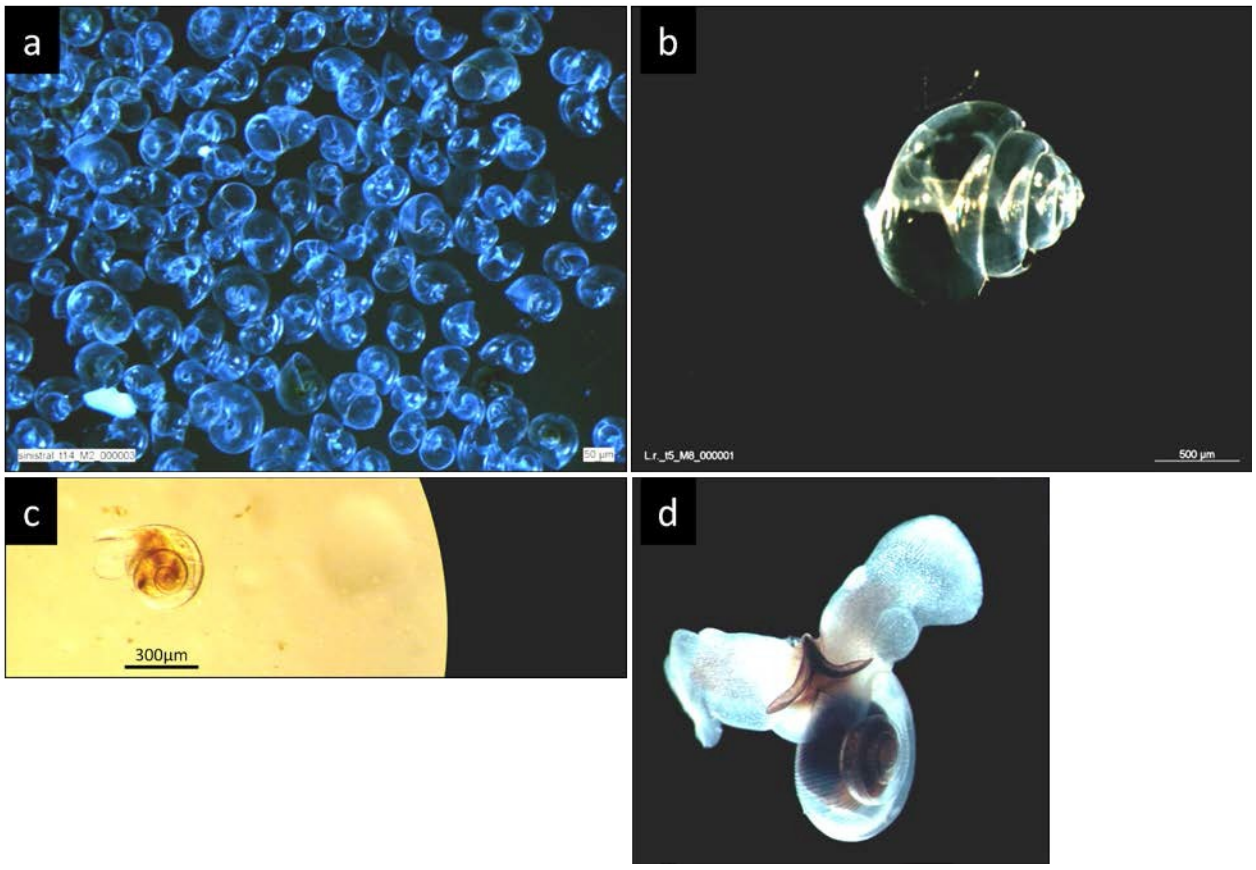

Figure 2 Examples of thecosome pteropods from the genus *Limacina*: a) cleaned shells of *L. retroversa* veliger larvae from the KOSMOS study 2011, Bergen, Norway; b) cleaned shell of an adult *L. retroversa* individual, Bergen, Norway; c) *L. retroversa* juvenile, Bergen, Norway; d) adult *L. helicina* individual photographed by Russell Hopcroft.

Thecosomes, due to their mineral shell, are negatively buoyant. It is assumed that they establish neutral buoyancy through the deployment of a mucus web several times their own size, which at the same time is their feeding device (Gilmer & Harbison 1986, Davenport & Bebbington 1990). During the 'feeding' mode the mucus web is deployed between their wings, thereby impeding any swimming movements. In the natural environment, thecosome pteropods spend most of their time motionless floating in the water column. Upon disruption they quickly release their mucus web and sink or actively swim away from their original position. To get back to the 'feeding' mode pteropods have to produce a new mucus web, which takes some time, during which they cannot swim but experience negative buoyancy and sink. Consequently, they need sufficient water column height in order to be able to produce a mucus web. In capture, neutral buoyancy is nearly never achieved, because the water column is too small to produce a mucus web and get into the feeding mode. Constant contact with boundaries like the water surface upon upward swimming or the walls of the cultivation unit upon sinking continuously interrupts the mucus web production. As a consequence, captured animals stay in an energy demanding 'escape' mode and additionally cannot feed, which limits their live time in cultivation. Recently, colleagues were able to cultivate *L. retroversa* for the first time from egg to reproduction outside the marine realm (Thabet et al. 2015).

Due to the use of a mucus web as feeding device the food size spectrum of thecosome pteropods is broad. Pico-seized particles are efficiently filtered of the water (Noji et al. 1997) but also motile organisms as big as copepods were found in limaciniid guts (Gilmer & Harbison 1991). At times swarm forming limaciniids can be the dominant zooplankton group and have major grazing pressure on phytoplankton blooms (Bathmann et al. 1991, Bednarsek, Mozina, et al. 2012, Bednarsek, Tarling, Fielding, et al. 2012).

In nature limaciniid life cycles can be annual to several years with sometimes more than one generation per year (Gannefors et al. 2005, Hunt et al. 2008, Thabet et al. 2015). After spawning eggs develop into veliger larvae over the period of a view days. Veliger larvae already have a shell and are identified by their two vela (Lebour 1932, Thabet et al. 2015). At the size of roughly 300 to 400 µm two wings start to grow (Fig. 2c) and vela disappear. Maturity is reached after ~ 3 months (Thabet et al. 2015). In polar regions *L. helicina* overwinters as lipid-rich veliger and juvenile stage at depth > 200 m (Gannefors et al. 2005).

From a food web and carbon cycle perspective thecosome pteropods are of special interest for marine scientists (Fortier et al. 1994): POC is produced by primary production and passed through the food web by consumption. On each trophic level, only about 10 % of the previous level POC is incorporated into body mass (Lindeman 1942), the remaining 90 % are respired. Therefore, the fewer trophic levels POC has to pass, the more POC will end in sinking particles or on the end-consumer level (Fortier et al. 1994). Microphage zooplankton like salps, appendicularians, doliolids and pteropods have the largest predator to prey size ratio in the marine system and therefore are of prior importance for efficient carbon channeling (Fortier et al. 1994). Pteropods make use of pico-seized plankton and particles down to 1µm and can grow themselves to sizes of centimeters putting them into the prey size spectra of end-consumers like e.g. salmon, birds and baleen whales (Lalli & Gilmer 1989, Noji et al. 1997, Armstrong et al. 2005, Hunt et al. 2008). With respect to the soft tissue pump they not only increase POC export by production of a ballasting shell, but even more importantly contribute to aggregation by heavy mucus production (Bathmann et al. 1991, Noji et al. 1997) and increase sedimentation rates by production of fast sinking fecal pellets (Yoon et al. 2001, Bernard & Froneman 2009, Manno et al. 2009).

3.10 Keystone species concept

Due to their ecological and biogeochemical relevance both organism groups, CCA and thecosome pteropods, can be considered keystone species for the Arctic marine realm.

A keystone species was originally defined as an organism with a disproportionally large effect on biodiversity or ecosystem functioning compared to its biomass (Paine 1969) e.g. like a sea otter reducing sea urchin abundance, which otherwise could totally out graze kelp forests. The kelp plant itself would not be called keystone species since its impact on the ecosystem is not disproportionally to its biomass. In an extended concept Jones et al. (1994) stated that organisms which due to their sheer existence alter resource and substrate availability and diversity for other organisms should be considered keystone species as well. "It is trite, but true, that a forest is a forest because it has trees, which also autogenically engineer the forest, climate, and modulate the flows of many other resources to forest inhabitants ..." (Jones et al. 1994). The depiction of CCA as keystone species is misleading in the original definition by Paine (1969) but truly fulfills requirements for the concept defined in Jones et al. (1994) (see 3.8). In the context of OA, thecosome pteropods can be considered Arctic calcifying keystone species since they are of major importance for efficient carbon channeling in the Arctic marine food web, significantly increase the efficiency of the Arctic soft tissue pump and are the dominant Arctic pelagic carbonate producer (see 3.9).

3.11 The Arctic Ocean at future climate scenarios

The Arctic Ocean is proposed to experience the largest changes with respect to pH, timing and volume of subsaturation and surface warming (Serreze & Francis 2006, Steinacher et al. 2009, Screen & Simmonds 2010) and thus is considered a bellwether for OA and warming impacts on the marine ecosystem (Fabry et al. 2009). With respect to ocean – climate change feedbacks, the Arctic Ocean is of significant interest. The Arctic Ocean takes up atmospheric CO_2 on the order of 66 to 199 PgC yr^{-1}, which is about 5 to 14% of the global sink and source balance (Bates & Mathis 2009). Sea ice loss and increased primary production are expected to further increase the CO_2 uptake by the Arctic surface ocean (Bates & Mathis 2009). “A future organic carbon sink of at least 1.4 x 10^9 tons C yr^{-1} might occur here” (Walsh et al. 1989).

OA effects on Arctic CCA have not been investigated so far, but tropic and temperate CCA were found to be highly OA sensitive. CCA were found to be absent in Mediterranean locations with naturally acidified seawater (Hall-Spencer et al. 2008) and in tropical species future OA conditions negatively affected the settlement and recruitment process (Kuffner et al. 2008) as well as growth and calcification rates (Jokiel et al. 2008, Anthony et al. 2008). A positive effect of increased CO_2 concentrations on calcification rates was reported for mild OA scenarios (Egilsdottir et al. 2012, Martin et al. 2013), but only under conditions where carbonate saturation states are high and CO_2 is possibly limiting algal photosynthesis (e.g. tropical waters) (Ries et al. 2009). Additionally, it was found that OA will bring increased metabolic costs for global CCA (McCoy & Ragazzola 2014). Increasing temperatures were found to amplify negative OA effects in Mediterranean and tropical CCA (Martin & Gattuso 2009, Diaz-Pulido et al. 2012). However, Arctic CCA are thought to live below their physiological temperature optimum, which can be at up to 10°C above present ambient temperatures (Adey 1970). Therefore, Arctic CCA could potentially benefit from warming waters.

Arctic pteropod mortality, shell corrosion and shell growth were shown to be affect by OA in laboratory based studies (Comeau et al. 2009, Lischka et al. 2011). In the same studies, authors reported continuous gross calcification at corrosive conditions (Comeau et al. 2009, Lischka et al. 2011). Observational studies found in-situ shell corrosion related to local subersaturated water masses (Bednarsek et al. 2012, 2014). In time series studies, however, pteropod abundances were not negatively correlated with decreasing carbonate saturation (Ohman et al. 2009, Mackas & Galbraith 2011, Beaugrand et al. 2012). Only increasing temperatures were found to correlate with a poleward movement of North Atlantic L. helicina (Beaugrand et al. 2012). Although it is not clear how thecosome pteropods will be affected by future climate change, many authors propose future Omega aragonite subsaturated oceans like the Arctic Ocean to be inhabitable for thecosome pteropods (Orr et al. 2005, Comeau et al. 2012, Bednarsek et al. 2014).

4 Publications

4.1 Thesis outline

The aim of this thesis is to improve our understanding of how OA and warming will impact Arctic calcifying keystone species and thereby add to an increased predictability of future Arctic Ocean ecosystem changes and carbon cycle feedbacks. Following this goal several publications are presented in this thesis thematically ordered by their subjects: Arctic CCA, Arctic and North Atlantic thecosome pteropods and methodological advances in pteropods science.

In chapter 4.3 I will show results of an OA experiment with Arctic CCA *Lithothamnion glaciale*, which I conducted in the laboratory of the GEOMAR. In this experiment I investigated CO_2 effects on Arctic CCA calcification rates under Arctic summer and winter conditions. In a co-authored paper the northern most Arctic benthic habitat is described, illustrating the importance of CCA (*Lithothamnion glaciale)* for the Arctic ecosystem.

In chapter 4.4 I will show results of two experiments investigating the effect of OA and warming on Arctic and North Atlantic thecosome pteropod species. I measured calcification, shell growth and size, as well as mortality in different life stages of *Limacina helicina* and *L. retroversa*. The first experiment was conducted in the marine laboratory in NyAlesund situated close to the Kongsfjord, Svalbard. The second experiment was conducted by a collaborative group of scientists in the framework of a KOSMOS study based at the Espegrend Marine Biology station, Bergen, Norway.

Experimental work with pteropods still is restricted prominent limitations; to my knowledge, the first successful long-term manipulative experiment with pteropods under controlled conditions was the mesocosm experiment we conducted in Bergen 2011. In chapter 4.5 I therefore include two co-authored papers focusing on methodological advances in this field: a recent review on pteropod culturing techniques and a description of the mesocosm design, which was used in Bergen. I also present some recent work on an optical particle counter (KielVision) hopefully improving pteropod science in mesocosms in the future.

4.2 Declaration of contribution

Publication I:
Idea: Armin Form, Jan Büdenbender
Experimental work: Jan Büdenbender, Armin Form
Analysis of data: Jan Büdenbender, Armin Form
Preparation of manuscript: Jan Büdenbender with comments from co-authors

Publication II:
Idea: Jan Büdenbender, Andre Freiwald
Experimental work: Sebastian Teichert
Analysis of data: Sebastian Teichert
Preparation of manuscript: Sebastian Teichert with comments from co-authors

Publication III:
Idea: Silke Lischka and Jan Büdenbender in equal contribution, Ulf Riebesell
Experimental work: Silke Lischka and Jan Büdenbender in equal contribution
Analysis of data: Silke Lischka and Jan Büdenbender in equal contribution
Preparation of manuscript: Silke Lischka with contributions of Jan Büdenbender and comments from co-authors

Manuscript I:
Idea: Jan Büdenbender, Ulf Riebesell
Experimental work: Jan Büdenbender, the KOSMOS Team
Analysis of data: Jan Büdenbender
Preparation of manuscript: Jan Büdenbender with comments from co-authors

Publication IV:
Idea: Ella Howes, Jean-Pierre Gattuso
Experimental work: Ella Howes and co-authors in equal contribution
Analysis of data: Ella Howes and co-authors in equal contribution
Preparation of manuscript: Ella Howes with contributions of co-authors

Publication V:
Idea: Ulf Riebesell
Experimental work: all authors in equal contribution
Analysis of data: all authors in equal contribution
Preparation of manuscript: Ulf Riebesell and Jan Czerny with comments from co-authors

Manuscript II:
Idea: Jan Büdenbender, Jan Czerny
Experimental work: Jan Büdenbender in cooperation with Develogic
Analysis of data: Jan Büdenbender
Preparation of manuscript: Jan Büdenbender with comments from co-authors

4.3 Arctic crustose coralline algae

4.3.1 Publication I

Calcification of the Arctic Coralline Red Algae *Lithothamnion glaciale* in Response to Elevated CO_2.

First-authored, published in Marine Ecology Progress Series

Vol. 441: 79–87, 2011
doi: 10.3354/meps09405

MARINE ECOLOGY PROGRESS SERIES
Mar Ecol Prog Ser

Published November 15

Calcification of the Arctic coralline red algae *Lithothamnion glaciale* in response to elevated CO_2

Jan Büdenbender*, Ulf Riebesell, Armin Form

Leibniz Institute of Marine Sciences (IFM-GEOMAR), University of Kiel, Düsternbrooker Weg 20, 24105 Kiel, Germany

ABSTRACT: Rising atmospheric CO_2 concentrations could cause a calcium carbonate subsaturation of Arctic surface waters in the next 20 yr, making these waters corrosive for calcareous organisms. It is presently unknown what effects this will have on Arctic calcifying organisms and the ecosystems of which they are integral components. So far, acidification effects on crustose coralline red algae (CCA) have only been studied in tropical and Mediterranean species. In this work, we investigated calcification rates of the CCA *Lithothamnion glaciale* collected in northwest Svalbard in laboratory experiments under future atmospheric CO_2 concentrations. The algae were exposed to simulated Arctic summer and winter light conditions in 2 separate experiments at optimum growth temperatures. We found a significant negative effect of increased CO_2 levels on the net calcification rates of *L. glaciale* in both experiments. Annual mean net dissolution of *L. glaciale* was estimated to start at an aragonite saturation state between 1.1 and 0.9 which is projected to occur in parts of the Arctic surface ocean between 2030 and 2050 if emissions follow 'business as usual' scenarios (SRES A2; IPCC 2007). The massive skeleton of CCA, which consist of more than 80% calcium carbonate, is considered crucial to withstanding natural stresses such as water movement, overgrowth or grazing. The observed strong negative response of this Arctic CCA to increased CO_2 levels suggests severe threats of the projected ocean acidification for an important habitat provider in the Arctic coastal ocean.

KEY WORDS: Calcification · CO_2 · Arctic · Coralline algae · Ocean acidification · Dissolution · *Lithothamnion*

INTRODUCTION

Crustose coralline red algae (Corallinales, Rhodophyta) are abundant and important components of benthic marine communities within the photic zone and are of global significance with respect to coastal calcium carbonate ($CaCO_3$) deposition (Nelson 2009). Their occurrence has been reported for most hard-substratum environments, from tide pools (Dethier & Steneck 2001) and shallow subtidal zones (Paine 1984) to the greatest depths (268 m) recorded for marine algae (Littler et al. 1985). Crustose coralline red algae (CCA) carbonates are important components of tropical reef structures (Adey 1998) and serve as triggers for the settlement and metamorphosis of coral larvae (Heyward & Negri 1999). Moreover, CCA are so called 'habitat modifiers' or 'bio-engineers' providing the habitat for entire benthic communities around the globe (Foster 2001, Barbera et al. 2003). The organic basis of these habitats is the unattached growth form of some CCA species, the so called rhodoliths (or maerl) (Foster 2001). In high latitudes, rhodoliths can build up large calcareous beds covering several square kilometers of the sea floor (Freiwald & Henrich 1994, Foster 2001). Rhodoliths significantly increase biodiversity through their 3-dimensional structure and facilitate settlement and recruitment for many invertebrate species, some of economic importance (Steller et al. 2003).

*Email: jbuedenbender@ifm-geomar.de

Calcification plays an important role for CCA in multiple ways. The total $CaCO_3$ content varies between algal species and can account for 80 to 90% of the biomass (Bilan & Usov 2001), making calcification an important process for organism growth and protection from grazing. For example, germination during early settlement is secured by hypobasal calcification, which cements the spores to the substrata (Walker & Moss 1984). Calcification also plays an important role in preventing overgrowth and fouling by bacteria and fleshy algae since the main defense mechanism is thought to be the sloughing off and regrowth of their outermost calcified epithelial cell layer (Littler & Littler 1999). Furthermore, calcification was hypothesized to liberate CO_2 for photosynthesis (Borowitzka 1982) and the thickness of the $CaCO_3$ layer in the cell walls was suggested to be relevant for the protection of the photosystem from ultraviolet radiation (Gao & Zheng 2010). CCA precipitate high magnesium calcite (Mg-calcite), e.g. *Lithothamnion glaciale* produces $CaCO_3$ with a fraction of 13 to 25 mol% magnesium carbonate ($MgCO_3$) (Kamenos et al. 2008). Biogenic Mg-calcite (>4 mol% $MgCO_3$; Reeder 1983), within the 'dominant composition range of 12–16 mol% $MgCO_3$', appears to be about 20% more soluble than aragonite (Morse et al. 2006, p. 5818). Therefore, CCA are among the most sensitive calcifying organisms to ocean acidification in terms of solubility. Recent work on Mg:Ca ratios of CCA showed that the Mg-fraction can decrease with increasing atmospheric CO_2 concentration, making algae less soluble at higher CO_2 concentrations (Ries 2011).

CCA seem to be highly sensitive to ocean acidification because they are found to be the first calcifying organism to disappear in areas with naturally acidified seawater (Hall-Spencer et al. 2008). Furthermore, recent studies found negative effects of ocean acidification on the settlement and recruitment process (Kuffner et al. 2008) and on growth and calcification rates of tropical CCA (Anthony et al. 2008, Jokiel et al. 2008). However, for a Mediterranean CCA species significant pCO_2 effects on net calcification rates were found only in combination with increased temperature (Martin & Gattuso 2009). A significant effect of pCO_2 alone was observed for net dissolution rates. Also a positive effect of increased CO_2 concentrations on calcification rates was reported, but only under conditions where carbonate saturation states are high and CO_2 is possibly limiting algal photosynthesis (Ries et al. 2009). The CO_2 effect became negative when aragonite saturation states were 1.7 and lower (Ries et al. 2009).

The polar oceans have a naturally low $CaCO_3$ saturation state due to low water temperatures (Fabry et al. 2009) and are therefore projected to turn corrosive for calcium carbonate earlier than other oceans (Orr et al. 2005, Steinacher et al. 2009). Decreasing sea ice cover in the Arctic ocean further accelerates the process of ocean acidification by allowing enhanced air–sea CO_2 gas exchange and increasing the freshwater input which is lowering alkalinity (Fabry et al. 2009, Steinacher et al. 2009). Annual mean aragonite subsaturation was projected as early as 2032 for the Arctic surface ocean if anthropogenic CO_2 emissions follow the IPCC (Intergovernmental Panel on Climate Change) 'business as usual' scenario (SRES A2) (Steinacher et al. 2009). Sea surface temperatures of the Arctic Ocean are expected to increase by 0.4 to 1.5°C until 2100 under this scenario (Steinacher et al. 2009).

In view of the ecological importance of CCA (Nelson 2009) and the severe threats to CCA in high latitudes (Andersson et al. 2008), we investigated the effects of ocean acidification and Arctic 'light seasons' on net calcification rates of the predominant rhodolith forming CCA *Lithothamnion glaciale* (Kjellman 1885). *Lithothamnion glaciale* is the most abundant CCA in the North Atlantic and is described from Cape Cod and the British Isles (Adey & Adey 1973) to the northern coast of Svalbard (Teichert et al. in press).

MATERIALS AND METHODS

Rhodolith specimens of *Lithothamnion glaciale* were collected during dives with the manned research submersible JAGO at 40 to 50 m depth near Cape Rubin (80° 32' 19" N, 19° 50' 40" E) on the north coast of Spitsbergen during cruise No. 2, Leg 3 of RV 'Maria S. Merian', from 31 July until 17 August 2006. Algae were stored in tanks and transferred to the Leibniz Institute of Marine Science (IFM-GEOMAR), where experiments were conducted. Rhodoliths were cultivated in aquaria with natural North Sea water with a salinity of 33 ppt at light intensities of 3 to 10 µmol photons m^{-2} s^{-1} and a temperature of 7°C for 2 yr before experiments were conducted.

For the experimental set up, rhodolith fragments of 22 ± 8 g buoyant weight were cleaned of epiphytic organisms and randomly distributed to 16 acrylglas reactors (radius = 5 cm, height = 40 cm). Four additional reactors were left empty serving as blanks in order to monitor bacterial background activity. The reactors contained 2 l of 0.2 µm filtered North Sea

water (salinity of 33) and were constantly aerated with ambient or premixed air. A water current inside the reactors was created by directing the air bubbles through an internal vertical acrylglas tube (4.5 × 25 cm), (air lift system). The water was renewed weekly to replenish nutrients and total alkalinity (A_T). Changes in nutrients and total alkalinity due to primary production, respiration, calcification and dissolution are accounted for in the calculations of the carbonate system. Premixed air at target pCO_2 levels was provided by enriching ambient air with pure CO_2 in analytical gas mixing pumps (DIGAMIX 5KA 36A/9, Wösthoff). For the summer experiment, 2 blue fluorescent lamps (Osram 36W) were installed and intensities were controlled with a quantum scalar laboratory irradiance sensor (QSL-2100). Two consecutive experiments were conducted with 2 separate sets of rhodolith fragments, where Arctic summer ('S'; 9.0 ± 0.25°C, 24 h 6.8 ± 0.2 µmol photons m^{-2} s^{-1}) and Arctic winter ('W'; 6.8 ± 0.15°C, 24 h darkness) conditions, in terms of light intensities (Table 1), were simulated at 4 pCO_2 levels of ~390, 815, 975 to 1570 ppm (Table 2). pCO_2 levels differed slightly between the summer and winter experiment (Table 2). Both experiments (S and W) were run for 4 wk encompassing 4 consecutive experimental phases (1 wk each): (1) first acclimatisation, (2) baseline, (3) second acclimatisation, and (4) treatment phase. Present day pCO_2 conditions (~390 ppm) were applied during the first acclimatisation and the baseline phase to all 16 replicates and 4 blanks, in order to measure the 'baseline' calcification for each rhodolith as a reference for changes in calcification rates in response to elevated pCO_2 levels. Elevated pCO_2 levels and a control level (Table 2) were applied during the second acclimatisation and the treatment phase each with 4 replicates and 1 blank.

Table 1. *Lithothamnion glaciale*. Culturing conditions (means ± SD; n = 20 per season)

Expt	Temperature (°C)	Light (µmol photon m^{-2} s^{-1})	Salinity
Summer	9.0 ± 0.26	6.8 ± 0.2	33 ± 0.2
Winter	6.8 ± 0.17	0	33 ± 0.2

Calcification rates and water properties (salinity, temperature, pH, total alkalinity (A_T) and inorganic nutrient concentrations) were quantified every second day during the baseline and treatment phase of each experiment (S and W). Salinity, temperature, and pH were measured with a WTW Multi 350i. The pH electrode was calibrated with certified reference material for seawater measurements (Prof. A.G. Dickson, Marine Physical Laboratory, University of California) to the total scale, precision was ±0.01 pH units. Water samples for dissolved inorganic nutrient measurements (nitrogen, NO_3, NO_2, NH_4; phosphate, PO_4; silicate, Si) were stored at 4°C and measured photometrically according to Grashoff et al. (1999). Ammonia (NH_4) was measured fluorometrically according to Holmes et al. (1999). Water samples for A_T measurements were poisoned with mercuric chloride and stored at 15°C. A_T was determined from duplicate measurements using an automatic titration device (Metrohm Titrando 808). Ten ml of the original A_T sample were 0.2 µm filtered and weighed to the nearest 0.0001g before the measurement, in order to determine the exact subsample volume. Certified reference material measurements (Prof. A.G. Dickson, Marine Physical Laboratory, University of California) were used to correct sample measurement for accuracy. Precision was within 2 µmol kg^{-1}.

Table 2. *Lithothamnion glaciale*. Summary of carbonate system parameters and nitrogen (as an example for the dissolved inorganic nutrients) from the summer and winter experiment. pH values are the means ± SD of all replicates. Each start and end value reported for total alkalinity (A_T) and nitrogen (NO_3 + NO_2) is the mean ± SD of 4 replicate water samples. Remaining parameters were calculated using CO2SYS (Seawater scale; K1, K2 from Mehrbach et al. 1973 refitted by Dickson & Millero 1987). $\Omega_{Aragonite}$ and $\Omega_{Calcite}$ refer to the saturation state of seawater with respect to calcium carbonate species

Expt	pH (total scale)	A_T (µmol kg^{-1}) Start	A_T (µmol kg^{-1}) End	NO_3 + NO_2 (µmol l^{-1}) Start	NO_3 + NO_2 (µmol l^{-1}) End	pCO_2 (ppm)	$\Omega_{Aragonite}$	$\Omega_{Calcite}$
Summer	8.06 ± 0.03	2419 ± 2	2159 ± 48	1.94 ± 0.12	0.18 ± 0.07	385 ± 26	1.99 ± 0.16	3.14 ± 0.25
	7.74 ± 0.03		2242 ± 51		0.07 ± 0.07	883 ± 49	1.06 ± 0.07	1.67 ± 0.12
	7.70 ± 0.03		2243 ± 62		0.43 ± 0.58	989 ± 57	0.96 ± 0.07	1.51 ± 0.11
	7.52 ± 0.02		2458 ± 31		0.07 ± 0.07	1573 ± 89	0.67 ± 0.03	1.06 ± 0.04
Winter	8.07 ± 0.05	2418 ± 5	2361 ± 11	1.09 ± 0.19	3.03 ± 0.70	388 ± 45	1.92 ± 0.19	3.04 ± 0.30
	7.82 ± 0.04		2453 ± 30		5.68 ± 1.46	754 ± 80	1.18 ± 0.11	1.87 ± 0.17
	7.72 ± 0.05		2450 ± 26		2.42 ± 0.45	958 ± 117	0.96 ± 0.11	1.51 ± 0.17
	7.53 ± 0.05		2601 ± 46		2.53 ± 0.65	1563 ± 187	0.65 ± 0.07	1.03 ± 0.11

A_T was calculated from the Gran function according to Dickson et al. (2003). Carbonate system parameters were calculated with the software CO2SYS (Lewis & Wallace 1998) from A_T, pH (total scale), temperature, salinity and inorganic nutrient concentrations using the constants from Mehrbach et al. (1973) refitted by Dickson & Millero (1987).

Net calcification rates (G_{net}) were calculated from the change in A_T over time (total alkalinity technique according to Smith & Key 1975). The net calcification rate is given by:

$$G_{net} = -0.5\ \rho_w V \frac{\Delta A_T}{\Delta t} \quad (1)$$

where G_{net} is the net calcification rate (µmol $CaCO_3$ d^{-1} ind.$^{-1}$), ρ_w is the seawater density (kg l^{-1}), V is the seawater volume (litres) and $\Delta A_T/\Delta t$ is the rate of change in total alkalinity per unit time (µmol kg^{-1} d^{-1} ind.$^{-1}$). The mean A_T change in the blanks of the 4 pCO_2 levels were below measuring precision and were thus not considered in the calculation of calcification rates. Normalisation of net calcification rates to a feasible standard was necessary for statistical analysis but was complicated by an irregular shape and varying weight to biomass ratio of rhodolith fragments due to varying amounts and type of inclusions, e.g. sand, stones, shells etc. Furthermore, culture organisms were slow growing, of limited availability, and needed to stay alive for further experimental purposes. For statistical analysis we calculated a relative calcification (G_{rel}) for each individual rhodolith fragment according to:

$$G_{rel} = \frac{G_{net,pH,t}}{G_{net,BL,t}} \times 100 \quad (2)$$

where G_{rel} is the relative calcification (%), $G_{net,pH,t}$ is the net calcification from the treatment phase and $G_{net,BL,t}$ is the net calcification from the baseline phase. G_{rel} is a measure for the impact of elevated pCO_2 levels on algal calcification performance: values >100% represent higher rates of calcification compared to the baseline phase, values of 100% represent equal rates of calcification as during the baseline phase, values between 0 and 100% represent reduced calcification compared to the baseline phase, and negative values represent net dissolution. We tested mean G_{rel} in a 2-way ANOVA for season (combination of light and temperature) and pCO_2 effects as well as possible interactions of these factors. Data were corrected for outliers with a modified Thompson tau test. A Fisher least significant difference (LSD) post-hoc test was applied to identify significant effects between different pCO_2 levels. The general regression of G_{rel} with respect to elevated pCO_2 levels was derived from a general linear regression analysis.

To estimate rhodolith bed $CaCO_3$ production rates, the maximum length and width of the rhodolith fragments used in experiments were measured with a measuring tape to the nearest 0.5 cm. From this, the area covered by each rhodolith fragment was calculated as a regular rectangle. $CaCO_3$ production of a square meter of rhodolith-covered sea ground was calculated from the mean of the measured areas and the calcification rates from the baseline phase. The standard deviation of the size measurements was used as error approximation for $CaCO_3$ production rates. Annual $CaCO_3$ production was calculated assuming 6 mo of summer and 6 mo of winter net calcification.

RESULTS

Light, temperature, and salinity were constant over time in the individual experiments (summer and winter) (Table 1), whereas dissolved nitrogen (NO_3 + NO_2) concentrations and A_T followed the biological processes of production and remineralisation and net calcification or net dissolution, respectively (Table 2). Dissolved phosphate (PO_4) concentration was 0.08 ± 0.03 µmol l^{-1} (mean ± SD of both experiments) and did not change significantly between the start and end of incubations or between treatments. Estimated annual $CaCO_3$ production per square meter of covered sea ground (mean ± SD) for *Lithothamnion glaciale* was 313.5 ± 78.4 g $CaCO_3$ m^{-2} yr^{-1}.

Net calcification rates (G_{net}) of *Lithothamnion glaciale* under present day pCO_2 conditions (390 ppm) were about 113% higher during the summer compared to the winter experiment (Fig. 1). With respect to time, G_{net} of algae in the 390 ppm pCO_2 treatment in the summer experiment increased from the baseline to the treatment phase, while it decreased during the winter experiment (Fig. 1). G_{net} values in both experiments (summer and winter) differed clearly between pCO_2 levels during the treatment phase, while they were similar during the baseline phase (Fig. 1). In the summer experiment (Fig. 1a), G_{net} of algae in the 1570 ppm pCO_2 treatment turned negative during the treatment phase, whereas algae in the 815 and 975 ppm pCO_2 treatments maintained G_{net} as high as during the baseline phase. In the winter experiment (Fig. 1b), G_{net} decreased in all pCO_2 treatments. The strongest decrease with a net dissolution during the treatment phase of twice the net cal-

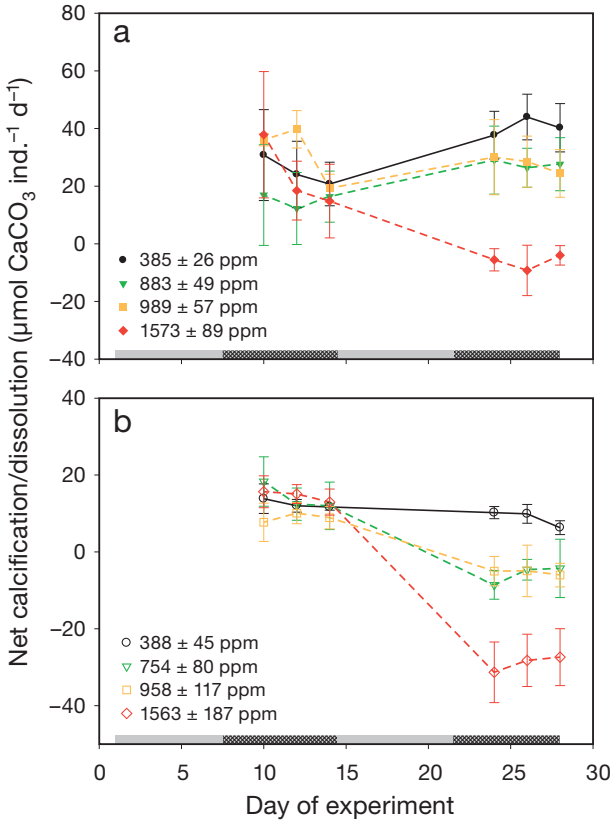

Fig. 1. *Lithothamnion glaciale*. Daily net calcification/dissolution rates from the (a) summer and (b) winter experiments. Data points are means ± SD of 4 replicates. The grey bars on the *x*-axis indicate acclimatisation (no pattern) and sampling phases (with pattern). From Days 1 to 14 all rhodoliths were exposed to the same pCO_2 level of ~390 ppm (baseline) and from Days 14 to 28, 3 sets of 4 rhodoliths were kept under elevated pCO_2 levels, as indicated

cification during the baseline phase was observed in the 1570 ppm pCO_2 treatment. A lower net dissolution occurred in the 815 and 975 ppm pCO_2 treatments, whereas algae kept at 390 ppm pCO_2 also had decreased net calcification rates during the treatment phase but experienced no net dissolution.

As G_{net} per individual was not a statistically meaningful normalisation, relative calcification (G_{rel}) was used in the statistical analysis. A 2-way ANOVA revealed a highly significant effect of pCO_2 and season on G_{rel} ($p < 0.001$) and no significant interaction between both factors ($p = 0.605$) (Table 3). Furthermore, post hoc tests (Fisher's LSD) revealed significant and highly significant differences between individual pCO_2 treatments (Table 3). G_{rel} was negatively affected by increasing CO_2 concentrations and the interpolated threshold pCO_2 for net dissolution was ~776 ppm lower in the winter compared to the summer experiment (Fig. 2). G_{rel} in the summer experiment still stayed above 100% in the 815 ppm pCO_2 treatment due to the fact that G_{net} was higher in the treatment phase than during the baseline phase. Reduced calcification relative to the baseline calcification ($G_{rel} < 100\%$) was observed in the 975 and 1570 ppm pCO_2 treatments. Linear interpolation yields a pCO_2 level of ~1430 ppm above which net dissolution ($G_{rel} < 0\%$) occurs. G_{rel} in the winter experiment was already decreased (<100%) at 390 ppm and turned to net dissolution (<0%) at a pCO_2 value of 654 ppm based on linear interpolation. The linear regression model revealed a high proportion of variation in calcification rates accounted for by pCO_2 in both experiments ($R^2 = 0.977$ and 0.997 for the summer and winter experiment, respectively).

Annual mean relative calcification (Fig. 2) was based on 2 assumptions: first, summer and winter calcification contributed equally to the annual mean, and second, calcification in the 390 ppm pCO_2 treatment represents acclimatised calcification rates. Accordingly the annual mean relative calcification estimated for the 390 ppm pCO_2 level is set to 100%.

G_{rel} of *Lithothamnion glaciale*, as a function of $CaCO_3$ saturation states for calcite ($\Omega_{Calcite}$) and aragonite ($\Omega_{Aragonite}$), is depicted in Fig. 3. In the present day pCO_2 level (390 ppm), water was always supersaturated with respect to $\Omega_{Calcite}$ and $\Omega_{Aragonite}$. In the summer experiment, net calcification occurred at $\Omega_{Aragonite}$ as low as 0.96. Net dissolution was first experienced by the algae when $\Omega_{Calcite}$ was approximately 1 and $\Omega_{Aragonite}$ was at 0.67. In the winter experiment, net dissolution already occurred at $\Omega_{Aragonite}$ of 1.18. Observed responses in G_{rel} were correlated to projected future changes in seawater carbonate chemistry, as reported by Steinacher et al. (2009) (SRES A2 Scenario, IPCC 2007) (Fig. 4). Steinacher et al. (2009)

Table 3. *Lithothamnion glaciale*. Results of 2-way ANOVA performed to test the effect of pCO_2 and season on algal relative calcification rates. p-values < 0.01 indicate highly significant results. For multiple comparison results (Fisher's LSD test) for the factor pCO_2, significant differences are in **bold**, 0 indicates $p < 0.001$. (1) to (4) indicate pCO_2 treatment: (1) 390 ppm; (2) 815 ppm; (3) 975 ppm; (4) 1570 ppm; df: degrees of freedom

Source of variation	df	*F*	p		LSD test (pCO_2) (1)	(2)	(3)
pCO_2	3	32.66	0.000	(2)	**0.012**	–	–
Season	1	63.24	0.000	(3)	**0**	0.098	–
pCO_2 × Season	3	0.63	0.605	(4)	**0**	**0**	**0**

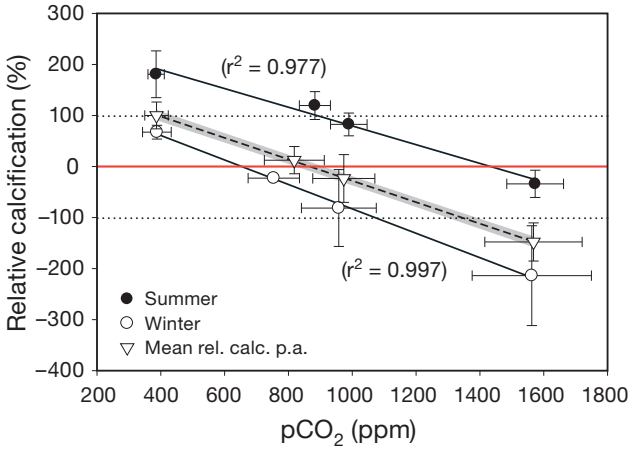

Fig. 2. *Lithothamnion glaciale*. Relative calcification as a function of pCO_2 levels from the summer and winter experiment. Data points are means ± SD of the 3 sampling days (see Fig. 1) for each of the 4 treatments. The linear regression analysis (black solid lines) shows trends of calcification with increasing pCO_2 levels for the summer and winter experiment. The upper and lower black dotted horizontal lines represent a relative calcification of 100% and −100% with respect to net calcification rates of the baseline phase (Fig. 1). The red horizontal line indicates zero growth. The black dashed line is the regression for the annual mean relative calcification calculated from the combination of summer and winter data. Annual mean relative calcification of the 390 ppm pCO_2 level was set to 100% by definition. The grey area fills the space between the upper and lower 95% prediction bands

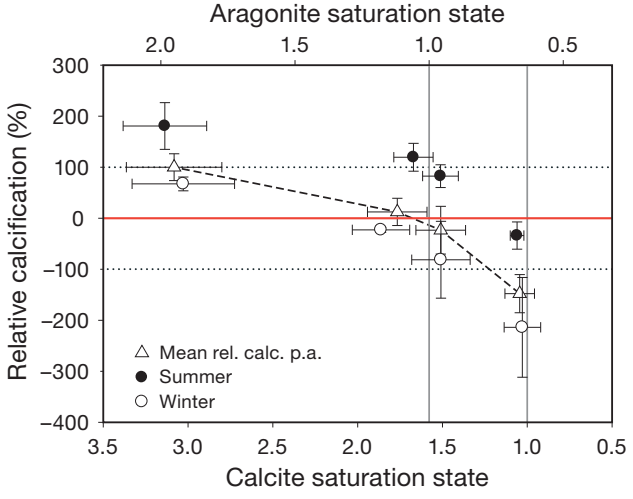

Fig. 3. *Lithothamnion glaciale*. Relative calcification ± SD as a function of calcium carbonate saturation states; the 4 data points of each set represent the 4 pCO_2 levels (compare with Fig. 2). Grey vertical lines separate supersaturated from subsaturated conditions for the calcium carbonate mineral phases aragonite and calcite. Black dotted horizontal lines represent relative calcification levels of 100% and −100% with respect to net calcification rates of the baseline phase (see Fig. 1). The red horizontal line indicates zero growth

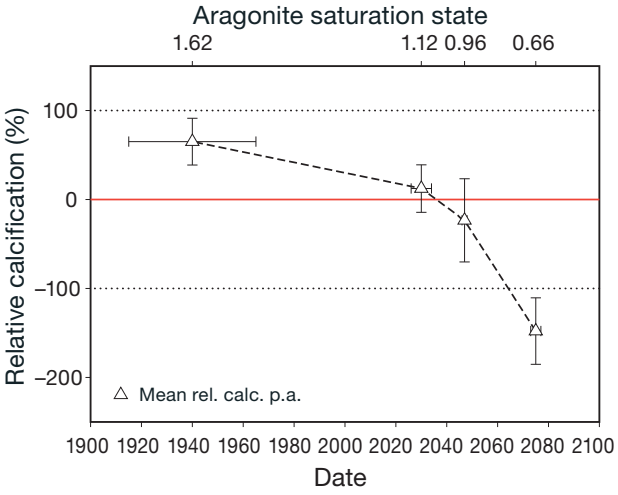

Fig. 4. *Lithothamnion glaciale*. Projected future annual mean relative calcification in the Arctic. Data points are the mean ± SD annual relative calcification rates, which were correlated to projected changes in the aragonite saturation state for the Arctic surface ocean according to Steinacher et al. (2009) and based on a 'business as usual' emission scenario (SRES A2; IPCC 2007). The error in time reflects the variability in the saturation states during the experiment (due to calcification or dissolution processes) translated to years according to the model. The upper *x*-axis gives corresponding aragonite saturation states

projected an annual mean subsaturation for $\Omega_{Aragonite}$ in the Arctic surface ocean by 2032. If we compare their calculations of past and future annual mean $\Omega_{Aragonite}$ levels in the surface ocean surrounding Svalbard (24 grid points) with the levels in our experiments, present annual mean net calcification of *L. glaciale* is already reduced by 40% compared to preindustrial conditions. Annual mean net dissolution could start by 2035 (±5 yr) (Fig. 4).

DISCUSSION

Our results indicate that increasing atmospheric CO_2 partial pressure causes reduced calcification to net dissolution in a key organism of the Arctic coastal ecosystem. The habitat-providing coralline algae *Lithothamnion glaciale* could experience annual mean net dissolution in the Arctic in 20 to 40 yr from today if CO_2 emissions follow a 'business as usual' scenario (SRES A2; IPCC 2007).

Light and temperature levels during the cultivation were chosen to provide optimum growth conditions (Adey 1970) in order to ensure successful long-term cultivation in the laboratory. Algae used in this study were maintained for 2 yr in culture before experiments were conducted. Adey (1970) reported accli-

matisation periods of several months for a temperature increase of 5°C. Temperatures of 6.8 and 9.0°C for the winter and summer experiment, respectively, were higher than observed *in situ* water temperatures of −1 to 4°C (J. Büdenbender unpubl. data) but were close to the range of temperatures reported to yield maximum growth rates (8 to 13°C; Adey 1970). Light intensities of 6.8 µmol photons m^{-2} s^{-1} simulated in the summer experiment were generally at the upper limit of measured *in situ* irradiance levels (Teichert et al. in press). To statistically distinguish between pCO_2 and season effects, our data were analysed in a 2-way ANOVA with pCO_2 and season as factors. As shown in the results, pCO_2 and season affected calcification rates but did not interact with each other. This allows us to discuss future pCO_2 effects separately from seasonal effects.

Elevated pCO_2 levels resulted in decreased net calcification rates. We found a negative linear correlation between pCO_2 and algal net calcification rates for the range of pCO_2 levels tested (Fig. 2). Additionally, we found an offset in pCO_2 of ~776 ppm for interpolated net dissolution between winter and summer experiment (Fig. 2). Possible reasons could be lower carbonate saturation due to higher CO_2 dissolution in colder water (which was not detectable in our experiment) and a lowering of the critical threshold pCO_2 for net dissolution due to lower temperature and/or absence of photosynthetic activity. Whatever the reasons are, net dissolution can be expected to occur first during the Arctic winter period.

Interestingly, algae in the summer experiment were able to increase (815 ppm) or maintain (975 ppm) their net calcification rates during the experimental period under elevated pCO_2 levels (Fig. 2). We attribute the increase or maintenance of net calcification rates in the 390, 815, and 975 ppm treatments in the summer experiment to an acclimatisation to the higher temperature compared to prior long-term cultivation conditions (+2°C). An additional reason could be carbon limitation of photosynthesis (Bowes 1993), possibly leading to CO_2 fertilisation at elevated CO_2 concentrations in our experiments.

As already mentioned, CCA precipitate high Mg-calcite, therefore the solubility is expected to be similar or higher than for aragonite. We calculated an aragonite saturation of 0.96 for the 975 ppm pCO_2 level in the summer experiment. Hence, algae were able to maintain net calcification in subsaturated conditions (Fig. 3). In contrast, previous studies found net dissolution in water supersaturated with respect to aragonite (Anthony et al. 2008, Martin & Gattuso 2009). However, this was attributed to bioerosion in addition to physiochemical erosion by Martin & Gattuso (2009) or to subsaturated conditions with respect to high Mg-calcite by Anthony et al. (2008). In the case of *Lithothamnion glaciale*, net calcification in subsaturated conditions could have been due to enhanced growth rates associated with still ongoing acclimatisation to a temperature higher than during the prior cultivation. Martin & Gattuso (2009) showed that algae living at lower than optimum temperatures are able to benefit from increasing temperatures with respect to growth rates. Since temperatures in our experiments were higher than projected for the Arctic ocean by the end of this century (Steinacher et al. 2009), effects of elevated pCO_2 levels on net calcification rates for *L. glaciale* are likely underestimated. Despite the apparent discrepancies, all previous studies reported possible net dissolution of CCA for 'business as usual' CO_2 emission until the end of this century (Anthony et al. 2008, Jokiel et al. 2008, Martin & Gattuso 2009, present study).

Acclimatisation to elevated pCO_2 was proposed and discussed by Martin & Gattuso (2009), who found a significant pCO_2 effect on net growth rates only for the first month of their experiment but not for the following 11 mo. The authors proposed a possible acclimatisation of algal growth rates to increasing CO_2 partial pressures but also mentioned that a simultaneous increase in net dissolution likely outbalances this effect. If acclimatisation of calcification rates is possible in Arctic CCA, an outbalancing of this positive effect by a simultaneously increasing dissolution rate is even more likely, because Arctic CCA will face subsaturated conditions much earlier than Mediterranean CCA (Steinacher et al. 2009). A second aspect is the possible modification of the skeletal Mg:Ca ratio and therefore skeletal solubility in response to increasing pCO_2 levels (Ries 2011). The observed change in skeletal Mg:Ca ratio would cause subsaturation for CCA carbonates to start at ~1900 ppm instead of ~1700 ppm pCO_2 at conditions as applied in Ries (2011). In summary, increasing temperature and/or changing Mg:Ca ratios have the potential to promote calcification or reduce dissolution in arctic CCA and thereby compensate for CO_2 stress to some extent.

The annual $CaCO_3$ production rate of *Lithothamnion glaciale* reported here is the first calcification rate reported from a CCA species collected in the high Arctic. Compared to CCA from other geographic regions *L. glaciale* has a production rate lower than a temperate species (Martin et al. 2006) and considerably lower than tropical species (Chisholm 2000) (Table 4). Hence, there could be a gen-

Table 4. $CaCO_3$ production rates of coralline red algae from 3 geographic zones. Annual production rates are estimations from measured calcification rates of isolated algae

Geographical zone	Species	Annual calcification (g $CaCO_3$ m^{-2} yr^{-1})	Source
Tropical	*Hydrolithon onkodes, H. reinboldii, Neogoniolithon brassica-florida, N. conicum*	1500–10 300	Chisholm (2000)
Temperate	*Lithothamnion coralloides*	300–3000	Martin et al. (2006)
Polar	*Lithothamnion glaciale*	235–391	Present study

eral trend of decreasing calcification rates with increasing latitude probably due to decreasing temperature and light availability. Because $CaCO_3$ production rates in this study were obtained for isolated algae and not for *in situ* communities, we only used data for isolated algae in the comparison shown in Table 4.

A characteristic feature of rhodoliths and an important aspect of the unique habitat they are providing is their irregular 3-dimensional structure. This growth form would not exist without a massive skeleton made of calcium carbonate. Based on the data shown in Fig. 4, *Lithothamnion glaciale* could experience annual mean net dissolution in the Arctic in 20 to 40 yr from today under 'business as usual' CO_2 emissions. Effects on the recruitment processes of *L. glaciale* have not been investigated yet. However, the early survival of spores, where calcification plays a vital role for settlement and further growth, was shown to be highly susceptible for ocean acidification effects in tropical CCA (Jokiel et al. 2008). Hence, our observations indicate severe consequences for the future survival of *L. glaciale* in the Arctic ecosystem due to increasing atmospheric CO_2 concentrations. Moreover, if the observed responses are representative for Arctic CCA in general, our data imply that rhodolith beds, which provide the habitat for diverse benthic communities in the Arctic ecosystem, could shrink or possibly disappear during this century under 'business as usual' CO_2 emission, potentially affecting Arctic food webs. Similar projections can be made for tropical and Mediterranean CCA (Anthony et al. 2008, Jokiel et al. 2008, Martin & Gattuso 2009), suggesting a global reduction of CCA in the coming decades in the case of unabated CO_2 emissions.

Acknowledgements. We thank J. Büscher, M. Meyerhöfer, P. Fritsche, A. Ludwig and the IFM-GEOMAR aquarium team for assistance in the laboratory and with logistics; and A. Freiwald for algae samples. We are grateful to M. Steinacher and A. Oschlies for their help with model data and general help on climate models. Special thanks go to M. Lenz and K. Schulz for their advice during the data processing and for general advice. This work was financially supported by the coordinated project BIOACID (Biological Impacts of Ocean Acidification) of the German Ministry for Education and Research (BMBF).

LITERATURE CITED

Adey WH (1970) The effects of light and temperature on growth rates in boreal-Subarctic crustose corallines. J Phycol 6:269–276

Adey WH (1998) Review — Coral reefs: algal structured and mediated ecosystems in shallow, turbulent, alkaline waters. J Phycol 34:393–406

Adey WH, Adey PJ (1973) Studies on the biosystematics and ecology of the epilithic crustose Corallinaceae of the British Isles. Br Phycol J 8:343–407

Andersson AJ, Mackenzie FT, Bates NR (2008) Life on the margin: implications of ocean acidification on Mg-calcite, high latitude and cold-water marine calcifiers. Mar Ecol Prog Ser 373:265–273

Anthony KRN, Kline DI, Diaz-Pulido G, Dove S, Hoegh-Guldberg O (2008) Ocean acidification causes bleaching and productivity loss in coral reef builders. Proc Natl Acad Sci USA 105:17442–17446

Barbera C, Bordehore C, Borg JA, Glémarec M, and others (2003) Conservation and management of northeast Atlantic and Mediterranean maerl beds. Aquat Conserv 13:S65–S76

Bilan MI, Usov AI (2001) Polysaccharides of calcareous algae and their effect on the calcification process. Russ J Bioorganic Chem 27:2–16

Borowitzka MA (1982) Mechanisms in algal calcification. Prog Phycol Res 1:137–177

Bowes G (1993) Facing the inevitable: plants and increasing atmospheric CO_2. Annu Rev Plant Physiol 44:309–332

Chisholm JRM (2000) Calcification by crustose coralline algae on the northern Great Barrier Reef, Australia. Limnol Oceanogr 45:1476–1484

Dethier MN, Steneck RS (2001) Growth and persistence of diverse intertidal crusts: Survival of the slow in a fast-paced world. Mar Ecol Prog Ser 223:89–100

Dickson AG, Millero FJ (1987) A comparison of the equilibrium constants for the dissociation of carbonic acid in seawater media. Deep-Sea Res A 34:1733–1743

Dickson AG, Afghan JD, Anderson GC (2003) Reference materials for oceanic CO_2 analysis: A method for the certification of total alkalinity. Mar Chem 80:185–197

Fabry VJ, McClintock JB, Mathis JT, Grebmeier JM (2009) Ocean Acidification at high latitudes: the bellweather. Oceanography 22:160–171

Foster MS (2001) Rhodoliths: Between rocks and soft places. J Phycol 37:659–667

Freiwald A, Henrich R (1994) Reefal coralline algal build-ups within the Arctic Circle: morphology and sedimentary dynamics under extreme environmental seasonality. Sedimentology 41:963–984

Gao K, Zheng Y (2010) Combined effects of ocean acidification and solar UV radiation on photosynthesis, growth, pigmentation and calcification of the coralline alga *Corallina sessilis* (Rhodophyta). Glob Change Biol 16:2388–2398

Grashoff K, Kremling K, Ehrhard M (1999) Methods of seawater analysis, 3rd edn. Wiley–VCH, Weinheim

Hall-Spencer JM, Rodolfo-Metalpa R, Martin S, Ransome E, and others (2008) Volcanic carbon dioxide vents show ecosystem effects of ocean acidification. Nature 454:96–99

Heyward AJ, Negri AP (1999) Natural inducers for coral larval metamorphosis. Coral Reefs 18:273–279

Holmes RM, Aminot A, Kérouel R, Hooker BA, Peterson BJ (1999) A simple and precise method for measuring ammonium in marine and freshwater ecosystems. Can J Fish Aquat Sci 56:1801–1808

IPCC (2007) The Physical Science Basis. Contribution of Working Group I to the Fourth Assessment Report of the Intergovernmental Panel on Climate Change. Cambridge University Press, Cambridge

Jokiel PL, Rodgers KS, Kuffner IB, Andersson AJ, Cox EF, Mackenzie FT (2008) Ocean acidification and calcifying reef organisms: a mesocosm investigation. Coral Reefs 27:473–483

Kamenos NA, Cusack M, Moore PG (2008) Coralline algae are global palaeothermometers with bi-weekly resolution. Geochim Cosmochim Acta 72:771–779

Kjellman FR (1885) The algae of the Arctic Sea. K Sv Vet-Akad Handl 20:1–350

Kuffner IB, Andersson AJ, Jokiel PL, Rodgers Ku S, Mackenzie FT (2008) Decreased abundance of crustose coralline algae due to ocean acidification. Nat Geosci 1:114–117

Lewis E, Wallace DWR (1998) Program developed for CO_2 system calculations. Carbon Dioxide Information Analysis Center, Oak Ridge National Laboratory, US Department of Energy, Oak Ridge, TN

Littler MM, Littler DS (1999) Epithallus sloughing: A self-cleaning mechanism for coralline algae. Coral Reefs 18: 204

Littler MM, Littler DS, Blair SM, Norris JN (1985) Deepest known plant life discovered on an uncharted seamount. Science 227:57–59

Martin S, Gattuso JP (2009) Response of Mediterranean coralline algae to ocean acidification and elevated temperature. Glob Change Biol 15:2089–2100

Martin S, Castets MD, Clavier J (2006) Primary production, respiration and calcification of the temperate free-living coralline alga *Lithothamnion corallioides.* Aquat Bot 85: 121–128

Mehrbach C, Culberson CH, Hawley JE, Pytkowicz RM (1973) Measurement of the apparent dissociation constants of carbonic acid in seawater at atmospheric pressure. Limnol Oceanogr 18:897–907

Morse JW, Andersson AJ, Mackenzie FT (2006) Initial responses of carbonate-rich shelf sediments to rising atmospheric pCO_2 and 'ocean acidification': role of high Mg-calcites. Geochim Cosmochim Acta 70:5814–5830

Nelson WA (2009) Calcified macroalgae — critical to coastal ecosystems and vulnerable to change: a review. Mar Freshw Res 60:787–801

Orr JC, Fabry VJ, Aumont O, Bopp L and others (2005) Anthropogenic ocean acidification over the twenty-first century and its impact on calcifying organisms. Nature 437:681–686

Paine RT (1984) Ecological determinism in the competition for space: the Robert H. MacArthur award lecture. Ecology 65:1339–1348

Reeder RJ (1983) Crystal chemistry of the rhombohedral carbonates. Rev Mineral Geochem 11:1–47

Ries JB (2011) Skeletal mineralogy in a high-CO_2 world. J Exp Mar Biol Ecol 403:54–64

Ries JB, Cohen AL, McCorkle DC (2009) Marine calcifiers exhibit mixed responses to CO_2-induced ocean acidification. Geology 37:1131–1134

Smith SV, Key GS (1975) Carbon dioxide and metabolism in marine environments. Limnol Oceanogr 20:493–495

Steinacher M, Joos F, Frölicher TL, Plattner GK, Doney SC (2009) Imminent ocean acidification in the Arctic projected with the NCAR global coupled carbon cycle-climate model. Biogeosciences 6:515–533

Steller DL, Riosmena-Rodríguez R, Foster MS, Roberts CA (2003) Rhodolith bed diversity in the Gulf of California: the importance of rhodolith structure and consequences of disturbance. Aquat Conserv 13:S5–S20

Teichert S, Woelkerling W, Rüggeberg A, Wisshak M and others (in press) Rhodolith beds (Corallinales, Rhodophyta) and their physical and biological environment at 80°31'N in Nordkappbukta (Nordaustlandet, Svalbard Archipelago, Norway). Phycologia

Walker R, Moss B (1984) Mode of attachment of six epilithic crustose Corallinaceae (Rhodophyta). Phycologia 23:321–329

Editorial responsibility: Gretchen Hofmann, Santa Barbara, California, USA

Submitted: March 18, 2011; Accepted: September 20, 2011
Proofs received from author(s): November 7, 2011

4.3.2 Publication II

Rhodolith Beds (Corallinales, Rhodophyta) and Their Physical and Biological Environment at 80°31′N in Nordkappbukta (Nordaustlandet, Svalbard Archipelago, Norway)

Co-authored, published in Phycologia

Phycologia (2012) Volume 51 (4), 371–390 Published 5 July 2012

Rhodolith beds (Corallinales, Rhodophyta) and their physical and biological environment at 80°31′N in Nordkappbukta (Nordaustlandet, Svalbard Archipelago, Norway)

Sebastian Teichert[1]*, William Woelkerling[2], Andres Rüggeberg[3], Max Wisshak[1], Dieter Piepenburg[4], Michael Meyerhöfer[5], Armin Form[5], Jan Büdenbender[5] and André Freiwald[1,6]

[1]*Senckenberg am Meer, Abteilung Meeresforschung, Südstrand 40, D-26282 Wilhelmshaven, Germany*
[2]*La Trobe University, Department of Botany, Kingsbury Drive, AUS-3086 Bundoora, Victoria, Australia*
[3]*Renard Centre of Marine Geology, Gent University, Krijgslaan 281–S8, B-9000 Gent, Belgium*
[4]*Akademie der Wissenschaften und der Literatur Mainz, c/o Institut für Polarökologie, Universität Kiel, Wischhofstraße 1–3, D-24148 Kiel, Germany*
[5]*Helmholtz-Zentrum für Ozeanforschung Kiel (GEOMAR), Düsternbrooker Weg 20, D-24105 Kiel, Germany*
[6]*MARUM, Zentrum für Marine Umweltwissenschaften, Leobener Straße 2, D-28359 Bremen, Germany*

Teichert S., Woelkerling W., Rüggeberg A., Wisshak M., Piepenburg D., Meyerhöfer M., Form A., Büdenbender J. and Freiwald A. 2012. Rhodolith beds (Corallinales, Rhodophyta) and their physical and biological environment at 80°31′N in Nordkappbukta (Nordaustlandet, Svalbard Archipelago, Norway). *Phycologia* 51: 371–390. DOI: 10.2216/11-76.1

Polar coralline red algae (Corallinales, Rhodophyta) that form rhodoliths have received little attention concerning their potential as ecosystem engineers and carbonate factories; although, recent findings revealed that they are much more widespread in polar waters than previously thought. The present study deals with the northernmost rhodolith communities currently known, discovered in 2006 at 80°31′N in Nordkappbukta (North Cape Bay) at Nordaustlandet, Svalbard. These perennial coralline algae must be adapted to extreme seasonality in terms of light regime (*c.* 4 months winter darkness), sea ice coverage, nutrient supply, turbidity of the water column, temperature and salinity. The rhodolith communities and their environment were investigated using multibeam swath bathymetry, CTD measurements, recordings of the photosynthetic active radiation (PAR) and determination of the water chemistry, seabed imaging and targeted sampling by means of the manned submersible JAGO as well as benthic collections with a dredge. The coralline flora was composed mainly of *Lithothamnion glaciale*, with a lesser amount of *Phymatolithon tenue*. Based on their distribution and development at different depth levels, a facies model was developed. Rhodoliths occurred between 30 and 51 m, while coralline algae attached to cobbles were present as deep as 78 m. Measurements of the PAR indicated their adaptation to extreme low light levels. Ambient waters were always saturated with reference to calcite and aragonite for the whole area. The rhodolith-associated macrobenthic fauna samples yielded 59 species, only one of which was typically Arctic, and the concomitant appearance of corallines and grazers kept the corallines free from epiphytes and coequally provided feeding grounds for the grazers. Overall, *L. glaciale* and *P. tenue* appeared to be well adapted to the extreme environment of the Arctic.

Key Words: *Lithothamnion glaciale*, Nordkappbukta, *Phymatolithon tenue*, Polar carbonate factory, Rhodolith community, Svalbard

INTRODUCTION

In polar regions, major physical oceanographic, chemical and biological parameters are affected by the strong seasonality in solar radiation. At 80° northern latitude, the polar night lasts for *c.* 4 months, and the annual solar radiation is 30–50% less than in temperate to tropical regions (Lüning 1990). This dark period is prolonged by sea ice covered by snow for several additional months. Multiyear sea ice can scour the seabed down to depths of 40 m (Gutt 2001). After the melting of the sea ice in coastal waters, the development of phytoplankton blooms and the inflow of turbid meltwater also affect the light transmission in the water column. Therefore, even under full-illuminated conditions during the polar summer, low irradiances often prevail (Wiencke *et al.* 2007). Under calm weather conditions, the meltwater generates a freshwater surface layer. At times when this stratification is disturbed by storms, the mixing of freshwater affects the upper 20-m water depth (Hanelt *et al.* 2001). Furthermore, biolimited macronutrients, such as nitrogen and phosphorus, follow a pronounced seasonal fluctuation. In Svalbard waters, macronutrients are abundant during the winter months but become rapidly depleted along with the development of the short-lived phytoplankton blooms in summer (Aguilera *et al.* 2002). All these environmental fluctuations led to the evolution of specific life strategies and ecophysiological adaptations amongst perennial polar algae to cope not only with low temperatures but also with depletion or absence of light and nutrients (see review in Wiencke *et al.* 2007). This study focuses on the environment of the northernmost known coralline algal rhodolith bed off the northern coast of Nordaustlandet, Svalbard, Norway.

* Corresponding author (sebastian.teichert@senckenberg.de).

Rhodoliths are free-living structures composed mostly (> 50%) of nongeniculate (i.e. lacking uncalcified joints) coralline red algae (Rhodophyta; Foster 2001). They are abundant from tropical to polar latitudes and from the lower intertidal zone to water depths of 150 m, where they provide a habitat for numerous animals and plants. Foster (2001) described rhodolith beds as one of the 'big four' benthic communities dominated by macrophytes in terms of area covered, ranking alongside kelp beds and forests, seagrass meadows and nongeniculate coralline reefs. Coralline algae are well adapted to a variety of environmental disturbances and hence are slow growing and probably long lived (Foster 2001). Many exhibit distinct banding patterns (Freiwald & Henrich 1994; Freiwald 1998; Foster 2001) and were successfully used in studies on climatic conditions (Kamenos *et al.* 2007; Halfar *et al.* 2008, 2010, 2011; Kamenos & Law 2010).

North of the Arctic Circle (66°33.73′N), rhodoliths have been reported to occur off Devon Island northern Canada (*c.* 75°N), northern mainland Norway (*c.* 70°N), Spitsbergen (Svalbard; including Treurenberg Bay, 79°56′N; see Kjellman 1883, 1885) and Novaya Zemlya (Russia; *c.* 75°N; see Kjellman 1883, 1885; maps in Bosence 1983b; Foster 2001). South of the Arctic Circle but still under Arctic climatic conditions, rhodolith beds are known from Herring Bay, Prince William Sound, Alaska (*c.* 60°N; Konar *et al.* 2006), and from Belle Isle Strait, Newfoundland (Halfar *et al.* 2000). Information on the environmental conditions of these high-latitude rhodolith beds are provided by Freiwald (1998) and Freiwald & Henrich (1994) for the northern Norwegian region and by Konar *et al.* (2006) for the Alaskan area. Examples for other well-investigated rhodolith beds at lower latitudes are the Sound of Arizaig, Scotland (*c.* 57°N; Davies & Hall-Spencer 1996); the Ryukyu Islands, Japan (*c.* 27°N; Matsuda & Iryu 2011), the southwestern Gulf of California, Mexico (*c.* 24°N; Hetzinger *et al.* 2006); the Gulf of Panama and the Gulf of Chiriquí, Panama (*c.* 8°N; Fortunato & Schäfer 2009; Schäfer *et al.* 2011); the coast of the State of Paraíba, Brazil (*c.* 7°S; Riul *et al.* 2004), Inhaca Island, Mozambique (*c.* 26°S; Perry 2005); and Arvoredo Island, Brazil (*c.* 27°S; Gherardi 2004).

In 2006, during the MSM 02/03 cruise of RV *Maria S. Merian*, the northernmost rhodolith communities currently known were discovered at 80°31′N in Nordkappbukta (North Cape Bay) off Nordaustlandet Island, Svalbard, Norway. The sites were intensively documented and sampled, thus providing an opportunity to determine the biological composition of and interactions within these rhodolith communities and to elucidate the physical and chemical conditions under which these apparently thriving communities were growing. This study of currently living rhodolith communities provides a basis for interpreting the geography, climatology and ecology associated with fossil rhodolith communities.

The study site is located on the Svalbard archipelago, which is situated about halfway between the Norwegian mainland and the North Pole and includes all islands in the region between 74°–81°N and 10°–35°E. Nordkappbukta (North Cape Bay; 80°31′N, 19°52′E; Figs 1–3), the focus of the present study, is located at the northern tip of the Laponiahalvøya, Nordaustlandet, and features the Early Neoproterozoic Laponiafjellet Granite (Harland 1997). Beverlysundet (Beverly Sound) extends 4.8 km SSE, separating the Nordaustlandet mainland from a disembarkation area around Nordkapp.

Nordkappbukta is currently the most northern known locality where well-developed coralline red algal rhodolith communities occur. The area is regularly exposed to sea ice formation for several months during winter, but ice cover often lasts into the summer, occurring mostly as open drift ice (Falk-Petersen *et al.* 2000; Spreen *et al.* 2008). The prevailing Arctic Ocean water is influenced by the West Spitsbergen Current (WSC), which is the northernmost extension of the Norwegian Atlantic Current, a relatively warm (> 3°C) and saline [>34.9 practical salinity scale (pss)] water mass (Orvik & Niiler 2002). These Atlantic waters mix with the Arctic Ocean water, but the impact of the Atlantic waters is pronounced only in periods of strong WSC activity; whereas, at other times the area is under the influence of Arctic Ocean water (Sapota *et al.* 2009).

Seasonally changing freshwater input from melting glaciers additionally contributes to the local attributes of the water column. The mean temperatures are 0.20°C and 0.46°C at the sea surface and at 50-m water depth, respectively. The mean salinities are 33.13 at the sea surface and 34.77 at 50-m water depth (data from NODC_WOA94).

MATERIAL AND METHODS

Samples and data were obtained on 9–10 August 2006 during the MSM 02/03 expedition of RV *Maria S. Merian* (Table 1, Figs 1–3; Lherminier *et al.* 2006). Seabed mapping was carried out with a Kongsberg EM 1002 multibeam echo sounder, operating at a nominal sonar frequency of 95 kHz and controlled with the software Seafloor Information System. Multibeam raw data were processed using the software packages Neptune and Cfloor. The Neptune bathymetric postprocessing software brought raw multibeam data through a data correction and cleaning process and was designed for graphical description of the raw data to identify problems. It also provided tools to correct or remove errors in navigation data, depth soundings or sound speed profiles. The Cfloor software was used for chart production starting with Neptune output data from which digital terrain models were generated.

For the measurements of physical and chemical variables in the water column, a Sea Bird CTD was mounted with a rosette of 24 water bottles with a capacity of 10 litres each. At the maximum water depth at each station, water samples were taken for total alkalinity (TA) and dissolved inorganic carbon (DIC). Additional near-bottom water samples were obtained by a 5-litre Niskin bottle attached to the submersible JAGO. The carbonate system parameters pH, carbon dioxide partial pressure (pCO_2), calcite (cal) saturation (Ω_{cal}) and aragonite (arg) saturation (Ω_{arg}) were calculated from TA, DIC, temperature and salinity.

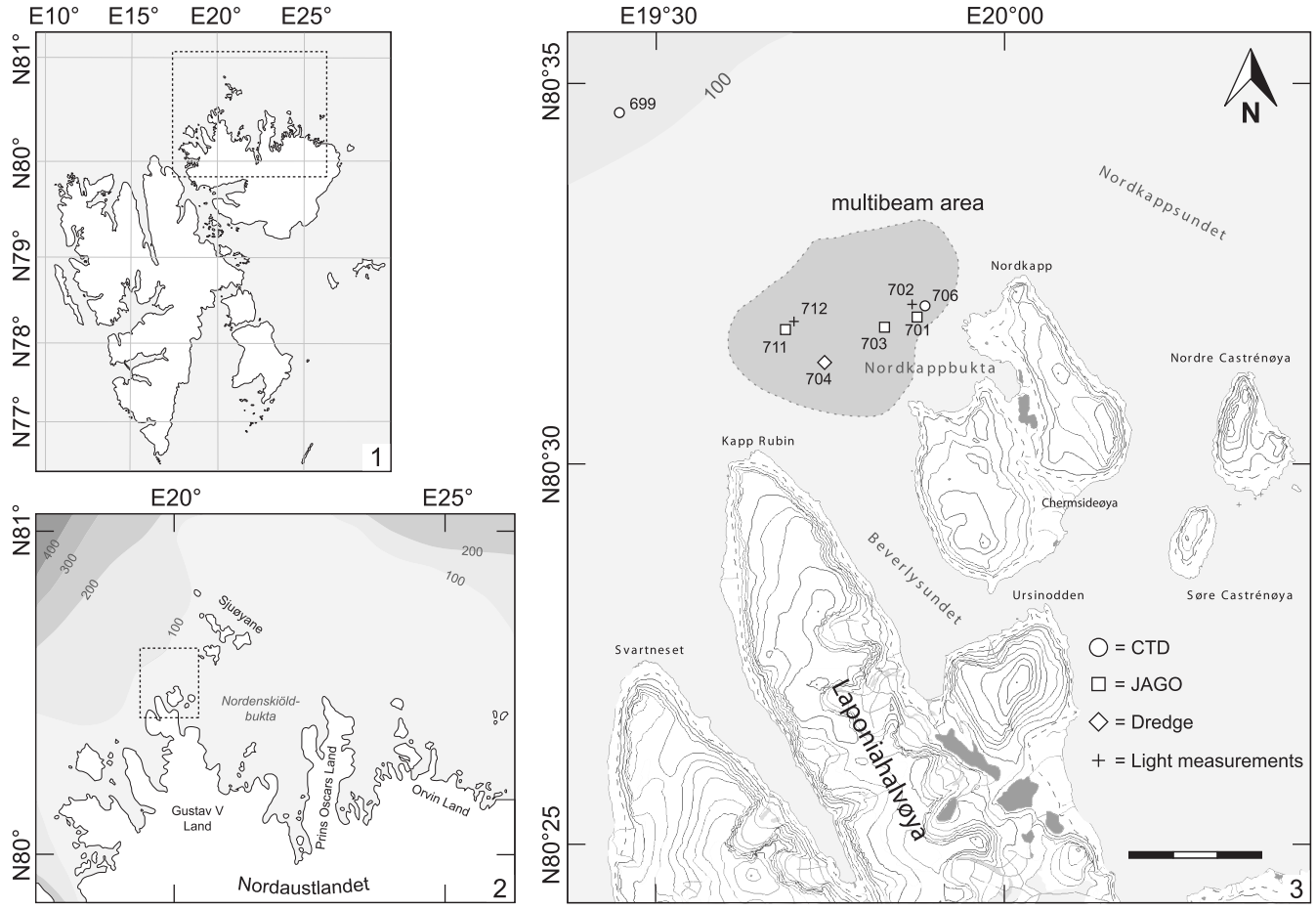

Figs 1–3. Maps of the study site and surrounding regions.
Fig. 1. Svalbard Archipelago, north of mainland Norway. Area enclosed in rectangle enlarged in Fig. 2.
Fig. 2. Northern part of Nordaustlandet Island where the study site is situated. Area enclosed in rectangle contains study site and is enlarged in Fig. 3.
Fig. 3. Study site and neighbouring regions showing the area mapped by multibeam echosounder (*c.* 16 km^2). Symbols denote sampling and measuring gear used. A detailed list of the applied gear is given in Table 1. Scale bar = 3 km, showing 1-km divisions.

Two light measurements were carried out with a LICOR Spherical Quantum Sensor (LI-193SA) in combination with a data logger (LI-1400) and a 100-m-long cable. The measured wavelength spectrum (400–700 nm) corresponds to the photosynthetic active radiation (PAR). Measurements were undertaken from the rescue boat of RV *Maria S. Merian* in order to minimise potential bias due to shadows cast by the research vessel and to enable controlled

Table 1. Station list and associated data.[1]

			Start				End			
Station no.	Gear	Date	Time UTC	Lat. °N	Long. °E	Depth (m)	Time UTC	Lat. °N	Long. °E	Depth (m)
699	CTD	9 Aug. 2006	07:09	80°35.01′	19°27.62′	142	07:15	80°35.03′	19°27.48′	144
700	MB	9 Aug. 2006	07:59	80°31.62′	19°39.45′	n.d.	11:34	80°31.00′	19°44.09′	41
701	JAGO	9 Aug. 2006	12:15	80°32.01′	19°50.77′	78	15:24	80°31.95′	19°51.30′	30
702	LS	9 Aug. 2006	12:46	80°32.00′	19°50.74′	75	12:46	80°32.00′	19°50.74′	75
703	JAGO	9 Aug. 2006	15:59	80°31.77′	19°48.70′	99	16:43	80°31.77′	19°48.42′	95
704	DRG	9 Aug. 2006	18:12	80°31.22′	19°44.23′	45	18:29	80°31.44′	19°43.02′	44
706	CTD	9 Aug. 2006	20:17	80°32.02′	19°50.78′	61	20:22	80°32.02′	19°50.77′	81
707	MB	9 Aug. 2006	20:39	80°31.76′	19°49.34′	87	21:16	80°32.23′	19°36.74′	84
710	MB	10 Aug. 2006	01:54	80°31.72′	19°39.79′	69	07:55	80°31.83′	19°39.40′	41
711	JAGO	10 Aug. 2006	09:03	80°31.76′	19°40.04′	70	11:54	80°31.86′	19°41.47′	30
712	LS	10 Aug. 2006	09:22	80°31.77′	19°40.32′	69	09:22	80°31.77′	19°40.32′	69
713	MB	10 Aug. 2006	12:36	80°32.09′	19°43.49′	112	16:16	80°31.76′	19°44.06′	60

[1] CTD, conductivity, temperature and depth measurements; MB, multibeam echosounder; JAGO, JAGO dive track; LS, light measurement; DRG, dredge; n.d., no data.

shallow measurements just below the water surface. Raw data were translated to percentages with respect to surface illumination to determine the water depth of the boundaries of the photic zoning at various study sites (see below). In addition to subaquatic measurements, the surface PAR was used as a reference for various weather conditions.

To gain information about the composition and diversity of the benthic community at the study site, a dredge (100-cm width, 40-cm height, 0.5-cm mesh size) was used to sample macro- and megabenthic epifauna. The samples were gently washed through a 1-mm sieve, and the organisms collected from the sieve residue were fixed in 70% alcohol for later

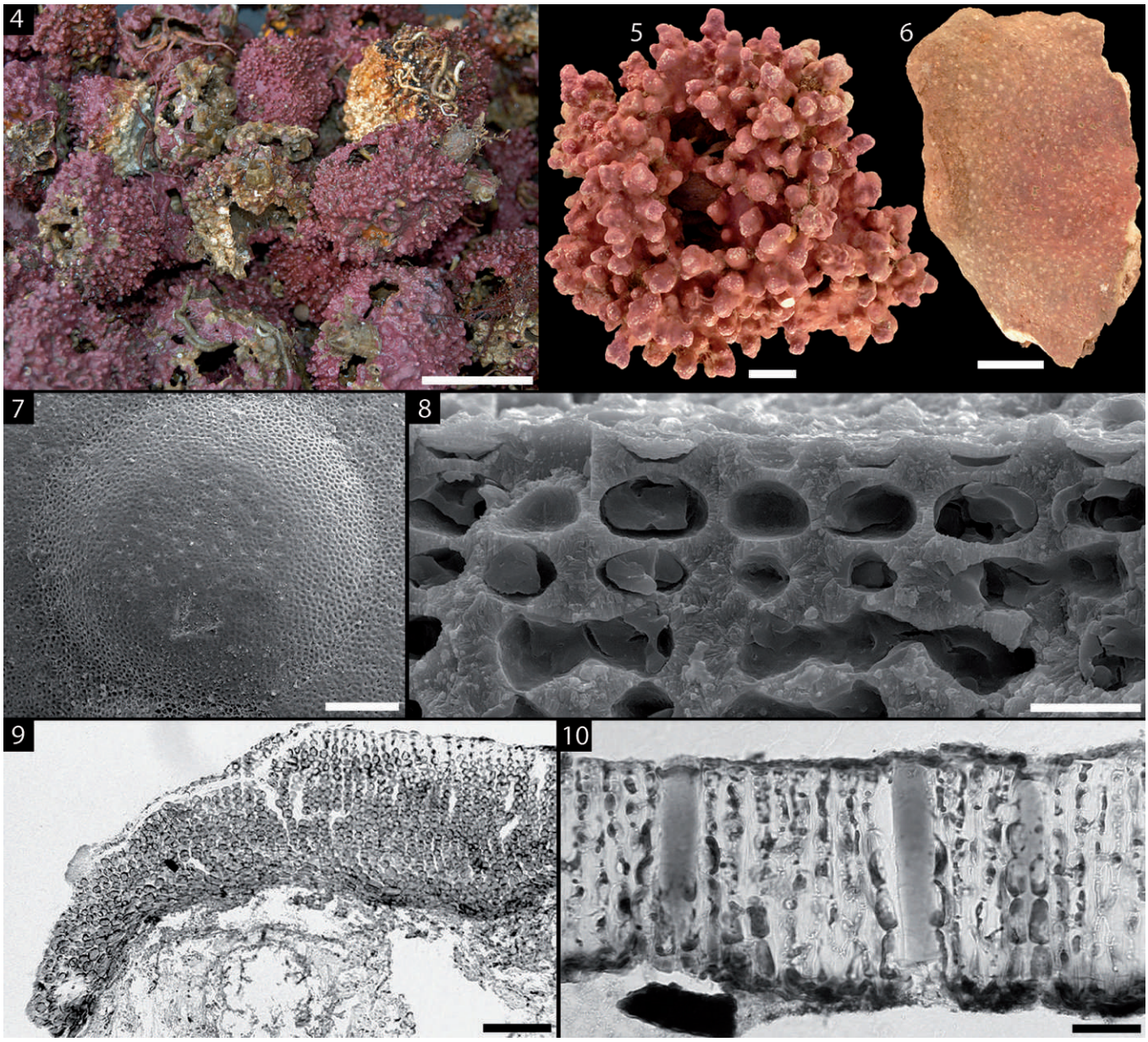

Figs 4–10. Principal species of coralline red algae in Nordkappbukta.
Fig. 4. Group of living rhodoliths of *Lithothamnion glaciale*, most of which are hollow. Scale bar = 10 cm.
Fig. 5. Individual living rhodolith of *Lithothamnion glaciale* (R_711_36). Scale bar = 1 cm.
Fig. 6. Part of a living plant of *Phymatolithon tenue* (R_704_3). White dots on upper surface denote positions of individual sporangial conceptacles. Scale bar = 1 cm.
Fig. 7. Tetrasporangial conceptacle of *Lithothamnion glaciale* in surface view (R_711_36_1). Note conceptacle pores on flattened part of roof. Scale bar = 100 μm.
Fig. 8. Section of thallus of *Lithothamnion glaciale* showing calcified filaments terminating in flattened and flared epithallial cells (R_711_36_4). Note fusions between some cells of adjacent filaments. Scale bar = 10 μm.
Fig. 9. Longitudinal section of edge of thallus of *Phymatolithon tenue* showing a ventral core of filaments portions of which curve upwards to the dorsal thallus surface (R_704_3_3). Scale bar = 100 μm.
Fig. 10. Part of a tetrasporangial conceptacle roof of *Phymatolithon tenue* showing three pore canals still blocked by sporangial plugs (R_711_31_1). Note that cells lining the pore canals characteristically are somewhat swollen compared with other roof cells. Scale bar = 25 μm.

analysis. Voucher specimens currently are housed at Senckenberg am Meer, Wilhelmshaven.

The manned submersible JAGO was used for visual inspection and video documentation of shallow-water slopes as well as for water sampling just above the seabed and for selective sampling of rhodoliths and their associated fauna. Video material was additionally used to analyse the distribution of rhodoliths and megafauna in a spatial context and to assess the sedimentary facies. The dredged material helps to identify major species. The video footage also included noncalcareous red algae that were mostly finely filamentous and resembled *Polysiphonia* (Rhodomelaceae, Ceramiales), but no specimens were collected during the 2006 cruise. Consequently, unequivocal identification was not possible, and these organisms are referred to hereafter as '*Polysiphonia*-like red algae'.

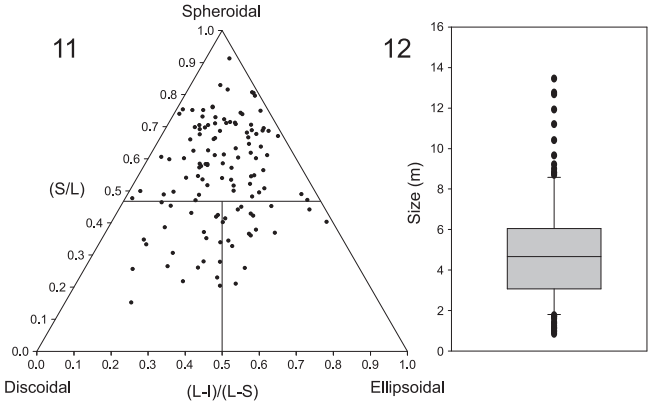

Figs 11, 12. Graphic analyses of rhodolith shape and size.
Fig. 11. Triplot shape distribution of rhodoliths based on measurements of long, intermediate and short axes as described in Bosence (1983a). $n = 128$.
Fig. 12. Box plot showing size range of rhodoliths based on measurements using the volume of an ellipsoid as described in Bosence (1976). $n = 128$.

RESULTS

Coralline red algal flora

The Nordkappbukta coralline red algal rhodolith community was mainly composed of *Lithothamnion glaciale* Kjellman (Figs 4, 5), with a lesser amount of *Phymatolithon tenue* (Rosenvinge) Düwel & Wegeberg (Fig. 6). Identification of thalli of *L. glaciale* was based on data in Adey (1964, 1966, 1970; includes species keys), Adey *et al.* [2005; includes comparisons of *L. glaciale* with *L. tophiforme* (Esper) Unger and *L. lemoineae* Adey], Irvine & Chamberlain (1994; includes species keys and accounts) and Kjellman (1883; contains the original account of *L. glaciale*). Living thalli (Figs 4, 5) were dull in texture and reddish to dull pink in colour, and tetrasporangial conceptacles had up to 50 pores in the roof (Fig. 7). This contrasts with another Arctic species, *L. tophiforme* (not identified in our samples), which is characterised by a glossy texture, an orange-red colour and tetrasporangial conceptacles with up to 85 pores in the roof (Adey *et al.* 2005). Like other species of *Lithothamnion*, the vegetative filaments of *L. glaciale* were terminated by epithallial cells with flared outer corners (Fig. 8). *Lithothamnion tophiforme* is said to be primarily an Arctic species that extends only into the deeper and colder parts of the subarctic Atlantic (Adey *et al.* 2005), while *L. glaciale* is said to be the dominant subarctic species of *Lithothamnion*. Elsewhere, Adey & Adey (1973) state that *L. glaciale* is the primary subarctic rhodolith builder, partly being replaced by *L. tophiforme* in Arctic waters. It should be remembered, however, that the type specimen of *L. glaciale* comes from Spitsbergen Island, Svalbard, and in the original account of the species (Kjellman 1883), *L. glaciale* is said to be common and plentiful on the west and north coasts of Spitsbergen Island and to occur as far north as Treurenberg Bay (79°56′N). According to Hansen & Jenneborg (1996, p. 372), *L. glaciale* is the dominant non-geniculate coralline at Spitsbergen Island. In Nordkappbukta, *L. glaciale* grew as unattached rhodoliths and also attached to cobbles or bedrock. Rhodoliths were more or less spherical to ovoidal to more irregular in form, consisted largely of knobby protuberances (branches) and were solid or hollow (see below). Attached thalli produced short (up to 19 mm) warty or knobby protuberances of varying diameter from a crustose base.

Identification of specimens of *P. tenue* was based on Düwel & Wegeberg (1996) and Rosenvinge (1893). *P. tenue* was originally described under the name *Lithothamnion tenue* by Rosenvinge (1893), but a modern examination of the lectotype specimen by Düwel & Wegeberg (1996) showed that the species belongs to *Phymatolithon.* The type specimen comes from Holsteinborg, Greenland. *Phymatolithon tenue* characteristically had a thin encrusting thallus (usually up to 200 μm thick; Figs 6, 9) that did not produce protuberances and had sporangial conceptacles that appeared as white dots on the upper thallus surface (Fig. 6). Pore canals of sporangial conceptacles were lined with cells that were mostly somewhat larger than other cells in the conceptacle roof (Fig. 10). These features were described and illustrated by Düwel & Wegeberg (1996, p. 478, figs 29–33) in the type and were clearly evident in algae from Nordkappbukta. In Nordkappbukta, thalli of *P. tenue* grew attached to cobbles or bedrock and occurred intermixed with *L. glaciale* but never produced protuberant branches.

Rhodolith morphology

The rhodoliths measured were collected from 45-m water depth. The shape of the rhodoliths was analysed as described in Bosence (1983a) by measuring the long (L), intermediate (I) and short (S) axes of all rhodoliths ($n = 128$), and the results were plotted in Sneed & Folk's (1958) pebble shape diagram using Tri-plot (Graham & Midgley 2000) (Fig. 11). The plot showed a majority of spheroidal shapes and the remaining rhodoliths dispersed on discoidal and ellipsoidal shapes in approximately equal parts.

The size of all rhodoliths ($n = 128$) was measured using the volume of an ellipsoid $[(L*I*S/4\pi)^{-2}]$ as shown in Bosence (1976). Plotting these values in a box plot showed that most rhodoliths ranged 3–6 cm in size but could also grow much bigger (Fig. 12).

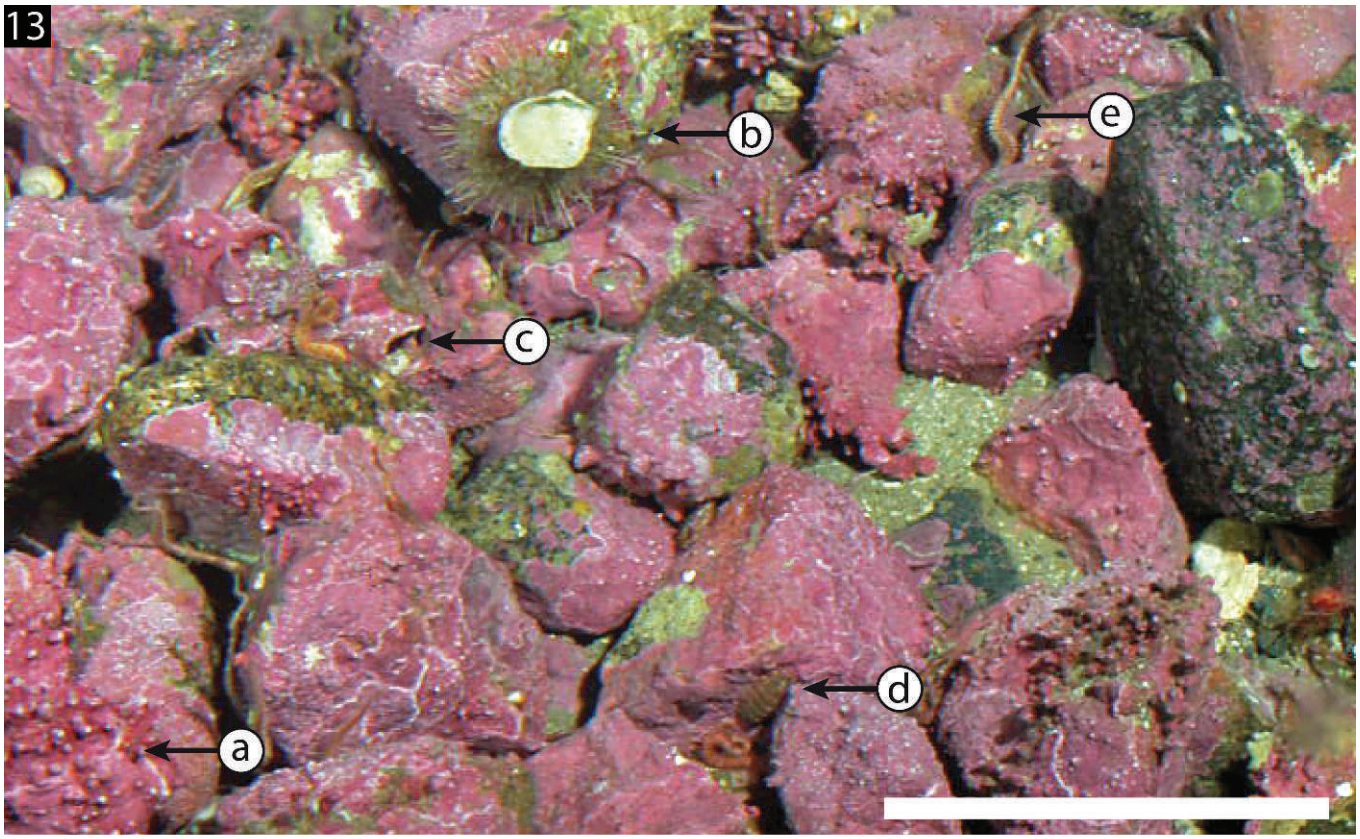

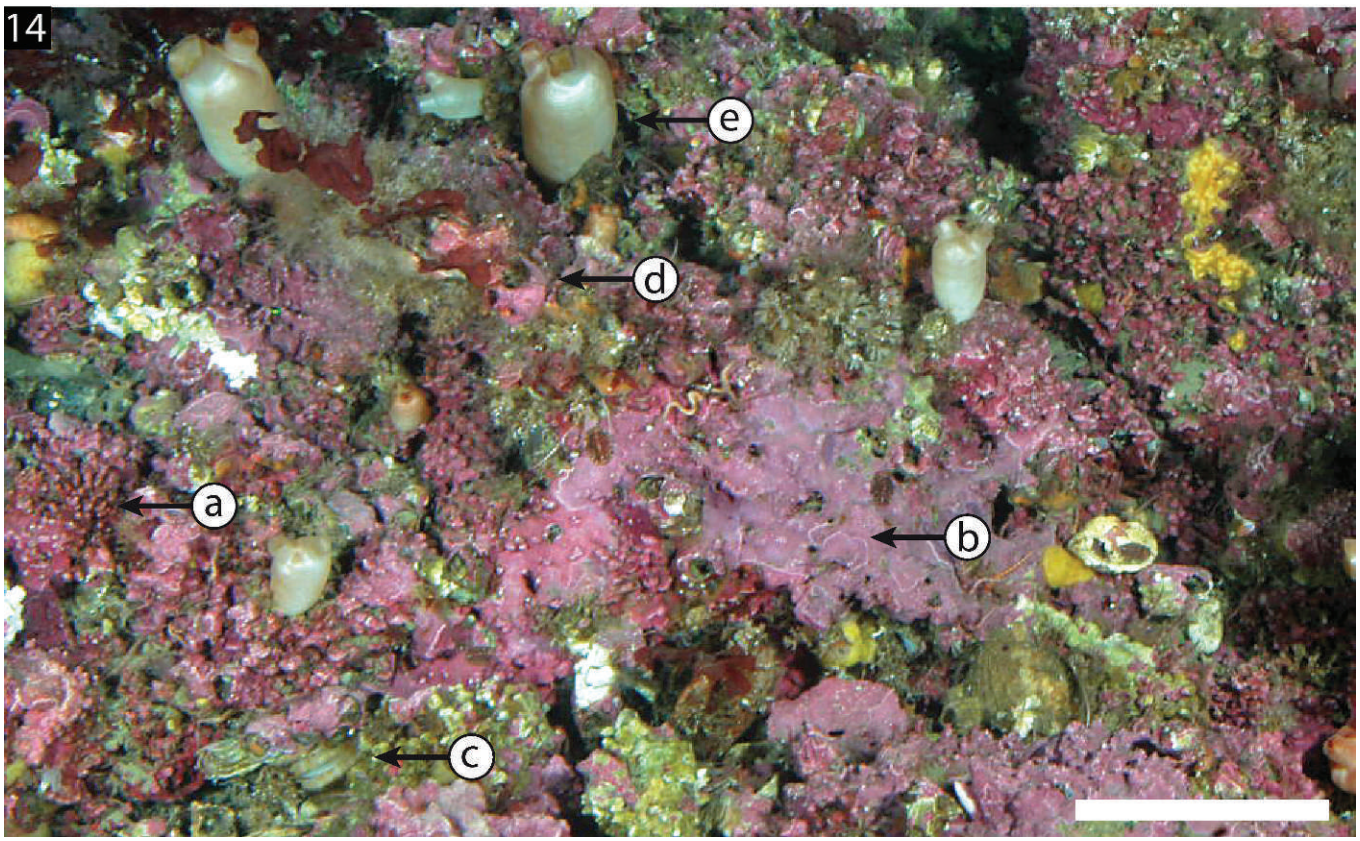

Figs 13–14. Examples of cobble communities and bedrock communities dominated by coralline red algae.

Fig. 13. Coralline red algal crusts of different stages of development and associated benthos covering cobbles on a glaciogenic gravel flat at 70-m water depth. a, *Lithothamnion glaciale*; b, *Strongylocentrotus* sp.; c, *Balanus* sp.; d, *Tonicella rubra*; e, *Terebellides stroemi*. Scale bar = 10 cm.

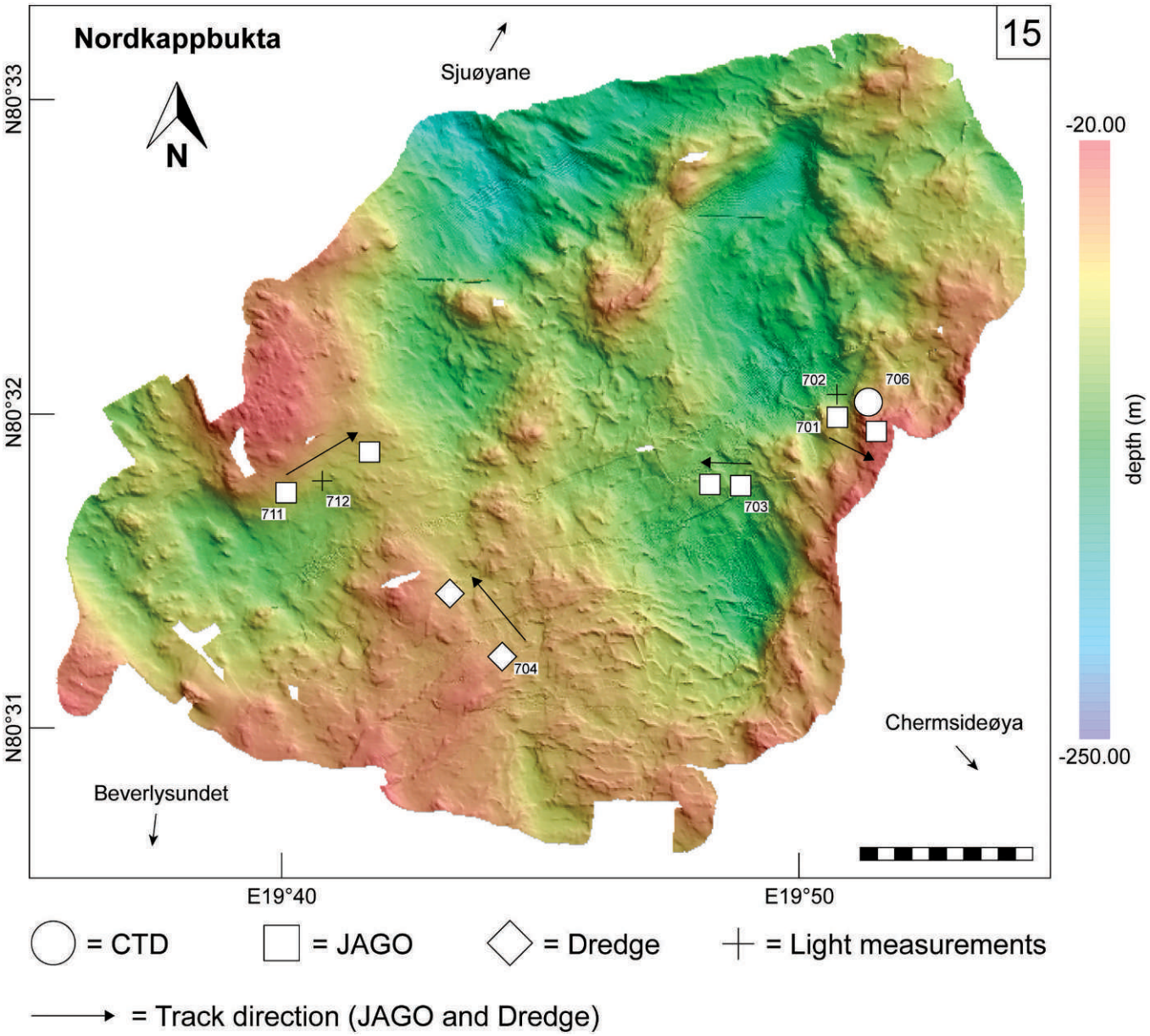

Fig. 15. Multibeam map of Nordkappbukta showing depth, morphology and positions of the applied gear. A detailed list of the applied gear is given in Table 1. Scale bar = 1 km, showing 100-m divisions.

Most rhodoliths were monospecific and consisted of *L. glaciale*. Some were multispecific, and both *L. glaciale* and *P. tenue* were present and overgrew each other. Overall, *L. glaciale* provided about 90% of the surface coverage. The coralline red algae settled on hard substratum (clastic or biogenic) above a distinctive size that provided enough stability (Fig. 13). If bedrock was present, it was also covered mainly by coralline red algae (Fig. 14). The fully developed rhodoliths generally contained a lithoclastic core and occurred both mixed with cobble communities and as distinct accumulations. Hollow rhodoliths with a wide-open space for internal colonisation and settlement to form a specific cryptic microhabitat also occurred. Although not yet fully understood, we believe that hollow rhodoliths have lost their lithoclastic nucleus at an earlier growth stage.

Seafloor and rhodolith bed features

The area mapped by the multibeam echosounder covered *c.* 16 km^2. The seafloor had a distinct morphology that featured zones of relatively flat depressions and plateaus alternating with steep ridges, ribs and slopes,

←

Fig. 14. Fully developed coralline red algal crusts and associated benthos nearly entirely covering the bedrock granite at 45-m water depth. a, *Lithothamnion glaciale*; b, *Phymatolithon tenue*; c, *Chlamys islandica*; d, *Balanus* sp.; e, *Actinia* sp. Scale bar = 10 cm.

while large iceberg scouring marks were not detected (Fig. 15).

Dive track 701 (78–30-m water depth; see Fig. 16 for facies profile) showed a bumpy, heavily structured seafloor and headed along a slope with a total inclination of *c.* 32°. The track started on a gravel pavement of poorly sorted material partly covered with a thin silty sediment layer, and some of the larger stones (> 10 cm) were covered with initial crusts of coralline algae. Crusts appeared only if the substratum was clean and were absent if it was smothered with soft sediment. At 75-m water depth, additionally large boulders occurred and were mostly completely covered with coralline algae crusts (Fig. 17). This boulder facies stopped at 70-m water depth and skipped to the same facies as in 78-m water depth and showed some shell accumulations of *Chlamys islandica* (O.F. Müller) and *Hiatella arctica* (Linnaeus) valves, which were restricted to patches. In 60-m water depth, shell beds were absent, and a boulder and gravel facies dominated again, while the degree of coralline algal encrustation and protuberance development increased. A steep slope at 51-m water depth made up of bedrock showed lots of encrustations of coralline red algae with fully developed protuberances, and the first individual rhodoliths accumulated in cracks (Fig. 18). The surface flattened again at 45 m, and nearly the whole substratum was covered with encrusting corallines, corallines with short protuberant branches and rhodoliths. Additional shell beds in this area were restricted to patches again. At 31-m water depth, a flat gravel pavement dominated, and coverage with *Polysiphonia*-like red algae increased, while rhodolith coverage decreased. Iceberg plough marks were absent, and epibenthos was very frequent along the entire track.

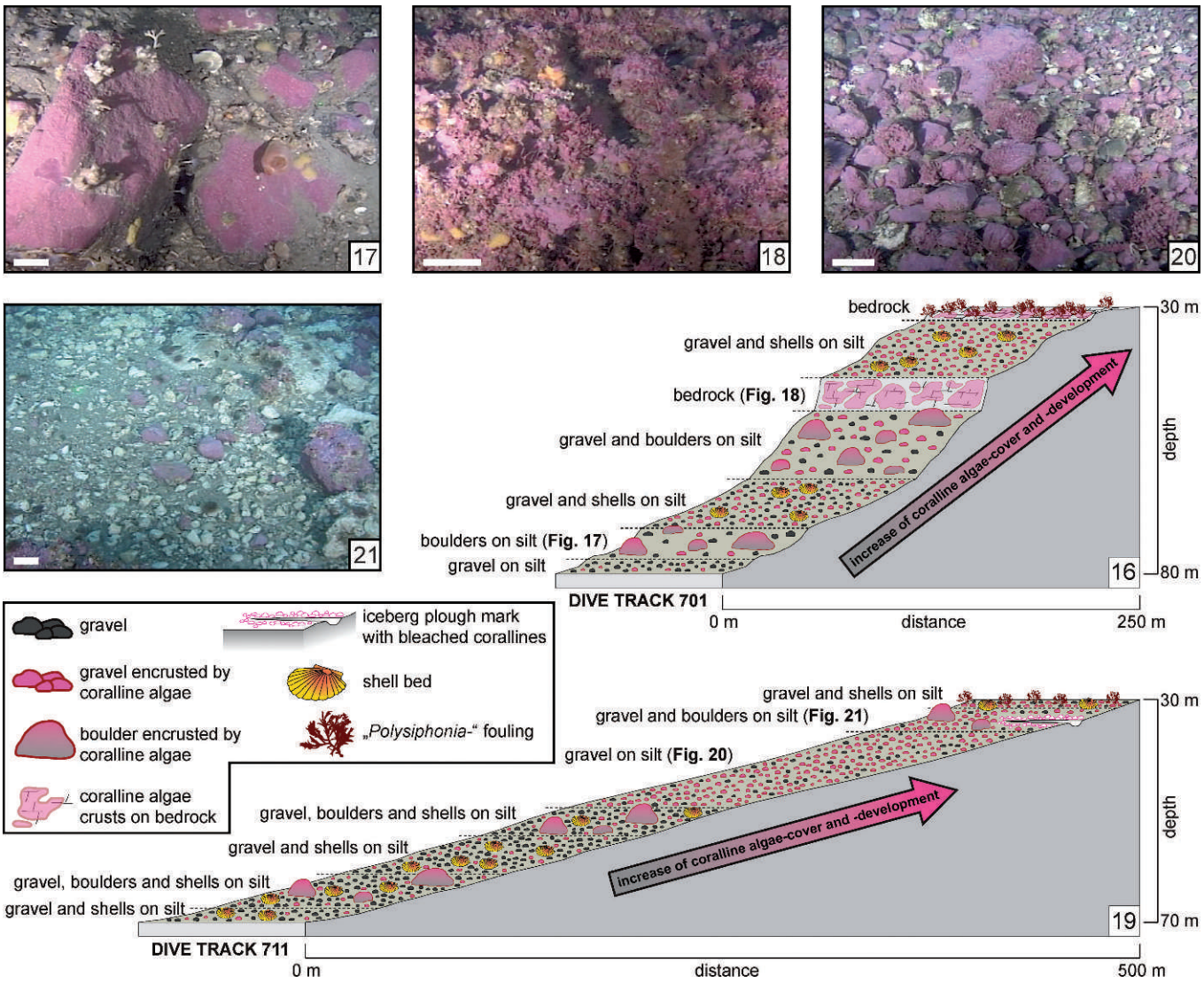

Figs 16–21. Facies profiles and associated sea floor pictures.
Fig. 16. Facies profile of dive track 701 showing the increase of coralline algae coverage with flattening and the prevailing substratum.
Fig. 17. Boulders with initial crusts in 75-m water depth (dive track 701). Scale bar = 10 cm.
Fig. 18. Fully developed protuberances attached to bedrock in 51-m water depth (dive track 701). Scale bar = 10 cm.
Fig. 19. Facies profiles of dive track 711 showing the increase of coralline algae coverage with flattening and the prevailing substratum.
Fig. 20. Rhodoliths in an intermediate stage of development on a gravel bottom in 45-m water depth (dive track 711). Scale bar =10 cm.
Fig. 21. Bleached crusts in an iceberg plough mark in 36-m water depth (dive track 711). Scale bar = 10 cm.

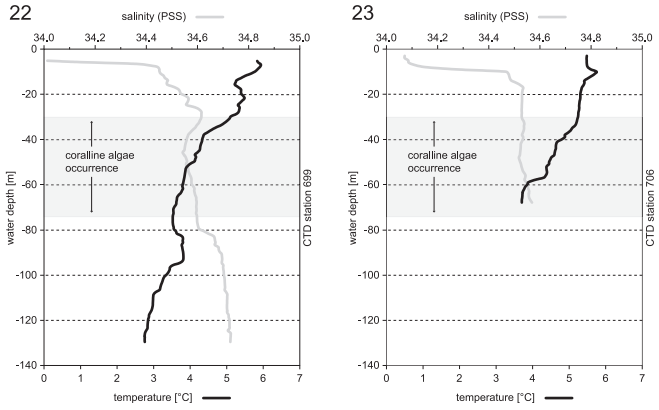

Figs 22, 23. CTD diagrams from stations 699 (Fig. 22) and 706 (Fig. 23) showing a similar pattern. Temperature decreases continuously with increasing water depth. Salinity strongly increases in the upper water column and stabilises at *c.* 20-m water depth. The coralline algae occurrence extends from 78- to 30-m water depth.

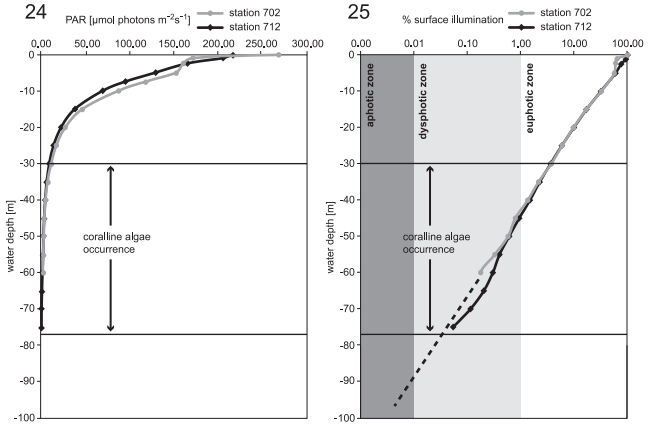

Figs 24, 25. Light measurements from stations 702 and 712 showing exponentially decreasing surface illumination toward deeper waters. The coralline algae occurrence extends from 78- to 30-m water depth.

Dive track 703 (95–110-m water depth) was very short and showed a partly washed-out pebble and cobble pavement with many large boulders on a smooth slope with *c.* 6° inclination. Epibenthos and shell accumulations were sparse and limited to depressions, where the pavement was also covered with a thin silty sediment layer. Coralline red algae were completely absent.

The seafloor at dive track 711 (70–30-m water depth; see Fig. 19 for facies profile) mainly conformed to the observations from dive track 701, but the morphology was less pronounced, the total inclination of the slope was *c.* 15° and bedrock was absent. The track started on a gravel pavement with shell accumulations that were restricted to patches. Thin coralline crusts appeared on individual larger cobbles at 70-m water depth, and the frequency and thickness of corallines increased with decreasing water depth. Occasionally, large boulders occurred, and the upper parts were completely covered with encrusting coralline algae. In 50-m water depth, shell beds and boulders were absent, and a flat gravel pavement dominated, while the bulk of the material was covered with encrusting coralline algae. Rhodoliths successively displaced the coralline-encrusted cobble community at 45-m water depth and partly covered the seafloor (Fig. 20). In 36-m water depth, encrusted boulders occurred again, and a small area was affected by an iceberg plough mark, and the affected rhodoliths and coralline crusts were bleached (Fig. 21). *Polysiphonia*-like red algae appeared and increasingly covered the seafloor at 32-m water depth, so that the rhodoliths and encrusting coralline algae were successively displaced.

Appearance and properties of the rhodolith beds slightly varied along the different dive tracks but showed the same overall pattern. Initial growth of encrusting algae started at *c.* 78-m water depth. With further flattening, thickness of crusts and development of protuberances increased. Coralline red algal coverage amounted to 30% below *c.* 45-m water depth. With further flattening, crust coverage strongly increased up to 100% if adequate substratum was available, and the coralline algae were not shaded and displaced by *Polysiphonia*-like red algae.

Environmental characteristics

The CTD records from stations 699 and 706 (Figs 22, 23) indicated a stratified summer situation characteristic for coastal Svalbardian waters. Temperatures decreased continuously with water depth from 5.8°C (surface) to 2.8°C (130-m water depth) at station 699 and from 5.5°C (surface) to 3.7°C (68-m water depth) at station 706. A surface layer with reduced salinity (*c.* 34) is developed in the upper 10 m of the water column at both stations. Underneath, more saline (> 34.5) waters, probably representing Atlantic-type water of the West Spitsbergen Current, prevail.

At stations 702 and 712 (Figs 24, 25), the ambient light levels decreased exponentially with water depth. The lower boundary of the euphotic zone (1% surface illumination) was at *c.* 45-m water depth at both stations. The lower boundary of the dysphotic zone (0.01% surface illumination) was not determined in the profiles, but extrapolation indicated a water depth of *c.* 90 m.

The bottom-near water parameters obtained by CTD and JAGO samples are compiled in Table 2. Despite the

Table 2. Water parameters obtained by CTD and JAGO.[1]

Station	T (°C)	p (dbars)	Salinity (PSS)	TA (µmol/kgSW)	DIC (µmol/kgSW)	pH	pCO_2 (µmatm)	Ω(cal)	Ω(arq)
699	3.0	131	35.0	2285	2106	8.15	294.10	2.97	1.88
703	3.0	30	35.0	2262	2096	8.12	314.78	2.84	1.79
706	3.7	62	34.6	2276	2110	8.11	323.70	2.86	1.80
714	3.0	50	35.0	2266	2084	8.16	285.17	3.06	1.93

[1] T, temperature; p, pressure; TA, total alkalinity; DIC, dissolved inorganic carbon; pCO_2, carbon dioxide partial pressure; Ω(cal), calcite saturation; Ω(arq), aragonite saturation.

Table 3. List of identified benthos.

Species	Interrelation to rhodoliths							
	No observations	Living on the surface of the rhodoliths	Attached to the surface of the rhodoliths	Living inside of hollow rhodoliths	Attached to the inside of hollow rhodoliths	Feeding on the surface of the rhodoliths	Living between the rhodoliths	Overgrowing rhodoliths and coralline crusts
Rhodophyta								
Lithothamnion glaciale								X
Phymatolithon tenue								X
Polysiphonia-like red algae								X
Porifera								
Calcaronea indet.	X							
Geodia sp.	X							
Porifera indet.								X
Cnidaria								
Alcyoniidae indet.	X							
Actinia sp.			X					
Gersemia rubiformis	X							
Gorgoniidae indet.			X					
Hormathia nodosa			X					
Hydrozoa indet.	X							
Lafeiodae indet.	X							
Mollusca								
Astarte crenata	X							
Chlamys islandica				X			X	
Hiatella arctica			X	X	X		X	
Musculus laevigatus	X							
Tridonta montagui	X							
Boreotrophon truncatus	X							
Lepeta caeca						X		
Margarites sp.	X							
Naticidae indet.	X							
Tectura sp.						X		
Tonicella rubra						X		
Sipunculida								
Golfingiidae indet.				X			X	
Polychaeta								
Flabelligera affinis				X			X	
Nephtys sp.				X			X	
Nereis zonata				X			X	
Sabellidea indet.			X			X		
Terebellides stroemi				X			X	
Thelepus cincinnatus				X			X	
Pantopoda								
Nymphon sp.	X							
Crustacea								
Anonyx laticoxae	X							
Balanus sp.			X					X
Hyas araneus	X							

Table 3. Continued

Species	Interrelation to rhodoliths							
	No observations	Living on the surface of the rhodoliths	Attached to the surface of the rhodoliths	Living inside of hollow rhodoliths	Attached to the inside of hollow rhodoliths	Feeding on the surface of the rhodoliths	Living between the rhodoliths	Overgrowing rhodoliths and coralline crusts
Lebbeus polaris	X							
Pagurus pubescens	X							
Pagurus sp.	X							
*Sclerocrangon ferox**	X							
Spirontocaris spinus	X							
Spirontocaris turgida	X							
Bryozoa								
Bryozoa indet.			X					X
Flustra foliacea			X					
Flustridae indet.			X					
Brachiopoda								
Hemithiris psittacea			X					
Echinodermata								
Cucumariidae indet.		X						
Gorgonocephalus sp.	X							
Heliometra glacialis	X							
Henricia sanguinolenta		X						
Ophiacantha bidentata							X	
Ophiocten sericeum							X	
Ophiopholis aculeata							X	
Ophiura robusta							X	
Ophiuridae indet.							X	
Solasteridae indet.	X							
Strongylocentrotus sp.						X		
Ascidiacea								
Ascidiacea indet.	X							
Boltenia echinata	X							
Styela rustica			X					
Pisces								
Artediellus atlanticus							X	
Cottidae indet.							X	

*Endemic Arctic species.

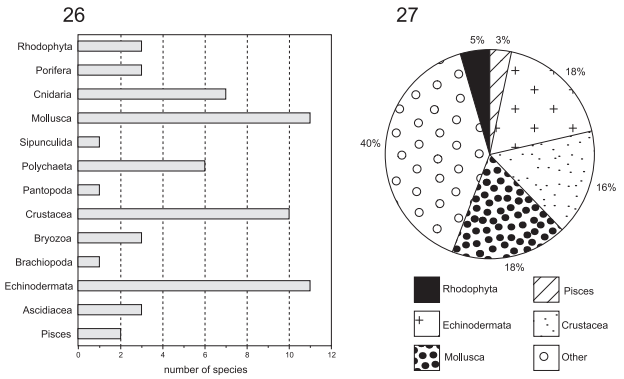

Figs 26, 27. Number and ratio of benthic species identified.
Fig. 26. Number of species in each major taxonomic group identified during present study.
Fig. 27. Pie chart showing percentage of species belonging to each major taxonomic group identified during present study. The Porifera, Cnidaria, Sipunculida, Polychaeta, Bryozoa, Brachiopoda and Ascidiacea have been collectively grouped under 'Other'.

low temperatures prevailing in the whole area, Ω_{Cal} and Ω_{Arg} were > 1 and thus in the range of saturation at any water depth in the study area.

Benthic community composition

A total of 61 benthic species were identified in the dredge sample and the video footage during the present study (Table 3; Figs 26, 27). However, this number, especially for taxa identified during the JAGO dives, probably will be an underestimate regarding the higher biodiversity that can be found when a larger variety of sampling tools is used (Hall-Spencer & Atkinson 1999). Mollusca and Echinodermata were richest in species (11 each), followed by Crustacea (10). The most prominent animal species are shown in Figs 28–36 and Figs 37–43. A clear depth zonation was evident in the distribution of the benthic fauna, with abundance and diversity decreasing with water depth. When rhodoliths were present, many species could be found on the surfaces of the rhodoliths, in gaps between them and even inside hollow rhodoliths (see Table 3 for the way of interrelation between benthos and rhodoliths).

DISCUSSION

Situated more than 1500 km north of the Arctic Circle, Nordkappbukta is an extreme environment in terms of water temperature, ice cover dynamics, light regime and salinity variability in response to meltwater formation. It is exposed both to cold Arctic Ocean water and, depending on seasonal activity, to the warmer Atlantic water of the West Spitsbergen Current. The mixing of the different water masses leads to a temperature range between the relatively warm (average 2°C; data from NODC_WOA94) upper-layer waters off western Spitsbergen (strongly influenced by the WSC) and the cold waters (average −1°C; data from NODC_WOA94) at the Barents Sea off eastern Nordaustlandet. All these characteristics exert high demands on the coralline red algae.

Comparisons with other rhodolith communities

Other polar and subpolar rhodolith communities occur, for example, in Alaska (Konar *et al.* 2006) and mainland Norway (Freiwald & Henrich 1994). The Alaskan community, situated in Herring Bay (Prince William Sound) at 60°28′N and 47°45′W, is the most northern known in the Pacific Ocean. In contrast to Nordkappbukta, Herring Bay features a monospecific rhodolith community composed of *Phymatolithon calcareum* (Pallas) W.H. Adey & D.L. McKibbin 1970 residing on a soft-bottom facies at 12–18-m water depth. The Alaskan rhodoliths have a similar ecological function as those in Nordkappbukta in providing a habitat for benthic organisms. Their branches are inhabited by specialized cryptofauna. This causes a strong increase in diversity of micro- and macrobenthos, a feature that seems to characterise many rhodolith communities (Foster 2001). At Herring Bay, the most abundant organisms are chitons (Konar *et al.* 2006), and thus the Herring Bay community seems to show the same interaction of coralline red algae and bioeroders as in Nordkappbukta and other localities (Steneck 1986).

In Norway, the Storvoll Plateau (Freiwald & Henrich 1994) situated in the Troms district at the southern tip of Rebbenesøy (69°59′N, 18°40′E) consists of rhodolith communities that fringe a rigid, *in situ* red algal buildup (14–15-m water depth). The community is multispecific, consisting of *Lithothamnion* cf. *glaciale*, *Lithothamnion* sp. and *Phymatolithon* sp., but the proportion of the two genera is much more balanced than in Nordkappbukta. However, the major sources for rhodolith production are detached heads from *Lithothamnion* branches, so most of the rhodoliths are not nucleated as they are in Nordkappbukta. The benthos is similarly diverse to that in Nordkappbukta, and many species [e.g. *C. islandica*, *H. arctica*

→

Figs 28–36. Prominent epibenthic animals at Nordkappbukta. All scale bars = 0.5 cm.
Fig. 28. *Flustra foliacea.*
Fig. 29. *Hemithiris psittacea.*
Fig. 30. *Astarte crenata.*
Fig. 31. *Chlamys islandica.*
Fig. 32. *Hiatella arctica.*
Fig. 33. *Lepeta caeca.*
Fig. 34. *Tonicella rubra.*
Fig. 35. Polychaete (suborder Terebellomorpha).
Fig. 36. *Balanus* sp.

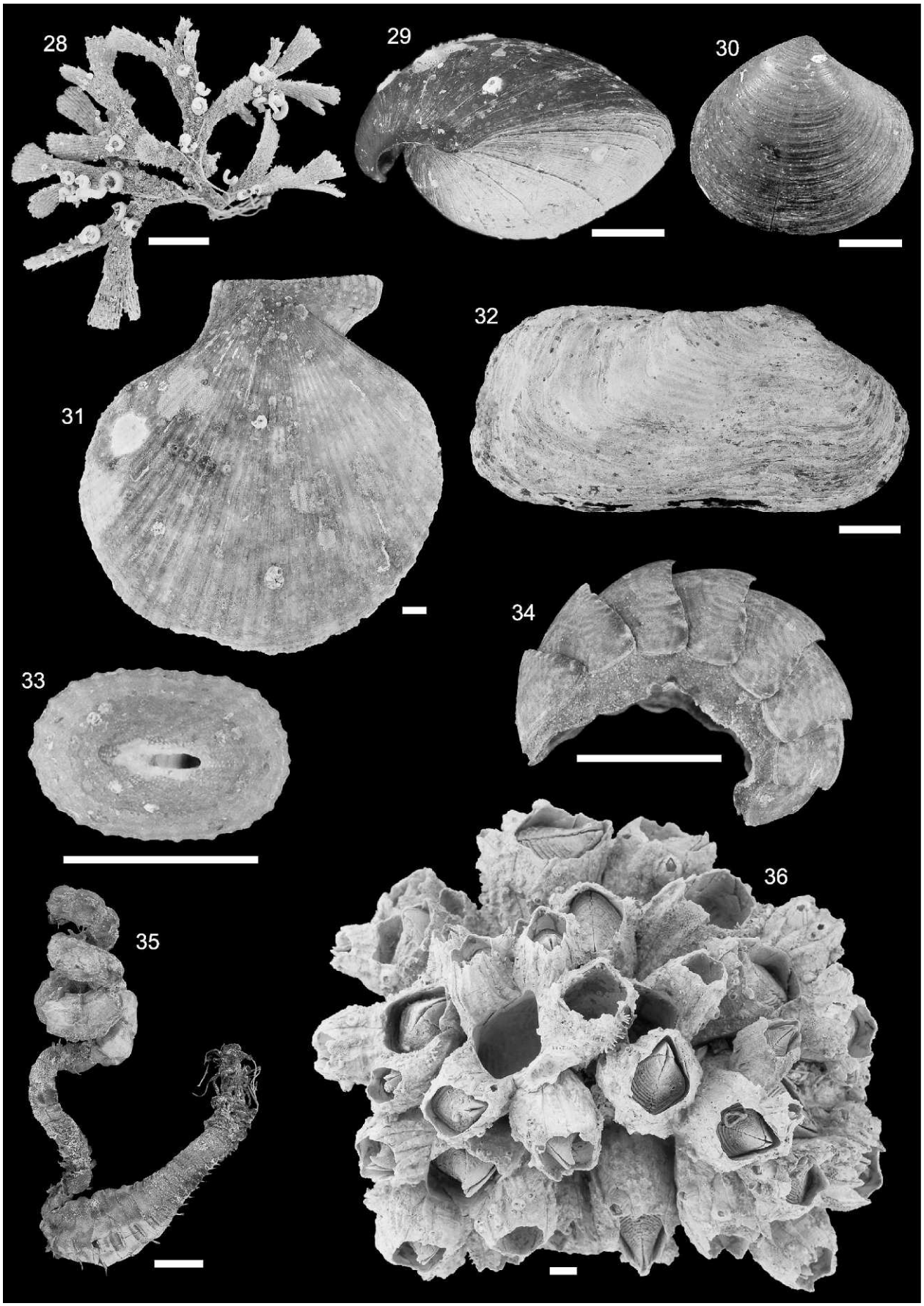
28
29
30
31
32
33
34
35
36

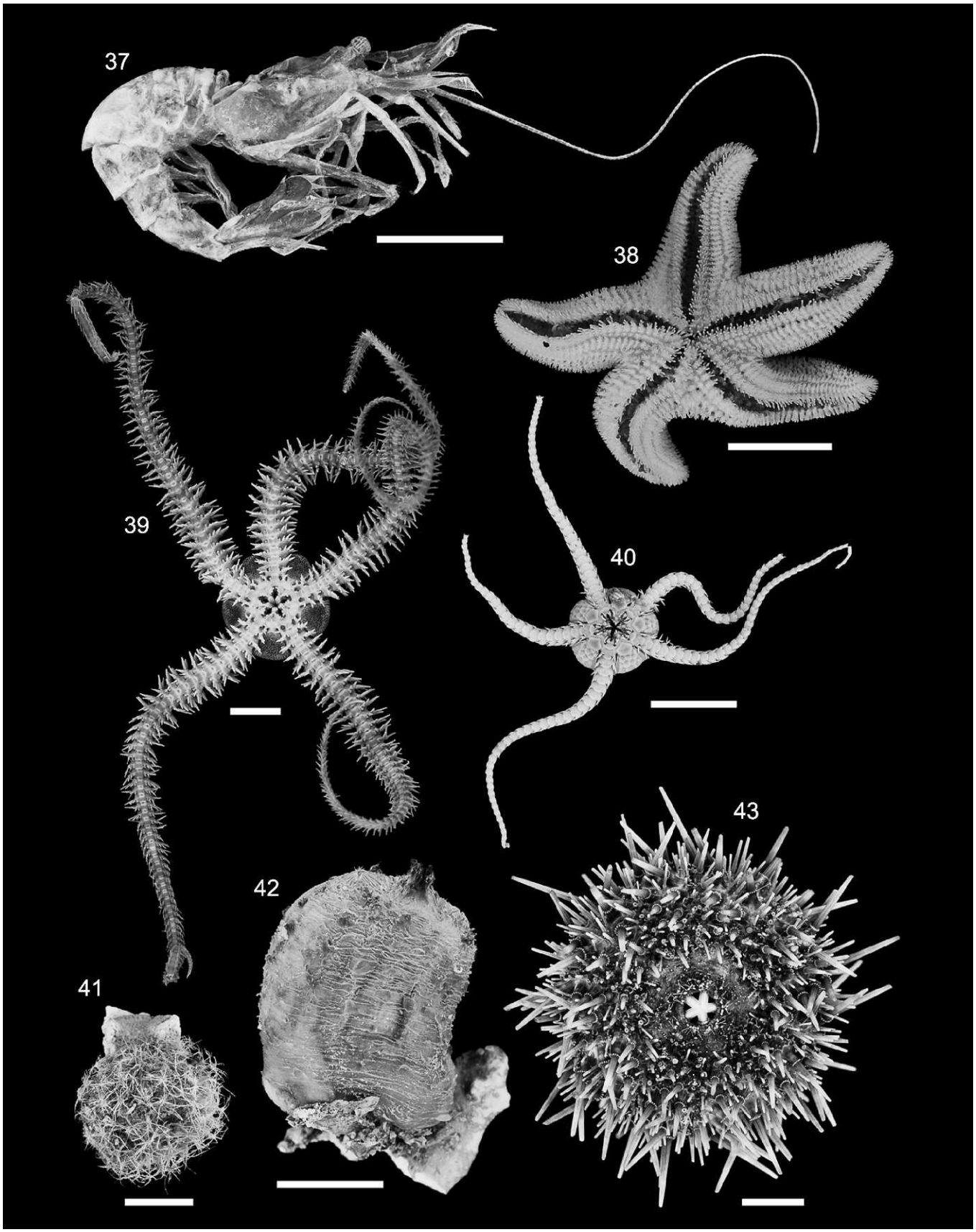

Figs 37–43. Prominent epibenthic animals at Nordkappbukta. All scale-bars = 0.5 cm.
Fig. 37. *Lebbeus polaris.*

and *Hemithiris psittacea* (Gmelin)] occur at both localities. Even bioeroders like *Strongylocentrotus droebachiensis* (O.F. Müller) and *Lepidopleurus asellus* (Gmelin) are common and take the same ecological niche as other grazers do in Herring Bay and Nordkappbukta.

Growth forms comparable to the hollow rhodoliths from Nordkappbukta are reported from the Storvoll Plateau but not from Herring Bay. Moreover, the Storvoll Plateau community (14–15-m water depth) and the Herring Bay community (12–18-m water depth) occur in considerably shallower water than the Nordkappbukta communities (mostly 30–75-m water depth).

Overall, these rhodolith assemblages seem to be ecologically very important, especially in providing substratum and protection for many benthic organisms. This system works similarly at different sites, even when the communities are composed of different species. If rhodoliths are present in a biocenosis like Nordkappbukta, which consists mainly of flat gravel pavements, they can greatly increase the diversity by providing a kind of microenvironment for cryptofauna between their branches (Steller *et al.* 2003) and in their partly hollow bodies. Coevally, several species present between and on the rhodoliths (e.g. polyplacophores) act as grazers and keep the corallines free from epiphytes (Steneck 1986).

Substratum and water movement

Most commonly, coralline red algae are attached to stable rock, but under suitable conditions of water depth and water movement, cobbles can also be colonized and rhodoliths can develop. If the substratum is disturbed seasonally, annual plants may predominate (Lieberman *et al.* 1979; Sousa 1979). Corallines can also occur as epiphytes, growing on the surface of other organisms (Kain & Norton 1990). Visible bedrock is very rare in Nordkappbukta, and the substratum is made up of a few larger (> 1 m^3) boulders and mainly by glaciogenic pebbles and cobbles appearing as gravel pavements. In a depth of 78 m, only cobbles above a distinctive size (> 10 cm) were colonized, but the minimum size of colonized cobbles and pebbles decreased with further seafloor flattening. Shell accumulations (mainly *Chlamys islandica* and *Hiatella arctica*) are of much lesser importance. The light shells as well as cobbles below a distinctive size do not provide enough stability, so storm waves and strong currents would intensely affect the coralline algal crusts. The reason why the minimum size of colonized material decreases with further flattening may be that other limiting factors, like irradiance, advance. Hence, the parts of the encrusted cobbles, which are currently buried, could be maintained sufficiently by the light-exposed part of the crust through secondary pits and cell fusions (Steneck 1986).

Another key factor for sufficient growth is water movement. Extensive beds of rhodoliths and maerl are found in areas with moderate to strong seabed currents that are relatively open yet sheltered (Bosence 1979). It has been suggested that these beds require both shelter from wave action to prevent burial of the thalli and enough water movement to prevent smothering with fine sediment (Hall-Spencer 1998); although, burial in coarse sediments has less severe effects on the algae (Wilson *et al.* 2004). Prevailing currents keep the exposed surfaces free from fine sediments due to the mostly flat topography in the Nordkappbukta coralline beds. Silt sedimentation, which is probably of seasonal origin due to meltwater transport, is limited to depressions. These depressions are generally devoid of living rhodoliths. The area, however, seems to be sufficiently protected from stronger wave and current action to enable the growth of large coralline crusts and rhodoliths. Shallower than *c.* 30-m water depth, crust and rhodolith coverage decreases and coralline algae are progressively replaced mostly by *Polysiphonia*-like red algae that shade the coralline red algae and inhibit further development. This change in algal cover could be caused mainly by increasing PAR (see below) and due to increasing wave action, which probably adversely affects *L. glaciale* and *P. tenue* more than the *Polysiphonia*-like red algae.

The action of waves and currents has a strong influence on the thriving of *L. glaciale* and *P. tenue* and is conducive to limit their main occurrence to a certain depth gradient between 70 and 30 m. Additionally, adequate substratum above a distinctive size has to be available to enable the development of initial encrustation. Hence, the bulk of the developed rhodoliths are nucleated or hollow, while rhodoliths with a core made up of coralline algae are rare. This also implies that the shape of the rhodoliths is controlled mainly by the shape of the encrusted material. Smothering of encrusted cobbles with soft sediment also seems to be harmful to the coralline algae. Signs of fresh-looking iceberg scour marks were not detected. Scouring of icebergs exerts a strong ecological disturbance to benthic ecosystems in polar waters (Heine 1989; Gerdes *et al.* 2003).

Temperature

Temperature has great effects on respiration, photosynthesis and growth rates of coralline red algae. The optimum temperature clearly varies geographically and with species, but the general pattern usually shows an increase in growth rate to a maximum that is near the top of the tolerated range (Kain & Norton 1990). Hence, temperature is the primary determinant of geographical distribution, and the boundaries of biogeographical regions are associated with isotherms (Lüning 1990). Adey & Adey (1973) showed that

←

Fig. 38. *Henricia sanguinolenta.*
Fig. 39. *Ophiopholis aculeata.*
Fig. 40. *Ophiura robusta.*
Fig. 41. *Boltenia echinata.*
Fig. 42. *Styela rustica.*
Fig. 43. *Strongylocentrotus* sp.

the distribution patterns of coralline red algae may be correlated with temperature boundaries.

In Nordkappbukta, the deepest occurrence starts at 78-m water depth, where the potential mean temperature is 0.7°C (data from NODC_WOA94). The maximum coverage appears at 45-m water depth, where the potential mean temperature is 0.4°C (data from NODC_WOA94). These relatively high temperatures result from mixtures of the warm Atlantic water with the colder Arctic Ocean water (Orvik & Niiler 2002; Sapota *et al.* 2009). However, this shows that *L. glaciale* is adapted to low temperatures compared to, for example, *Lithothamnion corallioides* (P.L. Crouan & H.M. Crouan) P.L. Crouan & H.M. Crouan, which has a minimum survival temperature of 5°C (Adey & McKibbin 1970). On the other hand, it is also temperature that seems to limit the southward distribution of *L. glaciale*, possibly because reproductive conceptacles are produced only when water temperatures are < 9°C (Hall-Spencer 1994). The Nordkappbukta CTD records (Figs 22, 23) show only snapshot conditions, but they were taken during summertime and under ice-free conditions. Hence, one can assume that they may show values close to the possible maxima. With values of 3.5°C in 78-m water depth, where coralline algae encrustation starts, and 4.2°C in 45-m water depth, where coralline algae development reaches its maximum, the water temperature is far below the 9°C limit, so conceptacle formation should be possible during summertime. This is a great advantage since the reproductive frequency of *L. glaciale* is annually protracted (Jackson 2003) and reproduction during summer implies sufficient light conditions, while it may fail during winter darkness.

Altogether, *L. glaciale* occupies a distinctive temperature range in Nordkappbukta, which is coequally warm enough to enable sufficient growth and cold enough to enable reproduction during summer.

Salinity

Fluctuations in salinity may cause osmotic stress, unfavourable ionic balances and shortage of essential metabolites (Kain & Norton 1990). Passing down a salinity gradient, the number of species of Rhodophyta commonly declines sooner than that of the Phaeophyta; whereas, that of the Chlorophyta may actually increase (Coutinho & Seeliger 1984). Despite this, *L. glaciale* favours full marine conditions but is also presumed to be tolerant to varying salinities (18–40 pss; Jackson 2003). Experiments by Wilson *et al.* (2004) also showed that *L. glaciale* appears to be not very sensitive to low salinities (< 18 PSS).

The salinity gradient in Nordkappbukta (Figs. 22, 23) seems to be quite stable except for the upper 10 m, which is subject to a thin incumbent freshwater lens deriving from terrestrial input (glacial meltwater, fluvial discharge). But this stable condition is only a snapshot and can change during times of melting sea ice or pronounced shifts of ocean currents and the coherent mixture of Atlantic water and Arctic Ocean water. Hence, it is an important attribute of *L. glaciale* to be suitably adapted to changing salinities. It may also be a reason why most of the red algal coverage in Nordkappbukta is made up of *L. glaciale*.

Irradiance

Coralline and other red algae can tolerate a wider range of light levels than any other group of photosynthetic plants, and many are low-light adapted (Kain & Norton 1990). This holds both for geniculate (jointed) corallines (Hader *et al.* 1996) and nongeniculate corallines (Kühl *et al.* 2001; Roberts *et al.* 2002), and such species often show an effective adaptation to low irradiance in polar latitudes and which is prolonged under sea ice conditions. Lüder *et al.* (2002) reported that the noncalcareous red alga *Palmaria decipiens* (Reinsch) R.W. Ricker could cope with complete darkness for several months before respiration suddenly drops, while photosynthetic capacity recovers rapidly after exposure to illumination. This enables sufficient growth even at high latitudes, such as in Nordkappbukta, where the polar night lasts for 120 days, and thus *L. glaciale* and *P. tenue* seem to be adapted very well to long-term dark periods.

Appearance and properties of the rhodolith beds slightly varied along different dive tracks but showed the same overall pattern. Initial growth of encrusting coralline algae started at *c.* 78-m water depth in the dysphotic zone (0.01–1% surface illumination), where the measured PAR was 0.1 μmol photons m^{-2} s^{-1} on average for both stations (Figs 24, 25). Roberts *et al.* (2002) showed that individuals of *P. tenue* have no significant net photosynthesis at such low irradiance. At 45-m water depth (2.1 μmol photons m^{-2} s^{-1}, averaged for both stations), coralline red algae cover nearly 100% of hard substratum, and protuberances of *L. glaciale* are fully developed. The relative abundance of *P. tenue* is 10% at most, and data from Roberts *et al.* (2002) show a net photosynthesis of only 2 mmol O_2 m^{-2} d^{-1} for individuals of this species at such irradiance conditions. Hence, the initial appearance of *L. glaciale* at $>$ 75-m water depth shows that these algae can cope with very low light conditions and are able to colonise a large range of the dysphotic zone. It could also be one reason why there is such a disequilibrium between the abundance of *L. glaciale* and *P. tenue*.

Wilson *et al.* (2004) showed that coralline red algae might lack the ability to perform additional photochemistry under high-irradiance conditions. The decrease in coverage with further topographic flattening ($<$ 30-m water depth) seems to be directly linked to the increasing coverage of *Polysiphonia*-like red algae, which do not calcify, grow much faster than the coralline red algae and find sufficient light conditions in the shallow waters. However, this seaweed cover seems not to be dense enough to enable the development of a shaded coralline algal understorey at shallow depths (see Irving *et al.* 2005). Irradiance is another factor that limits the appearance of coralline red algae at Nordkappbukta to a distinct depth gradient since light conditions seem not be sufficient in depths $>$ 78 m, while in a depth of $<$ 30 m, irradiance is high enough to favour other plants that displace the coralline red algae. The nearly 50-m-wide depth range for *L. glaciale* is much larger than characteristic depth ranges for algae in temperate and tropical environments. This observation indicates a very high degree of shade adaptation as has been demonstrated for coralline algae from the Ross Sea, Antarctica (Schwarz *et al.* 2005).

Overcoming nutrient and carbon depletions

Although not analysed by us, the ecophysiological adaptation of coralline algae to overcome the summer depletion of macronutrients (nitrogen, phosphorus) deserves some consideration. As stated before, these macronutrients are available during the dark winter period in Svalbardian waters and thus can be utilised by long-living algae instantaneously. Such an ecophysiological adaptation has been experimentally proven for some polar phaeophytes (see Wiencke *et al.* 2007 and further references therein). The carbon needed to maintain metabolism, biomass and even growth during the dark period derives from carbohydrates as storage products. Such carbohydrate products occur as starch grains in coralline algae, which are formed photosynthetically during the illuminated period and deposited within the vegetative cell compartments. During the dark period, the carbohydrates can be remobilised and may act as carbon source. A similar pathway has been detected by Lüning *et al.* (1973) for some polar laminarian phaeophytes.

Water chemistry

The concentration of calcium is critical for calcification in coralline red algae (King & Schramm 1982), and the maintenance of potassium in algal cells, relative to seawater, depends on the presence of adequate quantities of calcium ions (Kain & Norton 1990). The seawater carbon content, associated with its pH, has a marked effect on photosynthesis at the low salinities (Kain & Norton 1990) that can occur particularly during times of intense meltwater input, and hence carbonate saturation is an important factor for coralline growth at high latitudes. Martin *et al.* (2008) showed that an increasing acidification of seawater leads to a significant reduction in coralline algal cover, so a lowered pH and the reduction of carbonate saturation are important factors affecting rhodolith beds.

The water chemistry measured at four sites in Nordkappbukta (Table 2) shows carbonate saturation (cal and arq) and a pH > 8 for the whole area, which could be a very important factor for the thriving of the rhodolith beds. This is remarkable because high-latitude oceans should be the first to become unsaturated with respect to calcite and aragonite (Orr *et al.* 2005). Hence, it is one of the main factors that may be affected by the ongoing ocean acidification resulting in impaired conditions for the growth of coralline red algae. Modeling studies projected annual mean carbonate subsaturation as early as 2032 for the Arctic surface ocean if anthropogenic CO_2 emissions follow the Intergovernmental Panel on Climate Change's business-as-usual scenario (SRES A2; Steinacher *et al.* 2009). This could also imply that a possible acidification could lead to a decrease in rhodolith abundance and hence to more unfavourable conditions for many benthic organisms due to the loss of habitat.

Interactions between coralline red algae and other benthos

Distribution, composition and abundance of the benthos (excluding rhodophyceans) in Nordkappbukta seem to be controlled mainly by light penetration and the kinetic energy regime (waves, currents and tides). As these factors depend very much on water depth, depth zonation is the most pronounced pattern in the distribution of the benthic assemblages. If fully developed coralline crusts and rhodoliths are present, up to 55% of the observed organisms use them as a habitat, as they live in gaps between the rhodoliths, grow attached to their surface or even live inside hollow rhodoliths (see Table 3). Thus, rhodolith accumulations act as bioengineers and represent microenvironments for the otherwise nonprotected glaciogenic flats. Similarly, other studies report on rhodolith beds as refugia for scallops (Kamenos *et al.* 2004a) and as a habitat for juvenile cod (Kamenos *et al.* 2004b). Because of the influence of the WSC, most benthic species are of Atlantic origin and also occur at boreal latitudes. The only endemic Arctic species identified at Nordkappbukta is the shrimp *Sclerocrangon ferox* (Sars). Hence, the proportion of endemic Arctic fauna amounts to only 1.7%.

The surfaces of coralline algae represent a major source of food for a variety of herbivores like molluscs, crustaceans, sea urchins and fishes (Kain & Norton 1990). The grazing seems to be beneficial to the corallines, especially because fleshy algae are removed or limited (Adey & Macintyre 1973), so herbivory is often identified as the source of disturbance that keeps corallines clean and healthy (Steneck 1982, 1986). The most effective physical defence is seen in the calcareous thalli of the Corallinaceae, which are much tougher than those of most algae (Littler *et al.* 1983; Watson & Norton 1985). Such calcareous forms are among the most grazer-resistant algae; although, even these are not immune (Clokie & Norton 1974; Adey & Vassar 1975; Steneck 1982; Padilla 1984). Many calcareous crustose species seem to be dependent in some circumstances upon browsing animals to remove epiphytes or competitors that might otherwise swamp the algae (Brawley & Adey 1981; Steneck 1982). Both *L. glaciale* and *P. tenue* are among these grazer-resistant calcareous forms, and prominent grazers like *Tonicella rubra* (Linnaeus) and *Strongylocentrotus* sp. are very common in the coralline beds. The higher frequency of the intensely branched *L. glaciale* compared to the relatively smooth-surfaced *P. tenue* may be caused by the high abundance of *Strongylocentrotus* sp. because ecological studies have shown that branches in some nongeniculate corallines are an effective defence against deep-grazing sea urchins (Milliken & Steneck 1981). Competition for space is also important, and many red algae monopolise or virtually occlude the substratum by abutting with neighbours to form a continuous sheet (Littler & Kauker 1984; Johnson & Mann 1986). This also happens in Nordkappbukta, where many pebbles and cobbles are encrusted as a whole and appear completely pinkish red. Secondary to the encrusted stones, completely hollow rhodoliths are common and act as kind of microenvironment for benthic animals such as *Flustra foliacea* (Linnaeus), *C. islandica*, *H. arctica* and *Ophiura robusta* (Ayres). Not much is known about the formation of hollow rhodoliths, and this will be in the focus of another study, but their importance for the present ecosystem is clearly evident.

The environment of Nordkappbukta enables coralline red algal rhodolith formation if sufficient substratum is present and bottom currents are strong enough to prevent smothering of the corallines with fine sediments. *L. glaciale* occupies a distinctive temperature range in Nordkappbukta, which is warm enough to enable sufficient growth and does not exceed 9°C, so formation of reproductive conceptacles in *L. glaciale* is possible throughout the summer.

Nordkappbukta is exposed to strong seasonality, so changes in salinity due to changing currents and meltwater input are common. Hence, the occurrence of *L. glaciale* provides evidence of its adaptation to changing salinities.

The prevailing light conditions seem to be the main reason why the coralline algae are limited to a distinctive depth gradient since irradiance is too low in water depths > 80 m to enable sufficient photosynthesis. On the other hand, in water depths < 30 m, irradiance is high enough to favour faster-growing plants, which outcompete the coralline red algae, or is too high for the low-light-adapted corallines.

Carbonate saturation is of particular importance to maintain skeletal growth. Hence, the measured carbonate saturation in Nordkappbukta is another important factor that makes substantial rhodolith development possible. Coequally, it is the most sensitive parameter in view of possible ocean acidification.

The concomitant appearance of corallines and prominent grazers, such as *T. rubra* and *Strongylocentrotus* sp., keeps the corallines free from epiphytes and coequally provides feeding grounds for the grazers. Additionally, the rhodolith accumulations act as bioengineers and represent microenvironments for the otherwise nonprotected glaciogenic flats, with hollow rhodoliths being of particular significance as providers of microhabitats for the associated benthic fauna.

Overall, *L. glaciale* and *P. tenue* appear to be well adapted to the extreme environment of the Arctic. But like all ecosystems with highly specialised organisms present, even this environment is vulnerable to global change. The findings reveal that polar coralline algae are much more widespread in polar waters than previously thought, thus representing a unique polar carbonate factory. This will lead to further investigations using the collected material to estimate a budget for the carbonate production of these polar rhodolith communities and to assess their value as a recorder for historic environmental change.

ACKNOWLEDGEMENTS

This work was funded by the Deutsche Forschungsgemeinschaft (FR 1134/18). NODC_WOA94 data are provided by the NOAA/OAR/ESRL PSD, Boulder, Colorado, USA, from http://www.esrl.noaa.gov/psd. The authors would like to thank the captain and the crew of RV *Maria S. Merian*, the JAGO operating team (IFM-Geomar), Dirk Fleischer (Kiel) for helping with the epifauna sampling, Adele Harvey for the preparation of sections for light microscopy and Ines Pyko for her work as research assistant. The authors also acknowledge Matthias López Correa for fruitful discussions and Craig Schneider for providing a copy of and information about the abstract of Milliken & Steneck 1981. Comments from Steffen Hetzinger and an anonymous reviewer improved this manuscript.

REFERENCES

Adey W.H. 1964. The genus *Phymatolithon* in the Gulf of Maine. *Hydrobiologica* 24: 377–420.

Adey W.H. 1966. Distribution of saxicolous crustose corallines in the northwestern North Atlantic. *Journal of Phycology* 2: 49–54.

Adey W.H. 1970. The effects of light and temperature on growth rates in boreal-subarctic crustose corallines. *Journal of Phycology* 6: 269–276.

Adey W.H. & Adey P. 1973. Studies on the biosystematics and ecology of the epilithic crustose Corallinaceae of the British Isles. *British Phycological Journal* 8: 1–60.

Adey W.H. & Macintyre, I.G. 1973. Crustose coralline algae: a re-evaluation in the geological sciences. *Geological Society of America Bulletin* 84: 883–904.

Adey W.H. & McKibbin D.L. 1970. Studies on the maerl species *Phymatolithon calcareum* (Pallas) nov. comb. and *Lithothamnion corallioides* Crouan in the Ria de Vigo. *Botanica marina* 13: 100–106.

Adey W.H. & Vassar J.M. 1975. Colonization, succession and growth rates of Caribbean crustose corallines. *Phycologia* 14: 55–69.

Adey W.H., Chamberlain Y.M. & Irvine L.M. 2005. An SEM-based analysis of the morphology, anatomy, and reproduction of *Lithothamnion tophiforme* (Esper) Unger (Corallinales, Rhodophyta), with a comparative study of associated North Atlantic arctic/subarctic Melobesioideae. *Journal of Phycology* 41: 1010–1024.

Aguilera J., Bischof K., Karsten U., Hanelt D. & Wiencke C. 2002. Seasonal variation in ecophysiological patterns in macroalgae from an Arctic fjord: II. Pigment accumulation and biochemical defence systems. *Marine Biology* 140: 1087–1095.

Bosence D.W.J. 1976. Ecological studies on two carbonate sediment producing coralline algae from western Ireland. *Palaeontology* 19: 365–395.

Bosence D.W.J. 1979. Live and dead faunas from coralline algal gravels, Co. Galway. *Palaeontology* 22: 449–478.

Bosence D.W.J. 1983a. Description and classification of Rhodoliths (Rhodoids, Rhodolites). In: *Coated grains* (Ed. by T.M. Peryt), pp. 217–224. Springer-Verlag, Berlin.

Bosence W.J.D. 1983b. The occurrence and ecology of recent rhodoliths – a review. In: *Coated grains* (Ed. by T.M. Peryt), pp. 225–242. Springer-Verlag, Berlin.

Brawley S. & Adey W.H. 1981. The effect of micrograzers on algal community structure in a coral reef microcosm. *Marine Biology* 61: 167–177.

Clokie J.J. & Norton T.A. 1974. The effects of grazing on algal vegetation of pebbles from the Firth of Clyde. *British Phycological Journal* 9: 216.

Coutinho R. & Seeliger U. 1984. The horizontal distribution of the benthic algal flora in the Patos Lagoon estuary, Brazil, in relation to salinity, substratum and wave exposure. *Journal of Experimental Marine Biology and Ecology* 80: 247–257.

Davies J. & Hall-Spencer J. 1996. Mapping of the benthic biotopes in the proposed Sound of Arisaig Special Area of Conservation. Scottish Natural Heritage/Biomar Research Survey and Monitoring Report no. 83. 75 pp.

Düwel L. & Wegeberg S. 1996. The typification and status of *Leptophytum* (Corallinaceae, Rhodophyta). *Phycologia* 35: 470–483.

Falk-Petersen S., Hop H., Budgell W.P., Hegseth E.N., Korsnes R., Løyning T.B., Ørbæk, J.B., Kawamura T. & Shirawasa K. 2000. Physical and ecological processes in the marginal ice zone of the northern Barents Sea during the summer melt period. *Journal of Marine Systems* 27: 131–159.

Fortunato H. & Schäfer P. 2009. Coralline algae as carbonate producers and habitat providers on the Eastern Pacific coast of Panama: preliminary assessment. *Neues Jahrbuch für Geologie und Paläontologie, Abhandlungen* 253: 145–161.

Foster M.S. 2001. Rhodoliths: between rocks and soft places. *Journal of Phycology* 37: 659–667.

Freiwald A. 1998. Modern nearshore cold-temperate calcareous sediments in the Troms District, northern Norway. *Journal of Sedimentary Research* 68: 763–776.

Freiwald A. & Henrich R. 1994. Reefal coralline algal build-ups within the Arctic Circle: morphology and sedimentary dynamics under extreme environmental seasonality. *Sedimentology* 41: 963–984.

Gerdes D., Hilbig B. & Montiel A. 2003. Impact of iceberg scouring on macrobenthic communities in the high-Antarctic Weddell Sea. *Polar Biology* 26: 295–301.

Gherardi D.F.M. 2004. Community structure and carbonate production of a temperate rhodolith bank from Arvoredo Island, southern Brazil. *Brazilian Journal of Oceanography* 52: 207–224.

Graham D.J. & Midgley N.G. 2000. Graphical representation of particle shape using triangular diagrams: an Excel spreadsheet method. *Earth Surface Processes and Landforms* 25: 1473–1477.

Gutt J. 2001. On the direct impact of ice on marine benthic communities, a review. *Polar Biology* 24: 553–564.

Hader D.P., Herrmann H., Schafer J. & Santas R. 1996. Photosynthetic fluorescence induction and oxygen production in corallinacean algae measured on site. *Botanica Acta* 109: 285–291.

Halfar J., Zack T., Kronz A. & Zachos J.C. 2000. Growth and high-resolution paleoenvironmental signals of rhodoliths (coralline red algae): a new biogenic archive. *Journal of Geophysical Research* 105: 107–116.

Halfar J., Steneck R., Joachimski M., Kronz A. & Wanamaker A.D. Jr. 2008. Coralline red algae as high-resolution climate recorders. *Geology* 36: 463–466.

Halfar J., Hetzinger S., Adey W., Zack T., Gamboa G., Kunz B., Williams B. & Jacob D.E. 2010. Coralline algal growth-increment widths archive North Atlantic climate variability. *Palaeogeography, Palaeoclimatology, Palaeoecology* 302: 71–80.

Halfar J., Williams B., Hetzinger S., Steneck R., Lebednik P.A., Winsborough C., Omar A., Chan P. & Wanamaker A.D. Jr. 2011. 225 years of Bering Sea climate and ecosystem dynamics revealed by coralline algal growth-increment widths. *Geology* 39: 579–582.

Hall-Spencer J.M. 1994. *Biological studies on nongeniculate Corallinaceae*. PhD thesis. University of London.

Hall-Spencer J.M. 1998. Conservation issues relating to maerl beds as habitats for molluscs. *Journal of Conchology Special Publication* 2: 271–286.

Hall-Spencer J.M. & Atkinson R.J.A. 1999. *Upogebia deltaura* (Crustacea: Thalassinidea) in Clyde Sea maerl beds, Scotland. *Journal of the Marine Biological Association of the UK* 79: 871–880.

Hanelt D., Tüg U., Bischof K., Groos C., Lippert U., Sawall T., Karsten U. & Wiencke C. 2001. Light regime in an Arctic fjord: a study related to stratospheric ozone depletion as a basis for determination of UV effects on algal growth. *Marine Biology* 138: 649–658.

Hansen J.R. & Jenneborg L.H. 1996. Part 7. Benthic marine algae and cyanobacteria. *Norsk Polarinstitutt, Skrifter* 198: 361–374.

Harland W.B. 1997. *The geology of Svalbard*. The Geological Society, London. 521 pp.

Heine J.N. 1989. Effects of ice scour on the structure of sublittoral marine algal assemblages of St. Lawrence and St. Matthew Islands, Alaska. *Marine Ecology Progress Series* 52: 253–260.

Hetzinger S., Halfar J., Riegl B. & Godinez-Orta L. 2006. Sedimentology and acoustic mapping of modern rhodolith facies on a non-tropical carbonate shelf (Gulf of California, Mexico). *Journal of Sedimentary Research* 76: 670–682.

Irvine L.M. & Chamberlain Y.M. 1994. *Seaweeds of the British Isles, vol. 1. Rhodophyta, part 2B Corallinales, Hildenbrandiales*. Her Majesty's Stationery Office, London. 276 pp.

Irving A.D., Cionnell S.D., Johnston E.L., Pile A.J. & Gillanders B.M. 2005. The response of encrusting coralline algae to canopy loss: an independent test of predictions on an Antarctic coast. *Marine Biology* 147: 1075–1083.

Jackson A. 2003. *Lithothamnion glaciale*. Maerl. Marine Life Information Network: Biology and Sensitivity Key Information Sub-programme [online]. Marine Biological Association of the United Kingdom, Plymouth. Available at: http://www.marlin.ac.uk/reproduction.php?speciesID=3711.

Johnson C.R. & Mann K.H. 1986. The crustose coralline alga *Phymatolithon* Foslie inhibits the overgrowth of seaweeds without relying on herbivores. *Journal of Experimental Marine Biology and Ecology* 96: 127–146.

Kain J.M. & Norton T.A. 1990. Marine ecology. In: *Biology of the red algae* (Ed. by K.M. Cole & R.G. Sheath), pp. 377–422. Cambridge University Press, New York.

Kamenos N.A. & Law A. 2010. Temperature controls on coralline algal skeletal growth. *Journal of Phycology* 46: 331–335.

Kamenos N.A., Moore P.G. & Hall-Spencer J.M. 2004a. Attachment of the juvenile queen scallop (*Aequipecten opercularis* (L.)) to maerl in mesocosm conditions; juvenile habitat selection. *Journal of Experimental Marine Biology and Ecology* 306: 139–155.

Kamenos N.A., Moore P.G. & Hall-Spencer J.M. 2004b. Small-scale distribution of juvenile gadoids in shallow inshore waters; what role does maerl play? *ICES Journal of Marine Science* 61: 422–429.

Kamenos N.A., Cusack M. & Moore P.G. 2007. Coralline algae are global palaeothermometers with bi-weekly resolution. *Geochimica et Cosmochimica Acta* 72: 771–779.

King R.J. & Schramm W. 1982. Calcification in the maerl coralline alga *Phymatolithon calcareum*, effects of salinity and temperature. *Marine Biology* 70: 197–204.

Kjellman F.R. 1883. Norra Ishafvets Algflora. *Vega-expeditionens Vetenskapliga Iaktagelser* 3: 1–431. [Note: Subsequently published in English (Kjellman 1885).]

Kjellman F.R. 1885. The algae of the Arctic Sea. *Kongliga Svenska Vetenskaps-Akademien Handligar* 20: 1–350. [Note: Dated 1883 but first published in 1885. The original version (Kjellman 1883) is written in Swedish.]

Konar B., Riosmena-Rodriguez R. & Iken K. 2006. Rhodolith bed: a newly discovered habitat in the North Pacific Ocean. *Botanica Marina* 49: 355–359.

Kühl M., Glud R.N., Borum J., Roberts R. & Rysgaard S. 2001. Photosynthetic performance of surface-associated algae below sea ice as measured with a pulse-amplitude-modulated (PAM) fluorometer and O_2 microsensors. *Marine Ecology Progress Series* 223: 1–14.

Lherminier P., Meincke J., Freiwald A. & Schauer J. 2006. Circulation and ecosystems in the subpolar and polar North Atlantic, Cruise No. 2, May 23–September 16, 2006. *MARIA S. MERIAN-Berichte* 9(1). Universität Hamburg. 176 pp.

Lieberman M., John D.M. & Lieberman D. 1979. Ecology of subtidal algae on seasonally devastated cobble substrates off Ghana. *Ecology* 60: 1151–1161.

Littler M.M. & Kauker B.J. 1984. Heterotrichy and survival strategies in the red alga *Corallina officinalis*. L. *Botanica Marina* 27: 37–44.

Littler M.M., Littler D.S. & Taylor P.R. 1983. Evolutionary strategies in a tropical barrier reef system: functional-form groups of marine macroalgae. *Journal of Phycology* 19: 229–237.

Lüning K. 1990. *Seaweeds. Their environment, biogeography and ecophysiology*. Wiley Interscience, New York. 527 pp.

Lüning K., Schmitz K. & Willenbrink J. 1973. CO_2 fixation and translocation in benthic marine algae. III. Rates and ecological significance of translocation in *Laminaria hyperborea* and *L. saccharina*. *Marine Biology* 23: 275–281.

Lüder U.H., Wiencke C. & Knoetzel J. 2002. Acclimation of photosynthesis and pigments during and after six months of darkness in *Palmaria decipiens* (Rhodophyta): a study to simulate Antarctic winter sea ice cover. *Journal of Phycology* 38: 904–913.

Martin S., Rodolfo-Metalpa R., Ransome E., Rowley S., Buia M.C., Gattuso J.P. & Hall-Spencer J. 2008. Effects of naturally acidified seawater on seagrass calcareous epibionts. *Biology Letters* 4: 689–692.

Matsuda S. & Iryu Y. 2011. Rhodoliths from deep fore-reef to shelf areas around Okinawa-jima, Ryukyu Islands, Japan. *Marine Geology* 282: 215–230.

Milliken B. & Steneck R.S. 1981. The branching morphology of crustose corallines as a structural defence against herbivores and a refuge for filamentous algae. In: *Abstracts of papers and posters to be presented at the 20th Northeast Algal Symposium,* Marine Biological Laboratory, Woods Hole, MA, USA, April 11–12, 1981, p. 16 (abstract only).

Orr J.C., Fabry V.J., Aumont O., Bopp L., Doney S.C., Feely R.M., Gnanadesikan A., Gruber N., Ishida A., Joos F., Key R.M., Lindsay K., Maier-Reimer E., Matear R., Monfray P., Mouchet A., Najjar R.G., Plattner G.K., Rodgers K.B., Sabine C.L., Sarmiento J.L., Schlitzer R., Slater R.D., Totterdell I.J., Weirig M.F., Yamanaka Y. & Yool A. 2005. Anthropogenic ocean acidification over the twenty-first century and its impact on calcifying organisms. *Nature* 437: 681–686.

Orvik K.A. & Niiler P. 2002. Major pathways of Atlantic water in the northern North Atlantic and Nordic Seas towards Arctic. *Geophysical Research Letters* 29: 1896–1899.

Padilla D.K. 1984. The importance of form: differences in competitive ability, resistance to consumers and environmental stress in an assemblage of coralline algae. *Journal of Experimental Marine Biology and Ecology* 79: 105–127.

Perry C.T. 2005. Morphology and occurrence of rhodoliths in siliciclastic intertidal environments from a high latitude reef setting, southern Mozambique. *Coral Reefs* 24: 201–207.

Riul P., Lacouth P., Pagliosa P.R., Christoffersen M.L. & Horta P.A. 2009. Rhodolith beds at the easternmost extreme of South America: community structure of an endangered environment. *Aquatic Botany* 90: 315–320.

Roberts R.D., Kühl M., Glud R.N. & Rysgaard S. 2002. Primary production of crustose coralline red algae in a high Arctic fjord. *Journal of Phycology* 38: 273–283.

Rosenvinge L.K. 1893. Grønlands Havalger. *Meddelelser om Groenland* 3: 765–981.

Sapota G., Wojtasik B., Burska D. & Nowiński K. 2009. Persistent organic pollutants (POPs) and polycyclic aromatic hydrocarbons (PAHs) in surface sediments from selected fjords, tidal plains and lakes of the north Spitsbergen. *Polish Polar Research* 30: 59–76.

Schäfer P., Fortunato H., Bader B., Liebetrau V., Bauch T. & Reijmer J.J.G. 2011. Growth rates and carbonate production by coralline red algae in upwelling and non-upwelling settings along the Pacific coast of Panama. *Palaios* 26: 420–432.

Schwarz A.M., Hawes I., Andrew N., Mercer S., Cummings V. & Trush S. 2005. Primary production potential of non-geniculate coralline algae at Cape Evans, Ross Sea, Antarctica. *Marine Ecology Progress Series* 294: 131–140.

Sneed E.D. & Folk R.L. 1958. Pebbles in the lower Colorado River, Texas. A study in particle morphogenesis. *Journal of Geology* 66: 114–150.

Sousa W.P. 1979. Experimental investigations of disturbance and ecological succession in a rocky intertidal algal community. *Ecological Monographs* 49: 227–254.

Spreen G., Kaleschke L. & Heygster G. 2008. Sea ice remote sensing using AMSR-E 89-GHz channels. *Journal of Geophysical Research* 113, C02S03, DOI:10.1029/2005JC003384.

Steinacher M., Joos F., Frölicher T.L., Plattner G.-K. & Doney S.C. 2009. Imminent ocean acidification in the Arctic projected with the NCAR global coupled carbon cycle-climate model. *Biogeosciences* 6: 515–533.

Steller D.L., Riosmena-Rodriguez R., Foster M.S. & Roberts C.A. 2003. Rhodolith bed diversity in the Gulf of California: the importance of rhodolith structure and consequences of disturbance. *Aquatic Conservation – Marine and Freshwater Ecosystems* 13: 5–20.

Steneck R.S. 1982. A limpet-coralline algal association: adaptations and defenses between a selective herbivore and its prey. *Ecology* 63: 507–522.

Steneck R.S. 1986. The ecology of coralline algal crusts: convergent patterns and adaptive strategies. *Annual Review of Ecology and Systematics* 17: 273–303.

Watson D.C. & Norton T.A. 1985. The physical characteristics of seaweed thalli as deterrents to littorine grazers. *Botanica Marina* 28: 383–387.

Wiencke C., Clayton M.N., Gómez L., Iken K., Lüder U.H., Amsler C.D., Karsten U., Hanelt D., Bischof K. & Dunton K. 2007. Life strategy, ecophysiology and ecology of seaweeds in polar waters. *Reviews in Environmental Science and Biotechnology* 6: 95–126.

Wilson S., Blake C., Berges J.A. & Maggs C.A. 2004. Environmental tolerances of free-living coralline algae (maerl): implications for European marine conservation. *Biological Conservation* 120: 279–289.

Received 25 July 2011; accepted 10 October 2011
Associate Editors: Adele Harvey and Alan Millar

4.4 Thecosome pteropods

4.4.1 Publication III

Impact of Ocean Acidification and Elevated Temperatures on Early Juveniles of the Polar Shelled Pteropod *Limacina helicina*: Mortality, Shell Degradation, and Shell Growth.

Second-author (first- and second author had equal contribution to the publication), published in Biogeosciences

Biogeosciences, 8, 919–932, 2011
www.biogeosciences.net/8/919/2011/
doi:10.5194/bg-8-919-2011

Biogeosciences

Impact of ocean acidification and elevated temperatures on early juveniles of the polar shelled pteropod *Limacina helicina*: mortality, shell degradation, and shell growth

S. Lischka, J. Büdenbender, T. Boxhammer, and U. Riebesell

Leibniz-Institute for Marine Sciences (IFM-GEOMAR), Kiel, Germany

Received: 27 October 2010 – Published in Biogeosciences Discuss.: 5 November 2010
Revised: 11 April 2011 – Accepted: 12 April 2011 – Published: 15 April 2011

Abstract. Due to their aragonitic shell, thecosome pteropods may be particularly vulnerable to ocean acidification driven by anthropogenic CO_2 emissions. This applies specifically to species inhabiting Arctic surface waters that are projected to become temporarily and locally undersaturated with respect to aragonite as early as 2016. This study investigated the effects of rising partial pressure of CO_2 (pCO_2) and elevated temperature on pre-winter juveniles of the polar pteropod *Limacina helicina*. After a 29 day experiment in September/October 2009 at three different temperatures and under pCO_2 scenarios projected for this century, mortality, shell degradation, shell diameter and shell increment were investigated. Temperature and pCO_2 had a significant effect on mortality, but temperature was the overriding factor. Shell diameter, shell increment and shell degradation were significantly impacted by pCO_2 but not by temperature. Mortality was 46% higher at 8 °C than at in situ temperature (3 °C), and 14% higher at 1100 µatm than at 230 µatm. Shell diameter and increment were reduced by 10 and 12% at 1100 µatm and 230 µatm, respectively, and shell degradation was 41% higher at elevated compared to ambient pCO_2. We conclude that pre-winter juveniles will be negatively affected by both rising temperature and pCO_2 which may result in a possible decline in abundance of the overwintering population, the basis for next year's reproduction.

1 Introduction

Anthropogenic CO_2 emissions affect the seawater carbonate chemistry and cause a decrease of seawater pH (termed ocean acidification) and carbonate ions in the worlds' oceans, thereby also diminishing the saturation state of seawater with respect to calcite and aragonite. This effect is strongest in high-latitude surface waters, which are also experiencing the steepest increase in surface ocean temperature (Orr et al., 2005; Steinacher et al., 2009). Due to increasing CO_2 emissions since the industrial revolution, global mean surface temperatures have risen by 0.76 °C and global mean seawater pH has decreased by 0.1 unit (IPCC, 2007).

Calcite and aragonite are two common types of calcium carbonate secreted by marine organisms. Surface waters of the Arctic are specifically affected by carbonate undersaturation due to the high solubility of CO_2 in cold waters, for example in the Canada Basin, undersaturation with respect to aragonite was already detected in 2008 (Steinacher et al., 2009; Yamamoto-Kawai et al., 2009).

Changes in the carbonate chemistry can have severe consequences for marine organisms, particularly to those that build skeletons, shells, and tests of biogenic calcium carbonate. For instance, reduced calcification rates in corals, coralline macroalgae, coccolithophorids, bivalves, and echinoderms have been reported during the last years as a consequence of rising CO_2 partial pressures (e.g. Gattuso et al., 1999; Riebesell et al., 2000; Gazeau et al., 2007; Fabry et al., 2008). On contrast, a recent study by Gutowska et al. (2010) revealed increased calcification in the cuttlebone of the cephalopod *Sepia officinalis* during exposure to elevated CO_2 partial pressures. Hence, organisms' response of calcification to carbonate system variations is diverse.

A widely held view, as articulated by Wilson (1973), has been that "*living things during early developmental stages are more sensitive than at any other time in their life cycle to adverse influences in the environment*". Also with respect to ocean acidification, several studies corroborate this view in that early developmental and reproductive stages of calcifiers are the most vulnerable stages within a life cycle (e.g. Kurihara et al., 2007; Kurihara, 2008; Clark et al., 2009;

Correspondence to: S. Lischka
(slischka@ifm-geomar.de)

Comeau at al., 2010a). These authors reported, for example, on retarded larval development, reduced shell mineralization/calcification, increased mortality and degradation of larval skeleton in sea urchin and pteropod larvae, respectively. Acting on early developmental and reproductive stages, ocean acidification can have a direct impact on the size of the population, reduce fitness and increase mortality of the offspring (Kurihara, 2008). Thus it can lead to changes in species distribution and abundances that could propagate through multiple trophic levels of the marine food web (Guinotte and Fabry, 2008).

Thecosome pteropods are widely distributed small-sized holoplanktonic marine mollusks. While their species diversity is high in tropical regions, only two epipelagic species, both of the genus *Limacina*, occur in temperate areas of the North Atlantic and in Arctic regions (van der Spoel, 1967). In northern and polar regions, pteropods can dominate zooplankton communities at times and are key species in epipelagic food webs both as consumers of and prey for various marine organisms, including commercially important fish, seabirds and baleen whales (Gilmer and Harbison, 1991; Falk-Petersen et al., 2001; Karnovsky et al., 2008).

Shelled pteropods of the genus *Limacina* (*L. helicina*, *L. retroversa*) also contribute significantly to vertical fluxes of both organic matter and biogenic calcium carbonate (Berner and Honjo, 1981; Bathmann et al., 1991; Hunt et al., 2008). Furthermore, thecosomes have a very thin and fragile shell made of aragonite, a particularly soluble form of calcium carbonate, and are the main planktonic producers of aragonite in the worlds' oceans (Lalli and Gilmer, 1989; Seibel et al., 2007). Due to the chemical structure of their shell, pteropods are expected to be among the first major group of calcifying organisms to be adversely effected by undersaturation in $CaCO_3$ (Orr et al., 2005; Seibel et al., 2007). Hence, due to its polar distribution, this will specifically apply to *Limacina helicina*.

In Svalbard waters *Limacina helicina* has a one-year life cycle. It develops to adults in early summer, and after reproduction in July/August their veligers grow to juveniles that overwinter until the next spring before development is completed (Gannefors et al., 2005; Lischka unpublished data). To cope with the high seasonality of food supply, many polar organisms reduce their metabolism to save energy and/or live on their energy reserves during winter (e.g. Hirche, 1996; Hagen and Auel, 2001; Lee et al., 2006). As for *L. helicina* it is not clear whether or not it lowers its metabolism during overwintering and, if it does, to what extent. Juveniles accumulate lipids and probably utilize them during the dark period (Gannefors et al., 2005). Hence with respect to ocean acidification, *L. helicina* will have to withstand the most threatened period in a presumably vulnerable life stage and time.

Recently, the response to elevated partial pressure of CO_2 (pCO_2) of adult *L. helicina* was investigated by Comeau et al. (2009, 2010b). In the later study, calcification was reduced as a function of pCO_2 at control and elevated temperature, whereas respiration was unaffected at control temperature but increased significantly as a function of pCO_2 at higher temperature. Hence, temperature can be a contributing factor to a species' response to changing pCO_2. In another investigation, Comeau and co-workers studied larvae of the mediterranean species *Cavolinia inflexa* and reported on malformations, reduced shell growth and even shell-less, though still alive, larvae grown under low pH, respectively (Comeau et al., 2010a).

Furthermore, studies of pteropod shells collected in deep-sea sediment and traps provide evidence that shell integrity is lost with increasing degree of dissolution (Almogi-Labin et al., 1986; Acker and Byrne, 1989; Haddad and Droxler, 1996; Gerhardt et al., 2000; Manno et al., 2007). However, it is not possible from these findings to conclude on the effect of undersaturated waters on the shell of living pteropods. In fact, shell dissolution in live pteropods (*Clio pyramidata*) has so far only been described by Orr et al. (2005) by a coincidental observation and in larvae of *Cavolinia inflexa* by Comeau et al. (2010a).

The present paper reports on the first experimental study that focuses on the combined effects of ocean acidification and elevated temperature on juveniles of the pteropod *L. helicina* from the Arctic Kongsfjord (Svalbard) prior to the overwintering period (mid September to end of October 2009). To study the synergistic effects of elevated pCO_2 and temperature, incubation experiments were carried out at three different temperatures and four pCO_2 partial pressures to qualitatively assess the impact on species mortality, shell degradation, and shell growth. Levels of pCO_2 chosen cover a range from pre-industrial values to levels projected to occur within this century (according to the A2 scenario in the report of the Intergovernmental Panel on Climate Change, IPCC, 2007). The combination of three temperatures and four pCO_2 levels permitted conclusions regarding the separate, as well as combined, effects of temperature and CO_2.

2 Material and methods

2.1 Field sampling of pteropods

Juvenile *Limacina helicina* (Pteropoda, Thecosomata) were collected in Kongsfjord (northwest Spitsbergen) between 21 and 23 September 2009 using a plankton net (70 µm mesh size, 0.2 m^2 mouth opening, 1 l plastic cod end) onboard R/V *Teisten*. Integrated vertical hauls were taken in the deepest accessible part of the fjord from 300 or 200 m depth to the surface to allow collection of the deeper living overwintering individuals (Fig. 1). Onboard, freshly collected pteropods were stored in 20 l plastic containers in ambient seawater, and immediately transported to the Kings Bay Marine Laboratory where they were transferred into filtered seawater. About 200 individuals were caught per haul, less than 5% were damaged

due to collection. In the laboratory, specimens were kept for 1 to 2 days at in situ temperature (approximately 3 °C) in 1 µm filtered seawater until the start of experiments. Seawater supplied in the Marine Laboratory was pumped at 80 m depth from Kongsfjord and filtered through 20 µm filters. For experimental purpose, seawater was additionally filtered through Whatman GF/B filters (approximately retaining particles larger than 1 µm). Furthermore, to characterize abiotic parameters, depth, temperature, and salinity were measured with a STD/CTD model SD-204 (SAIV A/S, Bergen, Norway) prior to each sampling event.

2.2 Calcein staining

For qualitative assessment of shell growth under different temperature and pCO_2 conditions, pteropods were stained in a calcein bath (50 mg l^{-1}) for 1 h prior to incubation at experimental conditions. After staining, animals were rinsed with filtered seawater four times to remove excessive dye. Only actively moving individuals were taken for the experiments. Under UV-light, calcein has its fluorescence maximum at 515 nm (green) and marks the aperture margin at the time of staining (Comeau et al., 2009).

2.3 Experimental setup

In order to simulate past, present and future carbonate chemistries (atmospheric pCO_2 levels), GF/B filtered seawater was bubbled with air enriched with CO_2 using gas mixing pumps (Wösthoff, Germany) to CO_2 levels of 180, 380, 750 and 1150 ppm pCO_2 (target values) in storage containers at three temperatures (3, 5.5, and 8 °C). Temperatures were chosen according to a projected 1–2 °C temperature increase for the upper 100–200 m of the Arctic ocean (Steinacher et al., 2009). The natural temperature range of *Limacina helicina* goes from −0.4 °C to +4 °C, infrequently up to 7 °C (van der Spoel, 1967). Hence, experimental temperatures are within its natural range (3 and 5.5 °C) and according to a projected 2 °C increase slightly above the upper temperature limit (8 °C). Six replicates were set up for each of the twelve treatment combinations. Prior to pipetting 10 optically clean and actively moving juvenile *L. helicina* into each of the 440 ml jars (= one replicate), 5 ml filtered seawater were put in the jars to accommodate pteropods before filling the jars with the manipulated seawater. The whole procedure was done on crushed ice. After completion of all replicates of one temperature treatment (6 replicates × 4 pCO_2 levels = 24 jars), jars were filled with the manipulated seawater at treatment temperature, closed with an air-tight lid and stored in a water bath in a climate room at the experimental temperature. Incubations were performed in darkness in order to mimic the conditions at the depth of collection. Directly before filling experimental jars with manipulated seawater, water samples of each of the CO_2 manipulated seawater storage containers were taken for total alkalinity (A_T) and nutrients

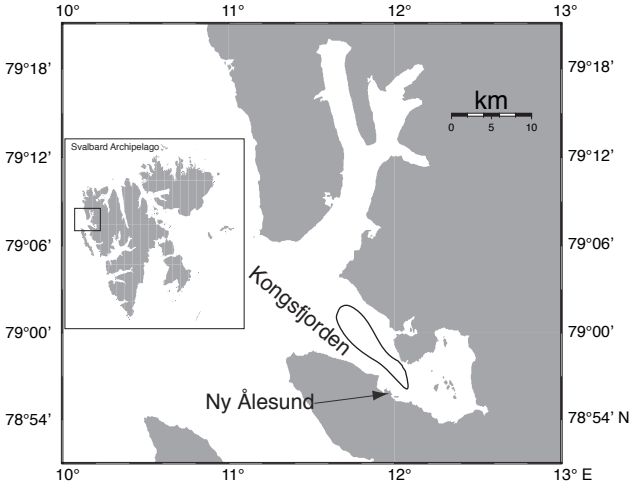

Fig. 1. Map of Kongsford highlighting the sampling area.

and pH on the total scale (pH_T) was measured (see below). Nutrient samples were immediately deep-frozen (−20 °C) whereas A_T samples were poisoned with $HgCl_2$ and stored at 4 °C (Dickson et al., 2007). After 29 days the experiment was terminated. Before harvesting juvenile *Limacina helicina*, pH_T was measured in each jar and water samples for A_T and nutrient analyses were taken. Subsequently, juveniles were collected from the jars and inspected for survival/mortality under a stereomicroscope and after rinsing in Milli-Q water, live (actively moving) individuals were preserved in 70% EtOH until inspection for shell degradation state and shell increment. Additionally, fjord water samples were taken for in situ A_T, dissolved inorganic carbon (C_T) and nutrient measurements.

2.4 Analyses of the carbonate chemistry

pH on the total scale was calculated from voltage readings according to SOP6a in Dickson et al. (2007). Instead of using TRIS buffers we used certified reference material (CRM) with a known pH calculated from known A_T and C_T (Prof. A. Dickson, Scripps Institution of Oceanography, La Jolla, California) as standard. Measurements were performed using a pH Mobile 826 pH meter (Metrohm, Switzerland), precision was within 0.2 mV units.

Total alkalinity (A_T) was determined using a potentiometric titration device (Titrando 808, Metrohm; Bradshaw et al., 1981). A_T was calculated from the Gran function as described by Dickson et al. (2003). The accuracy was determined by measuring CRM's as described for the pH measurements and precision was within 2 µmol kg^{-1} (max. difference between two replicate measurements). For fjord water, dissolved inorganic carbon (C_T) was quantified with continuous-flow analysis (Bran & Luebbe QUAATRO photometer) according to Stoll et al. (2001). A_T accuracy was between 1 to 15 µmol kg^{-1} (differences between measured

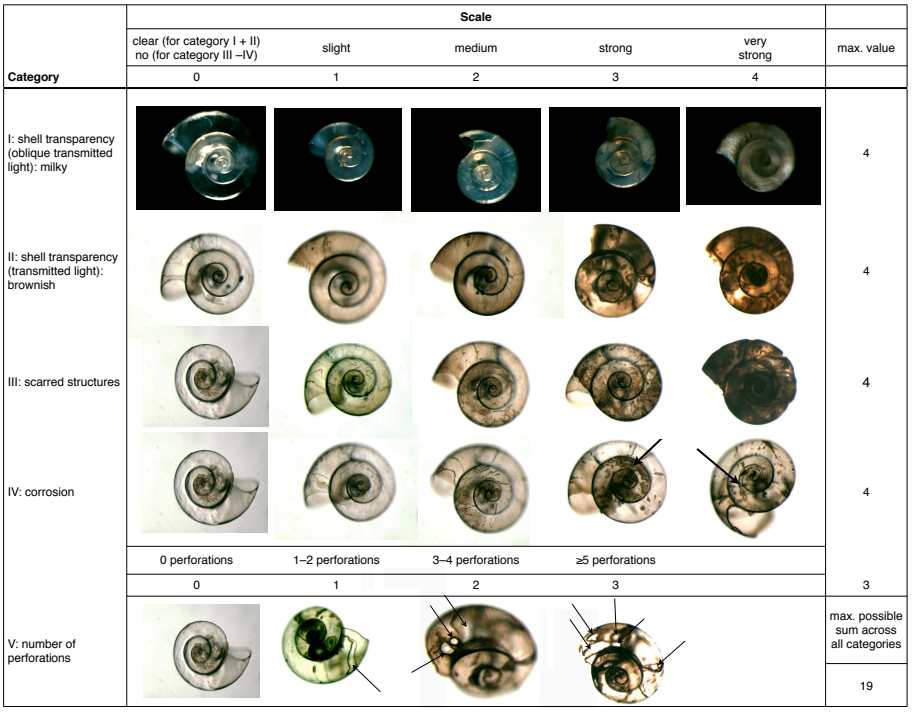

Fig. 2. Categories of shell degradation (I to V) and their levels of conspicuities on a scale from 0 to 4 (for category I to IV) and 0 to 3 (for category V). Examples for each level and its associated score in each category are shown. See also Figure 3 for category IV and V.

and target A_T in the CRM's from A. Dickson et al. (2003) depending on prepared solutions and temperatures etc.) and C_T accuracy was between 40 to 50 µmol kg^{-1}. Remaining carbonate system parameters for the experiments and fjord were calculated from A_T and pH, and A_T and C_T, respectively with the free software CO2SYS (Pierrot and Wallace, 2006) using the constants from Mehrbach et al. (1973) refitted by Dickson and Millero (1987). Nutrients were analyzed according to Koroleff and Grasshof (1983).

CO_2 partial pressures at the start of the experiment differed slightly between replicates of the same CO_2 level, with consistently lower values at lower temperatures. This difference is attributed to temperature dependent equilibration rates, which increase with increasing temperature. Apparently three days of bubbling with CO_2/air gas mixtures were insufficient to achieve full equilibration of the medium.

2.5 Mortality

After termination of the experiment, all juvenile *Limacina helicina* were inspected for survival under a stereomicroscope. For this, individuals were categorized optically into five different stages of activity (I = highest activity, V = no activity, identified as dead)

- Stage I: animal expanded, actively moving, soft tissue appears clear and in good condition
- Stage II: animal retracted, actively moving inside shell, soft tissue appears clear and in good condition
- Stage III: animal retracted, no discernable active movements, but soft tissue appears clear and in good condition, individual most likely alive
- Stage IV: animal retracted, no discernable movements, soft tissue appears decomposed, individual most likely dead
- Stage V: animal retracted, soft tissue appears strongly decomposed, individual clearly dead.

For statistical evaluation stages I–III (alive) and IV–V (dead) were pooled.

2.6 Shell degradation

The soft tissue was removed with chlorine bleach (24 h at room temperature) prior to analyzing shell degradation and growth (see below).

Shell integrity of all surviving individuals of all replicates was examined for surface degradation under a stereomicroscope (Leica MZ 16 F). Pteropod shells lose their integrity with increasing dissolution (e.g. Almogi-Labin et al., 1986; Gerhardt et al., 2000). Similar to Gerhardt et al. (2000), shell degradation was qualitatively described according to five categories, which are briefly described in the following (Fig. 2):

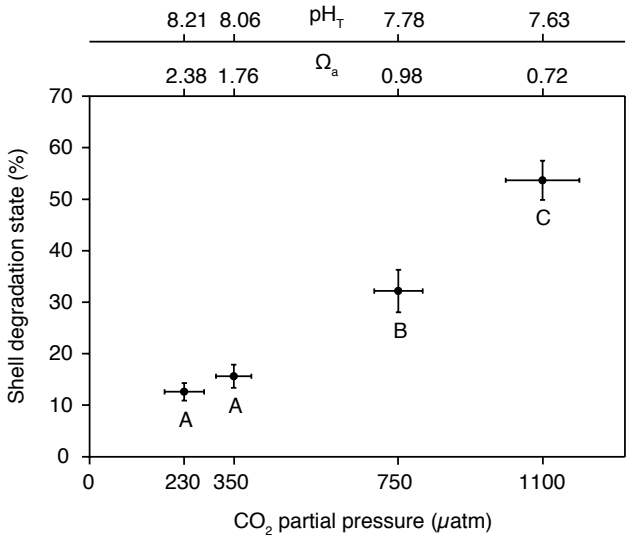

Fig. 3. Percent shell degradation of *Limacina helicina* after 29 days of incubation. Mean for the effect of pCO_2. Vertical bars denote 0.95 confidence intervals for shell degradation while horizontal bars denote 0.95 confidence intervals for pCO_2. Results from PERMANOVA pair-wise tests are depicted by letters with levels not connected by same letter being significantly different.

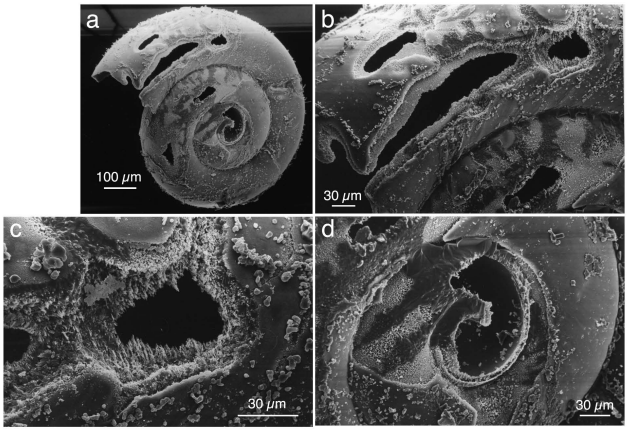

Fig. 4. Scanning electron micrographs (SEM) of representative *Limacina helicina* reared at 3 °C and 1100 µatm to illustrate shell degradation state specifically with respect to category IV and V. Magnification and scale bars are shown. The individual shown is the same as the one shown in Table 1 for category V with ≥ 5 perforations.

– Category I: Shell transparency (applying oblique transmitted light with mirror in an acute angle to the source of light). Shells were evaluated according to their transparency under oblique transmitted light. The scale extends from total transparency/clearness to different states of milky and cloudy shells, respectively.

– Category II: Shell transparency (applying transmitted light, with mirror in an obtuse angle to the source of light). Using transmitted light, shells appear brownish to various extents.

– Category III: Scarred structures. Category III describes the frequency of scarred structures of any kind.

– Category IV: Corrosion. Category IV describes the deepness of scarred structures in the shell that can be estimated by focusing the stereomicroscope, hence category IV describes the severity of corrosion.

– Category V: Perforation. In this category the number of holes in the shell is considered.

The condition of a single shell according to the different categories was described on a scale from 0 to 4 for categories I to IV and 0 to 3 for category V. The maximum possible sum of the five categories was 19 for a single shell. The maximum value was calculated for all inspected shells and graphically depicted as percentage of maximum possible surface degradation (see Fig. 3). For statistical evaluation, raw scores for each category were used (see below). In some cases, shells were mechanically damaged during processing. However, perforations due to corrosion can usually be distinguished from those resulting from mechanical damage. Therefore, only those perforations were counted in category V that could be identified as non-mechanical. Hence, shell surface degradation with respect to category V is underestimated.

Additionally, selected shells were examined by Scanning Electron Microscope (CamScan-CS-44, Institute of Geosciences, Kiel University) to illustrate shell degradation state in categories IV and V (Fig. 4).

2.7 Analysis of shell growth

Shell growth estimated from calcein staining was measured on a Leica MZ 16 F stereomicroscope equipped with a UV-epifluorescence lamp and the Leica Application Suite 3.5.0. To standardize for individual size differences, not only the shell increment was measured but also the shell diameter and the ratio of shell increment to shell diameter was used for comparison between temperature treatments and CO_2 levels. One individual of each of the 6 replicates was analyzed (Fig. 5).

2.8 Statistics

Multifactorial analysis was performed to test for significant effects of the factors temperature and pCO_2 on mortality, shell diameter and the ratio of shell increment to shell diameter using a general linear model Type IV (GLM) for equal sample size in case of mortality and a GLM Type III model for unequal sample size in case of shell diameter and shell increment/diameter. Percentage data of mortality

Table 1. Mean carbonate system parameters calculated from samples taken from the prepared manipulated seawater at start and from all experimental jars at the end of the experimental period. The treatment column refers to target temperature and pCO_2, of which the pCO_2 levels refer to glacial partial pressure CO_2 (180 µatm, 18 kyr BC), present day pCO_2 (380 µatm, year 1990), high pCO_2 I (750 µatm, year 2080), and high pCO_2 II (1150 µatm, > year 2100). The concentration of total CO_2 (C_T), partial pressure of CO_2 (pCO_2), and the saturation state of aragonite (Ω_a) were derived from pH_T, total alkalinity (A_T), salinity (S) and temperature (T). Si is silicate.

Treatment		S	T (°C)		A_T (µmol kg^{-1})		pH_T		C_T (µmol kg^{-1})		pCO_2 (µatm)		Ω_a		Si (µmol g^{-1})	
T (°C)	pCO_2 (µatm)		start	end	start	end	start	end	start	end	start	end	start	end	start	end
3	180	34.7	3.5	3.6	2280	2288	8.27	8.28	2045	2047	216	211	2.45	2.51	2.63	6.49
	380	34.7	3.3	3.5	2280	2287	8.12	8	2115	2164	323	435	1.81	1.45	2.63	7.27
	750	34.7	3.1	3.6	2280	2291	7.81	7.78	2223	2241	703	764	0.95	0.91	2.63	11.82
	1150	34.7	3	3.5	2280	2296	7.69	7.62	2260	2291	948	1110	0.72	0.65	2.63	11.25
5.5	180	34.7	5.4	5.4	2280	2288	8.24	8.09	2041	2118	231	347	2.5	1.87	2.63	3.47
	380	34.7	5.5	5.4	2280	2295	8.09	8.03	2111	2150	348	411	1.86	1.65	2.63	8.91
	750	34.7	5.6	5.4	2280	2293	7.8	7.74	2215	2246	732	851	1.02	0.9	2.63	4.38
	1150	34.7	5.6	5.4	2280	2299	7.66	7.63	2256	2283	1026	1104	0.76	0.71	2.63	12.28
8	180	34.7	8	7.6	2280	2290	8.26	8.12	2012	2092	223	322	2.8	2.15	2.63	7.3
	380	34.7	7.9	7.6	2280	2293	8.11	8	2086	2146	333	445	2.11	1.68	2.63	15.22
	750	34.7	7.9	7.5	2280	2302	7.81	7.73	2199	2247	711	876	1.15	0.96	2.63	16.18
	1150	34.7	8.1	7.5	2280	2305	7.62	7.58	2256	2297	1138	1279	0.77	0.69	2.63	16.46
Fjord (200 m)		35	3.9	4.3	2296	2287	7.98	8.03	2174	2145	448	398	1.45	1.61	3.27	3.13

were arcsin transformed, and values for the ratio shell increment/diameter were Box-Cox transformed ($\lambda = 2.467508$). Data were tested for normality (Shapiro-Wilks test). In case of significant effects of temperature and/or pCO_2, homogeneity of variances was tested with Levene's test. To determine significant differences between temperature and pCO_2 treatments, respectively, a post-hoc Tukey's honest significant difference test (HSD or HSD for unequal n, respectively) with α-level 0.05 was used.

Raw scores for each shell degradation category as well as the compound score for shell degradation were analyzed using non-metric multidimensional scaling (NMDS). PERMANOVA was applied using all five shell degradation categories as response variables to test for significant effects of the factors temperature and pCO_2 and possible interactions between factors. For NMDS and PERMANOVA Euclidean Distance was used to create a resemblance matrix. PERMANOVA was conducted according to a two-way crossed design (factors being temperature and pCO_2) with type III partitioning of the sums of squares. Permutation of residuals under a reduced model was applied based on 9999 permutations to obtain the P-value, α-level was 0.05.

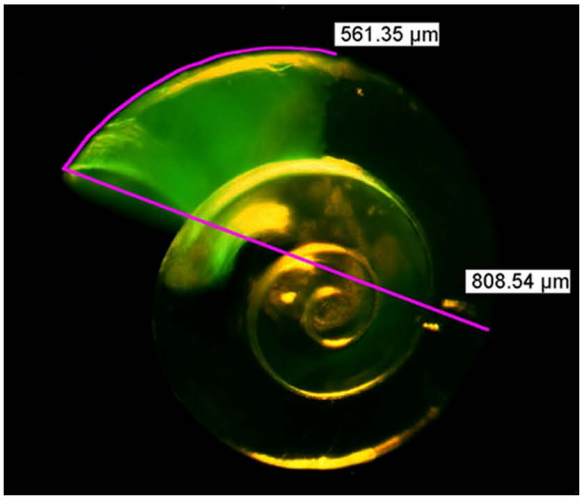

Fig. 5. Calcein stained shell of *Limacina helicina* showing shell increment during the experiment and measurement of increment length and diameter.

Statistics were carried out using Statistica version 8 (Statsoft) and PRIMER 6 (including PERMANOVA+, PRIMER-e Ltd), respectively.

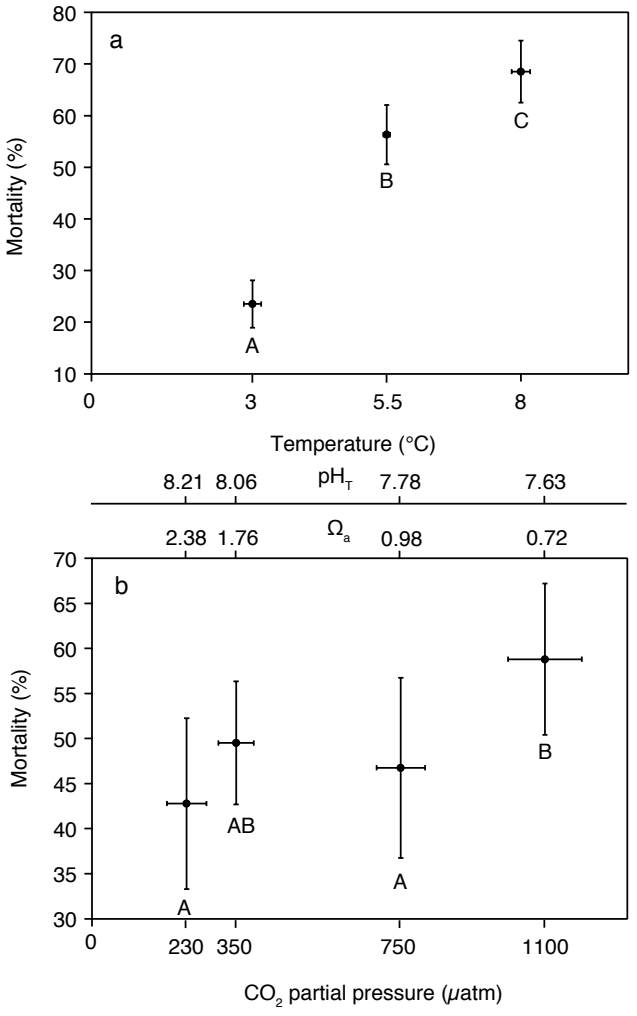

Fig. 6. Percent mortality after 29 days of incubation of *Limacina helicina*. Means for the effects of temperature **(a)** and pCO_2 **(b)**. Vertical bars denote 0.95 confidence intervals for mortality, horizontal bars denote 0.95 confidence intervals for temperature and pCO_2, respectively. Results from the Tukey HSD post-hoc test are depicted by letters with levels not connected by same letter being significantly different.

3 Results

3.1 Carbonate system

Carbonate chemistry conditions of the fjord (pCO_2 of 448 $\pm$15 µatm) were roughly simulated in the 380 µatm treatment as revealed by A_T, C_T and temperature (Table 1). Compared to in situ conditions the 180 µatm treatment had an increased pH level and Ω_a whereas the CO_2 enriched treatments had diminished pH levels and subsaturated Ω_a conditions. At the end of the experiment, CO_2 partial pressures were higher compared to initial partial pressures. Accordingly pH and Ω_a levels were lower and pCO_2 was higher. Interestingly, also A_T values were slightly higher.

Table 2. Univariate tests of significance indicating the effect of temperature and pCO_2 on mortality. Significant results are represented in bold.

Effect	SS	df	MS	F	p
Intercept	84.734	1	84.734	1362.562	0.000
Temp	7.469	2	3.735	60.055	**0.000**
pCO_2	1.088	3	0.363	5.831	**0.0009**
Temp × pCO_2	0.442	6	0.074	1.184	0.32
Error	8.209	132	0.062		

In the following, pCO_2 values (µatm) shown in figures are the means of values measured at experimental start.

3.2 Mortality

Temperature and pCO_2 both had a significant effect on mortality of *Limacina helicina* ($F = 60.055$, $p < 0.0001$ and $F = 5.831$, $p = 0.0009$, respectively) (Table 2). However, the temperature effect was stronger than the pCO_2 effect (Fig. 6a and b). There were no interactions between both factors ($F = 1.184$, $p = 0.32$). Tukey HSD post-hoc test showed mortality to be significantly higher at 5.5 °C and 8 °C ($p < 0.0001$ and $p < 0.0001$, respectively) than at in situ temperature (3 °C) (Fig. 6a). Moreover, mortality was significantly higher at 8 °C than at 5.5 °C ($p = 0.03$). pCO_2 caused a significantly higher mortality at 1100 µatm as compared to 230 and 750 µatm ($p < 0.0001$ and $p = 0.03$, respectively) (Fig. 6b), however, the mortality at 1100 µatm did not significantly differ from 350 µatm ($p = 0.10$).

3.3 Shell degradation

Ordination of the raw scores for each degradation category and the compound score by non-metric multidimensional scaling (NMDS) revealed differences in the effect size and direction of the factors temperature and pCO_2. Furthermore, sizes and/or directions of factor effects were different within different levels of the other factor, thus implying interactions between both factors. Distances between data clouds showed that the effect size of the factor pCO_2 was generally clearer and larger than the effect size of the factor temperature (Fig. 7). However, a temperature effect was specifically distinct for category V (perforation), where temperature has a clear and large effect within level four (1100 µatm) of factor pCO_2 (Fig. 7e). Moreover, temperature effects within all levels of factor pCO_2 were larger in categories III, IV and V (scarred structures, corrosion, perforation) as compared to categories I, II (milky, brownish) and the compound value for all categories.

Statistical significance of factor effects was determined applying PERMANOVA. PERMANOVA revealed a significant

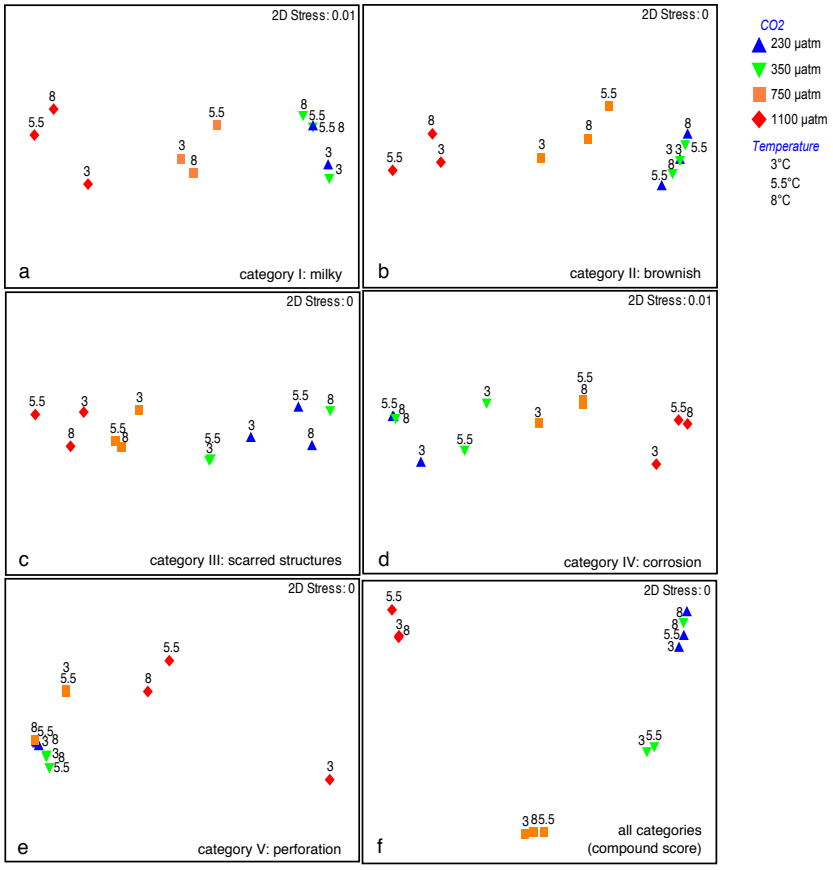

Fig. 7. MDS ordination of shell degradation categories with labels for the two-way crossed design: analyses of raw scores for each category (**a** to **e**) and of the compound value of all categories **(f)**. 2-D stress is the goodness of the representation, i.e. a stress of < 0.05 gives an excellent representation with no prospect of misinterpretation.

Table 3. PERMANOVA using all five shell degradation categories as response variables indicating the effect of temperature and pCO_2 on shell degradation. Significant results are represented in bold.

Source	df	SS	MS	Pseudo-F	P (perm)	Unique perms
Temperature	2	2.306	1.153	1.150	0.320	9938
pCO_2	3	146.03	48.678	48.565	**0.0001**	9947
Temp × pCO_2	6	9.560	1.593	1.590	0.095	9936
Res	60	60.139	1.002			
Total	71	220.36				

effect of pCO_2 on shell degradation (Pseudo-F = 48.565, P (perm) = 0.0001; Table 3). The effect of temperature was not statistically significant (Pseudo-F = 1.1501, P (perm) = 0.32), and no significant interaction between both factors was found (Pseudo-F = 1.59, P (perm) = 0.095). Pairwise tests for the factor pCO_2 showed significant differences in shell degradation between all level combinations of pCO_2 (P (perm) = 0.0001) except for the pair 230/350 µatm (P (perm) = 0.361) (Table 4, Fig. 3).

3.4 Shell growth

Univariate test of significance revealed a significant effect of pCO_2 on shell diameter (F = 4.955, df = 3, $p = 0.003$) but not of temperature (F = 1.767, df = 2, $p = 0.17$; Table not shown). Also, there was no significant interaction between the two factors (F = 0.548, df = 6, $p = 0.76$). Tukey HSD post-hoc test revealed shell diameter of the high pCO_2 treatment (1100 µatm) to be significantly lower than at 230 µatm and 750 µatm, however, it was not significantly different from the 350 µatm treatment (Fig. 8).

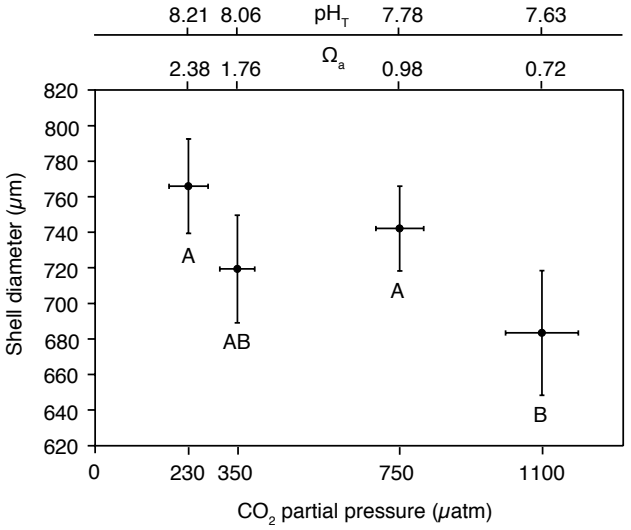

Fig. 8. Mean diameter of *Limacina helicina* after 29 days of incubation for the effect of pCO_2. Vertical bars denote 0.95 confidence intervals for diameter, horizontal bars denote 0.95 confidence intervals for pCO_2. Results from the Tukey HSD post-hoc test are depicted by letters with levels not connected by same letter being significantly different.

Table 4. PERMANOVA, Pair-wise tests for factor pCO_2. Significant results are represented in bold.

Groups	t	P (perm)	Unique perms
230, 350	1.027	0.3609	9946
230, 750	4.5986	**0.0001**	9944
230, 1100	8.7309	**0.0001**	9927
350, 750	6.1461	**0.0001**	9941
350, 1100	11.556	**0.0001**	9926
750, 1100	5.3049	**0.0001**	9941

Table 5. Univariate tests of significance indicating the effect of temperature and pCO_2 on the ratio of shell increment to shell diameter. Significant results are represented in bold.

	SS	df	MS	F	p
Intercept	34.772	1	34.772	4249.554	0.000
Temp	0.022	2	0.011	1.353	0.27
pCO_2	0.107	3	0.036	4.344	**0.008**
Temp × pCO_2	0.100	6	0.017	2.044	0.07
Error	0.507	62	0.008		

The ratio of shell increment versus diameter was significantly affected by pCO_2 ($F = 4.344$, $p = 0.008$), but there was no significant effect of temperature ($F = 1.353$, $p = 0.27$) and no significant interaction between both factors ($F = 2.044$, $p = 0.07$; Table 5). Tukey HSD post-hoc test revealed the shell increment/diameter ratio at the high pCO_2 treatment (1100 µatm) to be significantly lower than at 230 and 350 µatm, but not significantly different from the 750 µatm treatment (Fig. 9).

4 Discussion

The present experiments were carried out with unfed juvenile *Limacina helicina*; this species feeds on particles entangled in its mucus web, mainly on phytoplankton and small protozoa (Lalli and Gilmer, 1989). Phytoplankton biomass is low in Kongsfjorden already in late summer (Hop et al., 2002), and phytoplankton abundance was extremely low during the whole period of investigation (own observations from a 20 µm net haul in the upper 20 m). Moreover, *L. helicina's* downward migration to overwintering depth (>100 m) begins in the first half of September in Kongsfjorden (Lischka, unpublished data) and the larger part of the population already dwelled between 100 to 200 m in mid September (as determined by stratified vertical net hauls). Thus, feeding on phytoplankton can most likely be excluded. Rather lipid consumption during overwintering is likely (Gannefors et al., 2005) presumably at lower level metabolism (e.g. Lee et al., 2006). Although it is possible, that *L. helicina* still fed on organic particles during this time of the year, which could affect the effect size of temperature and pCO_2 on the response of *L. helicina*, a change in effect direction is unlikely since individuals in all treatments were kept under the same conditions with respect to food.

4.1 Carbonate system

A_T at the end of the experiment showed a slightly increased trend with increasing temperature and pCO_2 that correlates with silicate concentrations. Most likely the A_T increase resulted from silicate and other components dissolved from the experimental jars.

Increased C_T concentrations and therefore decreased pH and Ω values as well as increased CO_2 partial pressures at the end are most likely explained by respiration of pteropods (and bacteria) in the closed experimental set up.

4.2 Effects of elevated temperature

Concerning mortality, temperature was the dominant factor as revealed by the higher F and lower p value compared to those associated with pCO_2 (Table 2). *Limacina helicina* at the beginning of the overwintering phase are very sensitive to changes of 3 to 5 °C. *L. helicina* is a north Atlantic/polar species that is adapted to a relatively narrow and low temperature range between −0.4 °C and +4 °C and infrequently up to 7 °C (van der Spoel, 1967; Bé and Gilmer, 1977). As

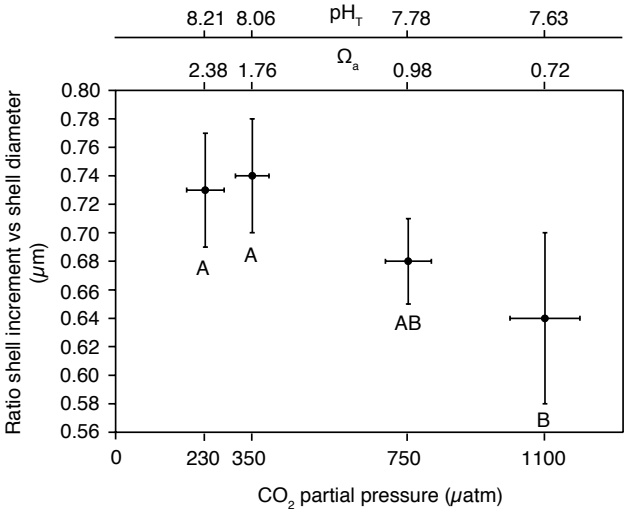

Fig. 9. Mean ratio of shell increment to diameter of *Limacina helicina* after 29 days of incubation for the effect of pCO_2. Vertical bars denote 0.95 confidence intervals for mean ratio while horizontal bars denote 0.95 confidence intervals for pCO_2. Results from the Tukey HSD post-hoc test are depicted by letters with levels not connected by same letter being significantly different.

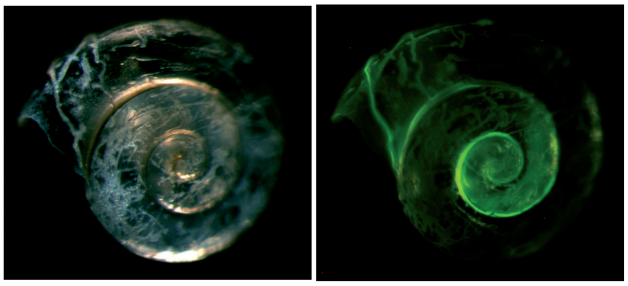

Fig. 10. Example for "repair" calcification: shell degradation of *Limacina helicina* (left, oblique transmitted light) and the respective regions of "repair" calcification indicated by enhanced fluorescence due to calcein incorporation (right).

mentioned earlier, peak occurrence of *L. helicina* during the present investigation was between 100 and 200 m depth. In September/October 2009, a relatively warm water lens of about 5 to 5.5 °C occurred in Kongsfjorden between 40 and 110 m depth. Below 110 m, temperature decreased quickly to values below 4 °C down to a minimum of about 2 °C at 300 m. Furthermore, at the time of this investigation, *L. helicina* was at the onset of the overwintering period presumably not feeding anymore, likely living on lipid reserves. Temperature adaptation is a complex and costly metabolic response and costs of existence (the sum of all processes that are necessary to maintain viability, excluding reproduction, growth, and activity) vary significantly with temperature (Clarke, 2003). Hence, temperature stress during this period of *L. helicina's* life cycle can be a severe threat for its ability not only to survive the food-scarce winter period, but to survive with still enough energy reserves available to proceed development to adults and fuel reproduction in spring/summer.

4.3 Effects of elevated pCO_2

4.3.1 Shell increment and shell diameter

Similar to Reusch (1998), calcein was used here as a qualitative measure of shell growth. In juvenile *L. helicina*, staining was not only depicted as a distinct green line at the growing margin, but usually two main regions of coloration indicating calcification activity were observed. One region usually started with a distinct line on the outer whorl extending to the aperture (the actual shell increment – in terms of lengthening), the other was found around the protoconch. This is in contrast to Comeau et al. (2009) who reported a distinct green line marking the shell edge (apertural margin) at the time of staining. The findings presented here are proposed as indication of "repair" calcification, since regions of coloration usually showed up where shell integrity was affected (Fig. 10). Indeed, thecosomes are able to repair shell parts (van der Spoel, 1967).

The question arising from this is why the region defined as shell increment was completely green instead of a single line marking the shell edge at time of staining and whether or not this region is indeed incremental or rather a region of enhanced shell thickening (in terms of increase of shell thickness) at the inner surface (presumably the inner prismatic layer, Sato-Okoshi et al., 2010)? Concomitant shell diameter measurements on juveniles freshly caught in the field during the whole period of the experiment (data not shown) as well as the increasing shell diameters of the incubated individuals indicate growth of juvenile *L. helicina* during September/October 2009. To further address this question, shell cross sections were made and revealed a fluorescence band at the inner shell surface, implying inward shell thickening (Fig. 11a and b). However, close to the aperture, the whole shell cross section (sensu Sato-Okoshi et al., 2010 the outer prismatic, middle crossed-lamellar, and inner prismatic layer) was fluorescent, thus implying shell increment (Fig. 11c). This region is suggested to exhibit shell increment, where the proximal ("older") part of new increment is still thickened inwardly (inner prismatic layer), and close to the apertural margin true shell increment proceeds. A similar process was described for the pteropod *Cuvierina columnella* (Cavoliniidae), which after attaining maximum shell length continues to thicken the entire shell inwardly (Lalli and Gilmer, 1989). Moreover, if our hypothesis is true for *L. helicina*, the fact that the entire region of increment was green points to storage of calcein during the entire incubation time.

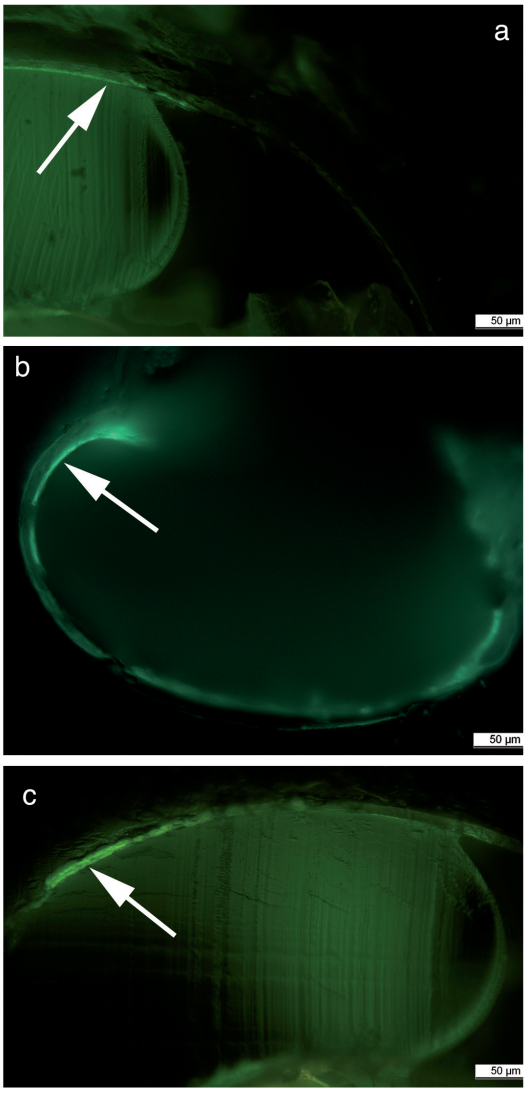

Fig. 11. Cross sections of *Limacina helicina* shells in the region of shell increment. **(a)** Dorso-lateral section (higher magnification of the right part of **(c)** showing a fluorescence band at the inner shell surface, arrow pointing at the thin inner fluorescence line). **(b)** Cross section of the aperture region distal from the area of increment, the arrow pointing at the line of constructive processes at the inner prismatic shell layer. **(c)** Dorso-lateral section showing calcein incorporation in all shell layers (prismatic, middle crossed-lamellar, inner prismatic) close to the aperture (arrow).

Shell growth of *Limacina helicina* kept at 1100 µatm was significantly reduced as compared to individuals kept at 350 and 230 µatm (Fig. 9). However, *L. helicina* was able to grow at $\Omega_a < 1$. Consequently, the present results principally agree with the conclusion by Comeau et al. (2009) deduced from adult *L. helicina* that seemed to be relatively well adapted to aragonite undersaturation. However, in addition to shell growth, shell degradation state of juvenile *L. helicina* revealed pronounced dissolution processes at the same time and as mentioned earlier, "repair" calcification is suggested. Therefore, three crucial questions arise: (1) How well can juvenile *L. helicina* adapt to aragonite undersaturation?, (2) What are the costs for different life stages of *L. helicina* to facilitate calcification and repair dissolution damage under aragonite undersaturation?, and (3) Will it be possible for *L. helicina* to maintain the integrity of its shell and, at the same time, sustain development, reproduction and accumulation of energy reserves to overwinter? The intensity of shell degradation under the two highest pCO_2 levels leads to the conclusion that juvenile pre-winter *L. helicina* may be seriously threatened under aragonite undersaturation.

The present study shows that pCO_2 is the driving factor influencing shell growth and calcification of juvenile *L. helicina*, whereas for temperature no significant influence was detected. This is in agreement with recent findings for adult *L. helicina* that exhibited declined precipitation rates of $CaCO_3$ as a function of pCO_2 (Comeau et al., 2010b). However, inconclusive results with respect to a temperature effect in the present study might be due to i.e. experimental constraints (i.e. experiment/test could not detect an effect) and does not necessarily mean that temperature had no effect.

4.3.2 Shell degradation

Both elevated pCO_2 levels caused a significant effect on shell degradation, especially at 1100 µatm (Fig. 3). Hence, shell degradation state gives clear evidence that the shell of juvenile *L. helicina* is negatively affected by aragonite saturation levels below 1. To the authors knowledge dissolution in live pteropods has so far only been reported by Orr et al. (2005) and Comeau et al. (2010a) from a Subarctic Pacific and a Mediterranean species, respectively (*Clio pyramidata* and *Cavolinia inflexa*). Similar to the present results, shell surface alterations due to $CaCO_3$ undersaturation are reported by e.g. Green et al. (2009) on live juvenile benthic bivalves, and from *Limacina* spp. shells collected in sediment traps by Gerhardt et al. (2000) and Manno et al. (2007).

PERMANOVA neither revealed a significant effect for temperature nor significant interactions between the two factors but P-value for the interaction term was quite small and thus rather inconclusive (Table 3). Although not statistically significant, NMDS ordination (Fig. 7), however, suggests that temperature may have an influence on shell degradation as well as the occurrence of interactive effects between temperature and pCO_2 are suggested. The ordination of the 3 °C and 1100 µatm CO_2 treatment in Fig. 7e shows a clear and large temperature effect. Highest incidence of perforated shells was at ambient temperature and high pCO_2, whereas at higher temperatures shells were considerably corroded but less perforated. Hence, at higher temperature and perhaps due to a higher metabolism, *L. helicina* might be better able to counteract dissolution processes by 'repair' calcification and therefore avoid perforation at least for a limited time. Similarly, McDonald et al. (2009)

describe compensatory calcification in the intertidal barnacle *Amphibalanus amphitrite* that was exposed to acidified conditions and showed compensatory calcification of their basal shell plates but central shell wall plates were significantly weakened.

5 Conclusion

The findings shown here give insight to the response (with respect to mortality, shell degradation and shell increment) of juvenile *Limacina helicina* just before overwintering as a function of temperature and pCO_2. Increased temperature and pCO_2 act differently on *L. helicina*, both significantly increasing species mortality but only the latter significantly affecting shell integrity and shell growth. pCO_2 change projected for the near future may severely affect pre-winter juveniles, and rising temperatures could contribute to a decline in abundance of the overwintering population, which represents the basis for next year's reproduction. Hence, population dynamics are likely to be changed and consequences for the Arctic epipelagic ecosystem may arise.

Various questions arise from this study with respect to *L. helicina's* fate in a high CO_2 ocean. This study suggests higher metabolic activity and thus higher metabolic costs to compensate for dissolution and as possible reason for higher mortality of *L. helicina* at higher temperature (Wood et al., 2008; Comeau et al., 2010b; Thomsen and Melzner, 2010). This raises the question as to energetic costs/trade offs and to what extent compensatory metabolic costs can be tolerated without seriously threatening winter survival and ultimately reproductive success? To address these questions, detailed physiological studies of the effects of rising CO_2 and temperature on different life stages of *Limacina helicina* are needed (e.g. respiration, lipid utilization).

Supplementary material related to this article is available online at: http://www.biogeosciences.net/8/919/2011/bg-8-919-2011-supplement.pdf.

Acknowledgements. We thank the staffs of the AWIPEV Station of the Alfred-Wegener-Institute for Polar and Marine Research and Kings Bay AS in Ny-Ålesund for excellent logistical support during our field campaign. The Institute for Polar Ecology in Kiel is acknowledged for making logistics and optical facilities available to us. The scanning electron microscopy work was performed in the Institute of Geosciences in Kiel, particularly we are indebted to Ute Schuldt for her supervision in the SEM Lab. Thanks are also due to Armin Form for helpful discussions. Dieter Piepenburg (Institute for Polar Ecology) provided access to PERMANOVA + for PRIMER. We also thank Jon Havenhand and an anonymous referee for their valuable suggestions and critics on the manuscript. This work is a contribution to the German BMBF (Federal Ministry of Education and Research) funded project "Biological Impacts of Ocean Acidification" (BIOACID, Grant number 03F0608A) as well as to the "European Project on Ocean Acidification" (EPOCA) which received funding from the European Community's Seventh Framework Programme (FP7/2007-2013) under grant agreement n° 211384. This work also received funding from the European Centre for Arctic Environmental Research (ARCFAC, Grant number 026129-2008-54).

Edited by: J.-P. Gattuso

References

Acker, J. G. and Byrne, R. H.: The influence of surface state and saturation state on the dissolution kinetics of biogenic aragonite in seawater, Am. J. Sci., 289, 1098–1116, 1989.

Almogi-Labin, A., Luz, B., and Duplessy, J.-C.: Quaternary paleo-oceanography, pteropod preservation and stable-isotope record of the Red Sea, Paleogr. Paleoclimatol. Paleoecol., 57, 195–211, 1986.

Bathmann, U. V., Noji, T. T., and von Bodungen, B.: Sedimentation of pteropods in the Norwegian Sea in autumn, Deep-Sea Res., 38, 1341–1360, 1991.

Bé, A. W. H. and Gilmer, R. W.: A zoogeographic and taxonomic review of euthecosomatous Pteropoda, in: Oceanic micropalaeontology, edited by: Ali, M. A., Academic Press, London, 773–808, 1977.

Berner, R. A. and Honjo, S.: Pelagic sedimentation of aragonite: its geochemical significance, Science, 211, 940–942, 1981.

Bradshaw, A. L., Brewer, P. G., Shafer, D. K., and Williams, R. T.: Measurements of total carbon dioxide and alkalinity by potentiometric titration in the GEOSECS program, Earth Planet Sci. Lett., 55, 99–115, 1981.

Clark, D., Lamare, M., and Barker, M.: Response of sea urchin pluteus larvae (Echinodermata: Echinoidea) to reduced seawater pH: a comparison among a tropical, temperate, and a polar species, Mar. Biol., 156, 1125–1137, 2009.

Clarke, A.: Costs and consequences of evolutionary temperature adaptation, Trends Ecol. Evol., 18, 573–581, 2003.

Comeau, S., Gorsky, G., Jeffree, R., Teyssié, J.-L., and Gattuso, J.-P.: Impact of ocean acidification on a key Arctic pelagic mollusc (Limacina helicina), Biogeosciences, 6, 1877–1882, doi:10.5194/bg-6-1877-2009, 2009.

Comeau, S., Gorsky, G., Alliouane, S., and Gattuso, J. P.: Larvae of the pteropod *Cavolinia inflexa* exposed to aragonite undersaturation are viable but shell-less, Mar. Biol. 157, 2341–2345, 2010a.

Comeau, S., Jeffree. R., Teyssié, J. L., and Gattuso, J. P.: Response of the Arctic Pteropod *Limacina helicina* to Projected Future Environmental Conditions PLoS ONe, 5(6), e11362, 2010b.

Dickson, A. G. and Millero, F. J.: A comparison of the equilibrium constants for the dissociation of carbonic acid in seawater media, Deep-Sea Res Part A, 34, 1733–1743, 1987.

Dickson, A. G., Afghan, J. D., and Anderson, G. C.: Reference materials for oceanic CO_2 analysis: a method for the certification of total alkalinity, Mar. Chem., 80, 185–197, 2003.

Dickson, A. G., Sabine, C. L., and Christian, J. R. (Eds.): Guide to the best practices for ocean CO_2 measurements, PICES Special Publication, 3, 191 pp., 2007.

Fabry, V. J., Seibel, B. A., Feely, R. A., and Orr, J. C.: Impacts of ocean acidification on marine fauna and ecosystem processes, ICES J. Mar. Sci., 65, 414–432, 2008.

Falk-Petersen, S., Sargent, J. R., Kwasniewski, S., Gulliksen, B., and Millar, R. M.: Lipids and fatty acids in *Clione limacina* and *Limacina helicina* in Svalbard waters and the Arctic Ocean: trophic implications, Polar Biol., 24, 163–170, 2001.

Gannefors, C., Böer, M., Kattner, G., Graeve, G., Eiane, K., Gulliksen, B., Hop, H., and Falk-Petersen, S.: The Arctic sea butterfly *Limacina helicina*: lipids and life strategy, Mar. Biol., 147, 169–177, 2005.

Gattuso, J.-P., Allemand, D., and Frankignoulle, M.: Photosynthesis and calcification at cellular, organismal and community levels in coral reefs: a review on interactions and control by carbonate chemistry, Am. Zool., 39, 160–183, 1999.

Gazeau, F., Quiblier, C., Jansen, J. M., Gattuso, J.-P., Middelburg, J. J., and Heip, C. H. R.: Impact of elevated CO_2 on shellfish calcification, Geophys. Res. Lett., 34, L07603, doi:10.1029/2006GL028554, 2007.

Gerhardt, S., Groth, H., Ruehlemann, C., and Henrich, R.: Aragonite preservation in late Quaternary sediment cores on the Brazilian Continental Slope: implications for intermediate water circulation, Int. J. Earth Sci., 88, 607–618, 2000.

Gilmer, R. W. and Harbison, G. R.: Diet of *Limacina helicina* (Gastropoda: Thecosomata) in Arctic waters in midsummer, Mar. Ecol. Prog. Ser., 77, 125–134, 1991.

Green, M. A., Waldbusser, G. G., Reilly, S. L., Emerson, K., and O'Donnell, S.: Death by dissolution: Sediment saturation state as a mortality factor for juvenile bivalves, Limnol. Oceanogr., 54, 1048–1059, 2009.

Guinotte, J. M. and Fabry, V. J.: Ocean Acidification and Its Potential Effects on Marine Ecosystems, Ann. NY Acad. Sci., 1134, 320–342, 2008.

Gutowska, M. A., Melzner, F., Pörtner, H. O., and Meier, S.: Cuttlebone calcification increases during exposure to elevated seawater pCO_2 in the cephalopod *Sepia officinalis*, Mar. Biol., 157, 1653–1663, 2010.

Haddad, G. A. and Droxler, A. W.: MetasTable $CaCO_3$ dissolution at intermediate water depths of the Caribbean and western North Atlantic: Implications for intermediate water circulation during the past 200 000 years, Paleoceanography, 11, 701–716, 1996.

Hagen, W. and Auel, H.: Seasonal adaptations and the role of lipids in oceanic zooplankton, Zoology, 104, 313–326, 2001.

Hirche, H.-J.: Diapause in the marine copepod, *Calanus finmarchicus* – a review, Ophelia, 44, 129–143, 1996.

Hop, H., Pearson, T., Hegseth, E. N., Kovacs, K. M., Wiencke, C., Kwasniewski, S., Eiane, K., Mehlum, F., Gulliksen, B., Wlodarska-Kowalczuk, M., Lydersen, C., Weslawski, J. M., Cochrane, S., Gabrielsen, G. W., Leakey, R. J. G., Lønne, O. J., Zajaczkowski, M., Falk-Petersen, S., Kendall, M., Wängberg, S.-Å., Bischof, K., Voronkov, A. Y., Kovaltchouk, N. A., Wiktor, J., Poltermann, M., di Prisco, G., Papucci, C., and Gerland, S.: The marine ecosystem of Kongsfjorden, Svalbard, Polar Res., 21, 167–208, 2002.

Hunt, B. P. V., Pakhomov, E. A., Hosie, G. W., Siegel, V., Ward, P. and Bernard, K.: Pteropods in Southern Ocean ecosystems, Prog. Oceanogr., 78, 193–221, 2008.

Karnovsky, N. J., Hobson, K. A., Iverson, S., and Hunt, G. L.: Seasonal changes in diets of seabirds in the North Water Polynya: a multiple-indicator approach, Mar. Ecol. Prog. Ser., 357, 291–299, 2008.

Koroleff, F. and Grasshoff, K.: Determination of nutrients, in: Methods of seawater analysis, edited by: Grasshoff, K., Ehrhardt, M., Kremling, K., Verlag Chemie, Weinheim, 419 pp., 1983.

Kurihara, H.: Effects of CO_2-driven ocean acidification on the early developmental stages of invertebrates, Mar. Ecol. Prog. Ser., 373, 275–284, 2008.

Kurihara, H., Kato, S., and Ishimatsu, A.: Effects of increased seawater pCO_2 on early development of the oyster *Crassostrea gigas*, Aquat. Biol., 1, 91–98, 2007.

Lalli, C. M. and Gilmer, R. W.: Pelagic snails: the biology of holoplanktonic gastropod molluscs, Stanford University Press, 1989.

Lee, R. F., and Hagen, W., and Kattner, G.: Lipid storage in marine zooplankton, Mar. Ecol. Prog. Ser., 307, 273–306, 2006.

Manno, C., Sandrini, S., Tositti, L. and Accornero, A.: First stages of degradation of *Limacina helicina* shells observed above the aragonite chemical lysocline in Terra Nova Bay (Antarctica), J. Mar. Syst., 68, 91–102, 2007.

McDonald, M. R., McClintock, J. B., Amsler, C. D., Rittschof, D., Angus, R. A., Orihuela, B., and Lutostanski, K.: Effects of ocean acidification over the life history of the barnacle *Amphibalanus amphitrite*, Mar. Ecol. Prog. Ser., 385, 179–187, 2009.

Mehrbach, C., Culberson, C. H., Hawley, J. E., and Pytkowicz, R. M.: Measurement of the apparent dissociation constants of carbonic acid in seawater at atmospheric pressure, Limnol. Oceanogr., 18, 897–907, 1973.

Orr, J. C., Fabry, V.J., Aumont, O., Bopp, L., Doney, S.C., Feely, R.A., Gnanadesikan, A., Gruber, N., Ishida, A., Joos, F., Key, R. M., Lindsay, K., Maier-Reimer, E., Matear, R., Monfray, P., Mouchet, A., Najjar, R. G., Plattner, G.-K., Rodgers, K. B., Sabine, C. L., Sarmiento, J. L., Schlitzer, R., Slater, R. D., Totterdell, I. J., Weirig, M.-F., Yamanaka, Y., and Yool, A.: Anthropogenic ocean acidification over the twenty-first century and its impact on calcifying organisms, Nature, 437, 681–686, 2005.

Pierrot, D. E. L. and Wallace, D. W. R.: MS Excel program developed for CO_2 System Calculations. ORNL/CDIAC-105, Oak Ridge, Tennessee, Carbon Dioxide Information Analysis Center, Oak Ridge National Laboratory, US Department of Energy, 2006.

Reusch, T. B. H.: Differing effects of eelgrass *Zostera marina* on recruitment and growth of associated blue mussels *Mytilus edulis*, Mar. Ecol. Prog. Ser., 167, 149–153, 1998.

Riebesell, U., Zondervan, I., Rost, B., Tortell, P. D., Zeebe, R. E., and Morel, F. M. M.: Reduced calcification of marine plankton in response to increased atmospheric CO_2, Nature, 407, 364–367, 2000.

Sato-Okoshi, W., Okoshi, K., Sasaki, H., and Fumihiro, A.: Shell structure of two polar pelagic molluscs, Arctic *Limacina helicina* and Antarctic *Limacina helicina antarctica* forma antarctica, Polar Biol., 33, 1577–1583, 2010.

Seibel, B. A., Dymowska, A., and Rosenthal, J.: Metabolic temperature compensation and coevolution of locomotory performance in pteropod molluscs, Integr. Comp. Biol., 47, 880–891, 2007.

Steinacher, M., Joos, F., Frölicher, T. L., Plattner, G.-K., and Doney, S. C.: Imminent ocean acidification in the Arctic projected with the NCAR global coupled carbon cycle-climate model, Biogeosciences, 6, 515–533, doi:10.5194/bg-6-515-2009, 2009.

Stoll, M. H. C., Bakker, K., Nobbe, G. H., and Haese, R. R.: Continuous-Flow Analysis of Dissolved Inorganic Carbon Content in Seawater, Anal. Chem., 73, 4111–4116, 2001.

Thomsen, J. and Melzner, F.: Moderate seawater acidification does not elicit long-term metabolic depression in the blue mussel *Mytilus edulis*, Mar. Biol., 157, 2667–2676, 2010.

van der Spoel, S. V. D.: Euthecosomata a group with remarkable developmental stages (Gastropoda, Pteropoda), Zoological Museum, Amsterdam, 375 pp., 1967.

Wilson, J. G.: Environment and birth defects, Academic, New York, 1973.

Wood, H. L., Spicer, J. I., and Widdicombe, S.: Ocean acidification may increase calcification rates, but at a cost, Proc. Royal Soc. London, Series B: Biol. Sci., 275, 1767–1773, 2008.

Yamamoto-Kawai, M., McLaughlin, F. A., Carmack, E. C., Nishino, S., and Shimada, K.: Aragonite understauration in the Arctic Ocean: effects of ocean acidification and sea ice melt, Science, 1098–1100, 2009.

4.4.2 Manuscript I

Canary for future Ocean Acidification not as Loyal as Proposed: What Mesocosms can add to Field and Laboratory Studies.

First-authored

Canary for Future Ocean Acidification not as Loyal as Proposed: What Mesocosms can add to Field and Laboratory Studies.

Jan Büdenbender, Nicole Hildebrandt, Kai Schulz, Barbara Niehoff and Ulf Riebesell

Abstract

Ocean acidification (OA), driven through anthropogenic CO_2 emissions since the industrial revolution, is already measurable (Bates et al. 2012) and has the potential to significantly affect marine organisms and ecosystems, with potential feedbacks to the climate system (Hoegh-Guldberg & Bruno 2010). Pteropods belong to the microphagous zooplankton representing a shortcut in the pelagic food chain by efficiently transporting carbon from the food web base to the end-consumer level (Fortier et al. 1994). Therefore, pteropods are important for the efficiency of the biological carbon pump (Bathmann et al. 1991). The development of a *Limacina retroversa* community was observed for several weeks at increasing CO_2 levels (ranging initially from 300 – 3000 µatm pCO_2) in a set up of 9 KOSMOS systems (Riebesell et al. 2013). Here, we show that in the first week after CO_2 manipulation pteropod veliger larvae experienced ~2 to 12 times higher mortality at increased CO_2 levels (620 – 3100 µatm pCO_2) compared to control conditions (320 µatm pCO_2). But, survivors of this initial phase showed CO_2 independent mortality and increased their shell size at highly subsaturated conditions during the remainder of the experiment. A second generation of pteropod larvae grew in the mesocosms, also independent of CO_2 concentrations. We propose *L. retroversa* is either able to acclimate or the population possessed a genetic variability allowing some individuals to survive increased CO_2 concentrations for at least 4 weeks under natural conditions.

Introduction

Absolute atmospheric CO_2 levels but also the rate of increase are higher respectively an order of magnitude faster than experienced by the Earth for millions of years (Doney & Schimel 2007, Lüthi et al. 2008). Increasing atmospheric CO_2 levels lead to a significant decrease in surface ocean pH of ~0.1 units (Caldeira & Wickett 2003). Recent ocean models predict surface waters of the high latitudes and the California Current System to become undersaturated with respect to aragonite (a calcium carbonate mineral form) within the next decades (Steinacher et al. 2009, Gruber et al. 2012). In these highly productive ocean regions thecosome pteropods like *Limacina retroversa* play an important, sometimes dominant role in the food web structure and carbon cycle (Bathmann et al. 1991, Hunt et al. 2008). Their filter feeding mode and their ratio of food particle- to body size makes them one of the most efficient carbon transfer pathways providing a direct link between primary production and the microbial loop and end consumers in the marine system (Fortier et al. 1994, Noji et al. 1997). Additionally, pteropods produce an aragonitic shell, rapidly sinking fecal pellets and through their active mucus production contribute to formation of marine snow thereby potentially increasing the transport of organic material from the surface ocean to deep sea sediments (Bathmann et al. 1990, 1991, Fortier et al. 1994). These attributes make them of concern for ocean-climate feedbacks (Manno et al. 2009).

Laboratory based studies provide evidence of potential OA effects on pteropods like increased mortality, shell corrosion and decreased shell growth (Comeau et al. 2009, Lischka et al. 2011). Recent open water studies could correlate in-situ shell corrosion with undersaturated water masses (Bednarsek et al. 2012, 2014). From time series, so far, scientists could not detect declining pteropod abundances in correlation to undersaturated conditions (Ohman et al. 2009, Mackas & Galbraith 2011, Beaugrand et al. 2012). Data on larval stages are so far rare (Comeau et al. 2010), but are typically thought to be the bottleneck with respect to OA effects for future pteropod generations. Based on their results, authors predict the future ocean at high latitudes or in upwelling regions to be inhabitable for thecosome pteropods like *Limacina retroversa*, with potential biogeochemical and socioeconomic impacts (Orr et al. 2005, Comeau et al. 2012, Bednarsek et al. 2014). However, both lab experiments and field surveys each suffer from inherent caveats such as missing in-situ variability and species interaction for the former and missing reproducibility and the possibility to re-sample the same community and water volume for the latter. These disadvantages can mostly be overcome in larger scale manipulative mesocosms studies, which furthermore minimize or even remove sampling and enclosure stress (Riebesell et al. 2013).

Methods

In this study we experimentally investigated OA effects on pteropods under close to natural conditions over a period of 40 days (t-4 to t35) as part of the interdisciplinary Bergen 2012 mesocosm study. Nine Kiel Off-Shore Mesocosms for Future Ocean Simulations (KOSMOS) systems (Riebesell et al. 2013) were deployed in the Bergen Raune Fjord, Norway. Pteropods were enclosed in the mesocosms as a part of the after spring bloom natural plankton community including their natural food sources and predators and 77 m^3 ± 3% of natural seawater. A 23 m long, 2m in diameter and 0.5 to 1 mm thick, transparent plastic bag separated the enclosed water body from the surrounding fjord closely mimicking in-situ temperature and light dynamics. Each bag was closed at the bottom with a cylindrical shaped sediment trap 2m in diameter and 2m long. Sedimenting material was removed daily in order to prevent potential remineralization and nutrient upwelling. Mesocosms were manipulated by adding CO_2 saturated Fjord water in four consecutive steps from t0 to t4. Two mesocosms served as control (M2 & 4) and seven mesocosm were enriched with increasing pCO_2 concentrations in the following order: M6, 8, 1, 3, 5, 7 & 9. M2 was excluded from data analysis due to a hole in the plastic bag leading to a constant water exchange with the fjord. Initial pCO_2 levels ranged from 280 to 3000 µatm on t5 and changed to 300 to 1300µatm on t33 due to constant air-sea gas exchange and autotrophic primary production. For data interpretation we will split the experiment into three phases: phase 0 (t-2 to t5 = before manipulation was finished), phase 1 (t5 to t12 = initial phase after CO_2 manipulation) and phase 2 (t12 to t33 = reminder duration, ¾ of experimental duration at increased CO_2). In order to stimulate a phytoplankton bloom, inorganic nutrients were added to all mesocosms on t14. Autotrophic primary production of blooming phytoplankton caused a significant decrease in pCO_2, leading to Ω_{arag} supersaturation in the upper water column (~0-7m) in all mesocosms thereby creating a potential "refugium" for aragonite producing organisms (Fig. 1).

Results and Conclusion

Abundances of adult *Limacina retroversa* (ad. *L.r.*) in the fjord was between 0 to 140 individuals (ind.) per m^3 in the upper 23 m. In the mesocosms ad. *L.r.* were of low abundances (Fig. 2a) of 0 to max 10 ind. m^{-3} (which is 0 to 5 ind. per net), and are therefore not representatively sampled. For analysis, sampling day's t12 to t33 were pooled. The first sample of ad. *L.r.* is from t7. We did not detect an effect of recent CO_2 manipulation on ad. *L.r.* abundance in phase 1 (Table 2). Pooled abundances of ad. *L.r.* in phase 2 (t12-t33) were 2 to 3 ind. m^{-3} ± 2 in the low and intermediate CO_2 mesocosms (M4,6,8,1) and 2 ± 4, 1 ± 1 and 0 ± 0 ind. m^{-3} in the high CO_2 mesocosms (M5,7,9), respectively. Mean shell size of ad. *L.r.* from all mesocosms was in the same size range as from ad. *L.r.* in the fjord (Fig. 3). We found no significant effect of CO_2 on abundances and on shell size of ad. *L.r.* (Table 2).

Total gastropod veliger larvae (proportion of *L.r.* was >80%) abundances were between ~ 9 and 500 ind. m^{-3} in the mesocosms over the experimental period (Fig. 2b), which is in the same order of magnitude as in the fjord (100 to 600 ind. m^{-3}). We found no significant difference in veliger larvae abundances in early phase 0 (t-2) (Table 2), which is two days after closing of the mesocosms and two days before CO_2 manipulations, and therefore consider replicate starting conditions for all mesocosms. In late phase 0 (t5), one day after the CO_2 manipulation was finished, we also found no significant effect of CO_2 (Table 2). In phase 1 (t5 to t12) veliger larvae experienced a mortality of 88%, 76%, 43%, 39%, 26%, 18%, -7% and 7% in mesocosms 9, 7, 5, 3, 1, 8, 6 and 4 respectively. During this period mesocosms 9, 7, 5 & 3 were subersaturated with respect to Ω_{arag} over the whole water column, M1 was partly undersaturated and M8, 6 and 4 were always supersaturated (Fig. 1). Mortality in phase 1 was significantly correlated to pCO_2 (Fig. 4, Table 2). In phase 2, mortality of veliger larvae was 2.4 % ± 0.6 SD (Fig. 4) independent of pCO_2 (Table 2). Veliger larvae were able to survive severe Ω_{arag} undersaturation of average 0.5 (M9/t5-33) for a period of 4 weeks and were present in the water column until the end of the experiment. Additionally, we found no effect of CO_2 on either the abundance (Fig. 2c, Table 2) or shell size (Table 2) of *L. retroversa* veliger larvae of a new generation (*L.r.* GenB) appearing in the mesocosms during phase 2, one week after this new generation appeared in the fjord (Fig. 5). The offspring of *L.r.* GenB was possible in M7, 5, 3, 1, 8 and 4. All of these mesocosms, except for M4, experienced undersaturation from 0.46 to 0.97 during phase 1, which is about the period when larvae hatched (Lebour 1932).

Qualitative analysis of shell corrosion for *L.r.* GenA from t33 (Table 1, Fig. 6): Shells without corrosion were only found in the fjord and in the control mesocosm (M4), which are the only water bodies, which never saw CO_2 saturated water. Shells without corrosion contributed 40 and 50% of the analyzed shells, respectively in the Fjord and in M4. Shells with minor or very minor corrosion contributed ~50% in the Fjord and in M4, between ~80 to 100% in M6, 8, 1 & 3, ~60% in M5 and ~ 30% in M7. Shells with major corrosion contribute ~10% in the Fjord, M6 & 3 and ~40% in M5 and ~70% in M7. Therefore all categories of corrosion occurred in the fiord (under natural conditions). Interestingly, very minor and minor shell corrosion is increased by 50% in CO_2 manipulated mesocosms (M6, 8, 1 & 3) compared to un-manipulated mesocosms (Fjord & M4). If this increase was an artifact of the manipulation with CO_2 saturated (highly corrosive) seawater, there would be no difference in shell corrosion between natural conditions (Fjord) and CO_2 increased mesocosms (M6, 8, 1 & 3). Major shell corrosion is nearly only found in mesocosms (M5 & 7) associated with very high levels of CO_2 (>1400 µatm). A statistically significant effect of CO_2 was found for the category major corrosion (Table 2). This effect is

driven by a high proportion of this category in the two high CO_2 treatments (M5 & 7). In the relevant CO_2 range ≤1100µatm CO_2 (M4, 6, 8, 1 & 3) no effect was found for any corrosion category.

Shell growth of *L. retroversa* veliger larvae of GenA (*L.r.* GenA) (Fig. 5) from phase 0 to 1 of ~7.5 µm d^{-1} is in the same order of magnitude as rates reported by Lebour (Lebour 1932). Growth rates during phase 2 of less than 1 µm d^{-1} is much smaller then reported by Lebour, also growth in *L.r.* GenB of ~2.8 µm d^{-1} in M5 is smaller than reported by Lebour and smaller than in *L.r.* GenA (t-2 to t12) although *L.r.* GenB is in an earlier developmental stage. Redirection of energy into other developments e.g. wings or inner organs could be an explanation for reduced shell growth at prolonging experimental duration in GenA. Nevertheless, low growth rates of *L.r.* GenA and B in phase 2 are in the same range as in the fjord population (Fig. 5). In phase 0 and 1 no significant effect of pCO_2 was detected for *L.r.* GenA shell sizes (Fig. 7, Table 2). In phase 2, only at t14 and t33 a highly significant CO_2 effect on shell size of *L.r.* GenA was detectable (Fig. 7, Table 2) with decreasing shell size at increasing CO_2 levels. On t33 *L.r.* GenA shell growth from the early phase 1 to end of phase 2 was 22%, 16%, 11%, 9% & 4% lower in M5, 3, 1, 8 and 6 compared to M4. On t33 pCO_2 levels ranged from 310 µatm (M4) to 800µatm (M5). Although highest growth rates were experienced during the period of severest undersaturation (Fig. 1) a detectable CO_2 effect was first seen 4 weeks later when growth rates were low. Interestingly the CO_2 effect on t33 does not generate from less growth in high CO_2, but from a reduction in shell size in high CO_2 mesocosms compared to shell size measurements from t26 &t28.

A potential refugium for aragonite producing organisms (supersaturation of $\Omega_{arag,}$ see Fig. 1) due to the artificially induced phytoplankton bloom became present in the upper water column (0 to ~7m). The refugium occurred for the first time on t15 to t18 in M3 to M7 and as late as t23 in M9 which is 3 to 10 days after mortality rates were shown to be independent of CO_2 levels. Hence the refugium cannot be a driver for the change in CO_2 effects on mortality of *L.r.* GenA. Moreover individuals of GenB must have hatched around t6 to t11 to get to a shell size of 100µm on t21 (Lebour 1932).

Increased mortality (Phase 1), decreased shell growth (end of phase 2) and shell corrosion at increased CO_2 levels of *L. retroversa* veliger larvae is in agreement to results published so far (Lischka et al. 2011, Bednarsek et al. 2012). However we found CO_2 level independent mortality (Phase 2), shell corrosion (between 300 and 1100 µatm CO_2), shell growth (Phase 1 & 2) and offspring of GenB (Phase 2). This was unexpected as the pCO_2 gradient was persistent and M7 and M9 were even undersaturated with respect to mean Ω_{arag} until the end of the experiment (Fig. 1). Why became mortality rates independent of CO_2 although they were initially highly CO_2 correlated?

We hypothesize, either genetic variability or physiological acclimation enabled some individuals to cope with high CO_2 concentrations as was discussed for marine cnidarians, invertebrates, mollusks and coccolithophores (Kurihara 2008, Ries et al. 2009, Thomsen et al. 2010, Form & Riebesell 2012, Lohbeck et al. 2012, Gazeau et al. 2013). Also, previews studies showed growth of thecosome pteropods at aragonite undersaturation (Lischka et al. 2011) or close to the saturation threshold and stated that *Limacina helicina*, a close relative to *L. retroversa*, seemed to be well adapted to low aragonite saturations (Comeau et al. 2009). Escape behavior (Harbison & Gilmer 1986) could also be an explanation of high mortality rates during phase 1. Larvae could have been trying to sink out of corrosive water, thereby getting caught in the sediment trap and being removed from the system by the daily sediment sampling.

In the future, OA and warming jointly impact the marine ecosystem potentially affecting pteropod biology but also interaction of the whole plankton community with unforeseeable feedbacks to individual species. OA effects on survival of pteropods were so far not detected in time series analysis (Ohman et al. 2009, Beaugrand et al. 2012) implying that changes in the ecosystem and the ecosystem itself is too complex to yet detect OA effects or that this natural complexity enables pteropods to cope with changing CO_2 concentrations. The latter hypothesis would be supported by results from our study where *L.r.* was able to survive, continue to grow and hatch at end of the century and more severe CO_2 scenarios (M8, 1, 3, 5 & 7). At least, our study implies that short-term effects after CO_2 manipulation are not necessarily valid for longer experiment durations. And, with respect to end of the century CO_2 emission scenarios, it seems possible that pteropods could survive without significantly increased shell corrosion compared to present conditions.

Full Methods

On the 1st of May nine KOSMOS (Kiel Off-Shore Mesocosms for future Ocean Simulation) systems were deployed in Raunefjord, Norway. For deployment, the mesocosm bag (2 m in diameter and 27 m long) is folded up at the water surface and openings at the top and bottom are sealed with a 3mm mesh-size screen to exclude large organisms from the water volume enclosed. For filling the bag with water, the bottom is slowly lowered to depth until the bag is fully extended, virtually cutting a water column out of the fjord. Afterwards, the bottom is sealed with a cylindrical shaped sediment trap and the top is lifted above the water surface. Detailed description of the mesocosm set up, manipulation, handling and sampling and parameter analysis is published for the Svalbard mesocosm campaign 2010 (Schulz et al. 2013, Riebesell et al. 2013). The Bergen mesocosm campaign is in principal the same set up and handling as in the Svalbard experiment. Artificial manipulations of the water body were a salinity increase on t-1 for volume determinations (Czerny et al. 2013), CO_2 manipulation t0–t4 in order to study OA effects on the plankton community, and a nutrient addition on t14 in order to trigger a phytoplankton bloom. CTD casts and water chemistry from depth integrating samples were measured on a daily basis (Salinity, temperature, light, pH, O_2, NH_4^+, NO_3^-, NO_2^-, PO_4^{3-}, H_4SiO_4, total alkalinity (TA), dissolved inorganic carbon (TC) and Chl *a*) (in preparation Schulz et al.).

Zooplankton was sampled twice a week from 23m water depth by vertical net twos with an Apstein net of 17 cm diameter and 55µm mesh size in the mesocosms and the fjord. All gastropod organisms of the sample were counted alive, sorted into veliger larvae, adult *Limacina retroversa* and others (benthic larvae older than the veliger stage) and fixed in 70% ethanol. In the GEOMAR veliger larvae were bleached with 10 % H_2O_2 and *L.r.* larvae were identified by their shell coiling (Lebour 1932). Shell size of all developmental stages were analyzed by measuring the shell height under a Leica MZ 1000 dissectioning microscope (Be & Gilmer 1977). For *L.r.* larvae, mean shell size was only calculated if 10 or more size measurements were available. Shell corrosion was examined under a Phenom pro desktop scanning electron microscope (Phenom-World B.V., Netherlands) and each shell was counted into one of four categories. No corrosion, very minor corrosion: only small superficial corrosion marks, minor corrosion: medium superficial or small profound corrosion marks & major corrosion: large superficial and profound corrosion marks. For analysis shells with minor and very minor corrosion marks were grouped.

For statistical analysis linear regression models and F-tests were calculated for individual sampling days or experiment phases always considering the actual CO_2 concentrations.

Since we did not expect pteropods to be part of the plankton community we first started to sample for pteropods after adults were identified in the first general zooplankton samples. Due to logistical needs pteropod live counting started on t12. Gastropod larvae counts and pteropod individuals could be recovered from formalin fixed subsamples from t-2 and t5 in order to prove equal starting conditions for the mesocosms.

From personal experience, pteropods were primarily sorted from the bottom of sampling jars since normally 99% aggregates there due to the heavy shell. On t14 we figured that this was not valid for veliger larvae, which could also be trapped at the water surface of the sampled volume and therefore the whole water volume was sorted from t19 onwards. Subsamples of the sediment trap were analyzed for gastropod individuals, but none were found. Although many veliger larvae left the water column in the high CO_2 mesocosms on relatively short time scales (Phase 1) only one to two individuals would have been expected per sediment trap subsample creating a high likelihood of not being identified.

References

Bates NR, Best MHP, Neely K, Garley R, Dickson AG, Johnson RJ (2012) Detecting anthropogenic carbon dioxide uptake and ocean acidification in the North Atlantic Ocean. Biogeosciences 9:2509–2522

Bathmann U, Noji TT, Bodungen B von (1991) Sedimentation of pteropods in the Norwegian Sea in autumn. Deep Sea Res Part I Oceanogr Res Pap 38:1341–1360

Bathmann UV, Peinert R, Noji TT, Bodungen B von (1990) Pelagic origin and fate of sedimenting particles in the Norwegian Sea. Prog Oceanogr 24:117–125

Be AWH, Gilmer RW (1977) A zoogeographic and taxonomic review of euthecosomatous Pteropoda (ATS Ramsay, Ed.). Academic Press, London New York

Beaugrand G, McQuatters-Gollop A, Edwards M, Goberville E (2012) Long-term responses of North Atlantic calcifying plankton to climate change. Nat Clim Chang 3:263–267

Bednarsek N, Feely RA, Reum JCP, Peterson B, Menkel J, Alin SR, Hales B (2014) Limacina helicina shell dissolution as an indicator of declining habitat suitability owing to ocean acidification in the California Current Ecosystem. Proc R Soc B 281:20140123

Bednarsek N, Tarling GA, Bakker DCE, Fielding S, Jones EM, Venables HJ, Ward P, Kuzirian A, Lézé B, Feely RA, Murphy EJ (2012) Extensive dissolution of live pteropods in the Southern Ocean. Nat Geosci 5:881–885

Caldeira K, Wickett ME (2003) Oceanography: anthropogenic carbon and ocean pH. Nature 425:365

Comeau S, Gattuso J-P, Nisumaa A-M, Orr JC (2012) Impact of aragonite saturation state changes on migratory pteropods. Proc Biol Sci 279:732–738

Comeau S, Gorsky G, Alliouane S, Gattuso J-P (2010) Larvae of the pteropod Cavolinia inflexa exposed to aragonite undersaturation are viable but shell-less. Mar Biol 157:2341–2345

Comeau S, Gorsky G, Jeffree R, Teyssie J-L, Gattuso J-P (2009) Impact of ocean acidification on a key Arctic pelagic mollusc (Limacina helicina). Biogeosciences 6:1877–1882

Czerny J, Schulz KG, Krug SA, Ludwig A, Riebesell U (2013) Technical Note: The determination of enclosed water volume in large flexible-wall mesocosms "KOSMOS." Biogeosciences 10:1937–1941

Doney SC, Schimel DS (2007) Carbon and climate system coupling on timescales from the Precambrian to the Anthropocene*. Annu Rev Environ Resour 32:31–66

Form A, Riebesell U (2012) Acclimation to ocean acidification during long-term CO2 exposure in the cold-water coral Lophelia pertusa. Glob Chang Biol 18:843–853

Fortier L, Fevre J Le, Legendre L (1994) Export of biogenic carbon to fish and to the deep ocean: the role of large planktonic microphages. J Plankton Res 16:809–839

Gazeau F, Parker LM, Comeau S, Gattuso J-P, O'Connor WA, Martin S, Pörtner H-O, Ross PM (2013) Impacts of ocean acidification on marine shelled molluscs. Mar Biol 160:2207–2245

Gruber N, Hauri C, Lachkar Z, Loher D, Frölicher TL, Plattner G-K (2012) Rapid progression of ocean acidification in the California Current System. Science (80-) 337:220–223

Harbison GR, Gilmer RW (1986) Effects of animal behavior on sediment trap collections: implications for the calculation of aragonite fluxes. Deep Sea Res Part I Oceanogr Res Pap 33:1017–1024

Hoegh-Guldberg O, Bruno JF (2010) The impact of climate change on the world's marine ecosystems. Science (80-) 328:1523–1528

Hunt BPV, Pakhomov EA, Hosie GW, Siegel V, Ward P, Bernard K (2008) Pteropods in Southern Ocean ecosystems. Prog Oceanogr 78:193–221

Kurihara H (2008) Effects of CO2-driven ocean acidification on the early developmental stages of invertebrates. Mar Ecol Prog Ser 373:275–284

Lebour M V (1932) Limacina retrouersa in Plymouth Waters. J Mar Biol Assoc United Kingdom 18:123–126

Lischka S, Büdenbender J, Boxhammer T, Riebesell U (2011) Impact of ocean acidification and elevated temperatures on early juveniles of the polar shelled pteropod Limacina helicina: mortality, shell degradation, and shell growth. Biogeosciences 8:919–932

Lohbeck KT, Riebesell U, Reusch TBH (2012) Adaptive evolution of a key phytoplankton species to ocean acidification. Nat Geosci 5:346–351

Lüthi D, Floch M Le, Bereiter B, Blunier T, Barnola J-M, Siegenthaler U, Raynaud D, Jouzel J, Fischer H, Kawamura K, Stocker TF (2008) High-resolution carbon dioxide concentration record 650,000-800,000 years before present. Nature 453:379–382

Mackas DL, Galbraith MD (2011) Pteropod time-series from the NE Pacific. ICES J Mar Sci 69:448–459

Manno C, Tirelli V, Accornero A, Fonda Umani S (2009) Importance of the contribution of Limacina helicina faecal pellets to the carbon pump in Terra Nova Bay (Antarctica). J Plankton Res 32:145–152

Noji TT, Bathmann UV, Bodungen B von, Voss M, Krumbholz M, Klein B, Peeken I, Noji CI, Rey F (1997) Clearance of picoplankton-sized particles and formation of rapidly sinking aggregates by the pteropod, Limacina retroversa. J Plankton Res 19:863–875

Ohman MD, Lavaniegos BE, Townsend AW (2009) Multi-decadal variations in calcareous holozooplankton in the California Current System: Thecosome pteropods, heteropods, and foraminifera. Geophys Res Lett 36:L18608

Orr JC, Fabry VJ, Aumont O, Bopp L, Doney SC, Feely RA, Gnanadesikan A, Gruber N, Ishida A, Joos F, Key RM, Lindsay K, Maier-Reimer E, Matear R, Monfray P, Mouchet A, Najjar RG, Plattner G-K, Rodgers KB, Sabine CL, Sarmiento JL, Schlitzer R, Slater RD, Totterdell IJ, Weirig M-F, Yamanaka Y, Yool A (2005) Anthropogenic ocean acidification over the twenty-first century and its impact on calcifying organisms. Nature 437:681–686

Riebesell U, Czerny J, Bröckel K von, Boxhammer T, Büdenbender J, Deckelnick M, Fischer M, Hoffmann D, Krug SA, Lentz U, Ludwig A, Muche R, Schulz KG (2013) Technical Note: A mobile sea-going mesocosm system – new opportunities for ocean change research. Biogeosciences 10:1835–1847

Ries JB, Cohen AL, McCorkle DC (2009) Marine calcifiers exhibit mixed responses to CO2-induced ocean acidification. Geology 37:1131–1134

Schulz KG, Bellerby RGJ, Brussaard CPD, Büdenbender J, Czerny J, Engel A, Fischer M, Koch-Klavsen S, Krug SA, Lischka S, Ludwig A, Meyerhöfer M, Nondal G, Silyakova A, Stuhr A, Riebesell U (2013) Temporal biomass dynamics of an Arctic plankton bloom in response to increasing levels of atmospheric carbon dioxide. Biogeosciences 10:161–180

Steinacher M, Joos F, Fröhlicher TL, Plattner G-K, Doney SC (2009) Imminent ocean acidification in the Arctic projected with the NCAR global coupled carbon cycle-climate model. Biogeosciences 6:515–533

Thomsen J, Gutowska MA, Saphörster J, Heinemann A, Trübenbach K, Fietzke J, Hiebenthal C, Eisenhauer A, Körtzinger A, Wahl M, Melzner F (2010) Calcifying invertebrates succeed in a naturally CO2-rich coastal habitat but are threatened by high levels of future acidification. Biogeosciences 7:3879–3891

Figures and tables

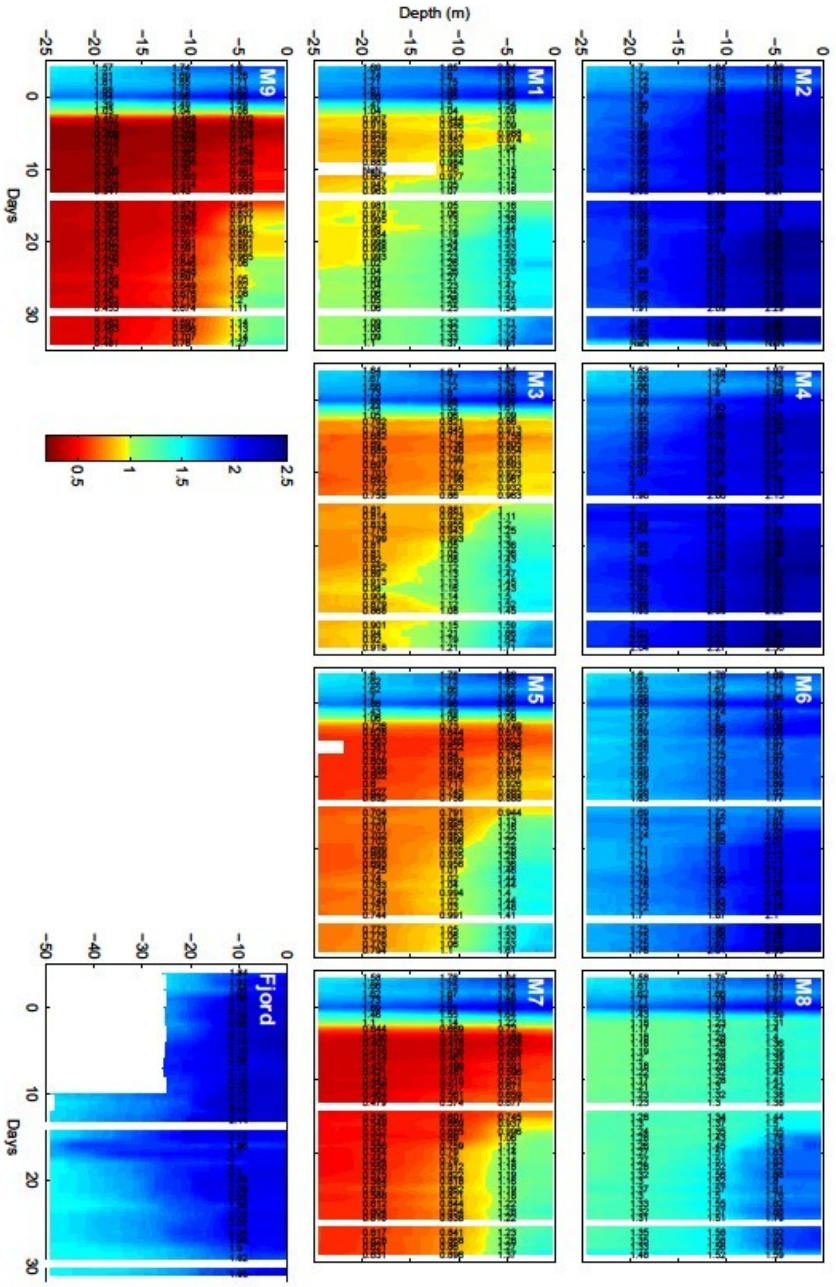

Figure 1 Temporal Ω_{arag} dynamics in each mesocosm and the fjord from t-4 to t34. Ω_{arag} profiles were calculated from daily CTD salinity, corrected pH and temperature measurements and a Sal corrected TA assumption. Three vertical rows of black numbers indicate mean Ω_{arag} for the upper 0.3 to 5m water column, 0.3 to 23m water column and the 15 to 23m water column. The color code indicates the saturation level with Ω_{arag} = 1 at the transition from green to yellow.

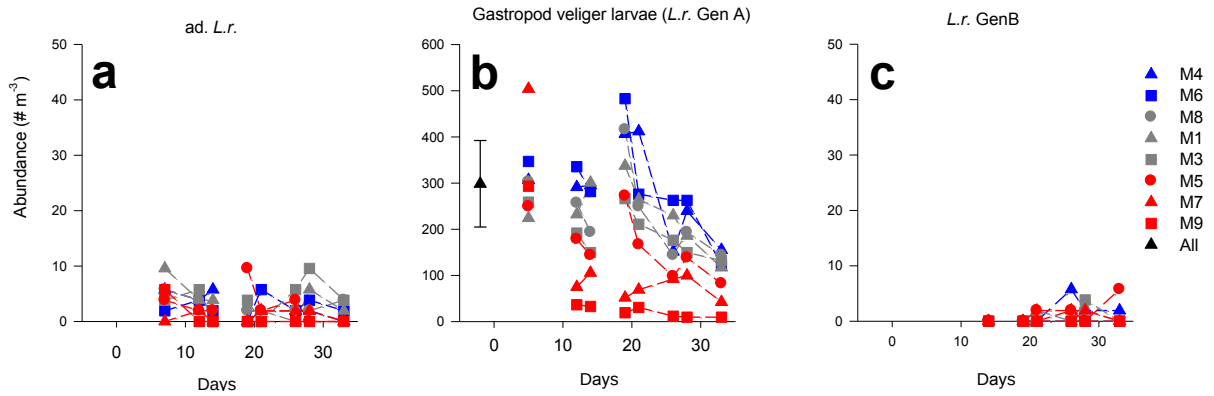

Figure 2 Abundance (# m^{-3}) of adult *L. retroversa* (ad. *L.r.*) (a), total gastropod veliger larvae (*L.r.* GenA) (b) and *L. retroversa* veliger larvae GenB (*L.r.* GenB) (c); blue triangle and blue square = control and low CO_2, grey circle, triangle and square = intermediate to high CO_2 and red circle, triangle and square = high to very high CO_2 levels, black triangle = all mesocosms ±SD. Adult *L.r.* individuals were of low abundance and no significant effect of CO_2 was detected (p= 0.08 Table 2). GenA was the dominant cohort in all mesocosms and significantly affected by CO_2 in phase 1 (t5-12) and unaffected by CO_2 in phase 2 (t12-33) (Table 2) where abundances were slowly declining in all mesocosms. GenB, a new generation of *L.r.* larvae, appeared in our nets from t14 onwards independent of prevailing Omega aragonite subsaturation in increased CO_2 mesocosms.

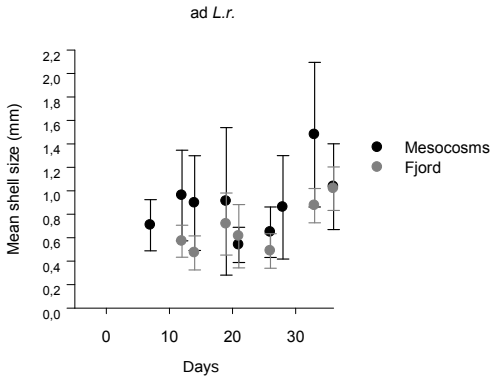

Figure 3 Shell size of adult *Limacina retroversa* as a mean of all mesocosms over the experimental duration, grey circles = mesocosms and black circles = fjord ±SD; Adult *L.r.* individuals in the mesocosms had the same lower but a higher upper size range as adult individuals found in the fjord.

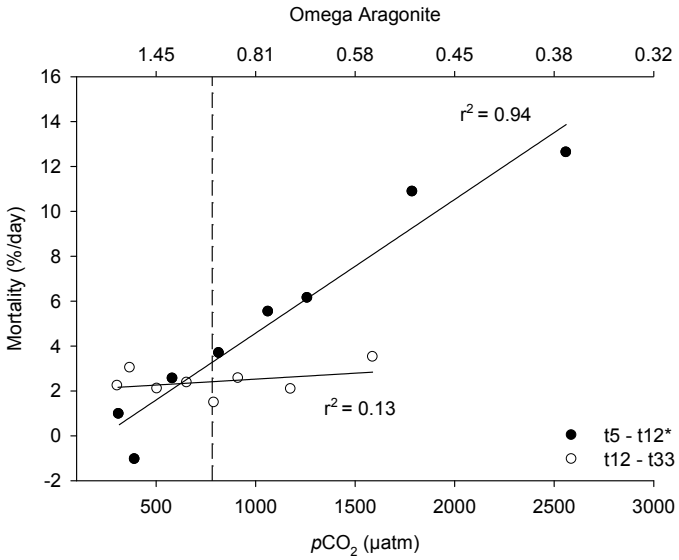

Figure 4 Mortality rates of gastropod veliger larvae living at different CO_2 levels in ~76 m^3 mesocosms. Filled circles and open squares represent daily rates from t5 to t12 and t12 to t33. Black solid lines represent a linear regression model. R^2 values represent the variation in the data explained by CO_2 levels; asterisks indicate a significant CO_2 effect. The top axis shows Omega aragonite for the corresponding CO_2 levels. Mortality rates were significantly correlated with CO_2 level during phase 1 (t5-12) and became independent of CO_2 level from t12 onwards although four mesocosms (M7,5,3&1) were still subsaturated with respect to Omega aragonite.

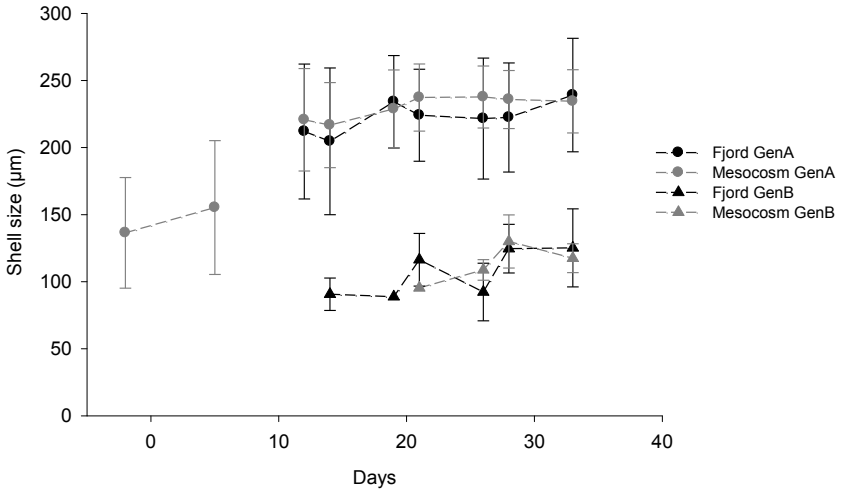

Figure 5 Mean shell size of *L. retroversa* veliger larvae from all mesocosms and the fjord over the experimental duration, circle and triangle symbols represent generation A (GenA) and generation B (GenB), grey and black color represent mesocosm and fjord ±SD. Shell size increased over the whole experimental duration and was similar to shell sizes from the fjord population. On t14 a new generation (GenB) of *L.r.* larvae was present in the fjord, which showed up in the mesocosms from t21 onwards.

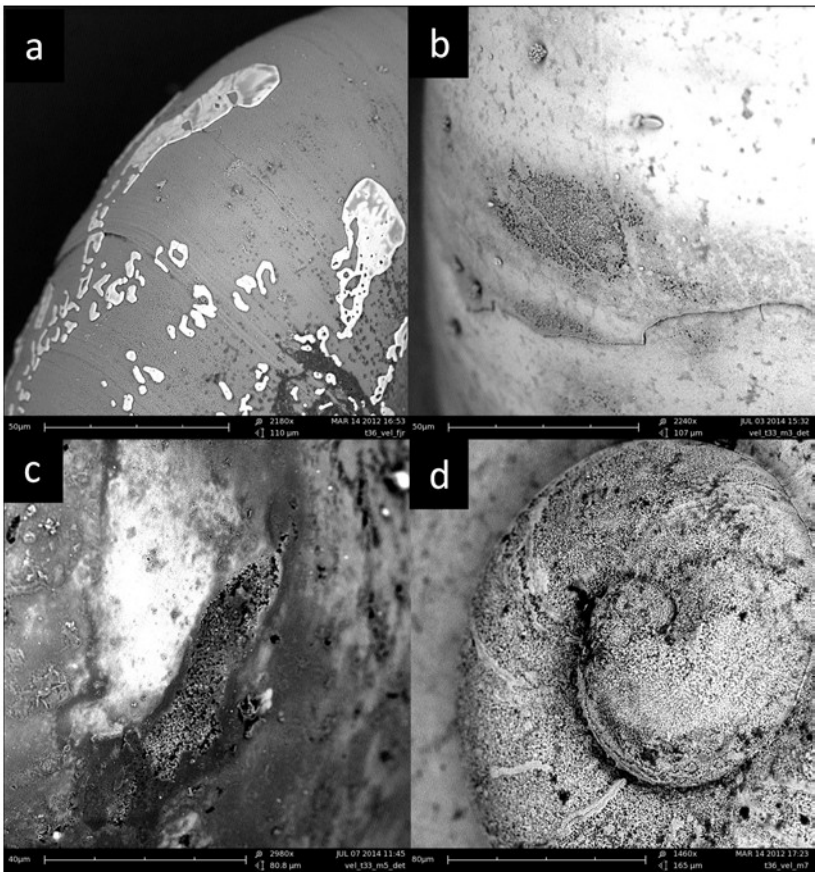

Figure 6 Scanning electron microscope photographs of representative *L. retroversa* larvae shells (GenA) from t33 for the four categories of shell corrosion. No corrosion (a): shells appear glossy and smooth, very minor corrosion (b): shells appear dull and show small superficial spots, minor corrosion (c): larger superficial spots (not shown) or small profound spots, major corrosion (d): large superficial and profound spots. Very minor corrosion is comparable to level I and II, minor and major corrosion is comparable to level II and III of Bednarsek et al. (2012). All categories of shell corrosion were found in the fjord samples (Table 1), a significant effect of CO_2 on shell corrosion was only detected for the category major corrosion, but not for the other categories (Table 2).

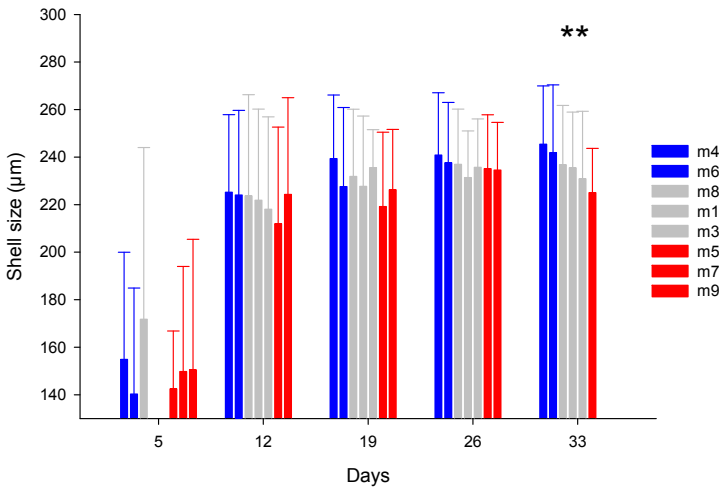

Figure 7 Shell size of *L.r.* GenA from individual mesocosms, blue, grey and red vertical columns represent control & low, intermediate and high CO_2 mesocosms +SD. Shell size of *L.r.* larvae of ~140 to 240 µm +- ~7 to 35% SD show a high variability in the cohort. Despite high pCO_2 levels (~3100µatm pCO_2 in M9 on t5) no correlation with shell size was detectable in most of the sampling days (Table 2). In the end of the experiment (t33) we detected a highly significant effect of CO_2 on shell size, marked with two asterisks.

	Proportion of corrosion category (%)		
	no	minor & very minor	major
Fjord	40	47	13
M4	50	50	0
M6	5	79	16
M8	0	94	6
M1	4	96	0
M3	0	88	12
M5	0	61	39
M7	0	32	68

Table 1 Relative proportion of corrosion categories in analyzed shells (n = 15 – 26) of *L.r.* GenA from t33. no: no signs of corrosion; minor & very minor: small superficial or single deep corrosion marks; major: large superficial and single or several deep corrosion marks (Fig. 6). All shells originate from live veliger larvae.

	ad. *L.r.*		gastropod veliger	*L.r.* GenA						*L.r.* GenB	
	abundance	shell size	abundance	abundance	shell size	shell corr.: minor	major	minor M4 - 3	major M4 - 3	abundance	shell size
t-2			0.23	0.92	0.62						
t5	(t7) 0.69		0.64	0.63	0.75						
t5-12			0.00005	0.0057							
t12					0.43						
t14					0.01						
t19					0.18						
t21					0.91						
t26					0.14						
t28					0.33						
t12 - 33	0.08	0.8	0.41	0.13						0.57	0.68
t33					0.001	0.36	0.014	0.15	0.9		

Table 2 *p*-values of F-test on linear regressions of all measurements for the individual sampling days or pooled periods. Experimental phases are highlighted, phase 0: blue, phase 1: red, phase 2: green. Statistically significant correlations are typed in red.

4.5 Methodological aspects

4.5.1 Publication IV

Sink and Swim, a Status Review of Pteropod Culture Techniques.

Co-authored, published in Journal of Plankton Research

Journal of
Plankton Research

plankt.oxfordjournals.org

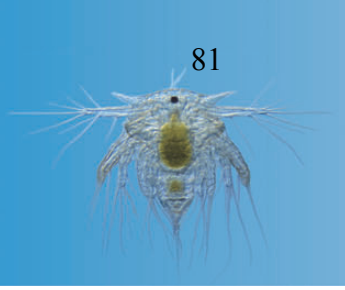

J. Plankton Res. (2014) 36(2): 299–315. First published online February 10, 2014 doi:10.1093/plankt/fbu002

REVIEW

Sink and swim: a status review of thecosome pteropod culture techniques

ELLA L. HOWES[1,2]*, NINA BEDNARŠEK[3], JAN BÜDENBENDER[4], STEEVE COMEAU[5], AYLA DOUBLEDAY[6], SCOTT M. GALLAGER[7], RUSSELL R. HOPCROFT[6], SILKE LISCHKA[4], AMY E. MAAS[7], JELLE BIJMA[2] AND JEAN-PIERRE GATTUSO[1,8]

[1]UNIVERSITÉ PIERRE ET MARIE CURIE, LABORATOIRE D'OCÉANOGRAPHIE DE VILLEFRANCHE, F-06230 VILLEFRANCHE-SUR-MER CEDEX, FRANCE, [2]ALFRED WEGENER INSTITUTE HELMHOLTZ CENTRE FOR POLAR AND MARINE RESEARCH, BREMERHAVEN, GERMANY, [3]NOAA PACIFIC MARINE ENVIRONMENTAL LABORATORY, 7600 SAND POINT WAY NE, SEATTLE, WA 98115, USA, [4]GEOMAR, HELMHOLTZ CENTRE FOR OCEAN RESEARCH KIEL, DÉSTERNRBOOKER WEG 20, 24105 KIEL, GERMANY, [5]DEPARTMENT OF BIOLOGY, CALIFORNIA STATE UNIVERSITY, NORTHRIDGE, CA, USA, [6]INSTITUTE OF MARINE SCIENCE, UNIVERSITY OF ALASKA FAIRBANKS, FAIRBANKS, AK 99775, USA, [7]WOODS HOLE OCEANOGRAPHIC INSTITUTION, WOODS HOLE, MA 02543, USA AND [8]CNRS-INSU, UMR 7093, LABORATOIRE D'OCÉANOGRAPHIE DE VILLEFRANCHE, F-06230 VILLEFRANCHE-SUR-MER, FRANCE

*CORRESPONDING AUTHOR: ella.howes@awi.de

Received October 16, 2013; accepted December 31, 2013

Corresponding editor: Roger Harris

The widespread distribution of pteropods, their role in ocean food webs and their sensitivity to ocean acidification and warming has renewed scientific interest in this group of zooplankton. Unfortunately, their fragile shell, sensitivity to handling, unknowns surrounding buoyancy regulation and poorly described feeding mechanisms make thecosome pteropods notoriously difficult to maintain in the laboratory. The resultant high mortality rates and unnatural behaviours may confound experimental findings. The high mortality rate also discourages the use of periods of acclimation to experimental conditions and precludes vital long-term studies. Here we summarize the current status of culture methodology to provide a comprehensive basis for future experimental work and culture system development.

KEYWORDS: pteropod; culture methods; ocean acidification; perturbation experiment

available online at www.plankt.oxfordjournals.org

INTRODUCTION

Pteropods are a cosmopolitan group of holoplanktonic molluscs, which consists of thecosome (shelled) and gymnosome (shell-less) species, both of which play an important role in trophic and biogeochemical fluxes (Lalli and Gilmer, 1989). For decades, pteropods have been understudied, but recently thecosome species have become the focus of renewed scientific interest within the rapidly expanding field of ocean acidification research, and as such are the primary focus of this review. Since the industrial revolution the oceans have absorbed approximately one-third of anthropogenic CO_2 (Sabine *et al.*, 2004), altering seawater carbonate chemistry. Ocean pH has dropped by 0.1 pH units since the industrial revolution and is projected to decrease by up to 0.3–0.4 units by 2100 (Orr, 2011).

Pteropods are predicted to be particularly vulnerable to the effects of lowered carbonate saturation states resulting from ocean acidification as their thin shells are made of aragonite, a form of calcium carbonate more soluble than calcite in sea water (Mucci, 1983). Studies have confirmed that pteropod larvae and adults exhibit negative calcification responses to projected future conditions with decreased calcification (Comeau *et al.*, 2010a,b; Lischka *et al.*, 2011) and shell dissolution (Lischka *et al.*, 2011). Studies of metabolic rate have also revealed that CO_2 acts in concert with other environmental stressors, such as temperature and salinity, influencing swimming speed and oxygen consumption in some pteropod species (Comeau *et al.*, 2010b; Maas *et al.*, 2011, 2012a, 2012; Bednaršek *et al.*, 2012a). These studies have been primarily of short-term duration due to constraints imposed by the difficulties of keeping pteropods in culture.

In their natural environment, pteropods have periods of active swimming, sinking and neutral buoyancy (Lalli and Gilmer, 1989). The weight of the shell causes the animals to sink relatively quickly, and culture vessels do not provide a sufficiently deep water column and/or adequate current conditions for the animals to attain neutral buoyancy. This often results in the animals repeatedly hitting the bottom of the culture vessel, causing shell breakage and the production of stress-induced mucus. The mucus can stick their wings together, impairing swimming ability and can adhere them to the bottom of the tank.

Lack of buoyancy, in turn, impedes feeding behaviour. Thecosome pteropods are suspension feeders, producing mucous webs from their wings (Fig. 1), several times their body size, to entrap phytoplankton and small motile prey and other particles (Gilmer, 1972). Production and retraction of the web can be relatively fast as little as 5 s for deployment and <20 s for retraction, although this is highly species specific (Gilmer and Harbison, 1986). Whilst the web is deployed the animal hangs motionless with the web between the parapodia; eventually the animal consumes the entire mucous structure with its attached particles. In culture, there is insufficient time to extend the wings and deploy the feeding web. Food deprivation has been shown to function as a synergistic stressor with CO_2 (Seibel *et al.*, 2012), and thus also acts as a confounding variable in long-term studies of captive animals.

In the course of experimental work with pteropods, various methods have been used to culture animals in the laboratory, with varying degrees of success. At the time of writing, only one laboratory has successfully reared a single species of pteropod, *Limacina retroversa*, through a full life cycle. Here we report, for the first time, the methods used. A common problem in developing culture systems is the patchy and seasonal abundance of pteropods, which limits opportunities for method testing and development. As negative results are often not published, these rare chances are often wasted by unknowingly repeating the unsuccessful tests of others, for this reason we also provide a summary of the varied and often-unpublished techniques tested in pteropod culture work. The aim of the present assessment is to summarize the different approaches used and discuss their efficacy as a starting point for the much-needed further development of pteropod culturing systems.

METHOD

Collection

Pteropods are often classified as gelatinous animals in zooplankton collections and are often in a poor state when retrieved using classical net tows (Hamner *et al.*, 1975; Robison, 2004). The shells of thecosome pteropods are fragile and many of the more highly evolved groups, including the subfamily *Cavolinidae* and the pseudothecosomes, have extremely delicate gelatinous pseudoconches and extensive external mantle structures. Damage by nets becomes particularly problematic when animals are collected for experimental or culturing purposes. Thus, collection of pteropods using specialized capture methods can greatly increase the proportion of undamaged animals. Although primarily open ocean animals, in some regions the topography and hydrography allow the collection of pteropods from the shore or using small boats. In these locations, researchers have used "jelly dippers" (beakers strapped to long handles) to allow the collection of these delicate animals (Seibel *et al.*, 2007; Maas *et al.*, 2011).

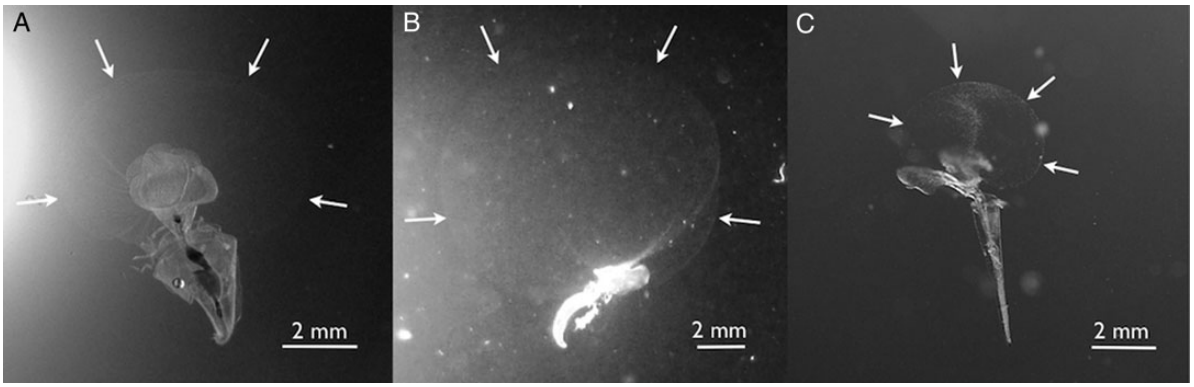

Fig. 1. Mucous web productions observed in pteropods maintained in temperature-gradient kreisel (Gorsky *et al.*, 1986). (**A**) The mucous web being retracted and (**B**) the mucous web at its maximum extension in Mediterranean *C. inflexa*. (**C**) The mucus production of the Mediterranean pteropod *C. virgula*. Photos: S. Comeau.

Hand collection can also be performed by sampling pteropods using SCUBA diving techniques (Gilmer, 1974; Fabry, 1990; Maas *et al.*, 2012a) to collect larger organisms with minimal stress. Successful collection using diving is limited by animal density and is much more time and effort intensive than net sampling (Haddock and Heine, 2005). It has, however, proven particularly useful in tropical regions (where cavolinids and pseudothecosomes are more abundant) and at night (when diel migratory individuals congregate in surface waters). Finally, a few species are exclusively meso- or bathy-pelagic, and gentle collection of these animals is particularly difficult. Such species have been sampled using remotely operated vehicles (Seibel *et al.*, 2007) and using a net with a thermally isolated cod end that closes at depth (i.e. Childress *et al.*, 1978), maintaining the animals in water from the depth of collection until retrieval.

Plankton net tows remain the most widely used for collection since they are relatively easy to operate and offer a variety of mesh sizes and designs (e.g. Bongo, WP-2, MOCNESS). Many pteropod species can be captured using >330-μm mesh nets, although small species and juveniles may be better sampled using 153-μm mesh or less (Lischka *et al.*, 2011; Bednaršek *et al.*, 2012b). Plankton tows have the advantage that they enable the user to easily collect large numbers of pteropods, including small individuals (<500 μm) and/or individuals that occur at great depths (>50 m). The disadvantage of damage by nets to both the soft tissues and the shell for work with live animals can be minimized if ship speeds of <1 knot are employed in conjunction with short duration, relatively vertical tows (Bednaršek *et al.*, 2012a). The use of a specialized cod end such as an extra-large cod end (Ikeda and Mitchell, 1982; Bouquet *et al.*, 2009) or thermally protected cod end (Childress *et al.*, 1978) can further limit physical and thermal stress.

After collection, pteropods should be inspected to ensure that the shell and soft tissue have not been damaged during collection. Damaged organisms must be discarded in order to avoid subsequent bacterial infection and the contamination/death of the whole population. Following inspection, it is recommended to immediately transfer the organisms into a large volume of filtered sea water at *in situ* temperature from the site of collection.

Water treatment

Pteropods produce mucous coverings, mucous webs and pseudofaeces, and rejected particles, expelled in mucous strings (Gilmer and Harbison, 1986), during feeding and buoyancy maintenance. These structures can attract bacterial populations that, in turn, can impact experiments and contaminate laboratory cultures. To deal with these issues researchers have used a combination of filtration, antibiotics and ultraviolet (UV) treatment of sea water (Comeau *et al.*, 2009, 2010b; Lischka *et al.*, 2011; Maas *et al.*, 2012a). Additionally, 0.5-mg L^{-1} disodium ethylenediaminetetraacetate (EDTA) can be used to chelate toxic metals from the sea water, even in areas where local water sources are relatively clean. Egg clutches/strings and juveniles are particularly susceptible to bacterial infections, and successful rearing through to adult stages is only possible with rigorously clean techniques using antibiotics and careful handling procedures (see below). For adult cultures, water filtration through <5-μm membrane filters is recommended as this reduces fouling and entanglement in aggregations of mucus and detritus; juvenile cultures require filtration using 1-μm filters.

To test directly whether antibiotics influenced the metabolism of pteropods, single adult *Limacina helicina* was held in glass syringe respiration chambers either treated or untreated with streptomycin and ampicillin (each

25 mg L^{-1}). During each experiment, a control syringe, without an animal, was simultaneously run as a control. After ~10–15 h, their oxygen (O_2) consumption (μmol g^{-1} h^{-1}) was measured using the methods detailed by Maas *et al.* (Maas *et al.*, 2012a). There was a no significant effect of exposure to antibiotics for a period of ~12 h (ANCOVA $F_{1,15} = 0.098$, $P = 0.760$) on the metabolic rate of *L. helicina* (Fig. 2). These results indicate that antibiotics may be an effective way to control bacterial activity during short duration respiration runs without physiological side effects. This is also particularly useful when oxygen consumption is being measured at warmer temperatures (>10°C) and longer duration experiments (>8 h) where bacterial respiration can be significant.

UV and microwave sterilization may also be used to sterilize culture water against fungi and viruses as well as bacteria. UV treatment is also more appropriate for use with large volumes than with antibiotics that need to be regularly replenished. A major drawback of UV sterilization, however, is its inefficiency in closed, recirculating systems (Spotte and Adams, 1981). In the Ny Ålesund Marine Laboratory, sea water is UV treated and 20-μm filtered, thus UV sterilization has been used for a number of pteropod perturbation experiments (Comeau *et al.*, 2009, 2010b; Lischka *et al.*, 2011). To our knowledge microwave sterilization has never been used in conjunction with pteropod culturing.

Aeration and gas bubbling

Gas bubbling is often used for aeration or to control the carbonate chemistry in ocean acidification perturbation experiments; however, it can also cause shell damage; particularly in juvenile pteropods. Thus, in closed vessels the bubbling should be performed before addition of pteropods, while in open vessels, bubbling should be made in such a way that the animals are not in direct contact with the stream of bubbles. This can be achieved by bubbling within a vertical tube placed in the vessel, thereby offering excellent control of the carbonate chemistry while also gently stirring the media. Veliger shells are hydrophobic (Gallager, personal observation), which can cause them to be trapped at the surface during bubbling or for gas bubbles to attach to the shell, causing buoyancy issues, in this instance the surface of the air–water interface can be covered with a few granules of polyvinyl alcohol, which forms a non-toxic surface coating eliminating the hydrophobic/hydrophilic interface. If bubbling occurs from a compressor, a series of filters decreasing in porosity to 0.45 μm should be used to avoid introducing airborne contaminates to the cultures. In humid conditions, air should be dehydrated using $CaCl_2$ or silica gel (Utting and Spencer, 1991).

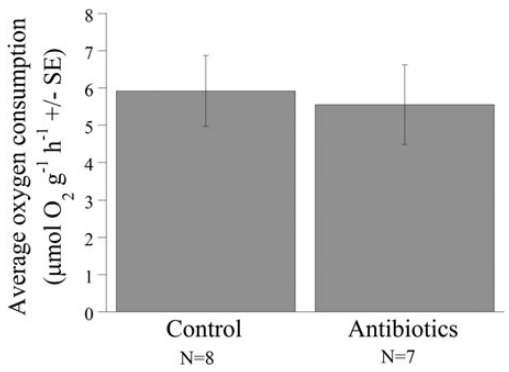

Fig. 2. The effect of antibiotics (25 mg each of streptomycin and ampicillin L^{-1}) on the respiration rate of *L. helicina*.

Diet

To date, very little experimental work has been undertaken to establish the appropriate dietary regime for cultures. Previous studies utilizing pteropod cultures have used enrichment of phytoplankton monocultures (Comeau *et al.*, 2010a). Alternatively, cultures have not been enriched with food (Lischka *et al.*, 2011) or *in situ*, unfiltered sea water is used. The use of motile species ensures that the entire water column remains evenly saturated with food with minimal agitation of culture vessels.

Successful cultures of *L. retroversa* have been maintained from juvenile stages through to adulthood with a mixed algal diet. Based on feeding studies with artificial microspheres (unpublished data), adults and juveniles were capable of feeding on particles 0.5 –30 μm in diameter. Accordingly, the flagellate *Isochrysis galbana* (clone T-ISO) and a cryptophyte *Chroomonas salina* (clone 3C) were used for larval and metamorphosing juvenile culture (Table I). Concentrations of 1×10^4 cells mL^{-1} are suitable for culture densities of ~1 veliger mL^{-1}. As parapodia developed, the dinoflagellate *Ceratium longipes* was added in addition to the two other species of microalgae. This dinoflagellate was used because of the frequent association of *C. longipes* and *Limacina* in the field (Gallager *et al.*, 1996). *Ceratium longipes*, *C. salina* and the flagellate *I. galbana* at a final concentration of 5×10^4cells mL^{-1} are an optimal combination of microalgae for juveniles and adults.

Food density was also found to be important during feeding trials using *L. helicina* juveniles to assess mixed algal diets at varying concentrations (Table I). Two cultures were maintained with high food concentrations (5×10^4cells mL^{-1}) and one with low food concentration (1×10^4cells mL^{-1}). Animals incubated in low food concentrations survived for 21 days, whereas animals in the high food concentrations survived for 37 days and

Table I: Summary of dietary regimes used in thecosome pteropod culturing

Diet	Algal species	Conc.	Pteropod species	Survival (days) and mortality (%)	Culture system	Reference
Unfed	–	–	*L. helicina* (j)	29 ~25% ~57% ~68% mortality	440 mL Jars, 3°C 5°C 8°C	Lischka *et al.* (2011)
Unfiltered seawater	–	–	*L. helicina* (j)	8 6% 8% 9% mortality	125 mL bottles, 1.6°C pH 8.05 7.90 7.75	Comeau *et al.* (2012)
Single algal species	*Isochrisis galbana*	–	*C. inflexa* (j)	13 70% mortality	1 L bottle, plankton wheel, 13°C	Comeau *et al.* (2010a)
Mixed algal diet	*Tetraselmis* spp., *Skelotonema* spp., *Gymnodinium simplex*, *Amphidinium carterii*, *Rhodomonas salina* *Pavlova*	1000 cells mL^{-1}	*L. helicina* (j) 100–2800 μm	5, 100% mortality	Stirred batch 2 μm filtered seawater, ~7°C	Doubleday, (personal observation)
Mixed algal diet	*Tetraselmis* spp., *Skelotonema* spp., *Gymnodinium simplex*, *Amphidinium carterii*, *Rhodomonas salina* *Pavlova*	>50 000 cells mL^{-1}	*L. helicina* (j) ~500 μm	40, 50% mortality	Stirred batch 2 μm filtered seawater, ~7°C	Doubleday, (personal Observation)
Mixed algal diet high conc.	*I. galbana, Chaetoceros calcitran Pavlova*	>50 000 cells mL^{-1}	*L. helicina* (j) 100–200 μm	37, 100% mortality	Stirred batch 2 μm filtered seawater, ~7°C	Doubleday, (personal observation)
Mixed algal diet low conc.	*I. galbana, Chaetoceros calcitran Pavlova* *I. galbana, C. salina* *I. galbana, C. salina, C. longipes*	1000 cells mL^{-1} 1000 cells mL^{-1} 50 000 cells mL^{-1}	*L. helicina* (j) 100–200 μm Larvae *L. retroversa* *L. retroversa*, adult, juvenile	21 100% mortality to maturity	Stirred batch 2 μm filtered seawater, ~7°C 2 L flasks, 10°C 1000 L tubes, 10°C	Doubleday, (personal observation) Gallager, (personal observation) Gallager, (personal observation)

For pteropod life stages: (j) juveniles, with shell diameters where available. It should also be considered that many of the methods listed were employed as part of perturbation experiments, therefore other stressors outside of diet regime may have contributed to mortality.

ciliary feeding was observed. These results suggest similar optimal algal concentrations for the two *Limacina* species.

Culture methods

A wide range of approaches have been used to maintain pteropods for experimental purposes. They can be grouped into three broad categories: batch cultures (with various modifications; agitation, tethering) (Table II), flow systems (circulating and flow through) (Table III) and mesocosm systems.

Closed systems

Small individuals (<1.5 mm) such as *Limacina inflata*, and juveniles of *L. helicina* (>5 mm) or *L. retroversa* can survive reasonably well in closed batch cultures. These small individuals can be maintained in smaller closed flasks with no water changes for up to 29 days at 3, 5.5 and 8°C (*L. helicina*, for percentage mortality see Table II) (Lischka *et al.*, 2011), and 7 days at 14°C (*L. inflata*) (Howes, personal observation). Adults and large species, however, appear to require much larger volumes for successful rearing. An appropriate culture vessel size is difficult to define, although the greater the water column depth the better the chance of mucous web production.

Often if the culture vessels are not gently swirled or shaken periodically, food particles, mucus and/or pseudofaeces collected at the bottom of the vessel then become entangled around pteropods incubated in the batch cultures, contributing considerably to mortality (Bednaršek *et al.*, 2012a). As with most culturing systems, particulate waste should be gently siphoned out routinely, along with periodic water changes. To maintain pteropods in suspension, tests have explored the effects of gently agitating cultures, either using external methods to move the whole vessel or by placing stirrers directly into the culture (Fig. 3 and Table II). While agitation methods work well for rearing egg clutches and juveniles (Table II) (Comeau *et al.*, 2010a) due to their light weight and slow sinking speed which allows them to be maintained in constant suspension, these techniques have been less successful for maintaining cultures of adults or juveniles >3 mm in size. Several of the agitation methods tested did appear to improve adult buoyancy, however, this was partially due to the pteropods swimming continually against the water currents precluding successful feeding behaviour. Alternatively, stirring can tumble pteropods either across the bottom of the culture vessels or into each other, and also cause an accumulation of mucus and detritus at the bottom of the culture vessel that can entangle individuals. Vibrations produced by some of the systems also appeared to disturb the animals.

To avoid some of the pitfalls of agitation, individual pteropods have been attached to mounted needles, prefixed in culture vessels, using gel-based superglue (Table II, Fig. 4). This method allows the use of smaller volumes of water and less space requirement when culturing adults. Great care and dexterity are needed to avoid damaging the fragile pteropod shell, the process is time consuming and likely very stressful. The success of the method depends greatly on the shell shape: those species with simple, straight or conical shells responded better than those with more complex shell forms. This can probably be attributed to the animals being fixed at slightly the wrong orientation. Tethered animals were never observed feeding. To date, the most successful culture of pteropods has been accomplished using a closed system with regular water changes, developed over eight separate attempts at culturing. In overview, egg strands of *L. retroversa* were collected from adults already in culture for several weeks. Larval development at 10°C in the egg capsules took ~10 days, followed by ~40 days for the veligers to reach metamorphic competency and begin to develop parapoda typical of the juvenile and adult. Metamorphosis took ~10 days to make the complete transition and loss of the velum. Development from metamorphosis to reproductive adult took ~40–50 days (Fig. 5). Egg strand production then began 90 days after hatching and continued until the F1 generation began to die out. After 110 days high mortality occurred and by 117 days all of the adults had died. Complete generation time from reproductive adult to reproductive adult was around 90–110 days at 10°C. Several F2 generations were again raised to reproduction.

To begin, the overall process adults were maintained for ~4 weeks in the laboratory in either 1000 L tubes or large tanks. Egg masses were separated by screening adult culture water through a 200-μm Nitex screen, rinsed and re-suspended in 2000 mL Erlenmeyer flasks in 1-μm filtered sea water. Water in the ova cultures was aerated at ~100 mL min^{-1} with 1-μm filtered air and not changed during the ova incubation period. Before hatching, as the ova strands darkened, eggs were treated to reduce bacterial and fungal contamination for 30 min with 2-mg L^{-1} polyvinylpyrrolidone iodine complex (PVP-I, Sigma Chemical) sea water solution whose pH has been adjusted to ~8.3 with Tris–HCL buffer (Trizma, pH 8.3). The egg masses were then treated with 0.1-M sodium thiosulphate to reduce the iodine to iodide prior to re-suspension in culture flasks prepped with antibiotics, EDTA and algal mix. Gentle agitation of flasks might also be useful in keeping egg masses off the bottom, minimizing the risk of bacterial infection

Table II: Summary of variations in batch techniques attempted

Technique description	Species	Survival (days) and mortality (%)	Reference	Comments
Batch: 440 mL jars, 10 individuals. Unfed. 3, 5, 8°C	*L. helicina* (j)	29 ~ 25%, 57%, 68%	Lischka *et al.* (2011)	–
Batch: 1l L, opaque, polyethylene jars. 1–6 individuals	*C. pyramidata*	≤1, 0%; short incubation	Fabry (1989)	Feeding not observed
	L. helicina		Fabry (1990)	
Batch: 1 litre Nalgene bottles, ≤15 individuals, −2°C	*L. helicina*	13, 0%	Maas *et al.* (2012a)	Feeding not observed
Batch: 2 L Schott bottles (opaque)	*L. helicina ant.*	14	Bednaršek *et al.* (2012a)	*L. inflata was* not observed feeding, but guts were full when inspected with a binocular microscope
2 L Schott bottles 14°C	*L. inflata*	3, 5%	Moya *et al.* (in prep)	
20 L, 0°C, 4°C	*L. helicina*	2, 0%; short incubation	Comeau *et al.* (2010b)	Feeding not observed
1000 L tubes, 10°C	*L. retroversa*	To reproduction	Gallager (personal observation)	Webs not observed, but guts full
50 000 L mesocosm (KOSMOS units)	*L. helicina* (a)	7, 95% 28, 99%	Riebesell *et al.* (2013)	Floating animals were observed
77 000 L mesocosm (KOSMOS units) (Fig. 6)	*L. retroversa* (a,j,l)	40, 50%	Büdenbender *et al.*, in prep	All life stages present until the end of the experiment
Larvacean system:	*L. helicina*	5, 0%	Comeau *et al.* (2009)	Technique effective for small individuals, egg clutches and larvae but failed to maintain pteropods >2 mm; should be used preferentially with individuals of reduced sizes
Plastic stirrers rotate (<10 rpm) in round culture vessels (e.g. 20 L beakers).	*C. inflexa* (e, j)	40, 50%	Doubleday (personal observation	
5°C		10, 100%	Howes (personal observation)	
7°C				
15°C				
Rollers 6 rpm: (Fig. 5A)	*L. inflata*	7, 60%	Howes (personal observation)	Slow speeds were more suitable for maintaining cultures
Incubation 14°C in 2 μm filtered seawater in 2 L glass bottles enriched with *I. galbana*. Bottles sealed with parafilm, ensuring no air bubbles. Every second day water was changed by gently pouring through a 100-μm sieve. Inspection and removal of dead individuals				
Rotatory shakers (varying speeds) (Fig. 5B): Preparation as described for rollers	*L. inflata*	7d, 60%	Howes (personal observation)	Slow speeds were suitable for maintaining cultures.
Plankton wheel (Fig. 5C)	*C. inflexa* (e, j)	13, 70%	Comeau *et al.* (2010a)	Successful for individual <3 mm
1 L glass bottles prefilled with 0.2 μm-filtered seawater. Partial water change every second day, 13°C				
Tethering: Rapid setting gel-based glue used to attach pteropods to needle. Needles and pteropods introduced to seawater (14°C) immediately after attachment (Fig. 8). Disposable pipettes used to keep pteropods wet at all stages of procedure. Fed with *I. galbana*	*C. acicula*	7, 100%	Howes (personal observation)	Stressful and time-consuming attachment procedure
	C. inflexa	2, 100%		Response species specific
	C. pyramidata	1, 100%		Feeding not observed
	S. subula	5, 100%		

For pteropod life stages employed: (a) adults (j) juveniles, (l) veliger larvae, (e) eggs. Note that the survival time represents the point at which the experiments were concluded and does not represent the time at which all individuals died. It should also be considered that many of the methods listed were employed as part of perturbation experiments, therefore other stressors outside of the culture environment may have contributed to mortality.

Table III: Summary of variations in flow systems

Technique description	Species	Survival (days) and mortality (%)	Reference	Comments
Temperature-gradient plankton Kreisel (Fig. 3)	*C. inflexa* *C. virgula*	7	Gorsky *et al.* (1986)	Successful feeding observed at high algal concentrations
Up flowing (Fig. 6A) Main body cylindrical water inflow at the base, positioned under 100 μm mesh, to disperse the flow evenly. Mesh at the top of the water column prevents animals being washed out	*C. inflexa*	3, 100%	Howes (personal observation)	Animals sunk beneath the lowest current and struggled to swim back up through water flow. Use of meshes traps biofilm and pteropods. Requires exact flow rate control
Circular water current (Fig. 6B): Circular current provided by water inflow at top of kreisel	*C. acicula*	2, 100%	Purcell *et al.* (2013)	System did not provide enough flow to maintain buoyancy and water column too small to allow production of mucous web
Circulating upward flow (Fig. 6C) Main body is cylindrical. Three equally spaced inflows running vertically down one side. Each inflow fed by its own tube allowing the speed of the flows to be differentially controlled	*C. acicula*	3, 70%	Graeve (unpubl.), Howes (personal observation thesis)	System was more successful for the smaller individuals, <1 cm, and one was observed with mucous feeding web. Once settled, they struggled to swim up the water column through water flows
Bi-directional elliptical flow (Fig. 6D) Rectangular design. Two elliptical flows: one from the top of the tank flowing vertically and a second from one end, flowing horizontally	*C. acicula*	3, 80%	Purcell *et al.* (2013)	The flows did not maintain the animals in suspension and forced them to swim continually or sink to the bottom
110 L aquaria: 110 L V-shaped aquaria (40 × 40 × 70 cm) ca. 80 individuals	*L. helicina*	14, 90%	Böer *et al.* (2006)	Feeding not observed Water column too short, sinking time ~15 s
600 L system: (Fig. 7) Horizontal circular current, constant flow (10 L min^{-1}) 20 μm filtered water directly pumped from Kongsfjord 100 individuals per tank	*L. helicina*	14, 50%	Büdenbender (personal observation)	Feeding not observed Animals were observed floating in water column Large volumes of water unsuited to perturbation experiments

For pteropod life stages: (j) juveniles, (e) eggs. Note that the survival time represents the point at which the experiments were concluded and does not document the time at which all individuals died.

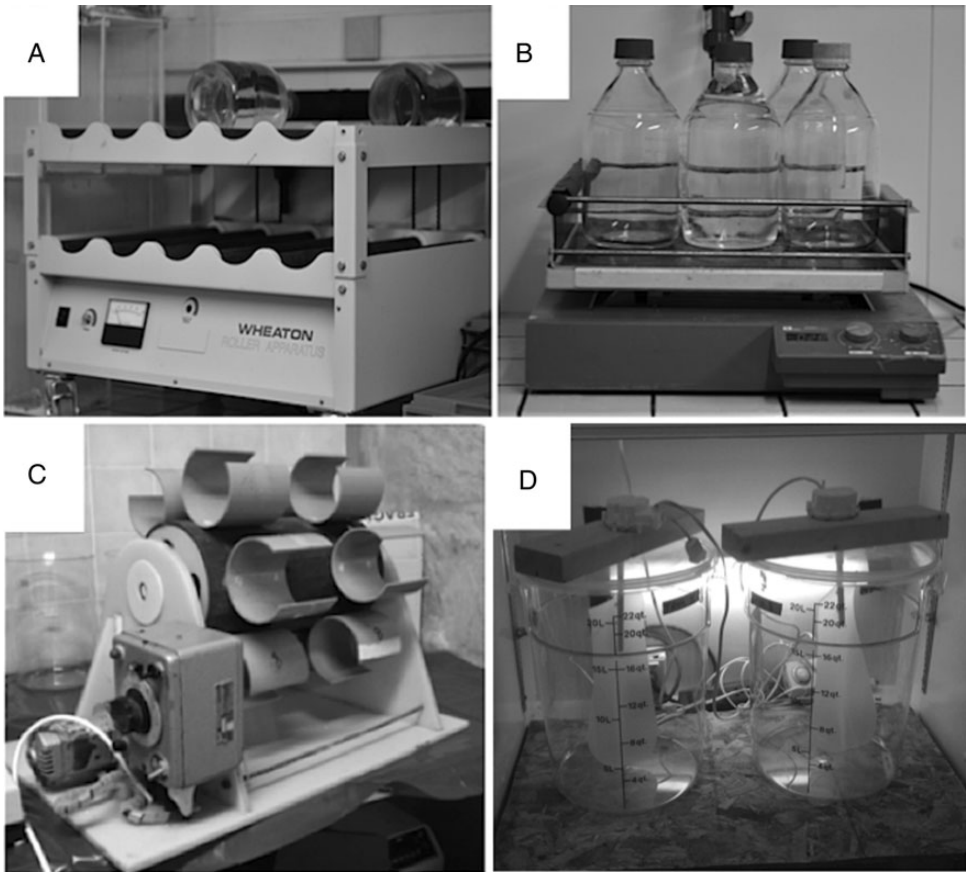

Fig. 3. Agitation methods: (**A**) rollers with sealed 2 L bottles containing *L. inflata* specimens. (**B**) Gyratory shaker with 2 L bottles containing *L. inflata* cultures. (**C**) Plankton wheel used for the culturing of *C. inflexa* egg clutches. (**D**) The larvacean system, used for appendicularian culturing. In this system, the organisms are maintained in suspension by creating a gentle current using plastic paddles that rotate slowly (<10 rpm) (Comeau *et al.*, 2009).

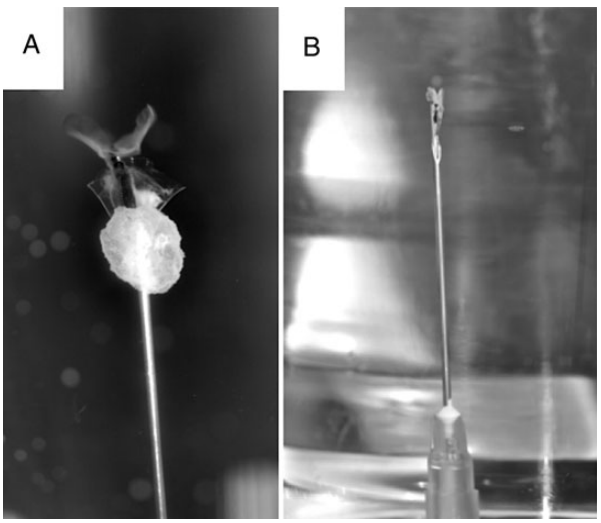

Fig. 4. Tethering method using needles and superglue. (**A**) *C. pyramidata*. and (**B**) *S. styliola*.

(Comeau *et al.*, 2010a). To avoid entrapment at the surface, the flask was filled to near overflowing and covered with Parafilm to eliminate air bubbles.

Initially, ~1 veliger mL^{-1} of culture water was considered optimal. Algae were added to the cultures to achieve a final concentration of 1×10^4 cells mL^{-1}. Flasks were inverted several times a day to mix algae and larvae. Cultures were screened using a 100-μm mesh and changed weekly at a minimum, and optimally every 3 days. At each culture water change, larvae were inspected and dead individuals removed using two drops of a 1:24 dilution of surgical scrub surfactant (Purdue Frederick, Norwalk, CT, USA) to re-suspend and facilitate handing the hydrophobic shells. Larvae were subsampled for measuring as necessary (typically 10–30 larvae were preserved per flask in 1% buffered formalin), and then concentrated into the centre of the dish by swirling. The larvae were then pipetted directly into a freshly prepared culture flask containing filtered sea water, algae and antibiotics. This

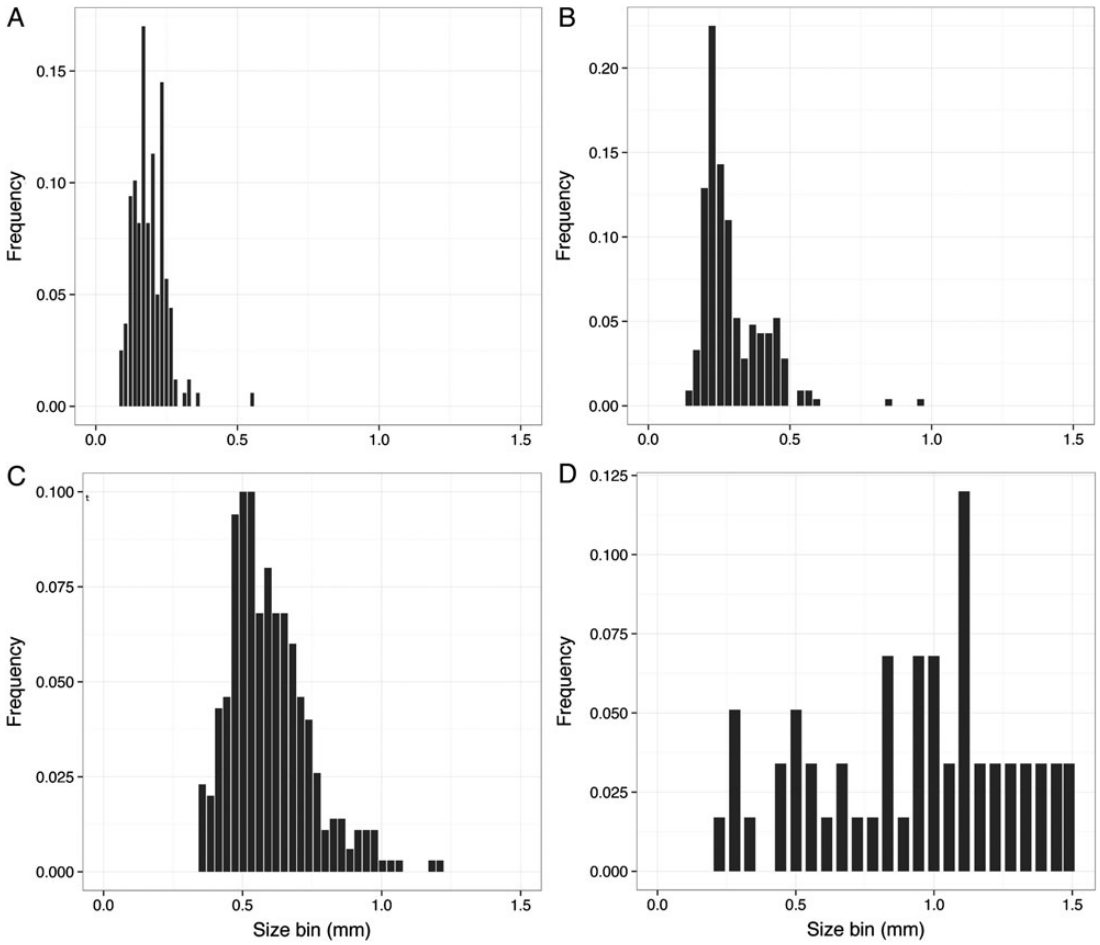

Fig. 5. Size distributions of juvenile and adult *L. retroversa* cultured at 10°C. (**A**) Metamorphosis, 50 days post-hatch, mean shell length 0.262 mm. (**B**) Sixty-two days post-hatch, mean shell length 0.459 mm. (**C**) Eighty days post-hatch, mean shell length 0.693 mm. (**D**) Ninety-eight days post-hatch, mean shell length 1.370 mm.

process minimized carryover of the surfactant from the glass dish. The flask is then sealed as before with parafilm or polyvinyl alcohol. As larvae developed and approached metamorphic competency, densities were reduced to 1 individual 10 mL^{-1}, and once metamorphosed, each flask of juveniles was transferred to 50-L culture vessels.

Recirculating systems

Variants on the original design of the plankton kreisel (Greve, 1968) have been used successfully to culture a variety of gelatinous zooplankton species (Dawson, 2000; Purcell *et al.*, 2013). A range of kreisels with different flow patterns have been tested for pteropod culture including circular, up-flow and multidirectional flow patterns (Fig. 6) (Table III). Notably, one of the only observed instances of pteropods producing mucuos webs under laboratory conditions (Fig. 1) was obtained using a variant of the "planktonkreisel" (Fig. 6E) (Gorsky *et al.*, 1986).

Kreisel systems typically use large volumes of water, and the movement produced by the currents gives buoyancy aid. The flow rate appears to be critical, and very fine control is required to keep the animals in suspension. If the flow is too strong, the pteropods will swim continuously, preventing feeding and resulting in rapid depletion of energy reserves. If too weak, it does not counteract the negative buoyancy of the shell and the animals come in contact with the sides and bottom of the vessel, causing shell damage and excess mucus production.

Flow-through systems

Flow through, or single-pass systems, utilize water currents and flows in the same way as circulating systems; however, in these aquaria, when the overflow water leaves the aquaria it is discarded. Gymnosome pteropods have been successfully maintained in large numbers (ca. 80 individuals) for 365 days using a 110-L, V-shaped

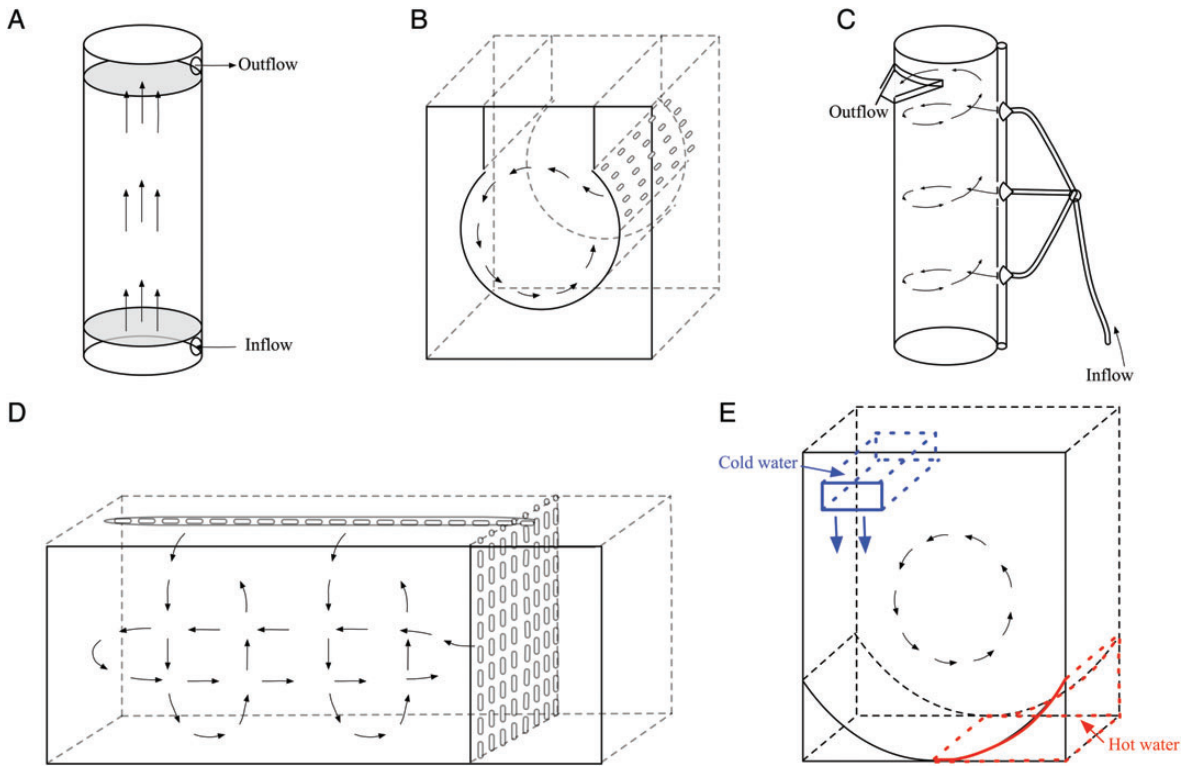

Fig. 6. Representations of the water flow kreisel systems, direction of water current represented by arrows. (**A**) Upflow system designed in Villefranche-sur-Mer (Mahacek, Moya and Howes). (**B**) Circular flow system used for ephyrae culture at Institut de Ciences del Mar, CSIC, Barcelona (Purcell *et al.*, 2013). (**C**) Circular upflow kreisel designed at Alfred Wegener Institute Helmholtz Centre for Polar and Marine Research Dr Martin Graeve. (**D**) Multidirectional jellyfish kreisel, Institut de Ciences del Mar, CSIC, Barcelona (Purcell *et al.*, 2013). (**E**) The temperature-gradient plankton kriesel (Gorsky *et al.*, 1986). The water current (black arrows) is generated by the difference in water density between low density water on one side of the tank on the bottom (created by warming up the water) and high density water on the top of the tank on the opposite side (created by cooling down the water).

aquaria (40 × 40 × 70 cm) (Lange and Kaiser, 1995) with constant circulation, to keep the animals swimming (Böer *et al.*, 2007). The same system was tested with *L. helicina*: the sinking from surface to the bottom of the aquaria was ∼15 s and after 14 days only 0–5 of 100 individuals survived.

Larger flow-through systems have been more successful. In the Marine Laboratory in Ny-Ålesund adult *L. helicina* were reared in 600-L flow-through system (10 L min^{-1}) (Table III) successfully for 14 days at 100 individuals per tank; mortality was <50%. A horizontal circular current transported the pteropods extending the time from surface to bottom by up to 1 min during which no swimming activity or interface collision occurred. Mucous feeding structures were not observed.

Mesocosm systems

The presence of a large water column, which can allow time for animals to deploy their mucous webs, makes mesocosm system candidates with high potential for successful pteropod culturing. To our knowledge, there have only been a few but promising attempts in this direction (Table II).

In 2010, nine KOSMOS mesocosms were deployed for 35 days in a high-arctic Fjord. The mesocosms contained ∼50 m^3 of natural fjord water, the enclosed water column was 15-m deep (Riebesell *et al.*, 2013). Controlled quantities of pteropods collected using jelly dippers were added to each mesocosm (4 individuals per m^3). Most died during the first 2 weeks due to a design shortcoming that trapped pteropods in the dead volume below the built-in sediment trap or in the sediment trap itself (Czerny *et al.*, 2012; Riebesell *et al.*, 2013). Only single individuals survived for the full period of the mesocosm deployment (30 days).

During the 2011 Bergen mesocosm campaign, nine KOSMOS units (Fig. 7) of ∼77 m^3 volume and the total bag length of 25 m were deployed in the Raunefjord close to the Espegrend Biological Station, Bergen, Norway. *Limacina retroversa* individuals of all life stages were part of the natural plankton community and were enclosed in the mesocosms during the filling process making the stressful collection process unnecessary.

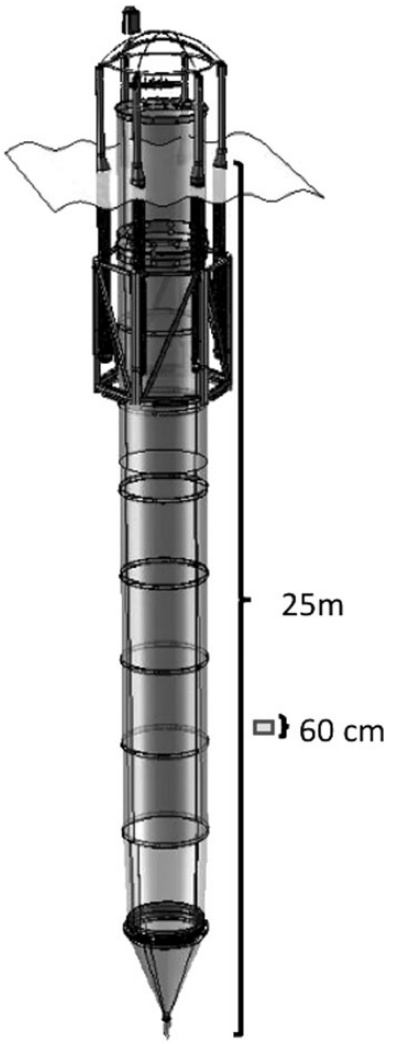

Fig. 7. KOSMOS system deployed for 40 days in Raunefjord Bergen Norway 2011, enclosing a natural plankton community including *L. retroversa*. Mesocosm drawing by D. Hoffmann.

Limacina retroversa as well as potential predators (e.g. *Clione limacina* and fish larvae) remained present for the full experiment (40 days) (Büdenbender *et al.*, in prep.). Mortality rates of veliger larvae under control conditions were ~50%.

DISCUSSION

Species selection

In general, when culturing thecosomes it seems that the size of the animals and the size of the culture vessels are both important. Although small species/juveniles (<1.5 mm) can be cultured in smaller vessels, larger species/adults require larger water volumes. Species of *Limacina* seem to be more robust than other body forms, with *L. retroversa* reared through larval stages to F3 generation under laboratory conditions. Healthy cultures of *L. inflata* have been maintained for at least 7 days in low densities (fewer than 10 individuals L^{-1}) in simple closed containers. Also, the slower metabolic rate at colder temperatures for polar Limacinidae allows longer survival when individuals are unable to feed (Hopcroft, personal observation).

Cavoliniidae are more problematic, possibly due to the increased shell and mantle complexity making them more prone to damage. Tethering methods showed some early promise when applied to Cavoliniidae species with simple conical shells, while some success has been reported with *Creseis virgula* and *Cavolinia inflexa* in the temperature-gradient plankton kreisel. Future attempts to improve culture systems should take into account the fact that the different forms respond differently to the same culture vessels; one size does not fit all. With the goal of performing successful perturbation experiments, effort should focus on developing techniques for a several key and widespread cosmopolitan species.

Larval rearing

The use of eggs laid in culture has been the only method that has successfully reared reproductive adults and refining this technique for polar species, e.g. *L. helicina*, and adapting it for Cavoliniidae should be a priority for future work. Whilst *L. retroversa* is relatively robust, there may also be advantages of working with F2 generations. The egg masses are not subjected to the rigours of sampling from the wild and can be kept in the most sterile conditions possible, limiting the risk of bacterial infestations. Experimentalists are able to work with many individuals of the same life stage that are already acclimatized to culture conditions. Successful work has already been undertaken using the egg clutches of *C. inflexa* (Comeau *et al.*, 2010a), with clutches raised through veliger stages to metamorphosis with low mortality. However, once individuals reach sizes of >1 mm, culture methods must be adapted, as mortality rapidly decreases populations by up to 50% in 24 h. Large adults can be induced to mass spawning in the laboratory when held in crowded conditions or exposed to mild heat or light stress (Howes, personal observation) making them good candidates for further work with careful application and adaptation of the methods presented here for *L. retroversa*.

Vessels

Batch cultures are easy, non-labour intensive and cheap for pteropod cultivation, but are much more suitable in small volumes for juveniles and small species than for

large adults as demonstrated for *L. retroversa*. With refinement, batch culturing should allow for easy experimental replication and could be implemented under field conditions. Nonetheless, fully closed batch culturing has its drawbacks: changes in sea water chemistry generated by biological activities (i.e. changes in oxygen availability, carbonate chemistry and the accumulation of potentially lethal nitrogenous wastes), along with the accumulation of faecal wastes and bacteria. Small closed volumes are also handicapped by increased contact rates with the sides or the base of the culture vessel. General husbandry of culture vessels and water changes appear critical to rearing success. In this regard, recirculating systems such as plankton kreisels or flow-through systems may offer some intermediate level of self-sufficiency albeit with higher cost and effort. With some specializations, manipulations of temperature and water chemistry are possible with kreisels and flow-through systems, e.g. as implemented in the indoor mesocosm facility at GEOMAR, Kiel.

Mesocosms such as those employed in the 2011 Bergen campaign show potential for new insights into pteropod ecology, particularly when tested with smaller *Limacinid* species. Mesocosms can provide conditions in which populations/species of pteropods are able to reach a state of neutral buoyancy and are able to feed with a mucous web on their natural food sources in a close to *in situ* environment. There is a need for new instruments, which allow *in situ* observation and controlled capture of single individuals within these systems due to their large body size/volume to water volume ratio (1:5.5 billion) (e.g. volume based camera systems and remotely operated sampling devices like small ROV's). Mesocosms like the KOSMOS system, due to their size, provide the most realistic and favourable conditions for pteropod culturing. As demonstrated in the 2010 experiments, the size and design of mesocosms must be taken into careful consideration in relation to the size and sinking rates of the pteropod species. Mesocosms with built-in sediment traps should be avoided as they act as a one-way gate, trapping animals at the bottom of the mesocosm (Büdenbender, personal observation). The labour, cost and logistics of setting up mesocosms are major drawbacks for experimental work where several treatments and replicates are required; the costs can, however, be greatly reduced by using pre-existing facilities such as the Espegrend biological station or by co-operation with existing projects. Further development of this work should focus on testing with non-polar or Cavoliniid species as it is not yet known how these less robust forms will respond to mesocosm conditions.

The common problem for all thecosome species is buoyancy and, as a direct result, feeding behaviour. As described above, many flow systems destabilize or trap animals and even the use of much larger culture vessels does not allow adequate sinking space. In a range of culture vessels used by Gallager with *L. retroversa*, healthy adults and juveniles of various species tended to congregate at the surface. Surface aggregation may have been a response to gravity, illumination, tank currents or food, with individuals observed vigorously swimming upwards and across the surface, followed by drifting downwards at various rates, usually quite slowly.

In the wild, pteropods undergo diurnal vertical migration (DVM), for some species of >300 m, which has been suggested to be linked to control of metabolic rate (Wormuth, 1981; Lalli and Gilmer, 1989; Maas *et al.*, 2012b). The migratory behaviour might account for sinking and could exacerbate feeding difficulties experienced by culture specimens. The development of culture vessels, dark incubations, opaque tanks or graduated opaque tanks with darker bases and transparent tops, might exploit the natural upward migrations during dark hours and reduce sinking periods in laboratory animals. Variegated mesocosms have been used to culture jellyfish found in meromictic lakes (Dawson, 2000) and such an introduction of a false halo, thermo or chemocline might counteract the downward migrations of the pteropods or satisfy metabolic needs related to DVM.

Diet and feeding

As a result of abnormal feeding behaviour in many culture vessels, it is unclear whether inadequate diet may be a further stressor for laboratory animals; several taxa of gelatinous zooplankton require mixed diets when maintained in artificial environments (Raskoff *et al.*, 2003). Sub-optimal food might account for the relatively slow growth rates encountered during culture of *L. retroversa*. Many other commonly cultured zooplankton genera can only achieve optimal fitness when provided with specific diets (Demott and Müller-Navarra, 1997; Sommer, 1998; Knuckey *et al.*, 2005). Gut content analysis of wild-caught, adult *L. helicina* indicates an omnivorous and, often, cannibalistic diet with juvenile life stages apparent in the gut contents (Gilmer and Harbison, 1991). Small disturbances to the mucous web provoke rapid ingestion and it has been hypothesized that adults may, in fact, be mucous trappers, using their webs as a spider would (Gilmer and Harbison, 1991). The guts of juveniles and smaller (<2.6 mm shell diameter) individuals contained only phytoplankton (Hopkins, 1987), suggesting a possible dietary shift in adult life stages. These *in situ* observations suggest that the mechanical feeding difficulties experienced by thecosomes in laboratory cultures of adults may be compounded by sub-optimal diets. The species selected for algal diets should

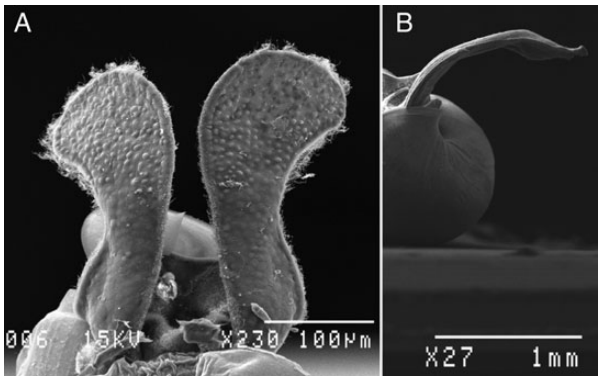

Fig. 8. (**A**) Long cilia fringing the periphery of the parapodia of *L. retroversa* (arrow). (**B**) Food groove travelling around the circumference of the parapodia of *L. retroversa* (arrow).

be tailored to the size and developmental stage of the culture individuals. Algal species that occur concurrently with the culture species of pteropods should be used where possible.

Observations of cultured *L. retroversa* have shown periods of negligible and sometimes slightly buoyant drift usually associated with web production. However, at no point during culture to the F3 generation were feeding webs observed, although phytoplankton was present in the guts of all life stages. The same phenomenon was also observed in healthy cultures of *L. inflata* (Howes, personal observation) and *L. helicina* (Doubleday, personal observation). Close examination of the parapodia of tethered *L. retroversa* indicated that the edges of the parapodia were fringed with several sets of cilia (Fig. 8A). Long cilia (~30 um) beat at a rate of ~15 Hz and together produced sufficient lift to keep the organisms floating with the parapodia extended but not moving. The longer cilia also provided flow to carry food particles past the parapodia edge where they were captured by the shorter cilia. These shorter cilia (~5 µm) surrounded the parapodia and formed a food groove (Fig. 8B) that transported particles to the mouth. Particles were observed moving at ~20 µm s^{-1} in the food groove towards the mouth where some form of particle selection occurred. Feeding appeared to occur when the parapodia were extended and not moving as the organism slowly drifted about as if it were neutrally buoyant. Yonge (Yonge, 1926) proposed ciliary feeding in pteropods and it was later described, in *L. retroversa* by Morton (Morton, 1954). Since the scuba observations of Gilmer and Harbison (Gilmer and Harbison, 1986), the mucous web has become the accepted feeding mechanism in all pteropods, but these recent studies suggest that a mucous web is not essential for feeding under at least some conditions. If the mucous trapper theory is correct, production of a mucous net might only be triggered when larger, motile prey is detected: future studies should explore if mixed cultures of pteropods with smaller zooplankton prey induce web production. Alternatively, the high food concentrations in culture means may only require ciliary feeding mechanisms and that webs, which are energetically expensive to produce, are only used to maximize capture when food is sparse.

Healthy *L. helicina* can survive starvation for 2–4 weeks (depending on condition at capture and body size) at 0–5°C by living off lipid and body reserves (Lischka *et al.*, 2011; Lischka and Riebesell, 2012), as can *L. helicina antarctica* at −2°C (Maas *et al.*, 2011) and also at higher temperatures of up to 4°C (Bednaršek *et al.*, 2012a). Cultures of veliger stage *L. helicina* have been observed to survive starvation for up to 7 days near 0°C (Hopcroft, personal observation). Ideally, successful culture methodology should confirm that feeding is taking place either by measuring metabolic rate (which decreases with food deprivation), or by direct observation of feeding structures or full guts. Designs utilizing camera systems may be required for feeding observations as production, and retraction of feeding webs can be very rapid (Lalli and Gilmer, 1989).

Established protocols

Culture of other taxa of gelatinous zooplankton has been markedly more successful than that of pteropods, although many of the challenges faced are very similar. The production of mucous feeding structures was a major issue for appendicularian culturing just as it is for thecosome pteropods (Paffenhöfer, 1973). Delicate gelatinous bodies are prone to damage from collection and handling and must be kept in suspension, protected from impacts with the walls and base of culture vessels. The traditional plankton kreisel (Greve, 1968) is suitable for many species and, in other cases, has provided an excellent starting point for more complex designs (Sommer, 1992, 1993). Pteropod culture tests have been relatively successful using flow through and temperature-gradient kreisels, and these prototypes should now be expanded upon. Many attempts at culture development are side projects or a means to an end for a wider research project, such that the inevitable lack of time prevents the further development of promising systems. It is our belief that progress could be vastly improved with dedicated projects focused on improving systems and increased cooperation with aquaculturists. In this manner, it would be possible to capitalize on the potential economic value to fisheries as well as usefulness to the scientific community.

The successful culture techniques used during rearing *L. retroversa* were developed in collaboration with mariculturists raising the opisthobranch *Aplysia californica* (Capo *et al.*, 1997).

Current pteropod culture techniques are insufficient to address many questions about their future under changing climate conditions. There is a pressing need to develop improved cultivating methods, as thecosome pteropods are major exporters of carbon to the deep oceans in some regions (Berner and Honjo, 1981) and important prey items for a number of animals, including commercially important species (Armstrong *et al.*, 2008). Focus should first be on establishing successful culture methods before attempting to adapt these methods for suitability in undertaking perturbation experiments.

Recommendations

(i) Dedicated projects to develop systems and increased co-operation with aquaculturists. In this manner it would be possible to capitalize on the potential economic value to fisheries as well as usefulness to the scientific community. This would also allow the further development of reasonably successful methods reported here, several promising methods have been attempted once or twice and then abandoned due to lack of time or other priorities.

(ii) At present, perturbation experiments should focus on smaller (<2 mm) species, larval or lipid rich life stages to ensure healthy cultures and minimize the effects of experimental stress on observed variables until solutions can be found for larger species and adults.

(iii) In the case that perturbation experiments with adults and larger species are attempted, large-scale facilities (>500 L) should be considered (e.g. Bergen mesocosm facilities, Kiel KOSMOS system).

(iv) Tailoring of mixed algal diets depending on species size, life stage and algal species that are associated with pteropod blooms. Introduction of small zooplankton prey items for large species should be explored. Since web production has been observed with the temperature-gradient kreisel, this apparatus should be used for investigation of potential links between food concentration and web production and

(v) Improved communication between researchers: whilst compiling this paper it has become clear that the same, largely unsuccessful, methods have been attempted and re-attempted by several research groups. Thecosome pteropod abundance is patchy and difficulties in developing useful techniques are often compounded by limited access to specimens. As such, it is vital that opportunities are not lost repeating unsuccessful methodology.

ACKNOWLEDGEMENTS

This work is a contribution to the European Union, Framework 7 "Mediterranean Sea Acidification under a changing climate" project (MedSeA; grant agreement 265103). The following funding agencies are also gratefully acknowledged: The Office of Naval Research and Alaska SeaGrant for funding under Project R/101-08". Research Associate P. Alatalo and T. Capo were instrumental in developing the *L. retroversa* culture techniques. We are also indebted to P. Mahacek for his skill and enthusiasm in helping design and building various culture system prototypes, V. Fuentes and M. Gentile for the use of the jellyfish systems at Institut de Ciences del Mar, CSIC, Barcelona, Dr M. Greave for the use of aquaria and discussion and F. Lombard and M. Lilley for invaluable assistance and advice. Thanks are also due to two anonymous reviewers whose constructive criticisms greatly improved an earlier draft of this paper.

FUNDING

The European Union, Framework 7 "Mediterranean Sea Acidification under a changing climate" project (MedSeA; grant agreement 265103), The Office of Naval Research and Alaska SeaGrant for funding under Project R/101-08.

REFERENCES

Armstrong, J. L., Myers, K. W., Beauchamp, D. A. *et al.* (2008) Interannual and spatial feeding patterns of hatchery and wild juvenile pink salmon in the Gulf of Alaska in years of low and high survival. *Trans. Am. Fish. Soc.*, **137**, 1299–1316.

Bednaršek, N., Tarling, G. A., Bakker, D. C. E. *et al.* (2012a) Description and quantification of pteropod shell dissolution: a sensitive bioindicator of ocean acidification. *Global Change Biol.*, **18**, 2378–2388.

Bednaršek, N., Tarling, G. A., Fielding, S. *et al.* (2012b) Population dynamics and biogeochemical significance of *Limacina helicina antarctica* in the Scotia Sea (Southern Ocean). *Deep-Sea Res. Pt. II*, **59–60**, 105–116.

Berner, R. A. and Honjo, S. (1981) Pelagic sedimentation of aragonite: its geochemical significance. *Science*, **3**, 940–942.

Böer, M., Graeve, M. and Kattner, G. (2006) Impact of feeding and starvation on the lipid metabolism of the Arctic pteropod *Clione limacina*. *J. Exp. Mar. Biol. Ecol.*, **328**, 98–112.

Böer, M., Graeve, M. and Kattner, G. (2007) Exceptional long-term starvation ability and sites of lipid storage of the Arctic pteropod *Clione limacina*. *Polar Biol.*, **30**, 571–580.

Bouquet, J. M., Spriet, E., Troedsson, C. *et al.* (2009) Culture optimization for the emergent zooplanktonic model organism *Oikopleura dioica*. *J. Plankton Res.*, **31**, 359–370.

Capo, T. R., Perrit, S. E. and Paige, J. A. (1997) Mass culture of Aplysia californica: embryonic through juvenile stages. Report to the Howard Hughes Medical Institution, Maryland, USA.

Childress, J. J., Barnes, A. T., Quetin, L. B. *et al.* (1978) Thermally protecting cod ends for the recovery of living deep-sea animals. *Deep-Sea Res.*, **25**, 419–422.

Comeau, S., Alliouane, S. and Gattuso, J. P. (2012) Effects of ocean acidification on overwintering juvenile Arctic pteropods *Limacina helicina*. *Mar. Ecol. Prog. Ser.*, **456**, 279–284.

Comeau, S., Gorsky, G., Alliouane, S. *et al.* (2010a) Larvae of the pteropod *Cavolinia inflexa* exposed to aragonite undersaturation are viable but shell-less. *Mar. Biol.*, **157**, 2341–2345.

Comeau, S., Gorsky, G., Jeffree, R. *et al.* (2009) Impact of ocean acidification on a key Arctic pelagic mollusc (*Limacina helicina*). *Biogeosciences*, **6**, 1877–1882.

Comeau, S., Jeffree, R., Teyssié, J.-L. *et al.* (2010b) Response of the Arctic pteropod *Limacina helicina* to projected future environmental conditions. *PLoS One*, **5**, e11362.

Czerny, J., Schulz, K. G., Boxhammer, T. *et al.* (2012) Element budgets in an Arctic mesocosm CO_2 perturbation study. *Biogeosci. Disc.*, **9**, 11885–11924.

Dawson, M. N. (2000) Variegated mesocosms as alternatives to shore-based planktonkreisels: notes on the husbandry of jellyfish from marine lakes. *J. Plankton Res.*, **22**, 1673–1682.

Demott, W. R. and Müller-Navarra, D. C. (1997) The importance of highly unsaturated fatty acids in zooplankton nutrition: evidence from experiments with *Daphnia*, a cyanobacterium and lipid emulsion. *Freshwat. Biol.*, **38**, 649–664.

Fabry, V. J. (1989) Aragonite production by pteropod molluscs in the subarctic Pacific. *Deep-Sea Res.*, **36**, 1735–1751.

Fabry, V. J. (1990) Shell growth rates of pteropod and heteropod molluscs and aragonite production in the open ocean: implications for the marine carbonate system. *J. Mar. Res.*, **48**, 209–222.

Gallager, S. M., Davis, C. S., Epstein, A. W. *et al.* (1996) High-resolution observations of plankton spatial distributions correlated with hydrography in the Great South Channel, Georges Bank. *Deep-Sea Res. II*, **43**, 1627–1663.

Gilmer, R. W. (1972) Free-floating mucus webs: a novel feeding adaptation for the open ocean. *Science*, **176**, 1239–1240.

Gilmer, R. W. (1974) Some aspects of feeding in thecosomatous pteropod mollusks. *J. Exp. Mar. Biol. Ecol.*, **15**, 127–144.

Gilmer, R. W. and Harbison, G. R. (1986) Morphology and field behavior of pteropod molluscs: feeding methods in the families Cavoliniidae, Limacinidae and Peraclididae (Gastropoda: Thecosomata). *Mar. Biol.*, **91**, 47–57.

Gilmer, R. W. and Harbison, G. R. (1991) Diet of *Limacina helicina* (Gastropoda: Thecosomata) in Arctic waters in midsummer. *Mar. Ecol. Prog. Ser.*, **77**, 125–134.

Gorsky, G., Fenaux, R. and Palazzoli, I. (1986) Une methode de maintien en suspension des organismes zooplanctoniques fragiles. *Rapp. Comm. int. Mer Médit.*, **30.2.204**, 21–22.

Greve, W. (1968) The "planktonkreisel", a new device for culturing zooplankton. *Mar. Biol.*, **1**, 201–203.

Haddock, S. H. D. and Heine, J. N. (2005) *Scientific Blue-Water Diving*. Vol. 1. California Sea Grant College Program, La Jolla, CA.

Hamner, W., Madin, L., Alldredge, A. *et al.* (1975) Underwater observations of gelatinous zooplankton: sampling problems, feeding biology, and behavior. *Limnol. Oceanogr.*, **20**, 907–917.

Hopkins, T. L. (1987) Midwater food web in McMurdo Sound, Ross Sea, Antarctica. *Mar. Biol.*, **96**, 93–106.

Ikeda, T. and Mitchell, A. W. (1982) Oxygen-uptake, ammonia excretion and phosphate excretion by krill and other antarctic zooplankton in relation to their body size and chemical-composition. *Mar. Biol.*, **71**, 283–298.

Knuckey, R. M., Semmens, G. L., Mayer, R. J. *et al.* (2005) Development of an optimal microalgal diet for the culture of the calanoid copepod *Acartia sinjiensis*: effect of algal species and feed concentration on copepod development. *Aquaculture*, **249**, 339–351.

Lalli, C. M. and Gilmer, R. W. (1989) *Pelagic Snails. The Biology of Holoplanktonic Gastropod Mollusks*. Stanford University Press, Stanford, CA.

Lange, J. and Kaiser, R. (1995) The maintenance of pelagic jellyfish in the Zoo-Aquarium, Berlin. *Int Zoo Yearb*, **34**, 59–64.

Lischka, S., Budenbender, J., Boxhammer, T. *et al.* (2011) Impact of ocean acidification and elevated temperatures on early juveniles of the polar shelled pteropod *Limacina helicina*: mortality, shell degradation, and shell growth. *Biogeosciences*, **8**, 919–932.

Lischka, S. and Riebesell, U. (2012) Synergistic effects of ocean acidification and warming on overwintering pteropods in the Arctic. *Global Change Biol.*, **18**, 3517–3528.

Maas, A. E., Elder, L. E., Dierssen, H. M. *et al.* (2011) Metabolic response of Antarctic pteropods (Mollusca: Gastropoda) to food deprivation and regional productivity. *Mar. Ecol. Prog. Ser.*, **441**, 129–139.

Maas, A. E., Wishner, K. F. and Seibel, B. A. (2012a) The metabolic response of pteropods to acidification reflects natural CO_2-exposure in oxygen minimum zones. *Biogeosciences*, **9**, 747–757.

Maas, A. E., Wishner, K. F. and Seibel, B. A. (2012b) Metabolic suppression in thecosomatous pteropods as an effect of low temperature and hypoxia in the Eastern Tropical North. *Mar. Biol.*, **159**, 1955–1967.

Manno, C., Morata, N. and Primicerio, R. (2012) *Limacina retroversa*'s response to combined effects of ocean acidification and sea water freshening. *Estuar. Coast. Shelf Sci.*, **113**, 163–171.

Morton, J. E. (1954) The biology of *Limacina retroversa*. *J. Mar. Biol. Assoc., U.K.*, **33**, 297–312.

Mucci, A. (1983) The solubility of calcite and aragonite in seawater at various salinities, temperatures, and one atmosphere total pressure. *Am. J. Sci.*, **283**, 780–799.

Orr, J. C. (2011) Recent and future changes in ocean carbonate chemistry. In Gattuso, J.-P. and Hansson, L. (eds), *Ocean Acidification*. Oxford University Press, Oxford, pp. 41–66.

Paffenhöfer, G.-A. (1973) The cultivation of an appendicularian through numerous generations. *Mar. Biol.*, **22**, 183–185.

Purcell, J. E., Baxter, E. J. and Fuentes, V. (2013) Jellyfish as products and problems for aquaculture. In: Allan, G. and Burnell, G. (eds), *Advances in Aquaculture Hatchery Technology*, 1st edn. Woodhead Publishing, Cambridge, UK.

Raskoff, K. A., Sommer, F. A., Hamner, W. M. *et al.* (2003) Collection and culture techniques for gelatinous zooplankton. *Biol. Bull.*, **204**, 68–80.

Riebesell, U., Czerny, J., Von Bröckel, K. *et al.* (2013) Technical note: a mobile sea-going mesocosm system—new opportunities for ocean change research. *Biogeosciences*, **10**, 1835–1847.

Robison, B. H. (2004) Deep pelagic biology. *J. Exp. Mar. Biol. Ecol.*, **300**, 253–272.

Sabine, C. L., Feely, R. A., Gruber, N. *et al*. (2004) The oceanic sink for anthropogenic CO_2. *Science*, **305**, 367–371.

Seibel, B., Maas, A. E. and Dierssen, H. M. (2012) Energetic plasticity underlies a variable response to Ocean acidification in the Pteropod, *Limacina helicina antarctica*. *PLoS One*, **7**, e30464.

Seibel, B. A., Dymowska, A. and Rosenthal, J. (2007) Metabolic temperature compensation and co-evolution of locomotory performance in pteropod moluscs. *Integr. Comp. Biol.*, **47**, 880–891.

Sommer, F. A. (1992) Husbandry aspects of a jellyfish exhibit at the Monterey Bay Aquarium. In American Associations of Zoological Parks and Aquariums Annual Conference Proceedings, Toronto, pp. 362–369.

Sommer, F. A. (1993) Jellyfish and beyond: husbandry of gelatinous zooplankton at the Monterey Bay Aquarium. In Proceedings of the Third International Aquarium Congress, Boston, MA, pp. 249–261.

Sommer, U. (1998) From algal competition to animal production: enhanced ecological efficiency of *Brachionus plicatilis* with a mixed diet. *Limnol. Oceanogr.*, **43**, 1393–1396.

Spotte, S. and Adams, G. (1981) Pathogen reduction in closed aquaculture systems by UV radiation: fact or artifact? *Mar. Ecol. Prog. Ser.*, **6**, 295–298.

Utting, S. D. and Spencer, B. E. (1991) *The Hatchery Culture of Bivalve Mollusc Larvae and Juveniles*. Vol. 68. Laboratory Leaflet ed. Ministry of Agriculture, Fisheries and Food, Lowestoft, UK.

Wormuth, J. H. (1981) Vertical distributions and diel migrations of Euthecosomata in the northwest Sargasso Sea. *Deep-Sea Res.*, **28A**, 1493–1515.

Yonge, C. M. (1926) Ciliary feeding mechanisms in the thecosomatous pteropods. *Zool. J. Linn. Soc.*, **36**, 417–429.

4.5.2 Publication V

Technical Note: A Mobile Sea-Going Mesocosm System – New Opportunities for Ocean Change Research.

Co-authored, published in Biogeosciences

Biogeosciences, 10, 1835–1847, 2013
www.biogeosciences.net/10/1835/2013/
doi:10.5194/bg-10-1835-2013

Biogeosciences Open Access

Technical Note: A mobile sea-going mesocosm system – new opportunities for ocean change research

U. Riebesell, J. Czerny, K. von Bröckel, T. Boxhammer, J. Büdenbender, M. Deckelnick, M. Fischer, D. Hoffmann, S. A. Krug, U. Lentz, A. Ludwig, R. Muche, and K. G. Schulz

GEOMAR Helmholtz-Zentrum für Ozeanforschung Kiel, 24105 Kiel, Germany

Correspondence to: U. Riebesell (uriebesell@geomar.de)

Received: 23 August 2012 – Published in Biogeosciences Discuss.: 19 September 2012
Revised: 25 February 2013 – Accepted: 26 February 2013 – Published: 19 March 2013

Abstract. One of the great challenges in ocean change research is to understand and forecast the effects of environmental changes on pelagic communities and the associated impacts on biogeochemical cycling. Mesocosms, experimental enclosures designed to approximate natural conditions, and in which environmental factors can be manipulated and closely monitored, provide a powerful tool to close the gap between small-scale laboratory experiments and observational and correlative approaches applied in field surveys. Existing pelagic mesocosm systems are stationary and/or restricted to well-protected waters. To allow mesocosm experimentation in a range of hydrographic conditions and in areas considered most sensitive to ocean change, we developed a mobile sea-going mesocosm facility, the Kiel Off-Shore Mesocosms for Future Ocean Simulations (KOSMOS). The KOSMOS platform, which can be transported and deployed by mid-sized research vessels, is designed for operation in moored and free-floating mode under low to moderate wave conditions (up to 2.5 m wave heights). It encloses a water column 2 m in diameter and 15 to 25 m deep (~50–75 m^3 in volume) without disrupting the vertical structure or disturbing the enclosed plankton community. Several new developments in mesocosm design and operation were implemented to (i) minimize differences in starting conditions between mesocosms, (ii) allow for extended experimental duration, (iii) precisely determine the mesocosm volume, (iv) determine air–sea gas exchange, and (v) perform mass balance calculations. After multiple test runs in the Baltic Sea, which resulted in continuous improvement of the design and handling, the KOSMOS platform successfully completed its first full-scale experiment in the high Arctic off Svalbard (78°56.2′ N, 11°53.6′ E) in June/July 2010. The study, which was conducted in the framework of the European Project on Ocean Acidification (EPOCA), focused on the effects of ocean acidification on a natural plankton community and its impacts on biogeochemical cycling and air–sea exchange of climate-relevant gases. This manuscript describes the mesocosm hardware, its deployment and handling, CO_2 manipulation, sampling and cleaning, including some further modifications conducted based on the experiences gained during this study.

1 Introduction

Of the more than 260 scientific papers published until now on ocean acidification and its impacts on marine life less than 5 % have been conducted on communities or ecosystems, with the vast majority of studies performed on individual species (Gattuso and Hansson, 2011). Extrapolating from organism-based effects to community and ecosystem impacts is difficult, because the observed responses are typically obtained in the absence of competition, trophic interactions, and with low or no genetic diversity (Riebesell and Tortell, 2011). For the same reasons parameterizations of biological processes in ecosystem and biogeochemical models based on physiological responses of individual organisms are problematic. In benthic systems, natural high CO_2 environments, such as CO_2-venting sites, provide a powerful test bed to assess effects of ocean acidification at the community and ecosystem level. Studies at volcanic CO_2 vents have revealed drastic changes in benthic community composition and biodiversity when compared to adjacent areas not exposed to high CO_2 (Barry et al., 2011). Because of

lateral advection and mixing of water masses, CO_2-venting sites generally do not provide useful testing grounds to study ocean acidification impacts on pelagic communities (Riebesell, 2008). Oceanographic transects along natural CO_2 gradients, e.g. from temperate to high-latitude waters (Charalampopoulou et al., 2011) or from recently upwelled high-CO_2 waters downstream towards lower-CO_2 waters (Beaufort et al., 2011), offer the opportunity for community-level comparisons. Because of the many other environmental factors varying in concert with CO_2, the interpretation of observed biotic differences along those gradients is complex.

For pelagic systems mesocosms provide a powerful approach to maintain a natural community under close-to-natural self-sustaining conditions, taking into account relevant aspects from "the real world" such as indirect effects, biological compensation and recovery, and ecosystem resilience, which commonly are not accounted for in small-scale laboratory experiments (Riebesell et al., 2010). The mesocosm approach is therefore often considered the experimental ecosystem closest to the "real world", without losing the advantage of reliable reference conditions and replication (Petersen et al., 2003). The main advantages unique to mesocosm experimentation are as follows:

1. The ability to investigate community dynamics of three or more levels for an extended period of time.
2. The ability to measure the pools and fluxes of bio-active and particle reactive elements and compounds and to perform mass balance calculations in complex systems.
3. The ability to study interactions of ecosystem dynamics and biogeochemical processes under experimental conditions.
4. The ability to bring together scientists from a variety of disciplines, ranging from, e.g., molecular and evolutionary biology, ecophysiology, marine ecology and biogeochemistry to marine and atmospheric chemistry.

It needs to be acknowledged, however, that some constraints of enclosures are to be considered when extrapolating mesocosm results to natural systems (see Riebesell et al., 2010, for a review). Enclosures of all kinds are inherently limited in their ability to include higher trophic levels (e.g. fish, seabirds and mammals), and to approximate vertical mixing of water column and small-scale shear occurring in nature (Menzel and Steele, 1978; Carpenter, 1996). Enclosure effects may also influence food web dynamics to varying degrees, creating trophic interactions that can differ with mesocosm dimension and which may deviate from those of the natural system intended to be mimicked (Kuiper et al., 1983; French and Watts, 1989, Petersen et al., 2009). Despite these difficulties and the intense debate they have spurred over the past decades (e.g. Pilson and Nixon, 1980; Brockmann, 1990; Drenner and Mazumber, 1999), mesocosm enclosure studies still remain the most generally applicable means to experimentally manipulate and repeatedly sample multi-trophic planktonic communities.

Considering the wide range of topics in ocean change research where mesocosm experimentation could greatly advance our science, there are surprisingly few marine mesocosm facilities in operation. Moreover, existing facilities are either stationary or confined to well-protected waters, limiting their scope of application. Here we describe a newly developed sea-going mesocosm facility which can be used in moored and free-floating mode under low to moderate wave conditions (up to 2.5 m wave heights). The new design in combination with new developments in mesocosm handling and sampling are intended to optimize mesocosm performance, prolong the duration of mesocosm experiments, and perform mass balance calculations by accounting for all relevant pools and fluxes of elements and compounds of interest.

2 Material and methods

Most of the following description relates to the 2010 experiment off Svalbard. The corresponding sections are written in past tense. Some aspects of the mesocosm hardware and handling used in 2010 were modified in subsequent experiments. To avoid providing detailed descriptions of the KOSMOS approach for each new experiment, we have included descriptions of those modifications in this manuscript. To distinguish between aspects specific for the 2010 experiment and those applicable to KOSMOS hardware and handling in general, we will use past tense in the case of the former and present tense for the latter.

2.1 Mesocosm hardware

The Kiel Off-Shore Mesocosms for Future Ocean Simulations (KOSMOS) consist of 9 mesocosm units, which are operated independently. Each unit comprises a floatation frame, the mesocosm bag, a bottom shutter and sediment trap, a dome-shaped hood on top of the floatation frame, weights at the bottom of the floatation frame and the lower end of the bags to maintain an upright position when exposed to wind and wave activity, and various ropes needed for mesocosm operation. The total weight of each KOSMOS unit, including all components described below, is approximately 1.7 tons.

2.2 Floatation frame

The KOSMOS floatation frame consists of six 7.5 m-long, 30 cm-diameter closed glass fibre tubes which are fixed to a steel structure in the lower part and by a steel metal ring at the top end. Steel weights are attached to the horizontal junctions at the bottom of the steel structure. The diameter of the glass fibre tubes, which generate the buoyancy, is reduced at and above the waterline to lower the up- and downward movement of the floatation frame due to wave action.

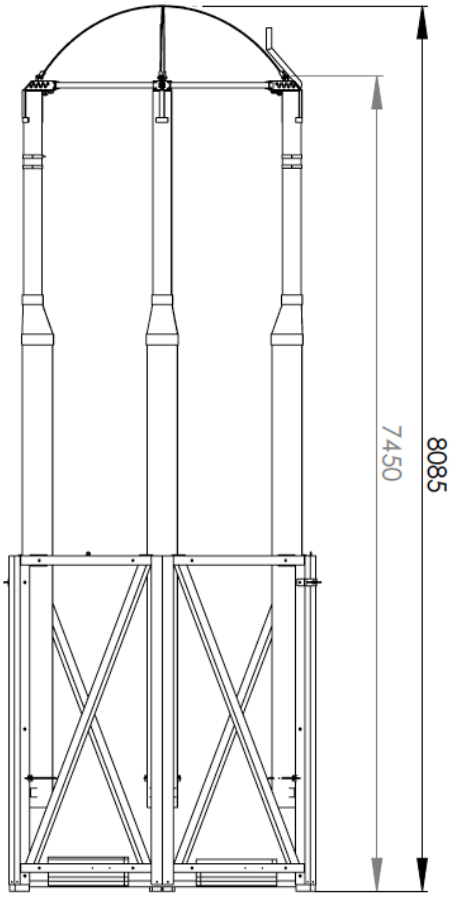

Fig. 1. Drawing of floatation frame with steel structure (lower part), glass fibre tubes for buoyancy, and steel ring at top, holding the dome-shaped PVC hoods. The tapering of the tubes in the above-surface section reduces buoyancy changes due to wave activity. Size indications in mm.

A dome-shaped roof made of polyvinyl chloride (PVC) covered with metal spikes is mounted on top of the floatation frame to reduce precipitation into the mesocosms and prevent seabirds from landing on the frame and defecating into the enclosures. The PCV foil has ca. 80 % light transparency in the spectral range > 400 nm wavelength. Below 400 nm the transparency strongly decreases, largely precluding the penetration of UV light. A flashlight with light sensor, solar panels and radar reflector is mounted on top of the frame, intended to alert passing ships. A set of clamps on either side of the frame above the waterline serves to fix various ropes needed to unfold, fix and operate the mesocosm enclosures (see mesocosm filling below). At the time of deployment the mesocosm bag is folded in a pack positioned above the water line (as displayed in Fig. 1).

2.3 Mesocosm bags

The enclosure bags are made of thermoplastic polyurethane (TPU) with a thickness of 1 mm in the upper 7 m and 0.5 mm below that. The bag diameter is 2 m. The length of the bag can be selected according to the scientific question and the conditions at the deployment location. For the 2010 experiment a total length of 17 m, 2 m above and 15 m below the water line, with a volume of approximately 50 m^3, was chosen. Follow-up experiments in the Raunefjord south of Bergen, Norway, in June/July 2011 used bag total lengths of 25 m, and off Hawaii in November/December 2011 and in the Finnish archipelago off Tvärminne in June to August 2012 19 m bag lengths. To maintain an approximately cylindrical shape of the mesocosm bags, rings of 2 m inner diameter made of 4 cm polyethylene pipes are positioned every 2 m in ring-shaped pockets made of TPU foil fixed onto the outside of the enclosure bag by high-frequency welding (Fig. 2).

Measurements of light intensities taken in parallel inside the mesocosms and outside in the fjord yielded similar surface layer light intensities and similar depth profiles in the PAR spectrum (see also Schulz et al., 2013). Light transparency measurements of the TPU foil revealed nearly 100 % absorbance of UV light. This together with the low light transparency below 400 nm of the PVC roof resulted in negligible UV light intensities inside the mesocosms.

2.4 Bottom shutter and sediment trap

At the bottom of the enclosure bag a steel ring holds two semi-circle plates made of 10 mm-thick Makrolon®. The plates are in upright position to allow water to enter the mesocosm bags during the lowering and unfolding of the bags (Fig. 3, left panel). A 2 m-long funnel-shaped sediment trap with a mouth of the same diameter as the mesocosm bag is connected to one of the bottom lids. It is tightly folded and attached between the bottom plates and unfolds and stretches automatically through an air-filled ring at the upper end of the funnel immediately after the bottom plates are closed (Fig. 3, right panel). A silicon tube connects to the lower end of the funnel from below the bottom lids and extends to the water surface on the outside of the mesocosms (Fig. 4). Material collected in the sediment trap is regularly sampled via this tube, using a manual vacuum pump system. Processing of the samples included sub-sampling for zooplankton counting, followed by concentrating the residual sediment material, freeze-drying, grinding and homogenizing for subsequent chemical analysis.

The sediment trap as described here created a "dead volume" underneath the funnel of approximately 8 % of the enclosure volume. Because this water gradually exchanged with the rest of the enclosed water over one to two days, there was a dilution effect after experimental manipulations such as CO_2 enrichment and nutrient addition. This complicated determining precisely the start value of the applied

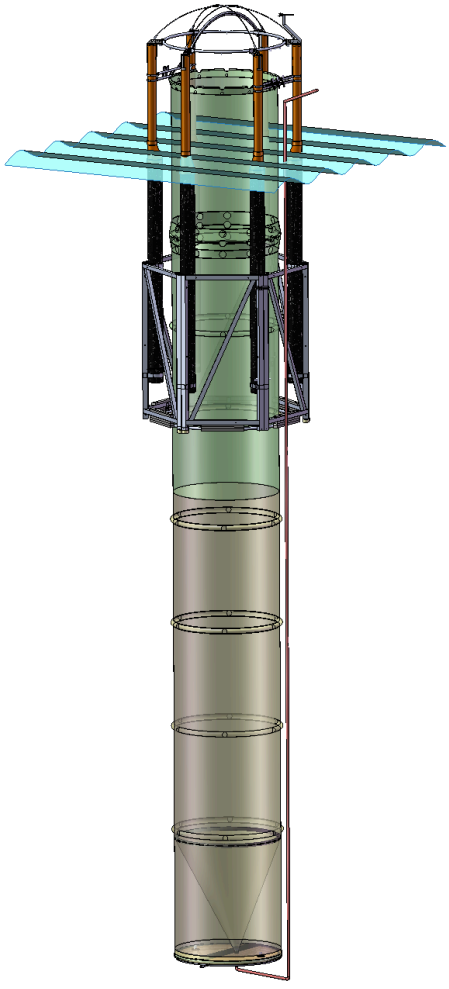

Fig. 2. Sketch of floatation frame with unfolded TPU enclosure bag; different colouring of the light-transparent bag indicates difference in TPU foil thickness: green, 1 mm; brown, 0.5 mm. The blue rippled plane represents the water line. At the bottom of the bag above the bottom plate the funnel-shaped sediment trap is indicated. The red line extending from the tip of the sediment trap to the water surface represents the tube used for sampling of sedimented matter.

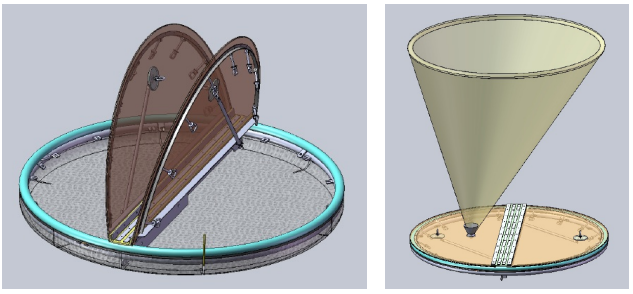

Fig. 3. Sketches of bottom plate. Left: lids in upright position, as applied during filling of the enclosure bags. A removable net (grey shaded area) with a mesh size of 3 mm is mounted below the bottom ring. Each bottom plate is equipped with 8 screws for tightening the lids after closing. Right: bottom plate in closed position with unfolded sediment trap.

Fig. 4. Left: sketch of sediment trap used in 2011 and 2012 campaigns. The funnel-shaped trap made of TPU foil is connected to the bottom of the enclosure bag via a flange (right panel). Note the tapering of the lowest section of the mesocosm bag. Sampling of sedimented matter is achieved via a silicon tube which connects to a 5 L sampling flask and a hand-operated vacuum pump. Right: flange ring made of laminated fibreglass to attach the external sediment trap to the lower end of the enclosure bag. The upper ring (connected to the bag) is equipped with steel weights to facilitate the sinking of the enclosure bag during mesocosm filling and to keep the bag in vertical position when exposed to currents. Bag and sediment trap are fixed to the upper and lower flanges by stainless steel clamps pressing the TPU foil in notches. Upper and lower flanges are connected with eight screws and sealed with a silicon rubber fitting.

manipulation. To avoid the dilution effect, a new sediment trap was designed after the 2010 campaign and applied in all later studies. This new trap is connected to the bottom of the mesocosm through a flange (Fig. 4). Mounted by divers after the filling of the bag, the trap closes off the mesocosm at the bottom end.

2.5 Mooring and deployment

The mesocosms can be operated in moored or free-floating mode. When moored, the mesocosms are deployed in groups of three at a distance of 30 to 50 m between mesocosm units (Fig. 5). Units of each group are connected to each other through ropes fixed to the floating frames at 2.5 m water depth. The groups are separated by approximately 50 m between each group and anchored on both ends with weights (1.2 tonnes) consisting of railway wheels. Buoys are mounted between mesocosms and the anchor weights to ensure that the downward pull generated by strong currents is absorbed by the buoys rather than acting directly on the mesocosms. When operated in moored mode, the water currents acting on the mesocosms should not exceed 0.5 knots to avoid strong vertical deflection of the mesocosm bags and wearing on the ropes. In free-floating mode, as applied in the 2011 campaign off Hawaii, a drogue was connected to one

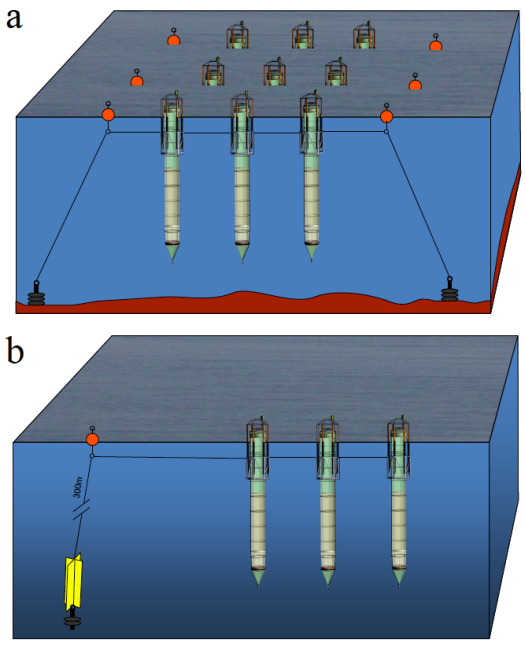

Fig. 5. Schematic drawing of the two modes of mesocosm operation: **(a)** mesocosms in moored mode in packs of three with anchor weight at each end as used in the Svalbard 2010 study; **(b)** mesocosms in free-floating mode connected to a weighted drogue hanging from a buoy at 150 m water depth. This approach was first tested in the 2011 campaign off Hawaii.

end of the three mesocosms. The weighted drogue was hanging from a large buoy at 150 water depth and thereby was exposed to water currents deviating from those at the surface. It served to generate a steady drag at one end of the mesocosm array in order to keep the mesocosms apart and in a straight line. In this mode there is no limit on the acceptable speed of water currents.

2.6 Filling and closing

The filling of the mesocosms started after all mesocosms were moored in position. For this the enclosure bags were untied at the bottom, allowing the weighted lower end of the bags to sink through the water column with open shutters until the bags were completely unfolded. With this approach the mesocosms were filled with minimal disturbance of the enclosed water body. To avoid capturing large organisms (e.g. fish, jelly fish) a removable net with a mesh size of 3 mm was mounted across the bottom opening. Several teams were involved in filling the mesocosms in parallel in close succession to reduce the effect of changing water masses due to lateral advection during the filling process. Nevertheless, because the mesocosms were not all filled simultaneously and because of possible small-scale patchiness in the plankton community (i.e. smaller than the distance between individual mesocosms), there was a risk of differences between enclosed water bodies in terms of seawater chemistry and plankton community abundance and composition. This could have caused large inter-mesocosm variability during the experiment. To minimize differences in starting conditions between enclosed water bodies, the mesocosms were left open for free exchange with the surrounding water for 48 h after filling. For this the bottom shutters were kept open and the upper part of the bags lowered to 1.5 m below the water surface with the top and bottom opening covered with a net of 3 mm mesh size. Test runs during previous years with dyes injected into the mesocosms indicated that, depending on bag length and current speed, a complete exchange of the enclosed water body occurs within 2–3 days. By gradually exchanging the enclosed and surrounding water masses, it is insured that spatial patchiness is averaged out over time. While the mesocosms were open for water exchange, frequent measurements were conducted for several chemical and biological parameters to test for differences between mesocosms. The absence of detectable differences in these parameters was a precondition for mesocosm closing.

The exchange between mesocosms and surrounding water was terminated by lifting the upper parts of the bags above the surface and having divers close the bottom plates. At this point the top and bottom nets are removed. With the closing of the bottom shutters the sediment trap, folded and fixed between the two bottom plates, unfolds and rises through an air-filled ring until fully extended (Figs. 2 and 3). The closing of the mesocosms marks the beginning of the experimental period.

As described above, bottom plate and internal sediment trap were replaced by a flange-connected external sediment trap after the 2010 campaign. In the following campaigns the sediment traps were put in place by divers after the full extension of the enclosure bags. In this new design the sediment trap also has the function of closing off the bottom of the bags. The sediment trap is put in place in two steps: initially it is connected by a hinge integrated in the flange (see Fig. 7, left side of the flange). At this stage the sediment trap is hanging parallel to the mesocosm bag, held by the hinge and tied to the first support ring. In a second step (e.g. on the following day), divers turn the lower flange ring in horizontal position to fully connect with the upper flange ring, thereby expending the TPU foil forming the funnel of the sediment trap. The two flange rings are tightly connected by 8 screws. As before, the mesocosms are closed by divers after 2–3 days of open exchange between mesocosm and surrounding water. After mounting of the sediment trap, three 5 kg weights are mounted at its lower end to keep the funnel stretched. A hose connected to the bottom of the funnel and reaching above the water surface is used for sampling of the sedimented material (Fig. 4).

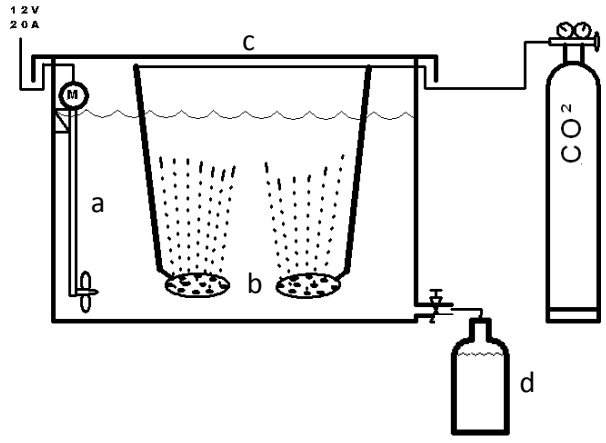

Fig. 6. Schematic drawing of the setup used for the preparation of CO_2-enriched water. An electric outboard motor **(a)** continuously mixed the water in the 1.4 m^3 polypropylene tank which was tightly closed by a lid **(c)**. Two large aerating disks **(b)** produced fine bubbles ensuring relatively low gas consumption. After aeration, the CO_2-enriched water was filled into 25 L polycarbonate carboys **(d)** for transport and quantitative addition into the mesocosms, using the "spider".

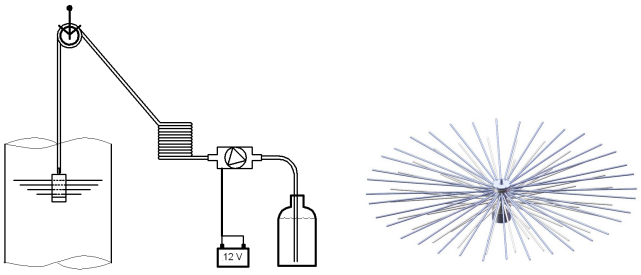

Fig. 7. Left: sketch of setup used for CO_2 manipulation. CO_2-enriched water is pumped from 25 L carboys via a garden hose into the "spider", which is gradually moved up and down over the entire length of the enclosure bag by manually heaving and hauling it via a pulley fixed above the centre of the enclosure bags underneath the hood. Right: the dispersion device ("spider") is composed of a polyoxymethylen body weighted with a 5 kg stainless steel stand. It has 84 jets (Ø 500 µm) of which 78 are equipped with elastic acryl branches of different lengths distributing the liquid evenly over a horizontal cross-section of the mesocosm. The diameter of the jets serves as a bottleneck, releasing ~ 80 mL min^{-1} of liquid dispensed through every jet irrespective of the length of the branch connected to it.

2.7 CO_2 and nutrient manipulation

CO_2 enrichment was carried out by adding CO_2-enriched fjord water into the mesocosms. The addition of CO_2-enriched seawater increases dissolved inorganic carbon (DIC) while leaving total alkalinity constant, perfectly mimicking on-going ocean acidification (cf. Schulz et al., 2009, Gattuso et al., 2010). With 9 mesocosms available for this study, the choice was made to apply a CO_2 gradient with 8 different CO_2 levels, duplicating only the ambient CO_2 conditions without CO_2 manipulation (considered as control). This approach involves the use of regression statistics for assessment of possible CO_2 effects. This choice was made for the following reasons:

(a) Because of the low number of experimental units available and considering the risk of losing one or several mesocosms (e.g. due to damage by ice floats), a CO_2-gradient approach carries a lower risk of failure compared to a replicated approach (e.g. 3 CO_2 treatments with triplicates each) relying on ANOVA statistics.

(b) If there is a threshold level for any of the CO_2/pH sensitive processes, a CO_2-gradient approach has a higher chance of detecting it.

(c) With a CO_2-gradient approach the opportunity arises to include one or two CO_2 levels outside the range recommended for ocean acidification perturbation experiments (Barry et al., 2010), which would be more difficult to justify if such extreme levels were replicated.

(d) Although CO_2 manipulation is relatively straightforward, it is challenging to precisely achieve the targeted CO_2 levels. While critical in a replicated approach, in a CO_2-gradient approach deviations from the targeted CO_2 levels can be tolerated.

It was decided to replicate the ambient CO_2 level (control treatment) in order to minimize the risk of completing the experiment with no control in case of losing one or several mesocosm units. The different CO_2 levels were randomly interspersed among the 9 mesocosms (cf. Riebesell et al., 2010).

The CO_2-enriched seawater was prepared in a 1.4 m^3 tank on land filled with filtered (pore size 20 µm) fjord water which was stirred by an electric propeller while aerated with pure CO_2 gas for approximately 24 h (Fig. 6). At this stage the CO_2 partial pressure in the water was close to saturation (pH $\sim$ 4.4).

The DIC concentration in the CO_2-enriched water was calculated based on measurements of total alkalinity, pH (presented in total scale unless stated otherwise), salinity and temperature, using the computer program CO_2SYS (Lewis and Wallace, 1997). Based on this the amount of CO_2-enriched water needed to achieve the target pCO_2 levels in the different CO_2 treatments was calculated. The CO_2-enriched water was filled into 25 L carboys and transported to the mesocosms. Depending on target pCO_2, between 0 and 320 L (see Schulz et al., 2013) of the CO_2-enriched seawater was injected into the mesocosms by means of a membrane pump and a dispensing device (termed "spider"; Fig. 7, right panel). To achieve an even distribution of the CO_2-enriched water throughout the mesocosms, the "spider" was

slowly moved up and down during the injection over the entire length of the enclosure bags (Fig. 7, left panel). Vertical pH profiles were conducted after CO_2 additions to check whether an even distribution was achieved.

The injection of CO_2-enriched water was done in steps over 4 consecutive days starting in the afternoon of 6 June (t-1). Two mesocosms served as controls, while 7 mesocosms were manipulated to establish treatments of elevated pCO_2 with an initial range of 185–1420 µatm. Mean values of pCO_2 during the experimental period ranged from 175–1085 µatm (for details see Bellerby et al., 2012). In mesocosms with no or low addition of CO_2-enriched water, similar amounts of filtered fjord water were added in order to apply the same physical perturbation to all mesocosms. Some fine-tuning to reach target CO_2 levels was conducted on 11 June (t4), at which time the target pCO_2 levels where reached with an offset generally smaller than ±50 µatm. After this no further CO_2 manipulation was done in any of the mesocosms. Because of the slow exchange of water in the "dead volume" below the sediment trap with that in the rest of the enclosure bag, there was a dilution of the initial CO_2 enrichment due to mixing of the CO_2 manipulated (open bag) and non-manipulated ("dead volume") water during the first couple of days. Budget calculations based on carbonate chemistry measurements starting after CO_2 manipulations needed to account for this dilution effect (Czerny et al., 2012a, 2013; de Kluijver et al., 2013; Silyakowa et al., 2013).

In the early morning of 20 June (t13), inorganic nutrients were added using the same dispersion device as described above and shown in Fig. 7 at concentrations of 5 µmol L^{-1} NO_3, 0.32 µmol L^{-1} PO_4, and 2.5 µmol L^{-1} Si. The precise amounts of inorganic nutrients added to each mesocosm were calculated based on volume determinations conducted for all mesocosms through salt additions on 3 June (t4) and 11 June (t4). For a detailed description of the volume determination see Czerny et al. (2012b).

Approximately 200 live adult pteropods (*Limacina helicina)* sampled individually from the fjord were added to each mesocosm during 11–13 June (t4–t6) to study their response to ocean acidification. For unknown reasons the pteropods rapidly disappeared from the water column. Some pteropods were collected in the sediment traps; others were seen by divers accumulating in the dead volume underneath the sediment traps. Very few specimen survived the experiment.

2.8 Cleaning of the mesocosm walls

To estimate the contribution of wall growth to the overall production and accumulation of particular organic matter (POM) in the mesocosms, the inside of the enclosure bags was cleaned with a ring-shaped brush on 7 July (t30). Various biological parameters were determined on suspended particulate matter immediately before and after brushing of the walls to quantify the amount of biomass released into the water column. As reported in Czerny et al. (2012a) on average 16 % of the nitrate and 32 % of the phosphate added on t13 had accumulated on the mesocosm walls due to biofilm formation on t30. In follow-up campaigns, the formation of biofilms on the inside of the enclosure bags (wall growth) was prevented by regular cleaning (once per week) with a ring-shaped, double-bladed wiper using a similar configuration as depicted in Fig. 8.

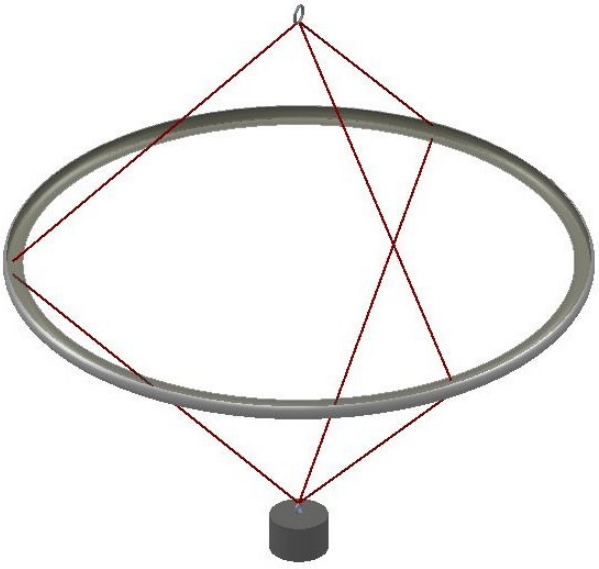

Fig. 8. Ring-shaped brush used for cleaning the inside of the enclosure walls. The brush is pulled downwards by a weight attached by ropes below the ring and pulled upwards manually by a rope run over a pulley fixed above the centre of the enclosure bags underneath the hood. In follow-up experiments the brush was replaced by a double-bladed wiper.

2.9 Sampling

Vertical profiles of temperature, conductivity, pH, oxygen, fluorescence, turbidity and light intensity were taken daily in each mesocosm and the surrounding water between 14:00 and 16:00 LT with a CTD60M (Sun and Sea Technologies). Sampling of seawater from the mesocosms was conducted with a depth-integrating water sampler (Hydro-Bios). The sampler is equipped with a pressure-controlled motor and continuously collects water (5 L volume) while being lowered from the surface to 12 m depth. Samples were collected in the morning between 9:00 and 11:00 In addition discrete samples were taken at fixed depths using Niskin bottles and pumping systems with sampling tubes lowered into the mesocosms (for details see M&M in the corresponding manuscripts). For measurements of DIC, total alkalinity, N_2O, inorganic nutrients, dissolved organic matter, volatile organic compounds, oxygen incubations, and other samples sensitive for contamination and gas exchange, subsamples

Table 1. Starting conditions in the nine mesocosms (M1-M9) and the surrounding fjord water. Data for salinity, pH and oxygen concentration (determined in situ with a CTD equipped with pH and oxygen sensors) for day t-4, all others for day t0. pH is in total scale, concentrations for oxygen, nitrate, ammonium, phosphate and silicate are in µmol L^{-1}. See Schulz et al. (2013) for details on the methodologies.

	M1	M2	M3	M4	M5	M6	M7	M8	M9	Fjord
Salinity	33.90	33.90	33.90	33.91	33.91	33.90	33.90	33.93	33.93	33.58
pH	8.36	8.36	8.37	8.35	8.36	8.35	8.37	8.37	8.39	8.36
O_2	466	462	461	462	460	460	462	463	466	476
NO_3^-	0.03	0.03	0.02	0.03	0.01	0.01	0.02	0.02	0.03	0.01
NH_4^+	0.59	0.59	0.60	0.60	0.59	0.59	0.49	0.59	0.69	0.22
PO_4^{3-}	0.04	0.05	0.05	0.06	0.05	0.06	0.05	0.06	0.06	0.04
$Si(OH)_4$	0.15	0.16	0.15	0.17	0.12	0.12	0.12	0.10	0.12	0.23

were taken directly from the depth-integrating samplers in a fixed order. For bulk measurements of suspended particulate matter, photosynthetic pigments, biogenic silica, phyto- and microzooplankton abundance and composition, and various other components (see M&M in the corresponding manuscripts), the depth-integrated samples were transferred to 10 L polyethylene containers which were kept in a dark cold room at in situ temperature for later subsampling.

Net hauls were done about once a week (for details see Niehoff et al., 2013). To minimize the effect of zooplankton catches on the plankton abundance and composition, the cross-sectional area sampled by the sum of all net hauls conducted over the course of the experiment was kept to less than one-sixth of the total cross-sectional area of the enclosure bags.

All sampling gear and sensors were plunged into fjord water next to the sampling boats before being deployed in the mesocosms to avoid contamination by adhering materials. All instruments were cleaned with fresh water when returning to land.

3 Results

A mesocosm CO_2-enrichment experiment was conducted in Kongsfjorden on the north-west coast of Spitsbergen (Fig. 9) between 31 May and 8 July 2010. Nine sea-going mesocosms were loaded in Kiel and deployed on the southern shore of Kongsfjorden near Ny-Ålesund at 78°56.2′ N und 11°53.6′ E (Fig. 10) by M/V *Esperanza* of Greenpeace International on 31 May (t-7). Before mesocosm deployment mooring weights were laid out by R/V *Viking Explorer* of the University Centre in Svalbard (UNIS). Upon deployment the mesocosms were towed to the mooring site by small boats and tied in three groups of three mesocosms each as indicated in Fig. 10.

3.1 Conditions in the fjord

At the time of mesocosm deployment Kongsfjorden off Ny-Ålesund was ice-free, while parts of the inner fjord were covered by sea ice. During the course of the study, the sea ice broke off and the glaciers surrounding Kongsfjorden started to calve. Floats of sea ice and glacier ice drifted towards the mouth of the fjord starting in mid-June. Most of the ice transport occurred along the northern side of the fjord, i.e. on the opposite side of the mesocosm mooring, following the general current pattern in the fjord system. At times of persistent north to north-east winds some ice floats occasionally drifted towards the mesocosm array. A 24 h ice watch was on duty for the duration of the experiment. In a few cases ice floats needed to be pushed out of their path by small boats to avoid collision with the mesocosms.

The initial pCO_2 of the ambient water in the fjord was ∼175 µatm, corresponding to a pH of ∼8.3 (Bellerby et al., 2012). Concentrations of mineral nutrients in the water were close to detection limit at the beginning of the experiment (0.11 µmol L^{-1} of nitrate, 0.7 µmol L^{-1} of ammonia, 0.13 µmol L^{-1} of phosphate). Additionally, there were 5.5 µmol L^{-1} of dissolved organic nitrogen, 0.20 µmol kg^{-1} of dissolved organic phosphorus (Schulz et al., 2013) and 75 µmol L^{-1} of dissolved organic carbon (Engel et al., 2013). Reduced pCO_2 and inorganic nutrient concentrations as well as increased concentrations of organic carbon, nitrogen and phosphorus indicated a post-bloom situation in the fjord at the start of the experiment.

3.2 Conditions in the mesocosms

Comparing the initial conditions after closing of the mesocosms provided an indication of the similarity between bags at the start of the experiment. As indicated in Table 1, the chemical conditions were almost identical in all mesocosms. Small differences between mesocosms and the surrounding fjord water were due to changing water masses in the fjord after closing the bags. Close agreement also exists for phytoplankton biomass and taxonomic composition (Table 2). Differences in group-specific chlorophyll *a* equiva-

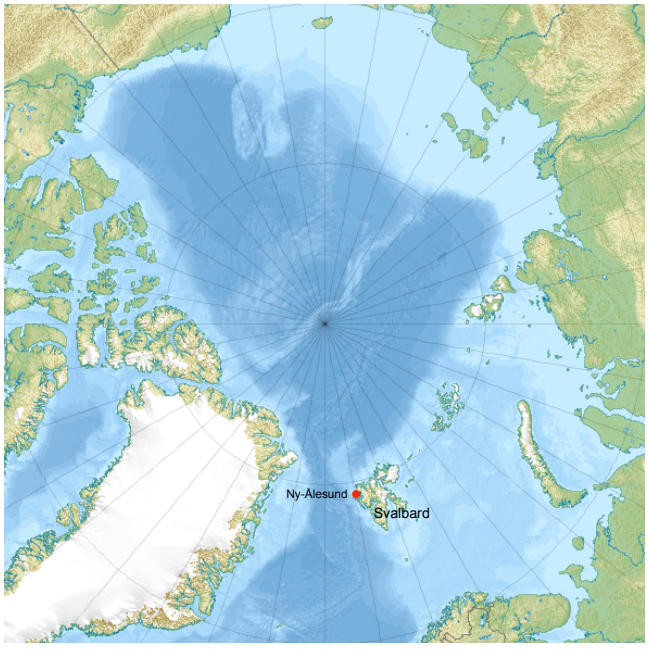

Fig. 9. Map of the Arctic. Red dot denotes the location of the study site (Kongsfjorden, Ny-Ålesund) on the north-west coast of Spitsbergen, the largest island of the Svalbard archipelago. Source: Wikipedia.

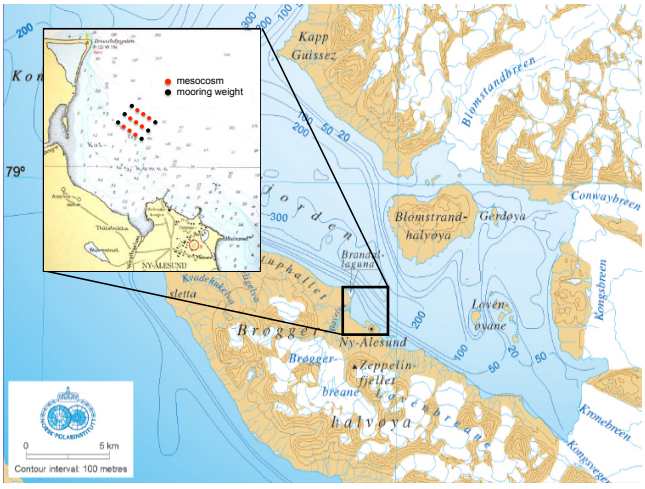

Fig. 10. Map of Kongsfjorden on the north-west coast of Svalbard. Insert shows the study area with the location and orientation of the mesocosm array. Source of map: Norsk Polarinstitutt.

lent concentrations between mesocosms for some of the taxonomic groups are more pronounced for those with predominantly large cell sizes combined with low abundances, such as diatoms and dinoflagellates. This difference is most likely due to a sampling bias rather than a true representation of biomass differences in the mesocosms. Almost identical concentrations in all mesocosms are obtained for bacteria and total virus counts (Table 2). Overall, the resemblance in initial values for a variety of chemical and biological parameters suggests proper conditions for the start of the experiment.

3.3 Temporal development

A short temporary increase in phytoplankton biomass during the first part of the experiment was probably fuelled by utilization of organic nutrients. Half way through the experiment inorganic nutrients were added to the mesocosms stimulating two additional phytoplankton blooms.

Based on the manipulations carried out over the course of the study, the deployment period is divided into 4 phases, one pre-experimental phase (phase 0) and three experimental phases (phases 1–3) as follows:

- phase 0: closing of the mesocosms until end of CO_2 manipulation (t-4 to t4),
- phase 1: end of CO_2 manipulation until nutrient addition (t5 to t12),
- phase 2: nutrient addition until 2nd chlorophyll minimum (t13 to t21),
- phase 3: 2nd chlorophyll minimum until end of experiment (t22 to t30).

The temporal changes in phytoplankton biomass and community composition observed in the mesocosms follow the same basic trends as those recorded in the waters surrounding the mesocosms (Brussaard et al., 2013; Schulz et al., 2013). Considering that lateral advection caused the water surrounding the mesocosms to exchange rapidly, the close agreement between enclosed and ambient plankton community development seems quite remarkable. This indicates that (1) major trends in plankton development persisted independent of small-scale patchiness in the study area and (2) the enclosed plankton community mimics the natural system reasonably well in terms of major developments in biomass and composition. The close agreement starts to weaken after nutrient addition in the mesocosms.

Aside from providing a comprehensive data set on plankton community responses to ocean acidification and their impacts on biogeochemical cycling, the study offered the opportunity for consistency checks between individual measurements. Particularly enlightening in this respect was the comparison of different approaches determining net community production, which was obtained from bottle incubations measuring O_2 production/consumption (Tanaka et al., 2013), estimates of changes in DIC concentration (Silyakowa et al., 2013), and incorporation of ^{13}C tracer added directly into the mesocosms (de Kluijver et al., 2013). These estimates were further compared with ^{14}C incorporation determined in bottle incubations (Engel et al., 2013). While at first sight the different approaches appeared to yield different rates and – more surprisingly – different relationships

Table 2. Concentrations of chlorophyll *a* equivalent (in ng L^{-1}) for eight taxonomic groups of phytoplankton determined from HPLC measurements using CHEMTAX and bacterial and viral numbers (10^6 mL^{-1}) measured by flow cytometry for day t0. See Schulz et al. (2013) for details on methodologies. Abbreviations for taxonomic groups refer to prasinophyceae, dinophyceae, crytophyceae, chlorophyceae, cyanophyceae, bacillariophyceae, chrysophyceae, and haptophyceae.

	M1	M2	M3	M4	M5	M6	M7	M8	M9	Fjord
Prasino	45.8	45.8	49.1	55.5	58.6	41.5	66.8	54.5	48.9	71.5
Dino	0	0.4	8.1	10.1	0	27.4	8.2	13.1	4.6	12.2
Crypto	25.2	15.5	19.7	34.6	45.6	23.1	29.5	20.7	18.3	73.3
Chloro	18.8	0	0	10.0	1.4	27.2	40.8	43.5	38.3	56.9
Cyano	29.9	31.3	41.4	41.4	44.2	36.5	28.3	22.2	38.7	37.2
Bacillario	28.4	18.5	27.7	31.4	31.8	19.6	37.2	15.3	35.7	97.8
Chryso	6.4	2.6	5.1	5.0	3.0	4.5	5.8	5.1	7.3	3.4
Hapto	28.0	65.4	28.7	35.1	51.3	25.3	16.1	25.4	19.7	18.5
Bacteria	2.0	2.1	2.0	2.1	2.0	2.1	2.2	2.0	2.0	1.7
Viruses	61.4	53.5	54.2	58.0	48.4	53.3	49.3	58.3	53.9	52.4

with CO_2 concentration, closer examination yielded some interesting insights into the underlying processes and eventually resulted in a coherent interpretation of plankton community responses to ocean acidification (see discussions in references cited above).

4 Discussions

4.1 The study area

The Arctic Ocean ecosystem is expected to undergo major climate-change-related transformations in the coming decades, ranging from surface layer warming and freshening to enhanced stratification and loss of sea ice. Due to the high CO_2 solubility and low carbonate saturation states of its cold surface waters, the Artic Ocean is also considered particularly vulnerable to ocean acidification. If CO_2 emissions continue to rise at current rates, half of the Artic Ocean will be undersaturated with respect to calcium carbonate and, therefore, corrosive for calcareous organisms within the next three to four decades (Steinacher et al., 2009). While several Arctic calcifying species have been shown to respond negatively to ocean acidification (e.g. Büdenbender et al., 2011; Comeau et al., 2009; Lischka et al. 2011; Walther et al., 2010; Wood et al., 2011), little is known about possible consequences of ocean acidification at the base of the Arctic food web. The experiment described here was intended as a first attempt at closing this gap by conducting a pelagic mesocosm CO_2-enrichment study in Kongsfjorden on the western coast of Spitsbergen – about 1000 nautical miles south of the North Pole.

Kongsfjorden, an open fjord system without sill, is about 26 km long and between 4 and 10 km wide, with a maximum depth of 400 m. The water in Kongsfjorden is influenced by (i) Arctic water masses transported by the coastal current flowing from the Barents Sea over the West Spitsbergen Shelf, (ii) Atlantic water masses coming in with the northbound West Spitsbergen Current, and (iii) freshwater input from calving and melting glaciers as well as precipitation (Hop et al., 2006). Discharge of freshwater and sediments from the adjacent glaciers strongly varies seasonally, peaking in the summer. During winter, the inner part of the fjord is covered by sea ice , with large interannual variability in ice thickness, time of formation and break-up (see Svendsen et al., 2002, for a detailed review of the physical environment of the Kongsfjorden area).

In the fjord the initiation of the phytoplankton spring bloom starts already under ice cover, culminating between April and early June after ice break-up (Eilertsen et al., 1989). The majority of studies conducted on the plankton community in Kongsfjorden focused on the spring period when high nutrient availability and increasing light levels support a substantial fraction of the annual primary production (Iversen and Seuthe, 2011; Seuthe et al., 2011). After the spring bloom, phytoplankton biomass remains moderately high during late spring and summer (Hop et al., 2002). At this time of the year, the plankton community is typically characterized by an efficient microbial loop (Iversen and Seuthe, 2011) that provides inorganic nutrients to phytoplankton and bacteria through rapid organic matter remineralization. These were the conditions encountered at the start of this mesocosm campaign. Accordingly, pico- and nanophytoplankton groups were the dominant autotrophs during the first part of this study (Brussaard et al., 2013). Due to the low seed population of dinoflagellates and diatoms, the dominance of pico- and nano-sized phytoplankton continued even after nutrient addition. The standing stock of microphytoplankton was building up slowly and dominated phytoplankton biomass only towards the end of the experiment (Schulz et al., 2013).

4.2 KOSMOS experimental facility

After a sequence of test runs in free-floating mode conducted in the Baltic Sea in 2006, 2007, and 2008, which led to considerable improvements in the mesocosm hardware and handling, and a four-week trial run in moored mode in 2009, which yielded some novel results on ocean acidification effects during a phytoplankton spring bloom (Schulz and Riebesell, 2012), the Svalbard 2010 campaign was the first full-scale experiment involving nine mesocosm units and covering a broad range of parameters over an extended period of time. Building on the experience gained during this campaign, this new sea-going experimental platform opens up new opportunities for mesocosm experimentation under a variety of hydrographic conditions and geographical locations. Important new features of this facility include

- the enclosure of large volumes (45–75 m^3) with minimal disturbance of the enclosed water body and plankton community,
- controlled carbonate chemistry manipulation with minimal agitation of the enclosed water,
- mass balance calculations through precise determination of mesocosm volume by full accounting of all relevant pools and fluxes for key elements (carbon, nitrogen, phosphorus, silica),
- extended experimental duration through routine cleaning of mesocosm walls (preventing extensive wall growth) and regular sediment sampling (preventing release of remineralization products from sedimented matter),
- operation in moored and free-floating mode under low to moderate wave conditions allowing mesocosm experimentation in areas previously not amendable to this kind of experimentation.

This mesocosm campaign, which involved 35 scientists from 12 institutes, provided the opportunity for a highly integrative, multidisciplinary study involving marine engineers, molecular and marine biologists, ecologists, biogeochemists, and marine and atmospheric chemists. By covering a wide range of parameters measured over 35 days (4 days prior to and 31 days after the start of CO_2 manipulation), it provided a comprehensive data set on pelagic community-level responses to ocean acidification and their impacts on nutrient cycling and air–sea exchange of climate-relevant gases.

Acknowledgements. The design, construction and field testing of the KOSMOS mesocosms was made possible through financial support of GEOMAR and the integrated project SOPRAN (Surface Ocean PRocesses in the ANthropocene) funded by the German Ministry for Education and Research (BMBF). GEOMAR and SOPRAN provided the KOSMOS facility for the Svalbard 2010 experiment and organized the logistics leading up to and during the experiment. GEOMAR was responsible for deploying the mesocosms, running the experiment and coordinating all scientific aspects before, during and after the experiment. The scientific work is a contribution to the European Project on Ocean Acidification (EPOCA), which received funding from the European Community's Seventh Framework Programme (FP7/2007–2013) under grant agreement no. 211384. Several participants of this study received funding from the European Community's Seventh Framework Programme under grant agreement no 228224, MESOAQUA. We gratefully acknowledge the logistical support of Greenpeace International for its assistance with the transport of the mesocosm facility from Kiel to Ny-Ålesund and back to Kiel. We also thank the captains and crews of M/V *Esperanza* of Greenpeace and R/V *Viking Explorer* of the University Centre in Svalbard (UNIS) for assistance during mesocosm transport and during deployment and recovery in Kongsfjorden. We thank the staff of the French-German Arctic Research Base (AWIPEV) at Ny-Ålesund, in particular Marcus Schumacher, for on-site logistical support.

The service charges for this open access publication have been covered by a Research Centre of the Helmholtz Association.

Edited by: J. Middelburg

References

Barry, J. P., Widdicombe, S., and Hall-Spencer, J. M.: Effects of ocean acidification on marine biodiversity and ecosystem function, in: Ocean acidification, edited by: Gattuso J.-P. and Hansson L., Oxford University Press, 192–209, 2010.

Barry, J. P., Tyrrell, T., Hansson, L., Plattner, G.-K., and Gattuso, J.-P.: Atmospheric CO_2 targets for ocean acidification perturbation experiments, in: Guide to best practices in ocean acidification research and data reporting, edited by: Riebesell, U., Fabry, V., Hansson, L., and Gattuso, J.-P., Office for Official Publications of the European Communities, Luxembourg, 53–66, 2011.

Beaufort, L., Probert, I., de Garidel-Thoron, T., Bendif, E. M., Ruiz-Pino, D., Metzl, N., Goyet, C., Buchet, N., Coupel, P., Grelaud, M., Rost, B., Rickaby, R. E. M., and de Vargas, C.: Sensitivity of coccolithophores to carbonate chemistry and ocean acidification, Nature 476, 80–83, 2011.

Bellerby, R. G. J., Silyakova, A., Nondal, G., Slagstad, D., Czerny, J., de Lange, T., and Ludwig, A.: Marine carbonate system evolution during the EPOCA Arctic pelagic ecosystem experiment in the context of simulated Arctic ocean acidification, Biogeosciences Discuss., 9, 15541–15565, doi:10.5194/bgd-9-15541-2012, 2012.

Brockmann, U.: Pelagic mesocosms: II. Process studies, in: Enclosed experimental marine ecosystems: A review and recommendations, edited by: C. M. Lalli, Springer-Verlag, New York, 81–108, 1990.

Brussaard, C. P. D., Noordeloos, A. A. M., Witte, H., Collenteur, M. C. J., Schulz, K., Ludwig, A., and Riebesell, U.: Arctic microbial community dynamics influenced by elevated CO_2 lev-

els, Biogeosciences, 10, 719–731, doi:10.5194/bg-10-719-2013, 2013.

Büdenbender, J., Riebesell, U., and Form, A.: Calcification of the Arctic coralline red algae *Lithothamnion glaciale* in response to elevated CO_2, Mar. Ecol. Progr. Ser., 441, 79–87, 2011.

Carpenter, S. R.: Microcosm experiments have limited relevance for community and ecosystem ecology, Ecology, 77, 677–680, 1996.

Charalampopoulou, A., Poulton, A. J., Tyrrell, T., and Lucas, M. I.: Irradiance and pH affect coccolithophore community composition on a transect between the North Sea and the Arctic Ocean, Mar. Ecol. Progr. Ser., 431, 25–43, 2011.

Comeau, S., Gorsky, G., Jeffree, R., Teyssié, J.-L., and Gattuso, J.-P.: Impact of ocean acidification on a key Arctic pelagic mollusc (Limacina helicina), Biogeosciences, 6, 1877–1882, doi:10.5194/bg-6-1877-2009, 2009.

Czerny, J., Schulz, K. G., Boxhammer, T., Bellerby, R. G. J., Büdenbender, J., Engel, A., Krug, S. A., Ludwig, A., Nachtigall, K., Nondal, G., Niehoff, B., Siljakova, A., and Riebesell, U.: Element budgets in an Arctic mesocosm CO_2 perturbation study, Biogeosciences Discuss., 9, 11885–11924, doi:10.5194/bgd-9-11885-2012, 2012a.

Czerny, J., Schulz, K. G., Krug, S. A., Ludwig, A., and Riebesell, U.: Technical Note: On the determination of enclosed water volume in large flexible-wall mesocosms, Biogeosciences Discuss., 9, 13019–13030, doi:10.5194/bgd-9-13019-2012, 2012b.

Czerny, J., Schulz, K. G., Ludwig, A., and Riebesell, U.: Technical Note: A simple method for air-sea gas exchange measurements in mesocosms and its application in carbon budgeting, Biogeosciences, 10, 1379–1390, doi:10.5194/bg-10-1379-2013, 2013.

de Kluijver, A., Soetaert, K., Czerny, J., Schulz, K. G., Boxhammer, T., Riebesell, U., and Middelburg, J. J.: A ^{13}C labelling study on carbon fluxes in Arctic plankton communities under elevated CO_2 levels, Biogeosciences, 10, 1425–1440, doi:10.5194/bg-10-1425-2013, 2013.

Drenner, R. W. and Mazumder, A.: Microcosm experiments have limited relevance for community and ecosystem ecology, Ecology, 80, 1081–1085, 1999.

Eilertsen, H. C., Taasen, J. P., and Weslawski J. M.: Phyto- plankton studies in the fjords of West Spitsbergen: physical environment and production in spring and summer, J. Plankton Res. 11, 1245–1260, 1989.

Engel, A., Borchard, C., Piontek, J., Schulz, K. G., Riebesell, U., and Bellerby, R.: CO_2 increases ^{14}C primary production in an Arctic plankton community, Biogeosciences, 10, 1291–1308, doi:10.5194/bg-10-1291-2013, 2013.

French, R. H. and Watts, R. J.: Performance of in situ microcosms compared to actual reservoir behavior, J. Environ. Eng., 115, 835–849, 1989.

Gattuso, J.-P. and Hansson, L.: Ocean acidification: background and history, in: Ocean acidification, Oxford, edited by: Gattuso, J.-P. and Hansson, L., Oxford University Press, Oxford, 1–20, 2011.

Gattuso, J.-P., Lee, K., Rost, B., and Schulz, K. G.: Approaches and tools to manipulate the carbonate chemistry, in: Guide to best practices in ocean acidification research and data reporting, edited by: Riebesell, U., Fabry, V., Hansson, L., and Gattuso, J.-P., Office for Official Publications of the European Communities, Luxembourg, 41–52, 2010.

Hop, H., Pearson, T., Hegseth, E. N., Kovacs, K. M., Wiencke, C., Kwasniewski, S., Eiane, K., Mehlum, F., Gulliksen, B., Wlodarska-Kowalczuk, M., Lydersen, C., Weslawski, J. M., Cochrane, S., Gabrielsen, G. W., Leaky, R. J. G., Lønne, O.J., Zajaczkowski, M., Falk-Petersen, S., Kendall, M., Wängberg, S.-Å., Bischof, K., Voronkov, A. Y., Kovaltchouk, N. A., Wiktor, J., Poltermann, M., di Prisco, G., Papucci, C., and Gerland, S.: The marine ecosystem of Kongsfjorden, Svalbard, Polar Res., 21, 167–208, 2002.

Hop, H., Falk-Petersen, S., Svendson, H., Kwasniewski, S., Pavlov, V., Pavlova, O., and Søreide, J. E.: Physical and biological characteristics of the pelagic system across Fram Strait to Kongsfjorden, Prog. Oceanogr., 71, 182–231, 2006.

Iversen, K. R. and Seuthe, L.: Seasonal microbial processes in a high-latitude fjord (Kongsfjorden, Svalbard): I. Heterotrophic bacteria, picoplankton and nanoflagellates, Polar. Biol., 34, 731–749, 2011.

Kuiper, J., Brockmann, U. H., van het Groenewoud, H., Hoornsman, G., and Hammer, K. D.: Influences of bag dimensions on the development of enclosed plankton communities during POSER, Mar. Ecol. Progr. Ser., 14, 9–17, 1983.

Lischka, S., Büdenbender, J., Boxhammer, T., and Riebesell, U.: Impact of ocean acidification and elevated temperatures on early juveniles of the polar shelled pteropod Limacina helicina: mortality, shell degradation, and shell growth, Biogeosciences, 8, 919–932, doi:10.5194/bg-8-919-2011, 2011.

Lewis, E. and Wallace, D. W. R.: Program developed for CO_2 system calculations. ORNL/CDIAC-105, Carbon Dioxide Information Center, Oak Ridge National Laboratory, US Department of Energy, Oak Ridge, Tennessee, 1998.

Menzel, D. W. and Steele, J. H.: The application of plastic enclosures to the study of pelagic marine biota, Rapp. P.-v. Réun. Cons. int. Explor. Mer., 173, 7–12, 1978.

Niehoff, B., Schmithüsen, T., Knüppel, N., Daase, M., Czerny, J., and Boxhammer, T.: Mesozooplankton community development at elevated CO_2 concentrations: results from a mesocosm experiment in an Arctic fjord, Biogeosciences, 10, 1391–1406, doi:10.5194/bg-10-1391-2013, 2013.

Petersen, J. E., Kemp, W. M., Bartleson, R., Boynton, W. R., Chen, C.-C., Cornwell, J. C., Gardner, R. H., Hinkle, D. C., Houde, E. D., Malone, T. C., Mowitt, W. P., Murray, L. Sanford, L. P., Stevenson, J. C., Sundberg, K. L., and Suttles, S. E.: Multiscale experiments in coastal ecology: Improving realism and advancing theory, BioScience, 53, 1181–1197, 2003.

Petersen, J. E., Kennedy, V. S., Dennison, W. C., and Kemp, W. M.: Enclosed experimental ecosystems and scale: tools for understanding and managing coastal ecosystems, Springer, New York, 221 pp., 2009

Pilson, M. E. Q. and Nixon, S. W.: Marine microcosms in ecological research, In Microcosms in ecological research, DOE Symposium series 52, Technical information center, US Department of Energy, Washington, DC, 724–741, 1980.

Riebesell, U.: Acid test for marine biodiversity, Nature 454, 46–47, 2008.

Riebesell, U. and Tortell, P.D.: Effects of Ocean Acidification on Pelagic Organisms and Ecosystems, in: Ocean Acidification, edited by: Gattuso, J.-P., Hansson, L., Oxford University Press, 99–121, 2011.

Riebesell, U., Lee, K., and Nejstgaard, J.C.: Pelagic mesocosms, in: Guide to best practices in ocean acidification research and data reporting, edited by: Riebesell, U., Fabry, V., Hansson, L., and

Gattuso, J.-P., Office for Official Publications of the European Communities, Luxembourg, 81–98, 2010.

Schulz, K. G. and Riebesell, U.: Diurnal changes in seawater carbonate chemistry speciation at increasing atmospheric carbon dioxide, Mar. Biol., doi:10.1007/s00227-012-1965-y, 2012.

Schulz, K. G., Barcelos e Ramos, J., Zeebe, R. E., and Riebesell, U.: CO_2 perturbation experiments: similarities and differences between dissolved inorganic carbon and total alkalinity manipulations, Biogeosciences, 6, 2145–2153, doi:10.5194/bg-6-2145-2009, 2009.

Schulz, K. G., Bellerby, R. G. J., Brussaard, C. P. D., Büdenbender, J., Czerny, J., Engel, A., Fischer, M., Koch-Klavsen, S., Krug, S. A., Lischka, S., Ludwig, A., Meyerhöfer, M., Nondal, G., Silyakova, A., Stuhr, A., and Riebesell, U.: Temporal biomass dynamics of an Arctic plankton bloom in response to increasing levels of atmospheric carbon dioxide, Biogeosciences, 10, 161–180, doi:10.5194/bg-10-161-2013, 2013.

Seuthe, L., Iversen, R. K., and Narcy, F.: Microbial processes in a high-latitude fjord (Kongsfjorden, Svalbard): II. Ciliates and dinoflagellates, Polar. Biol., 34, 751–766, 2011.

Silyakova, A., Bellerby, R. G. J., Czerny, J., Schulz, K. G., Nondal, G., Tanaka, T., Engel, A., De Lange, T., and Riebesell, U.: Net community production and stoichiometry of nutrient consumption in a pelagic ecosystem of a northern high latitude fjord: mesocosm CO_2 perturbation study, Biogeosciences Discuss., 9, 11705–11737, doi:10.5194/bgd-9-11705-2012, 2012.

Steinacher, M., Joos, F., Frölicher, T. L., Plattner, G.-K., and Doney, S. C.: Imminent ocean acidification in the Arctic projected with the NCAR global coupled carbon cycle-climate model, Biogeosciences, 6, 515–533, doi:10.5194/bg-6-515-2009, 2009.

Svendsen, H., Beszczynska-Møller, A., Hagen, J.O., Lefauconnier, B., Tverberg, V., Gerland, S., Ørbæk, J. B., Bischof, K., Papucci, C., Zajaczkowski, M., Azzolini, R., Bruland, O., Wiencke, C., Winther, J.-G., and Dallmann, W.: The physical environment of Kongsfjorden–Krossfjorden, an Arctic fjord system in Svalbard, Polar Res., 21, 133–166, 2002.

Tanaka, T., Alliouane, S., Bellerby, R. G. B., Czerny, J., de Kluijver, A., Riebesell, U., Schulz, K. G., Silyakova, A., and Gattuso, J.-P.: Effect of increased pCO_2 on the planktonic metabolic balance during a mesocosm experiment in an Arctic fjord, Biogeosciences, 10, 315–325, doi:10.5194/bg-10-315-2013, 2013.

Walther, K., Anger, K., and Pörtner, H. O.: Effects of ocean acidification and warming on the larval development of the spider crab *Hyas araneus* from different latitudes (54° vs. 79° N), Mar. Ecol. Progr. Ser., 417, 159–170, 2010.

Wood, H. L., Spicer, J. I., Kendall, M. A., Lowe, D. M., and Widdicombe, S.: Ocean warming and acidification; implications for the Artic brittlestar *Ophiocten sericeum*, Polar Biol., 34, 1033–1044, doi:10.1007/s00300-011-0963-8, 2011.

4.5.3 Manuscript II

KielVision: Automated High-Resolution Imaging System for Non-Invasive In-Situ Measurements of Marine Particles and Mesozooplankton

First-authored

KielVision: Automated high-resolution imaging system for non-invasive in situ measurements of marine particles and zooplankton

Jan Büdenbender, Jan Czerny, Jan Taucher, Bastian Rolf, Dominik Queißner, Anne Jordt-Sedlazeck, Rainer Koch, Reiner Kiko, Markus Motz and Ulf Riebesell

Abstract

In a recent opinion-paper in *Nature* entitled "Time to automate identification", MacLeod et al. (2010) called for "... a concerted interdisciplinary research and development effort ... to lead to automated systems capable of high-throughput identifications ... of living as well as non-living specimens." In marine science this effort should include the further development of underwater imaging systems capable to do non-invasive, in-situ analyses of plankton abundance and composition and particle size spectra (Culverhouse et al. 2006, Benfield et al. 2007). In-situ imaging systems have a number of advantages over traditional net-based approaches including high spatial resolution (e.g. to obtain vertical gradients), detection of unperturbed particle size spectra, detection of fragile and under-sampled objects and automated data analysis. Among the existing underwater imaging systems the ones most widely used are the Video Plankton Recorder (VPR) (Davis et al. 1992) and the Underwater Video Profiler (UVP) (Gorsky et al. 1992). Both systems have been extensively utilized in a variety of field applications (Guidi et al. 2008, 2009, Stemmann et al. 2008, Forest et al. 2012, Ohman et al. 2012) demonstrating the versatility and strong potential of this approach. Nevertheless, due to their large sizes and weight deployment of both systems rely on the support of a well-equipped research vessel. By to the use of state of the art computer and camera technology it is now possible to develop an underwater imaging system smaller, lighter and with higher resolution than existing systems, allowing the use in shallow water systems, mesocosm studies and from small boats.

Introduction

In the course of the KOSMOS studies our team became aware of a shortcoming in the scientific data compilation with respect to zooplankton ecology. In most studies zooplankton was sampled with a traditional Apstein 55µm net (Niehoff et al. 2013) and then used for secondary lab experiments. Mesocosms served as reservoir for CO2 acclimated organisms. From the ecological and biogeochemical point of view much more information on the in-situ community (development, abundances, size classes, biomass, trophic relations, sedimentation and gelatinous plankton) was desirable. Also a higher resolution in the spatial and temporal dimensions was needed. Additionally, parts of the community like gelatinous and fragile organisms as well as aggregates were, due to deformation, simply not identified in net samples. However, the major drawback of net sampling for the whole mesocosm system is the consecutive removal of mesozooplankton artificially changing community composition, grazing pressure and zooplankton recruitment success.

Simple underwater photography of the mesocosm water column with a GoPro 3 camera (GoPro Inc.) provided a surprisingly detailed picture of the dominant mesozooplankton species and generated the idea of a quantitative and qualitative non destructive in-situ data set

generated through a camera system to be developed. Since a prerequisite for non destructive observations is a physically undisturbed water body and lowest possible interference with the living organisms, enclosure of a water sample had to be avoided. At that state we came across the already existing Underwater Vision Profiler 5 (UVP5) (Picheral et al. 2010), which exactly was what we were looking for. After a collaborative test of the UVP5 system in the KOSMOS mesocosms we figured the UVP5's concept as ideal for our purposes, but the UVP5's dimensions and design as oversized and inappropriate. Due to the high pressure rating to 3000 m and an internal power supply the UVP5 weights 30 kg, which is not suited for handheld use. Additionally, the camera setup and electronics in the UVP5 are optimized for low and long battery use. As a consequence, the installed camera has low resolution and data acquisition rates if compared to today's state of the art machine vision technology. Especially the resolution and thereby the lower size limit for object identification had high potential for improvement if state of the art cameras could be implemented in such a system.

We decided to develop a system based on the UVP5 concept but with lower weight (<15kg) and 3 to 4 times higher resolution optimized for the use in mesocosm studies. After interviews with the UVP5 manufacturer and other potential industrial partners we decided to develop a system with a local industrial partner (Develogic) from scratch. The UVP5 concept was adopted in critical points, which are silhouette photography, 625 nm wave length spectrum for water illumination, optical capturing of an *in-situ* water volume, profiling casts and data structure and compatibility in order to use open source diagnostic software build for the UVP5 system. In contrast to the UVP5 system we choose an external power supply in order to save the weight of batteries and to allow unlimited operation time. Abandoning the batteries and the need for high pressure rating allowed us the implementation of a much more powerful camera and computer hardware at a still lower overall weight.

Technical specifications

The KielVision system weights 20 kg in air and is pressure rated to 100 m depth. The system consists of a camera system, an embedded windows PC and a light unit integrated in one housing (Fig. 1a). The camera (Dalsa Falcon2 12M) sensor contains 4096 x 3072 of 6 x 6 µm large pixels (12 Megapixel). It has a theoretical acquisition rate of 58 frames per second (fps) and a minimal exposure time of 20 µs. Data can be downloaded through a 2 x Full Camera Link – SDR26 interface allowing a transfer capacity of gross 6 Gbyte/s allowing a net transfer rate of images at 650 Mbyte/s. The acquisition rate limiting factor is the capacity of data storage on the cameras solid state drives, which were increased to 180 Mbyte/s using an embedded PC with Intel core i7 processor and 8 Gbyte RAM. In summary we could increase the resolution and data acquisition rate of the UVP5 system by a factor of 3 to 4. To allow the use of high data acquisition rates the systems storage capacities consist of a 128 Gbyte SSD system drive and 3 x 500 Gbyte SSD drives.

The lighting unit frames the sampled water volume in a horizontal direction from four sides (Fig. 1). The camera is mounted above the light unit and faces downwards (Fig. 1a). This arrangement guarantees an undisturbed volume of water on the downward profile. Upward profiles are not recorded. The optics consist of a 35 mm fixed focal lens (Rodagon 35 F4 Quioptic) and a modular focus (Modular Focus Helical Mount, Quioptic) for easy re focusing if image distance has to be changed and a narrow band pass filter centered on 635 nm (IFG BP 635-50, Schneider Kreuznach). The optics sits behind a dom port (BK-7). Depending on the adjustable object distance of 40, 20 and 10 cm, the captured field-of-view measures 28 x 21, 14 x 10.5 and 7 x 5.25 cm. At a light beam depth of average 2 cm the field-of-view corresponds to sampled volumes of 1.17, 0.29 and 0.07 l, respectively. Illumination by red light emitting diodes (LED) was chosen, in order to exclude interference

with sun light in surface waters (is excluded by the band pass filter) and to minimize zooplankton phototactic behavior (Forward 1987, Storz & Paul 1998). The quadrilateral illumination is generated by 160 LEDs of 625 nm wavelength. The LEDs can be pulsed with up to 500 Watt at maximum light intensity. The light flash is focused through an aperture – Fresnel lens – aperture system in order to parallelize the light and minimize the scattering angle to < 5°C (Fig. 1b). The flash is triggered by the camera and synchronized to the exposure time, which typically last for 100µs to prevent image blur. Deployment speeds up to 1.5 m s^{-1} are practicable.

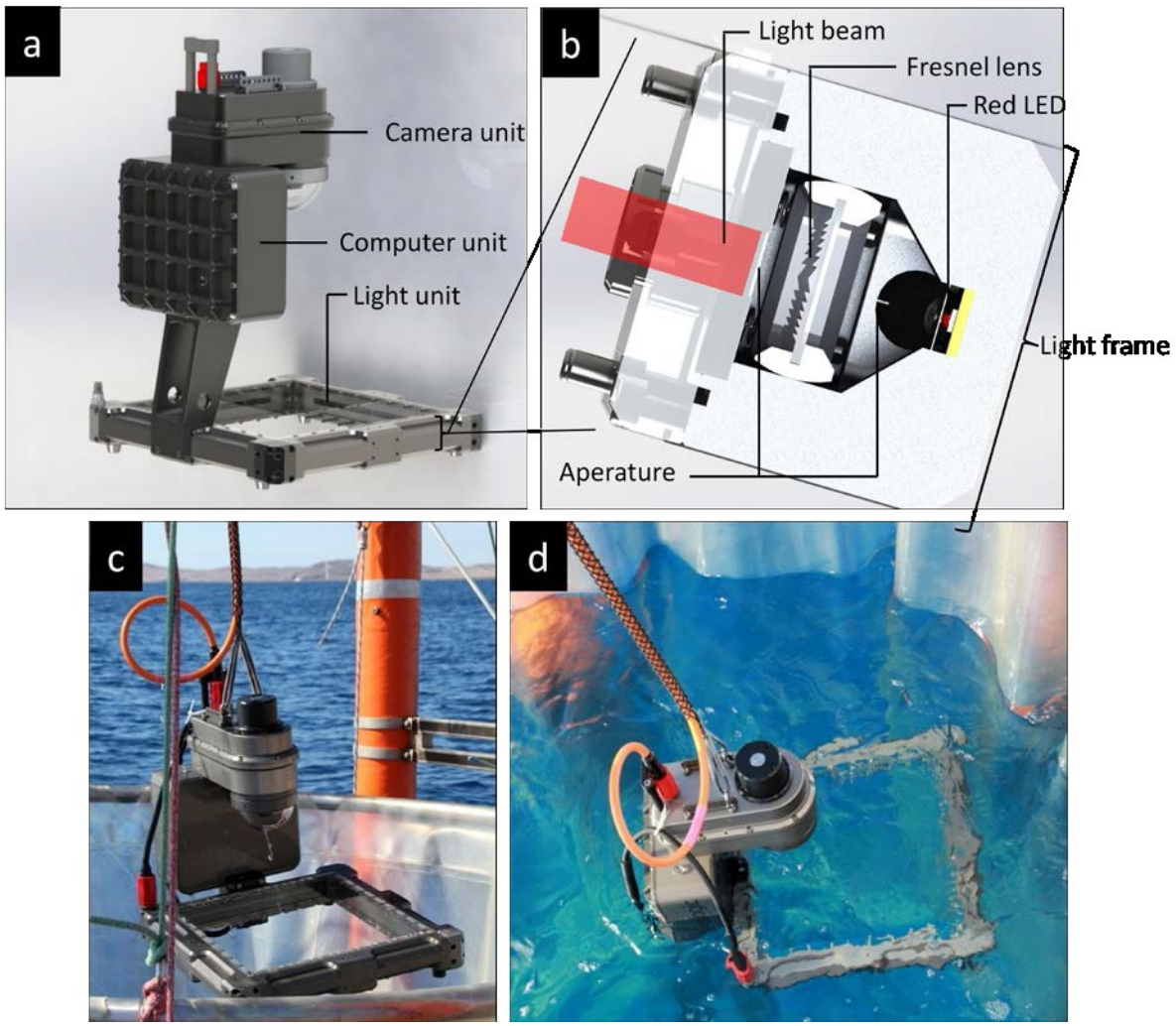

Figure 1 The KielVision, an automated high-resolution imaging system for non-invasive in-situ measurements of marine particles and zooplankton. Technical drawings by Develogic: a, the system from the back; b, cut through one bar of the light unit. Photographs from the deployment of the system during GC 1.0 by Tim Boxhammer: c, hanging in the opening of the mesocosm bag; d, at the water surface inside a KOSMOS mesocosm.

The control panel is implemented as a second windows embedded PC system in a separate IP67 rated housing. The control interface also contains a 150 W DC-DC voltage transformer providing 48 V instead of 12 V, thus decreasing the power loss through the 50 m supply cable for the camera system. The control panel allows direct control of the camera PC and the camera itself. The software surface on the control panel allows the configuration of the camera and depth sensor settings like acquisition mode (time controlled or depth controlled), exposure time (100 to 500 µs), stop conditions (time, depth or image number), ambient

pressure at sea surface and displays online depth readings and captured frame numbers. The system has GiGE and USB as well as RS232 interfaces for fast data transfer and easy access with external PC's.

Raw pictures and a log file linking each captured frame with the corresponding depth are stored on the cameras solid state drive and have to be downloaded for data procession. Data formats of the images and the log file are build according to data formats used with the open source software ZooProcess and PlanktonIdentifier developed by the founders of the UVP5 system (http://www.zooscan.com, Gorsky et al. 2010). Thereby, data comparability of both systems is guaranteed.

Exemplary results

After 1 year of development including a 2 month test- and 2 month revision phase, the prototype (Fig. 1) works as originally specified and was operated during two mesocosm campaigns of Gran Canaria in spring 'GC 1.0' and winter 'GC 2.0' 2014. The system generated an highly resolved dataset on particle size distributions in the vertical water column of nine mesocosms and the surrounding water over the experimental duration of almost 60 days (Fig. 2 & 3). We observed temporal and spatial dynamics of objects in the size range from 50 to 10000 µm (Fig. 2 & 3). Individual objects are eventually identified in the automated image analysis (Fig. 4). Objects not identified are simply treated as particles in different size classes (e.g. Fig. 2).

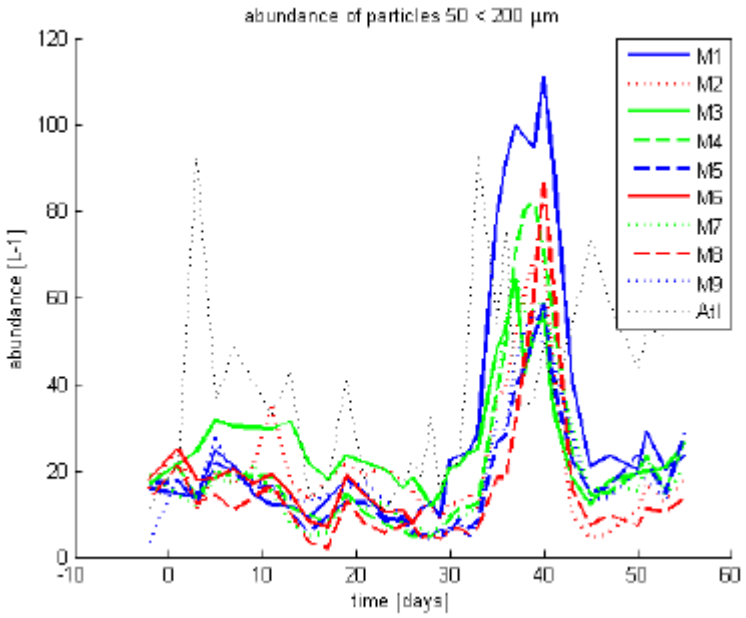

Figure 2 Particle abundances (# l^{-1}) in the size range 50 to 200 µm equivalent spherical diameter (ESD) from 9 mesocosms and the Atlantic (see color and line code) over the duration of the GC 2.0 KOSMOS experiment reprinted with kind permission of Dr. Jan Taucher (operator of the KielVision during GC 2.0).

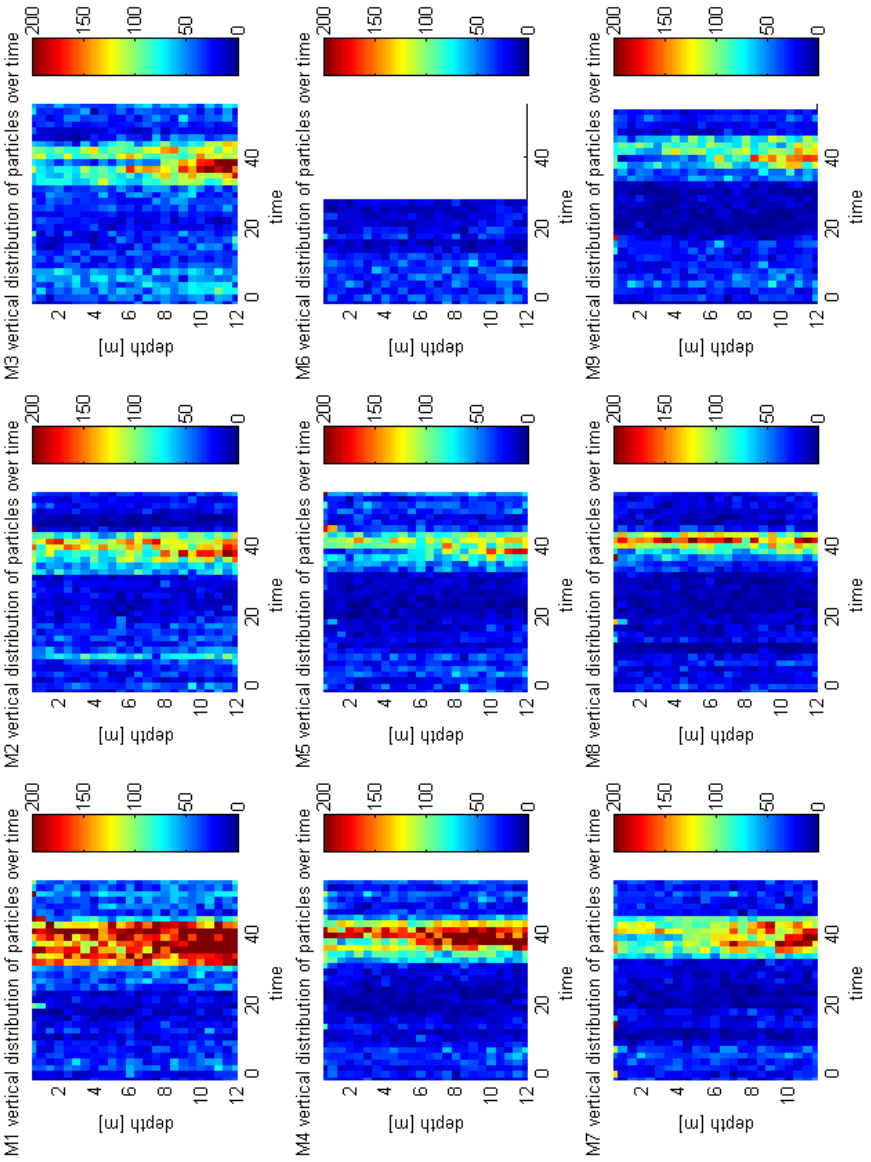

Figure 3 Temporal and spatial dynamic of all objects in the 50 to 200 µm size range captured during GC 2.0. Number of particles (# l^{-1}) are represented by the color code and are plotted for the water column of 12 m analyzed in 9 mesocosms and the Atlantic. With kind permission of Dr. Jan Taucher (operator of the KielVision during GC 2.0).

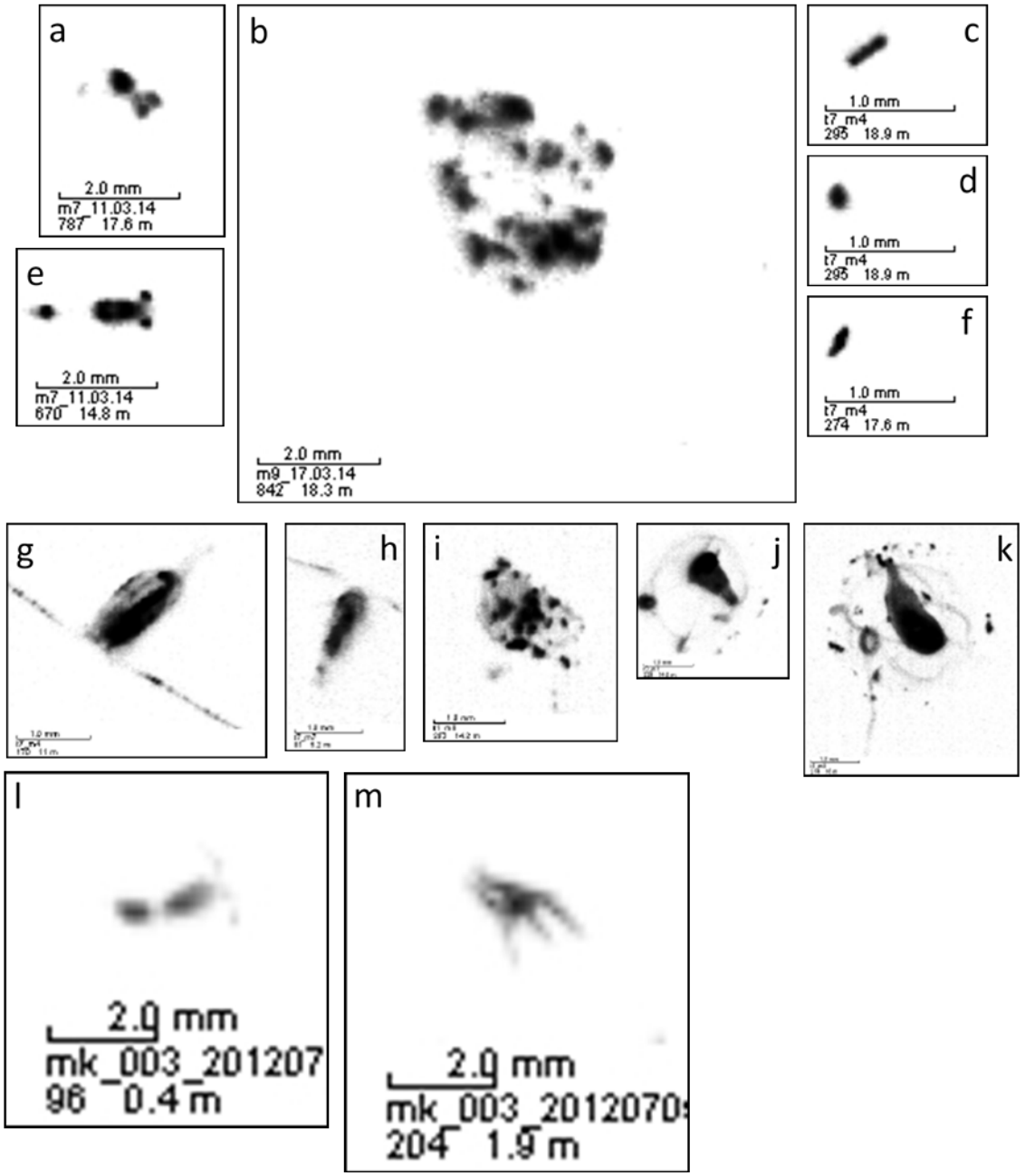

Figure 4 Exemplary objects from the KOSMOS mesocosm studies Finnland 2012, Kristineberg 2013 & GC 2.0. Objects a, b & e are from the Kristineberg study and are photographed at a distance of 40 cm from camera optics. Objects c, d & f – k are from GC 2.0 and were photographed at 20 cm distance, the scale bar always represents 1 mm (with kind permission from Dr. Jan Taucher, operator of the KielVision during GC 2.0). Objects l & m are photographed with the original UVP5 system at 40 cm distance during a collaborative test at the Finnland 2012 KOSMOS study. Copepod crustacean, a, g, h & l; decapod crustacean larvae, e; unidentified biogenic objects (likely zooplankton) making the bulk of captured objects, c, d & f; aggregates, b & i; gelatinous zooplankton (possibly *Mnemiopsis*), j & k; cyanobacteria aggregate 'puff', m.

Perspective

Summarizing the experience of the KielVision operation during the field studies, the performance with respect to camera resolution and operation is satisfactory. The system runs reliable over extended time periods and produces reproducible data. With respect to particle

size distributions scientific demands on data are fulfilled and new insights from this data for the particle dynamics in the KOSMOS system are looked forward to. Progress in size resolution relative to the UVP5 system was achieved (compare Fig. 4a&g to Fig. 4l). Still, resolution of photographed objects needs further improvement. Object blur and transparency are not sufficient for the desired level of identification. Problems most likely are generated by insufficient or improvable illumination. However, it could be possible that turbidity of natural sea water and the size range of objects relative to the object distance from the camera bring optical resolution to the boundaries of their technical feasibilities.

Potential for improvement was identified in the opening of the light frame apertures in order to increase the net light output, a second light source in a different angle (from above) to increase object plasticity on the images and in the use of optics with lower apertures. Additional light sources however, create problems for the volume definition and sun light independence. Optics with lower apertures and or focal length would decrease the field of view distance, which goes hand in hand with a reduction in depth resolution significantly reducing the photographed volume of water. All of these possibilities hold potential for improving the object resolution but make minor to major revisions in the KielVision system and another dedicated test phase necessary.

References

Benfield MC, Grosjean P, Culverhouse PF, Irigoien X, Sieracki ME, Lopez-Urrutia A, Dam HG, Hu Q, Davis CS, Hansen A, Pilskaln CH, Riseman EM, Schultz H, Utgoff PE, Gorsky G (2007) RAPID Research on Automated Plankton Identification. Oceanography 20:172–187

Culverhouse PF, Williams R, Benfield M, Flood PR, Sell AF, Mazzocchi MG, Buttino I, Sieracki M (2006) Automatic image analysis of plankton: Future perspectives. Mar Ecol Prog Ser 312:297–309

Davis CS, Gallager SM, Berman MS, Haury LR, Strickler JR (1992) The Video Plankton Recorder (VPR): Design and initial results. Arch für Hydrobiol Beih Ergebnisse der Limnol 36:67–81

Forest A, Stemmann L, Picheral M, Burdorf L, Robert D, Fortier L, Babin M (2012) Size distribution of particles and zooplankton across the shelf-basin system in southeast Beaufort Sea: combined results from an Underwater Vision Profiler and vertical net tows. Biogeosciences 9:1301–1320

Forward RB (1987) Comparative study of crustacean larval photoresponses. Mar Biol 94:589–595

Gorsky G, Aldorf C, Kage M, Picheral M, Garcia Y, Favole J (1992) Vertical distribution of suspended aggregates determined by a new underwater video profiler. Ann l'Institut océanographique 68:275–280

Gorsky G, Ohman MD, Picheral M, Gasparini S, Stemmann L, Romagnan J-B, Cawood A, Pesant S, Garcia-Comas C, Prejger F (2010) Digital zooplankton image analysis using the ZooScan integrated system. J Plankton Res 32:285–303

Guidi L, Jackson GA, Stemmann L, Miquel JC, Picheral M, Gorsky G (2008) Relationship between particle size distribution and flux in the mesopelagic zone. Deep Sea Res Part I Oceanogr Res Pap 55:1364–1374

Guidi L, Stemmann L, Jackson G a., Ibanez F, Claustre H, Legendre L, Picheral M, Gorsky G (2009) Effects of phytoplankton community on production, size, and export of large aggregates: A world-ocean analysis. Limnol Oceanogr 54:1951–1963

MacLeod N, Benfield M, Culverhouse P (2010) Time to automate identification. Nature 467:154–155

Niehoff B, Schmithüsen T, Knüppel N, Daase M, Czerny J, Boxhammer T (2013) Mesozooplankton community development at elevated CO_2 concentrations: results from a mesocosm experiment in an Arctic fjord. Biogeosciences 10:1391–1406

Ohman MD, Powell JR, Picheral M, Jensen DW (2012) Mesozooplankton and particulate matter responses to a deep-water frontal system in the southern California Current System. J Plankton Res 34:815–827

Picheral M, Guidi L, Stemmann L, Karl DM, Iddaoud G, Gorsky G (2010) The Underwater Vision Profiler 5: An advanced instrument for high spatial resolution studies of particle size spectra and zooplankton. Limnol Oceanogr Methods 8:462–473

Stemmann L, Youngbluth M, Robert K, Hosia A, Picheral M, Paterson H, Ibanez F, Guidi L, Lombard F, Gorsky G (2008) Global zoogeography of fragile macrozooplankton in the upper 100-1000 m inferred from the underwater video profiler. ICES J Mar Sci 65:433– 442

Storz UC, Paul RJ (1998) Phototaxis in water fleas (Daphnia magna) is differently influenced by visible and UV light. J Comp Physiol - A Sensory, Neural, Behav Physiol 183:709–717

5 Synthesis

In the synthesis section I will compare presented experiments with the literature and discuss overarching conclusions and hypotheses. I will elaborate the effects of OA and warming (only for pteropods) on Arctic calcifying key species biology in order to present a state of the art in this field. I will derive likely consequences for the Arctic marine ecosystem and present possible directions for subsequent research.

5.1 A high latitude ecosystem at risk: Arctic coralline algae

Crustose coralline algae (CCA) are adapted to extreme light and temperature conditions prevailing in the northern most benthic habitat described so far (80°31′N, publication II). By providing substrate, shelter and resources, CCA form the basis of a species-rich habitat at these latitudes, contributing to high fish stocks in Arctic waters (Kamenos et al. 2004a, b, Nelson 2009). This unique ecosystem is built on calcium carbonate ($CaCO_3$) which makes 80 to 90% of the plants biomass (Bilan & Usov 2001), and is thereby vulnerable to human induced changes in global ocean chemistry.

Recent studies described overall negative effects of OA for temperate and tropic CCA biology like reduced growth (Ragazzola et al. 2013), reduced calcification (Anthony et al. 2008; Jokiel et al. 2008), reduced settlement of spores (Kuffner et al. 2008) and absence in naturally acidified areas (Hall-Spencer et al. 2008), generating concern on the future fate of these keystone organisms. Annual mean net dissolution of Arctic CCA is experimentally determined for Omega aragonite (Ω_{Ar}) levels ≤ 1 (Publication I). Ω_{Ar} subsaturation was already measured in the Arctic surface ocean (Chierici & Fransson 2009). Widespread mean annual Ω_{Ar} subsaturation of the Arctic surface ocean is expected well before 2050 (Steinacher et al. 2009, Comeau et al. 2012). Therefore, unabated anthropogenic CO_2 emissions likely lead to significant annual mean net dissolution of Arctic CCA (Publication I, Fig. 4), putting CCA structures such as habitat forming rhodolith fields at risk.

As Arctic CCA likely live below optimum growth temperatures (Adey 1970), global warming could be beneficial for algae as shown for temperate species (Martin & Gattuso 2009, Martin et al. 2013). Additional to the direct positive effect of warming on growth, carbonate saturation increases at increasing temperatures, potentially delaying OA and associated problems for calcifying organisms. While the temperature effect on CO_3^{2-} saturation is small (Zeebe & Wolf-Gladrow 2001) (At an exemplary warming of 3°C, present day Ω_{Ar} saturation would increase by ~1%), the effect of increased light availability due to reduced seasonal ice cover at a warming surface ocean (Allison et al. 2009) could be large for Arctic CCA (Adey 1970; publication I). However, algae living at the sea bed may actually suffer from reduced light availability due to increasing snow and ice melt increasing the sediment load and turbidity in coastal waters (Labat et al. 2004). In publication I, experimental work was carried out at optimum growth temperature, ~5°C higher than prevailing in their natural habitat, such being higher than future proposed warming in the Arctic Ocean (Steinacher et al. 2009). We did not test whether increased temperature had a positive effect on calcification as shown for temperate species (Martin & Gattuso 2009, Martin et al. 2013), but if this would be the case, this positive effect is by far not sufficient to compensate negative CO_2 effects for Arctic algae as shown in publication I.

Summarizing, CCA, especially the unattached growth forms are important habitat providers in the northern most known CCA habitat (Publication II) and as a consequence of OA are expected to shrink or vanish from these latitudes (Publication I).

5.2 Dissolving Arctic coralline algae facies, a short term buffer for local OA?

Despite the importance of CCA for benthic ecology and carbonate production (Nelson 2009, van der Heijden & Kamenos 2015), until today no comprehensive data is published on the extent and volume of Arctic CCA standing stocks. Based on fossil records (Halfar & Mutti 2005) and present day significance in tropical and temperate regions (Bosence 1980, Foster 2001, Bosence & Wilson 2003, Nelson 2009) one could assume that CCA carbonates could be of significant volume on Arctic and subarctic shelves, too.

An aspect of CCA for the Arctic carbonate system, but also for other shelf oceans, not investigated yet is their potential as a short term buffer for local OA. Simply their high volume of accumulated $CaCO_3$ and their presence in the mixed surface layer could make them a short-term sink for anthropogenic CO_2. Could dissolution of the total quantity of Arctic CCA carbonates potentially delay local OA?

A similar hypothesis was tested for southern ocean carbonate sediments of macrozoobenthic and pelagic origin (Hauck et al. 2013). Here, authors stated benthic carbonates no matter of their origin to be of no relevance for the local CO_2 uptake capacity. They did not evaluate the potential role of CCA facies in Southern Ocean shelf areas.

Certainly, a representative mapping of CCA standing stocks, as was undertaken in temperate and tropical locations (Littler et al. 1991, Hetzinger et al. 2006, Riul et al. 2008, Ierodiaconou et al. 2011), would be a substantial contribution towards assessing their role in the Arctic carbonate system.

5.3 Are pteropods a canary in the coalmine for future OA?

Pteropods recently were called canaries in the coalmine for increasing OA (Kintisch 2014) proposing their hypothesized disappearance as an early warning system for first fatal acidification of the sea, like the birds used to sense dangerous CO_2 concentrations in ancient mining. In fact, most authors agree on overall negative effects of OA and warming on thecosome pteropods (Comeau et al. 2009, 2010, 2012; Bednarsek et al. 2012, 2014; Orr et al. 2005; Thabet et al. 2015; publication III) and propose future aragonite subsaturated oceans like the Arctic Ocean to be inhabitable for this organism (Comeau et al. 2010, 2012; Bednarsek et al. 2012, 2014). However, laboratory based work with these organisms is compromised by major limitations, like increased stress, mechanical damage and starvation, shown by high mortalities and no reproduction (Publication IV). Such limitations restrict the transferability of experimental results to in-situ conditions. Results derived from the Bergen mesocosm study (Manuscript I) question the hypothesis of pteropod absence in the future Arctic Ocean and raise concern towards the extrapolation of published laboratory experiments (Comeau et al. 2009; Orr et al. 2005; Thabet et al. 2015; Bednarsek et al. 2012; publication III) on future in-situ conditions.

Because of increased duration and higher sampling resolution in a mesocosm study (Manuscript I) we could identify different phases in the survival of pteropod larvae not shown so far. CO_2 correlated survival as shown previously (Thabet et al. 2015; publication III) was measured in the first phase, which was closely associated with manipulative acidification of the mesocosms (Manuscript I). In the second phase, covering the last two thirds of the experimental duration, survival became CO_2 independent (Manuscript I, Fig. 4) even at highly subsaturated conditions.

This contrary finding was likely not detectable in previous manipulative studies due to a lack of temporal resolution (Publication III) or duration (Thabet et al. 2015). With knowledge of only the final survival like e.g. in the Svalbard experiment (Publication III), we had to assume constant mortality over the experimental duration as the simplest possible model. Upon this assumption, CO_2 correlated survival is the only possible interpretation. Insight into temporal dynamics of pteropod survival as in the midterm OA mesocosm experiment disproves this assumption. Additional indications for the hypothesis of OA independent survival can be found in recent time series analyses (Ohman et al. 2009, Mackas & Galbraith 2011, Beaugrand et al. 2012), where no correlation between OA and pteropod abundances was detected, even not at already subsaturated waters of the California Current System (Ohman et al. 2009).

Shell growth as increase in shell diameter is in both studies (Publication III & manuscript I) negatively affected by increased CO_2 concentrations, resulting in smaller individuals under OA scenarios compared to present day or pre-industrial conditions. Shell preservation proposed to correlate with corrosiveness of the water and rate of repair calcification is expected to be CO_2 sensitive (Orr et al. 2005). In the Svalbard study we found a significant effect of CO_2 on shell corrosion (Publication III, Fig. 3). In the Bergen study, the CO_2 effect on shell corrosion was prominent at prolonged aragonite subsaturation, while if only end of the century representative OA scenarios were included in the statistic analysis no significant CO_2 effect was found (Manuscript I, Table 2). Variability in the significance of the CO_2 effect could indicate, that shell corrosion does not only depend on water chemistry, but e.g. also on sufficient food supply, certainly not given in lab experiments but likely in the mesocosm study. Furthermore, it is yet impossible to measure a rate of shell corrosion and thereby isolate the CO_2 effect on net calcification. Therefore, it remains speculative if corrosion at subsaturated conditions progresses until the entire shell is dissolved or if net calcification is sustainable.

Summarizing, pteropod survival is possible at Omega Ar subsaturation (Comeau et al. 2009, 2010; Lischka & Riebesell 2012; publication III; manuscript I), and is so far OA independent in nature (Ohman et al. 2009, Mackas & Galbraith 2011, Beaugrand et al. 2012) and in manipulative experiments closely mimicking in-situ conditions like mesocosm systems (Manuscript I). Further, OA affected survival, as proposed, likely is compromised by the lack of duration and/or temporal resolution of experimental laboratory studies and probably is associated with the CO_2 manipulation itself (Manuscript I). Unanimously, manipulative and observational studies propose corroded shells at subsaturated conditions (Orr et al. 2005; Bednarsek et al. 2012, 2014; Lischka & Riebesell 2012; Wall-Palmer et al. 2013; publication III; manuscript I) and reduced growth at end of the century scenarios (Comeau et al. 2009, 2012; publication III; manuscript I). But, if this will lead to absence of pteropods from subsaturated ocean regions in the worst case, or to similar abundances as today but at likely smaller sizes and weaker shells, remains unresolved. Development of a second pteropod generation at subsaturated conditions, as observed in the mesocosm experiment (Manuscript I), additionally indicate sustained pteropod survival at end of the century OA scenarios.

5.4 Impact of warming on pteropod survival

Warming of the pelagic realm (Levitus et al. 2001) is an additional consequence of manmade climate change likely affecting development of future pteropod generations. In publication III we could show that under laboratory conditions warming had a several fold higher impact on mortality as had OA. The hypothesis of temperature being the overriding factor for pteropod biology at ongoing climate change is confirmed in time series analysis of the North Atlantic Ocean (Beaugrand et al. 2012). Surface ocean warming was identified to be the main driver for a habitat shift of the pteropod population. Pteropods migrated to colder, northern regions. In the Svalbard experiment (Publication III), increased temperatures could also have stimulated viral and bacterial infection due to the absence of microphage consumers possibly leading to overestimated pteropod mortalities.

5.5 Pteropod perspectives

As consequence of here presented results, future research should focus on finding a cause for CO_2 correlated low survival shortly after manipulation and CO_2 independent survival in the following period. Mainly two hypotheses should be tested: Is CO_2 correlated survival an artifact of CO_2 manipulation (e.g. a triggered behavior) or does this effect derive from genetic diversity within the population meaning these individuals will sustain future pteropod presence. Verification of the first hypothesis causes concern on the applicability of CO_2 manipulation techniques and interpretations based on manipulative OA experiments, at least for the future of thecosome pteropod ecology. Verification of the alternative hypothesis would be of major significance for forecasting pteropod biology and biogeochemical consequences. By the use of molecular methods the number of different genotypes and their share in a pteropod population need to be identified before and after exposure to increased CO_2 concentrations. Ideally, the number of genotypes is reduced after exposure to increased CO_2 concentrations revealing the CO_2 tolerant genotypes.

After all, the effects of climate change on pteropods and subsequent biogeochemical consequences are controversial and call for further experimental work. Mainly the difficulties in culturing techniques so far prevent sound manipulative experiments (Publication IV). Most critic topics are the implementation of long-term and several generation experiments ensuring proper cultivation conditions and validating the extrapolation of derived hypotheses to future OA scenarios.

5.6 Advancing pteropod methodology

With respect to difficulties in culturing techniques from my experience, priorities for sound pteropod experiments should be:

- **Minimizing sampling stress:** Traditional plankton nets (e.g. Appstein) are not the best choice for catching individuals to be used in cultivation experiments. Acceptable results providing undamaged individuals were achieved by catching single individuals on sight with beakers or jars, by enclosing the whole water body to be used in the experiment as done in KOSMOS mesocosm experiments or by using specialized plankton nets with extra big collectors as described in Publication IV.
- **Minimizing cultivation stress:** Cultivation stress predominantly correlates with the likelihood of pteropods encountering an obstacle (e.g. water surface, aquarium walls, propellers, etc.). Therefore, important characteristics for sound cultivation are:
    - A as big as possible body volume to incubation volume ratio e.g. larvae in beakers (Publication III) or adult stages in mesocosms (Manuscript I) both had a ratio of $1{:}2x10^6$
    - A minimized surface to volume ratio of the enclosed water body e.g. no internal obstacles like rotators, hoses, filters, etc.
    - A increased depth to width ratio of the water column in order to give as much as possible room for the predominating sinking and ascending movements of pteropods. Cylindrical enclosures fulfill prior characteristics the best.
- **Minimizing manipulation stress:** The manipulation should be as gentle as possible. Increasing the stressor level should be preferred over diluting an unnatural high stressor level e.g. transferring organisms through a series of pre-equilibrated water volumes vs. manipulating a volume already containing the organisms with pure CO_2 gas or a CO_2 saturated solution.
- **Maximizing feeding success:** Feeding in cultivation in most cases is not possible. Two practicable strategies are the use of lipid rich overwintering stages to be captured at the beginning of the winter period as performed in Publication III or close to in-situ simulations of the natural habitat as in mesocosm set ups, where natural food sources are included and room for the deployment of a mucus web is optimized (Manuscript I).
- **Maximizing experimental duration:** Two reasons why extended experiment durations matter:
    - Acclimation to cultivation and manipulation likely takes several days (Thabet et al. 2015; manuscript I)
    - Successful long-term experiments are as well as reproduction the best indicator for sound cultivation conditions as pteropods quickly deteriorate (settling motionless in cultivation unit) at insufficient conditions.

  The acclimation phase should be analytically identified but excluded from analysis and experiment durations should be at least a multiple of the acclimation duration and optimally span over generation cycles.
- **Choosing the right set up for the right live stage:** Following the body volume to water volume argument it is conclusive that veliger larvae should be given preference in laboratory experiments, while adult stages should only be used in mesocosms.

Mesocosms like the KOSMOS system (Publication V) are especially promising for experimental pteropod studies since several of the above listed factors are met by this system. The KOSMOS system maximally reduces sampling stress by enclosing pteropods as part of their natural environment, largely increases the body size to incubation volume ratio, maximizes in-situ

simulation due to exposure to natural light and temperature dynamics as well as enclosure of the natural food sources, competitors and predators and at the same time enables replicated and manipulated experimental set ups. Additionally these systems can be used anywhere independent of large infrastructure with climate rooms and incubation labs (e.g. experiments were conducted using improvised labs in tents and containers illustrating the independence of urban structures).

Limiting the use of mesocosm systems, however, is besides high costs and a sophisticated technical and logistical handling, the ecological complexity urging the investigation of the complete plankton community (Publication V). Data of higher trophic levels and especially in-situ observations are still underrepresented in present KOSMOS experiments. To be able to observe in-situ effects of the experimental manipulation on zooplankton ecology, qualitative and quantitative non destructive sampling is to be performed. Traditionally, plankton nets are used to sample the zooplankton community or individual species of interest like pteropods. Disadvantages of this sampling strategy are a continuous artificial reduction of the population size and the damage of fragile organisms obscuring quantitative and qualitative sampling. A non-destructive method, which allows in-situ quantitative and qualitative measurements of population size, body size and growth and developmental stage had to be developed for the KOSMOS system.

5.7 Development of an automated in-situ observation system for mesocosm studies

The KielVision (Manuscript II) was developed as an automated high-resolution imaging system for non-invasive in-situ measurements of marine particles and zooplankton. In-situ imaging systems have a number of advantages over traditional net-based approaches: High spatial resolution (e.g. to obtain vertical gradients), detection of unperturbed particle shape and size spectra, observation of intact fragile objects (e.g. gelatinous plankton or aggregates) and automated data analysis. In mesocosms with limited population size a main advantage is preservation of stock. Further, automated data analysis enables online observation of in-situ dynamics in replicated set ups, impossible with traditional sorting techniques considering their tremendous time consumption.

We successfully operated the KielVision in mesocosm campaigns GC 1.0 & 2.0 off Gran Canaria 2014 and in Bergen 2015. The system generated a highly resolved dataset on particle size distributions in the vertical water column of nine mesocosms and the surrounding water and allowed the identification of large aggregate dynamics. However, most of the data is not yet quantified (e.g.: size, greyscale, geometrics) and awaits interpretation of temporal and spatial dynamics. Pteropods were present in low numbers and small size classes in the named studies (GC 1.0, 2.0, Bergen 2015) and were therefore not identified through the KielVision system. For the identification of objects < 500µm (Manuscript II, Fig. 4c,d & f) the system has to be further fine- tuned or in part (light source & magnification) reconstructed in order to increase plasticity of transparent and non-transparent body parts (Manuscript II). Nevertheless, important improvements compared to already existing systems (e.g. UVP5) are: the use of an external power supply, e.g. logistically flexible car batteries and the weight reduction, which ends the dependence on large research vessels and allows simple handheld deployments from e.g. zodiacs. These are tremendous advantages for mesocosm studies, were the sampling routine can only be performed from small boats, and also for other fresh water or shelf ocean activities were large research vessels or dedicated ship time is not available or affordable.

6 References

Adey WH (1970) The effects of light and temperature on growth rates in boreal-Subarctic crustose corallines. J Phycol 6:269–276

Allison I, Bindoff NL, Bindschadler RA, Cox PM, Noblet N de, England MH, Francis JE, Gruber N, Haywood AM, Karoly D, Kaser G, Quéré C Le, Lenton TM, Mann ME, McNeil BI, Pitman AJ, Rahmstorf S, Rignot E, Schellnhuber HJ, Schneider S, Sherwood SC, Somerville R, Steffen K, Steig EJ, Visbeck M, Weaver AJ (2009) The Copenhagen Diagnosis 2009: Updating the world on the latest climate science. Sydney, Australia

Anthony KRN, Kline DI, Diaz-Pulido G, Dove S, Hoegh-Guldberg O (2008) Ocean acidification causes bleaching and productivity loss in coral reef builders. Proc Natl Acad Sci U S A 105:17442–6

Armstrong JL, Boldt JL, Cross AD, Moss JH, Davis ND, Myers KW, Walker R von, Beauchamp DA, Haldorson LJ (2005) Distribution, size, and interannual, seasonal and diel food habits of northern Gulf of Alaska juvenile pink salmon, Oncorhynchus gorbuscha. Deep Sea Res Part II Top Stud Oceanogr 52:247–265

Armstrong RA, Lee C, Hedges JI, Honjo S, Wakeham SG (2002) A new, mechanistic model for organic carbon fluxes in the ocean based on the quantitative association of POC with ballast minerals. Deep Sea Res Part II Top Stud Oceanogr 49:219–236

Atkinson A, Siegel V, Pakhomov EA, Rothery P (2004) Long-term decline in krill stock and increase in salps within the Southern Ocean. Nature 432:100–103

Bates NR, Mathis JT (2009) The Arctic Ocean marine carbon cycle: evaluation of air-sea CO2 exchanges, ocean acidification impacts and potential feedbacks. Biogeosciences 6:2433–2459

Bathmann U, Noji TT, Bodungen B von (1991) Sedimentation of pteropods in the Norwegian Sea in autumn. Deep Sea Res Part I Oceanogr Res Pap 38:1341–1360

Be AWH, Gilmer RW (1977) A zoogeographic and taxonomic review of euthecosomatous Pteropoda (ATS Ramsay, Ed.). Academic Press, London New York

Beaugrand G, McQuatters-Gollop A, Edwards M, Goberville E (2012) Long-term responses of North Atlantic calcifying plankton to climate change. Nat Clim Chang 3:263–267

Bednarsek N, Mozina J, Vogt M, O'Brien C, Tarling GA (2012) The global distribution of pteropods and their contribution to carbonate and carbon biomass in the modern ocean. Earth Syst Sci Data 4:167–186

Bednarsek N, Tarling GA, Bakker DCE, Fielding S, Jones EM, Venables HJ, Ward P, Kuzirian A, Lézé B, Feely RA, Murphy EJ (2012) Extensive dissolution of live pteropods in the Southern Ocean. Nat Geosci 5:881–885

Bednarsek N, Tarling GA, Fielding S, Bakker DC. (2012) Population dynamics and biogeochemical significance of Limacina helicina antarctica in the Scotia Sea (Southern Ocean). Deep Sea Res Part II Top Stud Oceanogr 59-60:105–116

Bednarsek N, Feely RA, Reum JCP, Peterson B, Menkel J, Alin SR, Hales B (2014) Limacina helicina shell dissolution as an indicator of declining habitat suitability owing to ocean acidification in the California Current Ecosystem. Proc R Soc B 281:20140123

Bernard KS, Froneman PW (2002) Mesozooplankton community structure in the Southern Ocean upstream of the Prince Edward Islands. Polar Biol 25:597–604

Bernard KS, Froneman PW (2009) The sub-Antarctic euthecosome pteropod, Limacina retroversa: Distribution patterns and trophic role. Deep Sea Res Part I Oceanogr Res Pap 56:582–598

Berner RA, Kothavala Z (2001) GEOCARB III : A revised model of atmospheric CO2 over phanerozoic time. Am J Sci 301:182–204

Bilan MI, Usov AI (2001) Polysaccharides of calcareous algae and their effect on the calcification process. Russ J Bioorganic Chem 27:2–16

Blunden G, Campbell SA, Smith JR, Guiry MD, Hession CC, Griffin RL (1997) Chemical and physical characterization of calcified red algal deposits known as maerl. J Appl Phycol 9:11–17

Bosence DWJ (1980) Sedimentary facies, production rates and facies models for recent coralline algal gravels, Co. Galway, Ireland. Geol J 15:91–111

Bosence DWJ, Wilson J (2003) Maerl growth, carbonate production rates and accumulation rates in the northeast Atlantic. Aquat Conserv Mar Freshw Ecosyst 13:21–31

Boyd PW, Trull TW (2007) Understanding the export of biogenic particles in oceanic waters: Is there consensus? Prog Oceanogr 72:276–312

Broecker WS, Clarke E (2001) A dramatic Atlantic dissolution event at the onset of the last glaciation. Geochemistry, Geophys Geosystems 2:2001GC000185

Brown JH, Gillooly JF, Allen AP, Savage VM, West GB (2004) Toward a metabolic theory of ecology. Ecology 85:1771–1789

Caldeira K, Wickett ME (2003) Oceanography: anthropogenic carbon and ocean pH. Nature 425:365

Chierici M, Fransson A (2009) Calcium carbonate saturation in the surface water of the Arctic Ocean : undersaturation in freshwater influenced shelves. Biogeosciences Discuss 6:4963– 4991

Comeau S, Gorsky G, Jeffree R, Teyssie J-L, Gattuso J-P (2009) Impact of ocean acidification on a key Arctic pelagic mollusc (Limacina helicina). Biogeosciences 6:1877–1882

Comeau S, Gorsky G, Alliouane S, Gattuso J-P (2010) Larvae of the pteropod Cavolinia inflexa exposed to aragonite undersaturation are viable but shell-less. Mar Biol 157:2341–2345

Comeau S, Teyssié J-L, Gattuso J-P (2010) Response of the Arctic pteropod Limacina helicina to projected future environmental conditions. PLoS One 5:e11362

Comeau S, Alliouane S, Gattuso J-P (2012) Effects of ocean acidification on overwintering juvenile Arctic pteropods Limacina helicina. Mar Ecol Prog Ser 456:279–284

Comeau S, Gattuso J-P, Nisumaa A-M, Orr JC (2012) Impact of aragonite saturation state changes on migratory pteropods. Proc Biol Sci 279:732–738

Craigie JS (1990) Cell walls. In: Cole MK, Sheath RG (eds) Biology of the red algae. Cambridge University Press, Cambridge, p 221–259

Davenport J, Bebbington A (1990) Observations on the swimming and buoyancy of some thecosomatous pteropod gastropods. J Molluscan Stud 54:487–497

Diaz-Pulido G, Anthony KRN, Kline DI, Dove S, Hoegh-guldberg O (2012) Interactions Between Ocean Acidification and Warming on the Mortality and Dissolution of Coralline Algae. J Phycol 48:32–39

Dickson AG (1981) An exact definition of total alkalinity and a procedure for the estimation of alkalinity and total inorganic carbon from titration data. Deep Sea Res Part I Oceanogr Res Pap 28:609–623

Egilsdottir H, Noisette F, Noël LM-LJ, Olafsson J, Martin S (2012) Effects of pCO2 on physiology and skeletal mineralogy in a tidal pool coralline alga Corallina elongata. Mar Biol 160:2103–2112

Fabry VJ (1990) Shell growth rates of pteropod and heteropod molluscs and aragonite production in the open ocean: Implications for the marine carbonate system. J Mar Res 48:209–222

Fabry VJ, Seibel BA, Feely RA, Orr JC (2008) Impacts of ocean acidification on marine fauna and ecosystem processes. ICES J Mar Sci:414–432

Fabry VJ, McClintock J, Mathis J, Grebmeier J (2009) Ocean Acidification at High Latitudes: The Bellwether. Oceanography 22:160–171

Feely RA, Sabine CL, Lee K, Berelson W, Kleypas J, Fabry VJ, Millero FJ (2004) Impact of anthropogenic CO2 on the CaCO3 system in the oceans. Science (80-) 305:362–6

Fleming J (1823) On a reversed species of Fusus (Fusus retroversus). Mem Wernerian Nat Hist Soc 4:488–500

Fortier L, Fevre J Le, Legendre L (1994) Export of biogenic carbon to fish and to the deep ocean: the role of large planktonic microphages. J Plankton Res 16:809–839

Foster MS (2001) Rhodoliths : Between Rocks and Soft Places. J Phycol 37:659–667

Francey RJ, Farquhar GD (1982) An explanation of 13C/12C variations in tree rings. Nature 297:28–31

Frankignoulle M, Canon C, Gattuso J-P (1994) Marine calcification as a source of carbon dioxide: Positive feedback of increasing atmospheric CO_2. Limnol Oceanogr 39:458–462

Frantz BR, Foster MS, Riosmena-Rodriguez R (2005) Clathromorphum Nereostratum (Corallinales, Rhodophyta): the Oldest Alga? J Phycol 41:770–773

Freiwald A (1993) Coralline Algal Maerl Frameworks- Islands within the Phaeophytic Kelp Belt. Facies 29:133–148

Freiwald A, Henrich R (1994) Reefal coralline algal build-ups within the Arctic Circle : morphology and sedimentary dynamics under extreme environmental seasonality. Sedimentology 41:963–984

Froneman PW, Pakhomov EA (1998) Biogeographic study of the planktonic communities of the Prince Edward Islands (Southern Ocean). J Plankton Res 20:653–669

Gannefors C, Böer M, Kattner G, Graeve M, Eiane K, Gulliksen B, Hop H, Falk-Petersen S (2005) The Arctic sea butterfly Limacina helicina: lipids and life strategy. Mar Biol 147:169–177

Gattuso J-P, Frankignoulle M, Wollast R (1998) Carbon and Carbonate Metabolism in Coastal Aquatic Ecosystems. Annu Rev Ecol Syst 29:405–434

Gattuso J-P, Buddemeier RW (2000) Calcification and CO_2. Nature 407:311–313

Gilmer RW, Harbison GR (1986) Morphology and field behavior of pteropod molluscs: feeding methods in the families Cavoliniidae, Limacinidae and Peraclididae (Gastropoda: Thecosomata). Mar Biol 91:47–57

Gilmer RW, Harbison GR (1991) Diet of Limacina helicina (Gastropoda: Thecosomata) in Arctic waters in midsummer. Mar Ecol Prog Ser 77:125–134

Gruber N, Gloor M, Mikaloff Fletcher SE, Doney SC, Dutkiewicz S, Follows MJ, Gerber M, Jacobson AR, Joos F, Lindsay K, Menemenlis D, Mouchet A, Müller S a., Sarmiento JL, Takahashi T (2009) Oceanic sources, sinks, and transport of atmospheric CO_2. Global Biogeochem Cycles 23:GB1005

Guinotte JM, Fabry VJ (2008) Ocean acidification and its potential effects on marine ecosystems. Ann N Y Acad Sci 1134:320–42

Halfar J, Mutti M (2005) Global dominance of coralline red-algal facies: A response to Miocene oceanographic events. Geology 33:481

Hall-Spencer JM, Rodolfo-Metalpa R, Martin S, Ransome E, Fine M, Turner SM, Rowley SJ, Tedesco D, Buia M-C (2008) Volcanic carbon dioxide vents show ecosystem effects of ocean acidification. Nature 454:96–9

Hauck J, Arrigo KR, Hoppema M, Dijken GL van, Völker C, Wolf-Gladrow DA (2013) Insignificant buffering capacity of Antarctic shelf carbonates. Global Biogeochem Cycles 27:11–20

Heijden LH van der, Kamenos NA (2015) Reviews and sytheses: Calculating the global contribution of coralline algae to carbon burial. Biogeosciences 12:6429–6441

Hein M, Sand-Jensen K (1997) CO2 Increases Oceanic Primary Production. Nature 388:526–527 Henson SA, Sanders R, Madsen E, Morris PJ, Moigne F Le, Quartly GD (2011) A reduced estimate of the strength of the ocean's biological carbon pump. Geophys Res Lett 38:10–14

Hetzinger S, Halfar J, Riegl B, Godinez-Orta L (2006) Sedimentology and acoustic mapping of modern rhodolith facies on a non-tropical carbonate shelf (Gulf of California, Mexico). J Sediment Res 76:670–682

Hochachka PW, Somero GN (2002) Biochemical Adaptation: Mechanism and Process in Physiological Evolution. Oxford University Press

Hoegh-Guldberg O, Mumby PJ, Hooten AJ, Steneck RS, Greenfield P, Gomez E, Harvell CD, Sale PF, Edwards AJ, Caldeira K, Knowlton N, Eakin CM, Iglesias-Prieto R, Muthiga N, Bradbury RH, Dubi A, Hatziolos ME (2007) Coral reefs under rapid climate change and ocean acidification. Science (80-) 318:1737–42

Hoegh-Guldberg O, Bruno JF (2010) The impact of climate change on the world's marine ecosystems. Science (80-) 328:1523–8

Hunt BPV, Pakhomov EA, Hosie GW, Siegel V, Ward P, Bernard K (2008) Pteropods in Southern Ocean ecosystems. Prog Oceanogr 78:193–221

Ierodiaconou D, Monk J, Rattray A, Laurenson L, Versace VL (2011) Comparison of automated classification techniques for predicting benthic biological communities using hydroacoustics and video observations. Cont Shelf Res 31:28–38

IPCC 2007 Climate Change 2007: The Physical Science Basis. Contribution of Working Group I to the Fourth Assessment Report of the Intergovernmental Panel on Climate Change. In: Solomon, S., D. Qin, M. Manning, Z. Chen, M. Marquis, K.B. Averyt, M.Tignor and H.L. Miller (eds.). Cambridge University Press. Cambridge, United Kingdom and New York, NY, USA

Jackson JBC (2008) Ecological extinction and evolution in the brave new ocean. Proc Natl Acad Sci USA 105:11458–11465

Jokiel PL, Rodgers KS, Kuffner IB, Andersson AJ, Cox EF, Mackenzie FT (2008) Ocean acidification and calcifying reef organisms: a mesocosm investigation. Coral Reefs 27:473–483

Jones CG, Lawton JH, Shachak M (1994) Organisms as ecosystem engineers. Oikos 69:373–386 Kamenos NA, Cusack M, Moore PG (2008) Coralline algae are global palaeothermometers with bi-weekly resolution. Geochim Cosmochim Acta 72:771–779

Kamenos NA, Moore PG, Hall-Spencer JM (2004a) Nursery-area function of maerl grounds for juvenile queen scallops Aequipecten opercularis and other invertebrates. Mar Ecol Prog Ser 274:183–189

Kamenos NA, Moore PG, Hall-Spencer JM (2004b) Small-scale distribution of juvenile gadoids in shallow inshore waters; what role does maerl play? ICES J Mar Sci 61:422–429

Kamenos NA, Moore PG, Hall-Spencer JM (2004c) Maerl grounds provide both refuge and high growth potential for juvenile queen scallops (Aequipecten opercularis L.). J Exp Mar Bio Ecol 313:241–254

Keeling RF, Shertz SR (1992) Seasonal and interannual variations in atmospheric oxygen and implications for the global carbon cycle. Nature 358:723–727

Kintisch E (2014) Sea Butterflies are a Canary for Ocean Acidification. Science 344:569

Kjellman FR (1883) Norra Ishafvets algflora. Vega-expeditionens, Vetenskapliga Iakttagelser 1:1–431

Klaas C, Archer DE (2002) Association of sinking organic matter with various types of mineral ballast in the deep sea: Implications for the rain ratio. Global Biogeochem Cycles 16: 1116

Koenigk T, Brodeau L, Graversen RG, Karlsson J, Svensson G, Tjernström M, Willén U, Wyser K (2012) Arctic climate change in 21st century CMIP5 simulations with EC-Earth. Clim Dyn 40:2719–2743

Kuffner IB, Andersson AJ, Jokiel PL, Rodgers KS, Mackenzie FT (2008) Decreased abundance of crustose coralline algae due to ocean acidification. Nat Geosci 1:114–117

Kump LR (2008) The rise of atmospheric oxygen. Nature 451:277–278

Labat D, Goddéris Y, Probst JL, Guyot JL (2004) Evidence for global runoff increase related to climate warming. Adv Water Resour 27:631–642

Lalli CM, Gilmer RW (1989) Pelagic snails: the biology of holoplanktonic gastropod mollusks. Stanford university press, Stanford, California

Lebednik PA (1976) The Corallinaceae of northwestern North America. I. Clathromorphum Foslie emend Adey. Syesis 9:59–112

Lebour M V (1932) Limacina retrouersa in Plymouth Waters. J Mar Biol Assoc United Kingdom 18:123–126

Lee K, Millero FJ, Byrne RH, Feely RA, Wanninkhof R (2000) The recommended dissociation constants for carbonic acid in seawater. Geophys Res Lett 27:229-232

Levitus S, Antonov JI, Wang J, Delworth TL, Dixon KW, Broccoli AJ (2001) Anthropogenic warming of Earth's climate system. Science (80-) 292:267–270

Levitus S, Antonov J, Boyer T (2005) Warming of the world ocean, 1955–2003. Geophys Res Lett 32:L02604

Lindeman RL (1942) The Trophic-Dynamic Aspect of Ecology. Ecology 23:399–417

Lischka S, Büdenbender J, Boxhammer T, Riebesell U (2011) Impact of ocean acidification and elevated temperatures on early juveniles of the polar shelled pteropod Limacina helicina: mortality, shell degradation, and shell growth. Biogeosciences 8:919–932

Lischka S, Riebesell U (2012) Synergistic effects of ocean acidification and warming on overwintering pteropods in the Arctic. Glob Change Biol 18:3517–3528

Littler MM, Littler DS, Dennis Hanisak M (1991) Deep-water rhodolith distribution, productivity, and growth history at sites of formation and subsequent degradation. J Exp Mar Bio Ecol 150:163–182

Lopez-Urrutia A, San Martin E, Harris RP, Irigoien X (2006) Scaling the metabolic balance of the oceans. Proc Natl Acad Sci U S A 103:8739–8744

Lüning K (1985) Meeresbotanik. Thieme

Mackas DL, Galbraith MD (2011) Pteropod time-series from the NE Pacific. ICES J Mar Sci 69:448–459

Manno C, Tirelli V, Accornero A, Fonda Umani S (2009) Importance of the contribution of Limacina helicina faecal pellets to the carbon pump in Terra Nova Bay (Antarctica). J Plankton Res 32:145–152

Martin S, Gattuso J-P (2009) Response of Mediterranean coralline algae to ocean acidification and elevated temperature. Glob Change Biol 15:2089–2100

Martin S, Cohu S, Vignot C, Zimmermann G, Gattuso J-P (2013) One-year experiment on the physiological response of the Mediterranean crustose coralline alga, Lithophyllum cabiochae, to elevated pCO2 and temperature. Ecol Evol 3:676–693

Maxwell JC (1860) Illustrations of the Dynamical Theory of Gases. Part I . On the Motions and Collisions of Perfectly Elastic Spheres. Philos Mag Ser 4:19–32

McCoy SJ, Ragazzola F (2014) Skeletal trade-offs in coralline algae in response to ocean acidification. Nat Clim Chang 4:719–723

Morse JW, Andersson AJ, Mackenzie FT (2006) Initial responses of carbonate-rich shelf sediments to rising atmospheric pCO2 and “ocean acidification”: Role of high Mg-calcites. Geochim Cosmochim Acta 70:5814–5830

Nelson WA (2009) Calcified macroalgae - critical to coastal ecosystems and vulnerable to change: a review. Mar Freshw Res 60:787-801

Noji TT, Bathmann UV, Bodungen B von, Voss M, Krumbholz M, Klein B, Peeken I, Noji CI, Rey F (1997) Clearance of picoplankton-sized particles and formation of rapidly sinking aggregates by the pteropod, Limacina retroversa. J Plankton Res 19:863–875

O’Connor MI, Bruno JF, Gaines SD, Halpern BS, Lester SE, Kinlan BP, Weiss JM (2007) Temperature control of larval dispersal and the implications for marine ecology, evolution, and conservation. Proc Natl Acad Sci U S A 104:1266–1271

O’Connor MI, Piehler MF, Leech DM, Anton A, Bruno JF (2009) Warming and resource availability shift food web structure and metabolism. PLoS Biol 7:e1000178

Ohman MD, Lavaniegos BE, Townsend AW (2009) Multi-decadal variations in calcareous holozooplankton in the California Current System: Thecosome pteropods, heteropods, and foraminifera. Geophys Res Lett 36:L18608

Orr JC, Fabry VJ, Aumont O, Bopp L, Doney SC, Feely RA, Gnanadesikan A, Gruber N, Ishida A, Joos F, Key RM, Lindsay K, Maier-Reimer E, Matear R, Monfray P, Mouchet A, Najjar RG, Plattner G-K, Rodgers KB, Sabine CL, Sarmiento JL, Schlitzer R, Slater RD, Totterdell IJ, Weirig M-F, Yamanaka Y, Yool A (2005) Anthropogenic ocean acidification over the twenty-first century and its impact on calcifying organisms. Nature 437:681–686

Paine RT (1969) The Pisaster-Tegula Interaction: Prey Patches, Predator Food Preference, and Intertidal Community Structure. Ecology 50:950–961

Pakhomov EA, Perissinotto R (1997) Mesozooplankton community structure and grazing impact in the region of the Subtropical Convergence south of Africa. J Plankton Res 19:675–691

Pakhomov EA, Verheye HM, Atkinson A, Laubscher RK, Taunton-Clark J (1997) Structure and grazing impact of the mesozooplankton community during late summer 1994 near South Georgia, Antarctica. Polar Biol 18:180–192

Pakhomov EA, Froneman PW (2004) Zooplankton dynamics in the eastern Atlantic sector of the Southern Ocean during the austral summer 1997/1998—Part 2: Grazing impact. Deep Sea Res Part II Top Stud Oceanogr 51:2617–2631

Perissinotto R (1992) Mesozooplankton size-selectivity and grazing impact on the phytoplankton community of the Prince Edward Archipelago (Southern Ocean). Mar Ecol Prog Ser 79:243–258

Phipps CJ (1773) A Voyage towards the North Pole undertaken by His Majesty's Command. J. Nourse, London

Pirenne H (1914) The Stages in the Social History of Capitalism. Am Hist Rev 19:494–515 Plummer LN, Mackenzie FT (1974) Predicting mineral solubility from rate data; application to the dissolution of magnesian calcites. Am J Sci 274:61–83

Pörtner H-O, Langenbuch M, Reipschläger A (2004) Biological Impact of Elevated Ocean CO2 Concentrations: Lessons from Animal Physiology and Earth History. J Oceanogr 60:705–718

Post WM, Peng T, Emanuel WR, King AW, Dale VH, DeAngelis DL (1990) The global carbon cycle. Am Sci 78:310–326

Quéré C Le, Raupach MR, Canadell JG, Marland et al. G, Quéré et al. C Le, Marland G, Bopp L, Ciais P, Conway TJ, Doney SC, Feely RA, Foster P, Friedlingstein P, Gurney K, Houghton R a., House JI, Huntingford C, Levy PE, Lomas MR, Majkut J, Metzl N, Ometto JP, Peters GP, Prentice IC, Randerson JT, Running SW, Sarmiento JL, Schuster U, Sitch S, Takahashi T, Viovy N, Werf GR van der, Woodward FI (2009) Trends in the sources and sinks of carbon dioxide. Nat Geosci 2:831–836

Ragazzola F, Foster LC, Form AU, Büscher J, Hansteen TH, Fietzke J (2013) Phenotypic plasticity of coralline algae in a High CO2 world. Ecol Evol 3:3436–3446

Raven JA, Caldeira K, Elderfield H, Hoegh-Guldberg O, Liss P, Riebesell U, Shephard J, Turley CM, Watson A (2005) Ocean acidification due to increasing atmospheric carbon dioxide. London

Reeder RJ (1983) Crystal chemistry of the rhombohedral carbonates. Rev Mineral Geochemistry 11:1–47

Ridgwell A, Zeebe R (2005) The role of the global carbonate cycle in the regulation and evolution of the Earth system. Earth Planet Sci Lett 234:299–315

Ridgwell A, Zondervan I, Hargreaves JC, Bijma J, Lenton TM (2007) Assessing the potential long-term increase of oceanic fossil fuel CO2 uptake due to CO2-calcification feedback. Biogeosciences 4:481–492

Riebesell U, Wolf-Gladrow DA, Smetacek V (1993) Carbon dioxide limitation of marine phytoplankton growth rates. Nature 361:249 – 251

Riebesell U, Zondervan I, Rost B, Tortell PD, Zeebe RE, Morel FM (2000) Reduced calcification of marine plankton in response to increased atmospheric CO2. Nature 407:364–367

Riebesell U, Körtzinger A, Oschlies A (2009) Sensitivities of marine carbon fluxes to ocean change. Proc Natl Acad Sci U S A 106:20602–20609

Ries JB, Cohen AL, McCorkle DC (2009) Marine calcifiers exhibit mixed responses to CO2-induced ocean acidification. Geology 37:1131–1134

Riul P, Targino CH, Farias JDN, Visscher PT, Horta PA (2008) Decrease in Lithothamnion sp. (Rhodophyta) primary production due to the deposition of a thin sediment layer. J Mar Biol Assoc United Kingdom 88:17–19

Roberts RD, Kühl M, Glud RN, Rysgaard S (2002) Primary Production of Crustose Coralline Red Algae in a High Arctic Fjord. J Phycol 283:273–283

Sabine CL, Heimann M, Artaxo P, Bakker DC, Chen C-TA, Field CB, Gruber N, Quéré C Le, Prinn RG, Richey JE, Lankao PR, Sathaye JA, Valentini R (2004) Current status and past trends of the global carbon cycle. In: Field CB, Raupach MR (eds) The Global Carbon Cycle: Integrating Humans, Climate, and the Natural World. Island Press, :17–44

Sarmiento JL, Gruber N (2006) Ocean biogeochemical dynamics. Princeton University Press Screen JA, Simmonds I (2010) The central role of diminishing sea ice in recent Arctic temperature amplification. Nature 464:1334–1337

Serreze MC, Francis JA (2006) The Arctic Amplification Debate. Clim Change 76:241–264

Siegel DA, Buesseler KO, Doney SC, Sailley SF, Behrenfeld MJ, Boyd PW (2014) Global assessment of ocean carbon export by combining satellite observations and food-web models. Global Biogeochem Cycles 28:181–196

Spoel S van der, Dadon JR (1999) Pteropoda. In: Boltovskoy D (ed) South Atlantic Zooplankton. Backhuys Publishers, Leiden, The Netherlands, :649–706

Steinacher M, Joos F, Fröhlicher TL, Plattner G-K, Doney SC (2009) Imminent ocean acidification in the Arctic projected with the NCAR global coupled carbon cycle-climate model. Biogeosciences 6:515–533

Steller DL, Riosmena-Rodriguez R, Foster MS, Roberts CA (2003) Rhodolith bed diversity in the Gulf of California: the importance of rhodolith structure and consequences of disturbance. Aquat Conserv Mar Freshw Ecosyst 13:5–20

Thabet AA, Maas AE, Lawson GL, Tarrant AM (2015) Life cycle and early development of the thecosomatous pteropod Limacina retroversa in the Gulf of Maine, including the effect of elevated CO2 levels. Mar Biol 162: 2235-2249

Toggweiler JR, Gnanadesikan A, Carson S, Murnane R, Sarmiento JL (2003) Representation of the carbon cycle in box models and GCMs: 1. Solubility pump. Global Biogeochem Cycles 17:1–10

Toggweiler JR, Murnane R, Carson S, Gnanadesikan A, Sarmiento JL (2003) Representation of the carbon cycle in box models and GCMs: 2. Organic pump. Global Biogeochem Cycles 17:1027

Turner J (2002) Zooplankton fecal pellets, marine snow and sinking phytoplankton blooms. Aquat Microb Ecol 27:57–102

Volk T, Hoffert MI (1985) Ocean Carbon Pumps: Analysis of Relative Strengths and Efficiencies. In: Sundquist ET, Broecker WS (eds) Ocean-Driven Atmospheric CO2 Changes, in The Carbon Cycle and Atmospheric CO: Natural Variations Archean to Present. American Geophysical Union, Washington, D. C.

Wall-Palmer D, Smart CW, Hart MB (2013) In-life pteropod shell dissolution as an indicator of past ocean carbonate saturation. Quat Sci Rev 81:29–34

Walsh JJ, McRoy CP, Coachman LK, Goering JJ, Nihoul JJ, Whitledge TE, Blackburn TH, Parker PL, Wirick CD, Shuert PG, Grebmeier JM, Springer AM, Tripp RD, Hansell DA, Djenidi S, Deleersnijder E, Henriksen K, Lund BA, Andersen P, Müller-Karger FE, Dean K (1989) Carbon and nitrogen cycling within the Bering / Chukchi Seas : Source regions for organic matter effecting AOU demands of the Arctic Ocean. Prog Oceanogr 22:277–359

Woelkerling WJ (1988) The coralline red algae: an analysis of the genera and subfamilies of non geniculate Corallinaceae. Oxford University Press, London

Woelkerling WJ (1990) An introduction. In: Cole KM, Sheath RG (eds) Biology of the red algae. Cambridge University Press, Cambridge, p 1–7

Wolf-Gladrow DA, Zeebe RE, Klaas C, Körtzinger A, Dickson AG (2007) Total alkalinity: The explicit conservative expression and its application to biogeochemical processes. Mar Chem 106:287–300

Yoon WD, Kim SK, Han KN (2001) Morphology and sinking velocities of fecal pellets of copepod, molluscan, euphausiid, and salp taxa in the northeastern tropical Atlantic. Mar Biol 139:923–928

Zeebe RE, Wolf-Gladrow DA (2001) CO2 in seawater: equilibrium, kinetics, isotopes. Gulf Professional Publishing, Amsterdam

7 Danksagung

Ich bedanke mich!

Bei Ulf für deine Unterstützung und Vertrauen und dein Beispiel an Verhandlungsgeschick und Durchsetzungskraft, und dafür, dass ich die Möglichkeit bekommen habe, diese Arbeit zu machen und für das Erschaffen und Amlaufenhalten der KOSMOS Experimente, die für mich die schönste Form der Wissenschaft verkörpern.

Vielen Dank an Frank Melzner für das zweite Gutachten und an die Mitglieder meiner Kommission für deren Mitarbeit in dieser Aufgabe.

Wissenschaftlich habe ich am meisten von Armin, Kai & Silke gelernt, jeder war auf seinem Spezialgebiet ein unersetzlicher Mentor - sei es die eigenverantwortliche und kreative Art von Armin (Experimentelle Aufbauten), die allwissende und höchst wissenschaftliche Verkörperung durch Kai S (Karbonatsystem, Methoden, Lösungsorientiertheit, Genialität & Genauigkeit), oder die organisierte, unbeirrbare und ordentliche Art von Silke (Zooplankton & Arktis).

Für die Hilfe bei Messungen und Methoden, für die vielen Espressi und Nervennahrungseinheiten, den Esprit und die vielen netten Worte bedanke ich mich bei Peter, Andrea, Kerstin, Annegret und Michael.

Für die Diskussionen, die gemeinsame Doktoranden-Zeit innerhalb und außerhalb des Instituts, die geteilten Erfahrungen und die kompensatorischen Lauf-, Schwimm- und Radeinheiten Kai, Luke, Lennart, Jan C, Jasmin, Sarah, Scarlett, Matze F, Jörn, Kristin, Rainer, Matthes und eine zweite Heimstätte Herr und Frau Herzog.

Meinen Hiwis und Studenten für Ihre Unterstützung, geduldigen Ohren für meine Lebensweisheiten und Wertschätzung Tim, Dana, Hauke, Isabell, Paul und Janina.

Meinen Tauchern Jan C, Matze F, Matze H, Mischa, Jens, Sebastian, Sarah K, Christus und Chrischan für Ihre absolute Verlässlichkeit und Ihr Vertrauen immer dann, wenn es darauf Ankommt, egal ob der Tag schon rum ist oder noch gar nicht angefangen hat, ob müde, krank, oder total fertig, dann wenn jeder vernünftige schon umgekehrt wäre, ihr seid die echten Kerle, diejenigen mit denen ich ohne zu zögern alles gemacht habe und weiterhin machen werde egal wie groß die Herausforderung ist. Ich hoffe, wir verlieren uns nie aus den Augen. Meinen Ausbilder und Mentoren Hubert und Max, besser hätte ich nicht lernen können.

Für das gemeinsam Er- und Durchlebte und die tiefe Freundschaft Matze L und David.

Meinen Eltern und meinem Bruder für den Beweis, dass egal welchen (Um)weg man im Leben geht, alles wieder gut werden kann und es zum Glücklich sein nicht viel braucht. Meinen Großeltern für das Vorleben von sozialem Engagement, speziell Walter und Henni die neben 6 eigenen und zwei adoptierten Kindern keinem Hilfesuchendem die Tür je verschlossen hätten, und meinem Opa Hans für die pädagogische, philosophische, logische, Vernunft getriebene und wissbegierige Lebensart.

Kathrin und Janosch für ihre Liebe, Verständnis, Unterstützung und Lebensfreude, Ihr seid mein Zuhause.

8 Eidesstattliche Erklärung

Hiermit bestätige ich, dass die vorliegende Arbeit mit dem Titel:

Impacts of ocean acidification and warming on Arctic calcifying key species: Benthic coralline red alga (*Lithothamnion glaciale*) and pelagic thecosome pteropods (*Limacina helicina* & *L. retroversa*)

von mir selbstständig verfasst worden ist und keine weiteren Quellen und Hilfsmittel als die angegebenen verwendet wurden. Die vorliegende Arbeit ist unter Einhaltung der Regeln guter wissenschaftlicher Praxis der Deutschen Forschungsgemeinschaft entstanden und wurde weder im Rahmen eines Prüfungsverfahrens an anderer Stelle vorgelegt noch veröffentlicht. Ich erkläre mich einverstanden, dass diese Arbeit an die Bibliothek des GEOMAR und die Universitätsbibliothek der CAU weitergeleitet wird.

Kiel, den Dezember 2015 Jan Büdenbender